THE DISCOVERY AND CHARACTERIZATION OF LENALDEKAR: A SELECTIVE COMPOUND FOR THE TREATMENT OF T CELL ACUTE LYMPHOBLASTIC LEUKEMIA

by

Suzanne Ridges

A dissertation submitted to the faculty of
The University of Utah
in partial fulfillment of the requirements for the degree of

Doctor of Philosophy

Department of Oncological Sciences

The University of Utah

May 2013

The University of Utah Graduate School

STATEMENT OF DISSERTATION APPROVAL

The dissertation of **Suzanne Ridges**

has been approved by the following supervisory committee members:

Nikolaus S. Trede	, Chair	**7/30/2012** Date Approved
David A. Jones	, Member	**7/30/2012** Date Approved
Bryan E. Welm	, Member	**7/30/2012** Date Approved
David J. Bearss	, Member	**7/30/2012** Date Approved
Amy M. Barrios	, Member	**7/30/2012** Date Approved

and by **Bradley R. Cairns** , Chair of

the Department of **Oncological Sciences**

and by Charles A. Wight, Dean of The Graduate School.

ABSTRACT

Acute lymphoblastic leukemia (ALL) is the most common cancer of childhood, with approximately 2000 cases diagnosed annually in the US. Although cure rates for childhood ALL are currently ~80%, T-cell ALL (T-ALL) is still more difficult to treat than B-cell ALL, requiring harsher treatments with concomitant harsher side effects. The goal of this study was to identify more targeted therapies for treating T-ALL with the intent of reducing harsh treatment side effects, thus preserving both lives and long-term quality of life.

To meet this goal, 26,400 compounds from the ChemBridge library were screened utilizing zebrafish larvae since they have the combined attributes of vertebrate physiology and small size. The transgenic *lck:*eGFP zebrafish line with T-cell specific GFP was chosen since compounds which eliminate immature T-cells in the thymus might also eliminate developmentally arrested leukemic blasts. The screen identified five "hit" compounds that cause reduction in GFP without sickening the larvae or causing general cell cycle effects. Of these five compounds, one compound, "Lenaldekar" (LDK), was effective in killing human Jurkat T-ALL without harming healthy lymphocytes.

In vivo, LDK shows efficacy in treating leukemia in both zebrafish and mouse xenograft models of T-ALL without observable toxicity or endorgan damage. Furthermore, expanded leukemia testing showed that T-ALL, B-ALL, and CML are all largely LDK-sensitive, including most treatment-refractory relapsed Ph+ leukemias and

primary patient samples. Moreover, some AML and multiple myeloma cell lines also show LDK sensitivity.

Molecular characterization shows that LDK down-regulates the PI3K/AKT/mTOR (P/A/mT) pathway, which pathway is up-regulated in ~50% of T-ALL cases. Recent results suggest that LDK may achieve this effect via inactivation of the insulin-like growth factor 1 receptor (IGF1-R), which activates the P/A/mT pathway. In addition, LDK treatment elicits a second activity of G2/M arrest in most sensitive cell lines, which arrest appears to be independent of P/A/mT pathway inhibition.

Future directions include identifying and modeling LDK's direct biochemical target(s) with the intent of utilizing structure-activity relationships to optimize LDK's chemical structure and efficacy. This study's ultimate goal is to bring LDK into clinical trials for the treatment of T-ALL in both monotherapy and combination therapy applications.

This work is dedicated to my family without whom I could never have even started, let alone finished, this journey. I also dedicate it to the clinicians and staff at Huntsman Cancer Hospital and Huntsman Cancer Institute for their excellent care and support for me while being treated for breast cancer while pursuing my own graduate work in cancer research.

TABLE OF CONTENTS

LIST OF FIGURES

LIST OF TABLES

ACKNOWLEDGMENTS

I wish to thank Nikolaus Trede and David Jones for their guidance, support and encouragement during the time that I have spent in my thesis program. I also wish to thank all members of the Trede and Jones labs, both past and present, for their untiring support, without which this project could not have been completed. I especially want to acknowledge and thank Deepa Joshi and Will Heaton for their enormous contribution to this project and for their unconditional and invaluable friendship to me while working in the lab.

I also wish to give special thank to all personnel at Huntsman Cancer Institute, and particularly to the Deininger, Engel, Lessnick, Cairns, and CIT Labs for their cooperation and collaboration in many aspects of this work. Special thanks also go to the CZAR staff and to all University of Utah CORE facilities and personnel for their constant support. Many thanks also go to the off-campus collaborating labs elsewhere in the country that supported and advised us and contributed data to this study.

The clinicians and staff of Huntsman Cancer Hospital also must be thanked for their phenomenal kindness and skill in treating me for cancer myself while pursuing my own doctoral degree in Oncological Sciences. And finally, I wish to thank my family for their untiring love, support and encouragement during this chapter of my life, without which I could not have survived, let alone succeeded.

CHAPTER 1

INTRODUCTION TO T CELL ACUTE LYMPHOBLASTIC LEUKEMIA

Definition of T-ALL

Acute lymphoblastic leukemia (ALL) is a clinically aggressive disease. It is defined as the uncontrolled clonal expansion of an immature lymphocytic precursor cell of either the T- or B-cell lineage, which overwhelms the bone marrow, causing cessation of normal hematopoiesis in the bone marrow. If left untreated, it is inevitably lethal. T-ALL (T-cell acute lymphoblastic leukemia) pathogenesis is a multistep process consisting of acquisition by a T cell precursor of a series of genetic abnormalities, which disturb its normal maturation process, leading to differentiation arrest and uncontrolled proliferation. T-ALL is a specific and rare subtype of ALL that arises from a precursor cell of the T-cell lineage which becomes developmentally arrested early within certain defined stages of intrathymic differentiation.

T-cell acute lymphoblastic leukemias (T-ALL) and lymphomas (T-LBL) are often considered to be the same disease, differing only in burden of the leukemic disease in the bone marrow (over 25% of blasts in T-ALL and below 25% in T-LBL). Indeed, pathological inspection of blasts from both diseases manifests no difference in cell morphology and they are often treated in the same manner in the clinic setting.[1] However, recent findings indicate that some molecular markers differ between T-LBL and T-ALL,

for example BCL2 expression is more elevated in the former.[2] For diagnostic purposes, these two types of T-cell neoplasms can be segregated into two groups: precursor T-cell lymphoblastic neoplasms, derived from immature thymocytes, and peripheral T-cell lymphomas, arising from T-cells with varying stages of differentiation.[3] Peripheral T-cell lymphomas can be further subclassified by specific clinical features (Table 1.1).[4]

T-ALL demographics and statistics

Each year approximately 6,050 new cases of ALL are diagnosed in the United States alone (3,450 male and 2,600 female), of which an estimated 2,400 occur in children and adolescents, with an estimated 1440 total deaths from ALL.[5] This represents an incidence of approximately 3 to 4 cases per 100,000 in children ages 0-14 and 1 per 100,000 for ages 15 and older.[6] Altogether ALL constitutes 35% of new cancer cases diagnosed in childhood as well as almost 75% of all childhood leukemias (ages 0-19), making it the most common pediatric malignancy.[7] Approximately 15% and 25% of new ALL cases in children and adults, respectively, are T cell ALL. It is primarily a pediatric disease, with diagnoses peaking between 2-5 years of age, but T-ALL can also affect adults and exhibits a second incidence peak in the elderly.[5] In contrast to pediatric leukemias, the most common forms of leukemia in the adult population are acute *myeloid* leukemia (AML) and chronic lymphocytic leukemia (CLL).[8,9]

T-ALL occurs primarily as *de novo* disease and rarely as a secondary neoplasm, but it has been correlated to certain genetic and environmental factors. It has a slightly higher occurrence in patients with Down syndrome, Bloom syndrome, neurofibromatosis type I, and ataxia-telangiectasia. It has also been linked to environmental exposure *in utero* to ionizing radiation, pesticides, and solvents.[10] In all age groups, there is a slight

predominance of cases among males as well as notable excess incidence among Caucasian children.[6]

Overall, T-ALL is more difficult to treat and carries a worse prognosis than B-ALL due to the additional difficulties encountered in T-ALL, such as CNS infiltration as well as a worse risk of failure of initial induction therapy. As a result, in recent decades, treatment outcome improvements for T-ALL have lagged behind B-ALL. Nevertheless, treatment expectations for ALL patients have improved dramatically in recent years due to the application of intensified chemotherapy regimens. Consequently, 5-year relapse-free survival currently is ~80% in pediatric[11] and ~50% in adult cases of ALL (Figure 1.1).[12]

The poorer outcome in adult T-ALL patients can be attributed to multiple factors, including decreased tolerance for intensive chemotherapy regimens, higher incidence of poor-prognosis cytogenetics, and lower incidence of favorable subtypes such as the t(12;21) translocation.[13,14] In all groups of patients, relapsed cases of T-ALL still carry a dismal prognosis since they often correlate with development of chemoresistance in the refractory disease and still constitute a significant clinical problem.[15,16]

T-ALL diagnosis and classification

Patient presentation and symptoms

T-ALL usually presents as acute disease. However, in rare cases disease may evolve insidiously over several months.[17] A patient may present with fever caused by either the leukemia or by leukemia-induced secondary infection. Patients may also experience fatigue and lethargy caused by anemia, bone and joint pain, and bleeding diathesis related to thrombocytopenia. Other symptoms may include loss of appetite and

weight, excessive unexplained bruising, enlarged lymph nodes, pitting edema, petechiae due to low platelet levels, and wheezing due to an enlarged thymus (in T-ALL and T-LBL). Because of similarity of symptoms to many common maladies, T-ALL patients may not realize at first that they have a serious disease until it progresses to the point where medical attention is mandatory. Furthermore, T-ALL may initially be misdiagnosed as asthma due to observed wheezing and because it often can be relieved by corticosteroid treatment.

Clinical diagnosis and pathology

Due to its acute nature, T-ALL patients usually exhibit large tumor burdens upon initial presentation. The examining physician may observe organomegaly, particularly mediastinal masses with or without pleural effusions leading to respiratory distress, and often infiltration of the central nervous system at the time of diagnosis. Leukemic blasts may also spread to lymph nodes or other common extramedullary sites of involvement, including lymph nodes, liver, spleen, and meninges. Less commonly, ALL may infiltrate orbital tissues, testes, tonsils, and adenoids.

Pathological diagnosis includes a complete blood analysis and bone marrow smear. Normal bone marrow from a healthy patient will exhibit a mixture of several heterogeneous cell types (Figure 1.2A). By contrast, a bone marrow smear from a T-ALL patient will show a largely homogeneous cell population of small to medium-sized blasts overwhelming the bone marrow (Figure 1.2B). T-ALL blasts are typically cells with round to irregular or convoluted nuclei and high mitotic activity. T-ALL blasts also usually exhibit expression of nuclear terminal deoxynucleotidyl transferase (TdT). Most

commonly, ALL blasts have scanty cytoplasm, open nuclear chromatin, and sometimes presence of nucleoli.

Hematological assessment will usually show high numbers of circulating lymphoblasts in peripheral blood. Other blood count abnormalities include anemia, thrombocytopenia, neutropenia, and leucopenia or leucocytosis with hyperleukocytosis (>100 $x10^9$/L) present in approximately 15% of the pediatric patients.[17] Laboratory findings may also include elevated serum uric acid and lactose dehydrogenase levels because of excessive cell turnover.

T-cell development

A discussion on T-ALL leukemogenesis first requires an understanding of T-cell ontogeny since many of the molecular mistakes that result in T-ALL arise from this normal process gone awry. Normal lymphocyte development takes place in the central lymphoid organs: in the bone-marrow for B-cells and in the thymus for T-cells. The thymus provides the microenvironment essential for the development of T-cells from common lymphoid progenitors (CLP). When CLPs leave the bone marrow and enter into the thymus, they receive signals from the thymic microenvironment, particularly NOTCH signaling, engaging them definitively in the T-cell lineage (Figure 1.3).[18]

Immature committed lymphocytes, called thymocytes, undergo two crucial steps. First, they acquire a unique mature T-cell receptor (TCR) following the rearrangement of the genes coding for the different chains of the receptor. Second, they undergo selection steps that will retain only thymocytes with a functional receptor able to recognize specific antigens presented by thymic epithelial cells via the major histocompatibility complex (MHC). If thymocytes receive signals from the functional TCR, they are transmitted to

the nuclei through different signaling proteins, initiating the transcription of survival genes (positive selection), while T-cells without a functional TCR die by neglect.[19] Toward the end of this maturation process T-cells undergo negative selection, or "clonal deletion", of T-cells with high affinity for self-antigens to avoid self-reactivity.[19] During this maturation and selection process, T-cells undergo a series of transitions in their expression of CD4 and CD8 cell surface markers from double negative (DN,CD4-/CD8-) to double positive (DP, CD4+/CD8+), to finally single positive (SP, either CD4+ or CD8+) before leaving the thymus (Table 1.2).[20]

Thymocyte development is regulated by a series of transcription factors and regulators of hematopoiesis such as E2A proteins. Other proteins such as HOX, MYB, IKAROS, and especially NOTCH family proteins all play a role in T-cell commitment, differentiation, and proliferation. NOTCH proteins also play an important role in self-renewal of progenitors.[21] In T-ALL, alterations of these key proteins are common findings responsible for leukemic transformation. At the time when rearrangement of the different segments, variable (V), diversity (D), and joining (J), of the TCR genes takes place, illegitimate recombinations between TCR receptor gene promoter elements and genes that are in an open chromatin conformation at this stage of T-cell development, and thus susceptible to the recombinase enzyme activity of RAG1/2, can occur. Hence, though rare, translocations between TCR and HOX genes or genes coding for proteins interacting with E2A are recurrently found in T-ALL and point to the importance of these proto-oncogenes that are frequently over-expressed in T-ALL. [19]

T-ALL subtype classifications

Historically, T-ALL and T-NHL were once considered to be the same disease, differing only in the degree of bone marrow infiltration (>25% for T-ALL and <25% for T-NHL). Indeed, leukemic blasts from both disease classifications are largely indistinguishable under the microscope and are treated much the same in many cases. However, due to advances in molecular diagnostic and sequencing technologies in recent years, it has become apparent that T-cell neoplasms, though relatively rare, are a much more heterogeneous group of diseases than previously thought. In addition, Feng et al demonstrated that BCL2 is more strongly expressed in T-NHL than in T-ALL.[2] Likewise, differential response to identical therapy regimens in different patients with seemingly identical diseases has spurred investigation into the molecular causes of such disparate clinical outcomes. It was also anticipated that a more in-depth understanding of the molecular mechanisms driving T-ALL could better inform customized treatment regimen decisions.

Two classification systems have been proposed for T-ALL. The first classification system is from the European Group for the Immunological Characterization of Leukaemias (EGIL).[22] Briefly, in the EGIL classification system cellular expression of CD3 defines T-ALL. The system further separates T-ALL into four categories depending on the maturation status of the cells involved, ie. pro-T, pre-T, cortical-T, and mature T-cell stages, depending on the expression status of CD markers exhibited by the malignant cells (Table 1.3).

The second and more recent T-ALL classification system, developed by Macintyre et al.,[23] is based on T-cell receptor (TCR) status (Table 1.4). It contains

classifications of immature stage (IM), the pre-αß stage, and the TCRαß or TCRγδ stages.[24] Based on actual TRD, TRG, and TRB gene rearrangements, the IM group can be further differentiated into the IM0, IMδ, IMγ, or IMβ subtypes. Both of these T-ALL stage classification systems are intended to correlate with normal maturation steps involved in healthy T-cell development. However, only about half of T-ALL cases characterized by them can be assigned to equivalent developmental stages by both classification systems simultaneously.[25]

Molecular genetics and translocations

Modern advances in chemotherapy regimen intensification, although currently successful in curing ~80% of pediatric patients, are not without liability in the form of short- and long-term detrimental side effects. Furthermore, 20% of pediatric patients still cannot be cured of T-ALL. Clearly novel treatment strategies are needed beyond mere chemotherapy intensification and/or hematopoietic stem cell transplant to improve treatment outcomes. These observations as well as advances in molecular diagnosis technology have spurred much research in recent years concerning cytogenetic abnormalities in T-ALL with the intent of identifying druggable T-ALL-specific biochemical targets.

Many of the mutations in T-ALL (Summarized in Figure 1.4) can be attributed to chromosomal aberrations, which can be observed in ~50% of T-ALL cases by utilizing standard karyotyping techniques.[26] Other cytogenetic abnormalities are far more subtle or "cryptic", requiring FISH (Fluorescence *In Situ* Hybridization) for detection (Figure 1.5). The genetic abnormalities observed in T-ALL may be grouped into four general categories as follows (summarized in Table 1.5): 1) Juxtaposition of a T cell receptor

(TCR) promoter or enhancer next to a strong transcription factor, 2) The creation of fusion proteins, 3) Deletions and amplifications, and 4) Mutations. Each of these will be discussed in turn.

TCR-transcription factor gene juxtaposition

T-cell progenitors rearrange their TCRD, TCRG, TCRB, and TCRA loci, which if successful, will lead to expression of a mature TCR. In T-ALL, alterations of these key proteins are common findings responsible for leukemic transformation. At the time when rearrangement of the different segments (V(D)J) of the TCR genes takes place, illegitimate recombinations between TCR receptor genes' promoter and enhancer elements and genes that are active and therefore in an open chromatin conformation at this stage of T-cell development can occur. Hence, translocations between TCR and HOX genes or genes coding for proteins interacting with E2A are recurrently found in T-ALL.[19] Transcription factor genes are the preferred targets of these rare pathogenetic chromosomal translocations in the acute T-cell leukemias. Notable examples include the bHLH genes MYC, TAL1, and LYL1 which are essential for the development of other lineages such as erythroid cells, but with the exception of MYC, they are not normally expressed in T-lymphoid cells. Hence, over-expression or mutation of these proteins are pathogenetic mechanisms in T-ALL.[27]

Fusion proteins

The MLL (Mixed Lineage Leukemia) protein methylates histone H3 at lysine 4 (H3K4) and is the gene most associated with the formation of fusion oncoproteins in T-ALL. Under healthy circumstances it regulates gene expression, especially HOX gene

expression, to control skeletal patterning and HSC and early hematopoietic progenitor cell development.[28] Over 40 different balanced chromosomal translocations have been identified as fusion partners for MLL in T-ALL, all of which produce a fusion protein possessing the NH2-terminus of MLL fused to the COOH-terminus of the fusion partner.[27] The most common MLL-partner fusion genes are listed in Table 1.6. An 8.3KB breakpoint cluster region between exons 8 and 13 is the site for most MLL rearrangements, which always produce in-frame fusion proteins with fusion partners.[29] The SIL-TAL1 fusion is also very common in T-ALL and results from a t(1;14) translocation (3% of cases) or from an interstitial deletion of the SIL-TAL locus (~25% of cases).[30] Fusion proteins including ABL1 also occur recurrently in T-ALL, such as NUP214-ABL1 in 6% of T-ALL[31] or EML1-ABL1.[32]

Genomic deletions and amplifications

Often cryptic, genomic deletions and amplifications lead to the loss of tumor suppressor genes such as CDKN2A (p14/p16), which encodes a cell cycle regulator. Loss of CDKN2A is the most common genetic abnormality in T-ALL and is found in the vast majority of patients.[33] Other deletions may fall upstream or downstream of transcription factor genes and thus activate the ectopic expression as in the cases of LMO2 in T-ALL.[34,35] Duplications or amplifications of genes in T-ALL may include MYB or the amplification of the ABL1 variant fusion gene NUP214-ABL1 on amplified episomes.[31]

Mutations

Mutations are commonly found with or without chromosomal abnormalities in T-ALL. The most commonly mutated gene in T-ALL is NOTCH1, which exhibits

activating mutations in over 50% of T-ALL. Mutations in the *Notch1* gene occur in the homodimerization (HD) and PEST domains, resulting in the constitutive activation of the Notch pathway or in an increase of its half-life, respectively. The NOTCH1-associated gene, FBXW7, which is responsible for ubiquitinylating NOTCH1 as well as cyclin E1, c-Myc, and c-Jun protein, is also often mutated in T-ALL, resulting in lack of proteosomal degradation of NOTCH1 protein.[36,37]

In addition to these types of aberrations, T-ALL may also exhibit aneuploidy in the form of either hyperdiploidy or hypodiploidy. Hyperdiploidy (51-65 chromosomes) usually indicates a good prognosis, whereas hypodiploidy (45 or fewer chromosomes) is usually accompanied by a worse prognosis (Reviewed in Harrison 2002[38]). Unfortunately, with the exception of haploid/diploid status, cytogenetics in T-ALL are not as well understood as they are in B-ALL and have not been as informative in risk group classification or treatment planning for T-ALL as desired.[39]

Despite ~50% occurrence in T-ALL, cytogenetic abnormalities are not entirely responsible for all aberrant gene regulation that contributes to T-ALL ontogeny. In fact, gene expression analysis has demonstrated that up-regulation of oncogene expression in T-ALL can happen in the complete absence of such abnormalities. For instance, the *Notch1* gene undergoes translocation in less than 1% of T-ALL. This translocation results in lack of the extracellular portion but retains the transmembrane and intracellular subunits, resulting in a constitutively active form of intracellular NOTCH1 protein.[40] However, gain-of-function mutations in *Notch1* have been observed in over 50% of T-ALL which are not caused by this translocation.[37] If one includes mutations in *Fbxw7,*

which is responsible for ubiquitinylating and degrading NOTCH1 protein, mutations in *Notch1/Fbxw7* may be observed in 80% of T-ALL.[41,42]

Micro RNA contributions

More recent investigations indicate that there may be other gene misregulation phenomena which may also contribute to T-ALL. For instance, Mavrakis et al. (2011)[43] demonstrated that specific micro RNAs (miRNA) targeted towards T-ALL tumor suppressor genes were upregulated in T-ALL. Five specific miRNAs with relevance to T-ALL were identified including MIR19B, MIR20A, MIR26A, MIR92, and MIR223, which were predicted to silence T-ALL tumor suppressor genes including IKZF1, PTEN, BCL2L11, PHF6, NF1, and FBXW7.

Epigenetic contributions

Epigenetic gene misregulation may also play a role in T-ALL development, as has been found to apply to other forms of cancer. Abnormal levels of DNA methylation in T-ALL can result in silencing of WNT pathway elements as well as the cell cycle regulators P15INK4B and P16INK4A.[44,45] Furthermore, in two separate studies, Kraszewska et al. (2011)[46] and Roman-Gomez et al. (2005)[47] found that DNA methylation status of particular genes is different in T-ALL patients, healthy children, and normal thymic cell populations. However, it seems that the hypermethylation status of particular genes is not as important as assessing the general pattern of methylation of cancer cells, or the CpG island methylator phenotype (CIMP status).[48]

Both of these studies defined CIMP- status as two or less hypermethylated genes and CIMP+ status as three or more hypermethylated genes. In both studies, strong

positive genomic methylation (CIMP+) status correlated with poor outcome, whereas lack of high methylation status (CIMP-) correlated with good outcome. Specifically, in the Roman-Gomez et al. study (2005),[47] relapse rates for CIMP- and CIMP+ were 0% vs 58%, mortality rates were 20% and 59%, and 13-year overall survival were 91% and 17%, respectively. For both studies, 12-year disease-free survival for patients who achieved complete remission was significantly different at 100% and 20% for CIMP- and CIMP+, respectively. Furthermore, 13-year overall survival was 91% for CIMP- and 17% for CIMP+ patients.[49] However, although these data seem significant, larger high-powered studies need to be done to confirm these findings.

Moreover, pre-existing germline mutations in enzymatic processing genes may result in pharmacogenetic inhibition of chemotherapeutic drug activity. These germline polymorphisms and mutations affect drug metabolizing genes, which may influence negatively the response of leukemic blasts to specific chemotherapy agents.[50,51] Such genes may include thiopurine methyltransferase, glutathione S-transferase, cytochrome P450 3A4, and methylene-tetrahydrofolate reductase. All molecular contributors to T-ALL leukemogenesis are summarized graphically in Figure 1.6.

T-ALL risk level assessment

One of the most critical determinations that must be made before treating a patient for T-ALL is the relative risk level of the disease. Assessment of the risk category ensures that patients with high-risk T-ALL receive treatment of appropriate life-saving intensity and that low-risk patients are spared unnecessary toxic effects of treatment. A fine balance must be struck between these two considerations.

Many factors have been found to be contributory to T-ALL relative risk level. The first risk factors taken into consideration are patient characteristics, such as age and sex. The second set of considerations relate to the T-ALL disease features, such as WBC count, immunophenotype, and genetic abnormalities. Additional factors considered are the presence or absence of central nervous system (CNS) or testicular involvement, and early therapy response as determined in the initial 1-2 weeks of therapy.[17,52]

Within the last 10 years, pediatric T-ALL risk stratification classifications have expanded from two classes (standard and high risk) to four classes currently. The prior two-class risk stratification system relied only on patient age and WBC at the time of diagnosis. Currently the Children's Oncology Group (COG) defines four classes of T-ALL risk as low risk, standard risk, high risk, and very high risk.[53] The estimated 4-year event-free survival (EFS) for these groups is 91%, 86%, 76%, and 46%, respectively.[54] These groups were defined after examining clinical and cytogenetic data from more than 6000 patients enrolled on previous studies.

However, risk level assessment can be much more complicated due to several contributing factors beyond those mentioned above. High risk factors include older age (with the exception of infancy), MLL rearrangements, hypodiploidy, CNS involvement, drug metabolizing enzyme polymorphisms, hepatosplenomegaly, mediastinal mass, male gender, Caucasian race, an immature T-ALL immunophenotype, and hypermethylation of tumor suppressor genes. A few of these factors will be discussed further here.

Gene expression profiling

With the recent development of microarray platforms for global gene expression assessment, it has become possible to assess comprehensively differential T-ALL gene

expression patterns. Lugthart et al.[55] determined *in vitro* drug sensitivity of ALL cells in 441 patients. They used a genome-wide approach to identify 45 genes differentially expressed in ALL, exhibiting cross-resistance to multiple chemotherapeutic agents. The expression of these genes discriminated treatment outcome in two independent patient populations, identifying a subset of patients with a markedly inferior outcome. Furthermore, Golub et al.[56] demonstrated the feasibility of using microarrays to accurately distinguish subtypes of leukemia using a set of genes as class predictors.

T-ALL treatment regimens

Once T-ALL has been definitively diagnosed, a course of clinical action is chosen. The primary clinical goal of treatment is to achieve a lasting remission, defined as the absence of detectable cancer cells in the body and a negative minimal residual disease (MRD) reading as determined by FACS. Treatment includes high-dose chemotherapy administered both intravenously and intrathecally (IV and IT).

Chemotherapy regimens typically include three steps: 1) remission induction 2) intensification, and 3) maintenance therapy. The purpose of remission induction is to rapidly kill most leukemic blasts and achieve an initial remission regardless of non-debilitating toxicity. This allows the patient to achieve sufficient hematological recovery to proceed to further therapy as promptly as possible. CNS prophylactic (or therapeutic, in the case of CNS positive disease) chemotherapy is also administered at this point.

Glucocorticoid therapy

Glucocorticoids (prednisone/prednisolone and dexamethasone) play a fundamental role in the treatment of all lymphoid tumors because of their capacity to

induce apoptosis in lymphoid progenitor cells.[57,58] For this reason, they will be discussed more in-depth as an example of T-ALL treatment. The importance of glucocorticoid therapy in leukemias and lymphomas is underscored by the strong association of glucocorticoid response with prognosis in childhood ALL. Thus, the initial response to 7 days of glucocorticoid therapy is a strong independent prognostic factor in this disease.[59,60] Resistance to glucocorticoids *in vitro* is associated with an unfavorable prognosis.[61,62] Moreover, the majority of patients with ALL in relapse show increase resistance to glucocorticoid therapy, identifying glucocortocid resistance as a major contributor to treatment failure.[61,63] The glucocorticoids used in T-ALL therapy are predisone (or its derivative prednisolone) and dexamethasone. Though structurally very similar as derivatives of cortisol (Figure 1.7), these compounds have different efficacy and toxicity.[64]

Relative strengths of dexamethasone in comparison to prednisone include a longer plasma half-life (200 min vs 60 min),[65,66] reduced sodium retention,[66] and lower IC_{50} of ALL cells *in vitro* (0.2μM vs 3.5μM).[67] Furthermore, treatment regimens which include dexamethasone have higher CNS penetration with a concomitant reduction in CNS relapse (14.3% vs 25.6%, p=0.017),[68,69] and are associated with overall better event-free survival (81% vs 49%).[70,71]

However encouraging dexamethasone treatment outcomes may be in comparison to those of prednisone treatment, care must still be taken to consider the detrimental side effects of dexamethasone use. Prior studies have shown a consistent increase in side effects with dexamethasone use over prednisone, including bacterial and fungal infections,[72,73] bone fractures and osteonecrosis (especially for patients age > 10

years),[74,75] steroid psychosis,[76,77] neurocognitive dysfunction,[78,79] and proximal myopathy.[76,80]

Tyrosine kinase inhibitors

With the recent trend toward more targeted therapies for cancer, tyrosine kinase inhibitors (TKIs) have become a useful treatment modality for leukemia. The first TKI to be used in treating leukemia was imatinib mesylate (STI-571, brand name Gleevec®), a small molecule inhibitor designed to inhibit a small group of tyrosine kinases, including BCR-ABL, also referred to as the Philadelphia (Ph+) chromosome.[81] Imatinib acts as a competitive inhibitor for ATP cofactor binding and locks the Abelson kinase portion of BCR-ABL in an inactive conformation.[82,83] Imatinib has been highly successful as frontline therapy for treating chronic myeloid leukemia (CML). In CML, imatinib induces complete hematologic remission in ~95% of cases, with complete cytogenetic responses in ~75% of patients with chronic phase CML.[84]

Philadelphia chromosome-positive B cell ALL

Ph+ B-ALL usually carries a poor prognosis even with modern intensive chemotherapy regimens. Historically, bone marrow transplant had been recommended for children with this subtype of B-ALL, especially those with poor early response to induction therapy.[85] Imatinib also serves as therapy for treating BCR-ABL B-cell ALL (Ph+ B-ALL) and has constituted a revolutionary development in treating this disease.[86] In Ph+ B-ALL, remission is frequently achieved with imatinib alone.[87] Unfortunately, unlike CML, these responses in Ph+ B-ALL are often transient and in most cases relapse within months. Hence, subsequent studies evaluated combinations of imatinib with

chemotherapy.[86,88] Concurrent administration of imatinib with a multiagent regimen in an adult cohort led to molecular remission in 54% of patients compared with 19% in those who received an alternative chemotherapy regimen.[89]

Imatinib resistance

CML in remission, maintained on imatinib, can become treatment resistant over time.[90,91] Imatinib resistance in patients with Ph+ ALL also develops in most cases. A common mechanism of resistance is the development of point mutations within the kinase binding domain of BCR-ABL, most often in the P-loop or at codon 315 (T315I). These mutations can be detected in a small subclone of leukemic cells in 40% of newly diagnosed patients. But it becomes the dominant clone in 90% of cases at relapse, thus implying selective pressure of the resistant clone after treatment with tyrosine kinase inhibitors.[92] Other mechanisms leading to imatinib resistance in Ph+ B-ALL include gene amplification and overexpression of BCR-ABL, and activation of the SRC family of kinases.[93]

The development of resistance to imatinib in CML and Ph+ B-ALL spawned the development of a second generation of tyrosine kinase inhibitors, including dasatinib and nilotinib, which are both effective in treating imatinib-resistant ALL with the exception of cases harboring the T315I mutation. Dasatinib is a multikinase inhibitor targeting several tyrosine kinases, including BCR-ABL and SRC kinases. It is 325 times more potent than imatinib, binds to both the active and inactive forms of BCR-ABL, and has excellent CNS penetration.[94,95] Nilotinib is a derivative of imatinib in which modification of the aminopyrimidine backbone resulted in improved binding and a 30-fold increase in potency.[96]

Third generation TKIs

A third generation of tyrosine kinase inhibitors, including ponatinib, are being actively developed, especially to overcome the problematic T315I mutation that confers resistance to all existing BCR-ABL-specific tyrosine kinase inhibitors. Though not found as often as in cases of B-ALL, ABL1 translocations can also be found in T-ALL in the form of NUP214-ABL1 and EML1-ABL1 translocations. TKIs have been found to be effective in treating these cases of T-ALL. Dasatinib inhibits NUP214-ABL1 (Nuclear pore complex protein 214-V-abl Abelson murine leukemia viral oncogene homolog 1) cell proliferation while EML1-ABL1 (Echinoderm microtubule-associated protein-like 1-V-abl Abelson murine leukemia viral oncogene homolog 1) cells show sensitivity to imatinib.[97] However, despite encouraging results seen in utilizing second and third-generation TKIs, it is still likely that these drugs will have to be used in combination with other standard chemotherapies, as resistance to single kinase inhibitors is becoming an expected outcome in cancer.[90]

Maintenance therapy

The goal of maintenance therapy is to eradicate any residual leukemia cells that were not eliminated by remission induction or intensification regimens. Maintenance therapy typically includes daily oral intake of mercaptopurine as well as weekly oral intake of methotrexate and a monthly injection of IV vincristine and a 5-day course of oral corticosteroids. The duration of maintenance therapy is typically 2 years for girls and adults and 3 years for boys.[98]

T-ALL relapse therapy

Relapsed cases of T-ALL are the most difficult to treat and carry the worst prognosis since the disease has already undergone selection for chemoresistance characteristics. Overall, ALL relapses occur in 25% of pediatric and 50% of adult cases, respectively, with the rate of relapse being correlated with the immunophentotype and genetic subtype of the disease.[17,52] The majority of ALLs relapse in the initial 3 to 5 years following initial diagnosis with a small percentage relapsing more than 5 years from diagnosis and up to as many as 10 to 20 years later in a small minority of patients.[99]

Relapsed ALL may involve the bone marrow or extramedullary tissues, often at "sanctuary sites," such as the CNS, gonads, or both. Statistically, relapses with isolated bone marrow involvement seem to correlate with a poorer prognosis than those of isolated extramedullary or combined bone marrow and extramedullary relapses.[17] The morphologic and immunophenotypic features of relapsed ALL are often similar to that found at initial diagnosis and treatment. However, due to genomic instability coupled with drug-induced selection, imunophyenotypic variations may be present at relapse, wherein some cell surface antigens present at initial diagnosis may increase or decrease in intensity or may have been lost altogether at the time of relapse.[100,101]

The primary goal of T-ALL relapse therapy is to obtain a remission and to move to allogeneic transplantation as quickly as possible. Allogeneic transplantation must proceed quickly since most relapsed patients die shortly after relapsing. One study of 607 relapsed patients showed a 5-year survival of only 7%. In the same study, transplanted patients only experienced 14-16% survival for sibling and unrelated donors, respectively, a poignant reminder of how much progress has yet to be made in this field.[102] In a French

study, 44% of relapsed patients achieved a second remission (CR2), but only 12% survived.[103] These statistics clearly indicate a need to focus on optimizing initial therapy since salvage therapy in relapsed cases rarely succeeds long-term. These data also underscore a need to develop a much better understanding of the molecular mechanisms involved in relapsed T-ALL with the intent of using this knowledge to develop better targeted T-ALL therapies.

Minimal residual disease (MRD) determination

More than 80% of childhood and 35% of adult ALL patients can be cured with modern chemotherapy supplemented with HSCT (hematopoietic stem cell transplant) in high risk patients.[104] Still, a substantial number of ALL patients relapse and the prediction of relapse with conventional prognostic factors as above and classical clinical risk group assignment is far from optimal. Mortality rates for relapsed patient cases of ALL are a particularly sobering reminder of such treatment limitations. For instance, in the FRALLE-93 study, ~80% of patients with induction failures achieved a complete second remission utilizing various salvage therapies. However, only 30% were long-term survivors, emphasizing the need for early treatment success via complete initial elimination of all remaining residual disease.[105]

Prior techniques for determination of early induction therapy success relied on morphological examination of bone and peripheral blood specimens to detect the presence of residual disease. However, the bulk of residual tumor burden is below this limit of visual detection. For that reason, molecular techniques for detection of residual disease are now available that can detect “submicroscopic disease” not previously

identifiable. Techniques are now available that can detect 1 tumor cell in a background of 10,000 (using FACS) to more than 1 million normal cells (using PCR).

Correlation of MRD with treatment outcome has obvious applicability to treatment-making decisions in T-ALL. As the treatment side-effects in T-ALL can be very harsh, the overriding goal in risk level assessment is to assure that the patient receives only as intense a treatment regimen as necessary to eradicate the disease without excessive and undue toxicity. Patients who achieve MRD negativity after 2 to 3 weeks of remission induction, and therefore have an excellent prognosis, are good candidates for treatment de-intensification. At the very least they should not be subjected to further treatment intensification.[106,107] Conversely, MRD determination has the prognostic ability to inform treatment decisions when treatment intensification is warranted in resistant cases of T-ALL. Augmentation of subsequent therapy for patients who demonstrate a slow early response can significantly improve cure rates as extended induction and consolidation are used to deepen morphologic remission.[108,109]

Relapsed cases of T-ALL are the most difficult to treat and carry the worst prognosis. In such cases, MRD determination can be utilized to herald impending relapse, thus accelerating the planning of salvage therapy and/or HSCT. In patients who relapse but manage to achieve a second remission, MRD assays can be used to guide the selection of optimal post-remission treatment (i.e., chemotherapy versus HSCT). MRD measurements can also be used to determine the optimal timing of HSCT. MRD measurements post HSCT can also be used to guide the administration of donor lymphocyte infusions or other agents.[110]

Detection of MRD can be achieved through utilization of three different molecular techniques, including flow-cytometry, PCR detection of leukemia-associated fusion genes, and PCR detection of Ig/TCR gene arrangements. PCR detection of Ig/TCR gene re-arrangements is the third MRD methodology. Since individual T-cell receptor and immunoglobulin genes undergo a unique clonal rearrangement, they can be used as specific targets for residual tumor detection.[107] Although this MRD strategy is the most laborious, expensive, and time-consuming, it is reproducible not only within the same laboratory but also between different laboratories. Furthermore, it is the most sensitive technique. The junctional regions of clonal Ig and TCR gene rearrangements are fingerprint-like sequences for each lymphoid malignancy and can be identified in the vast majority of ALL patients using the standardized primer sets established through the European collaboration within the BIOMED-1 and -2 frameworks.[111,112] Consensus primers can be used to amplify junctional sequences and the length of the product will allow discrimination from a background of normal cells. The sensitivity of this approach can be as high as 1 cell in 10,000 with sequencing of the initial product and the creation of allele-specific primers.[113] Due to oligoclonality and clonal evolution of Ig/TCR gene rearrangements between diagnosis and relapse, it is recommended that at least two Ig/TCR targets be followed per patient.[114,115]

Regardless of the technique used, the following broad conclusions can be made. Patients with no detectable MRD at the end of induction have an exceedingly good outcome (EFS >90% at 3 years). Those children with a high MRD ($>10^{-2}$) have a poor prognosis (3-year EFS of approximately 25%). Patients with intermediate levels (10^{-4} to 10^{-3}) make up one-third to one-half of all patients depending on the technique used.

These patients can be further subdivided based on analysis of a second time point. For example, in the study by Coustan-Smith, of 32 patients who were MRD+ by flow cytometry at the end of remission induction who then became MRD- at week 14, only one relapsed. In comparison, 10 relapses occurred among 18 patients who remained MRD+ at the second time point.[116] It is probable that MRD diagnostics will be included in all T-ALL treatment protocols, as MRD data provide so far the most optimal reflection of the *in vivo* response to treatment, which gives the clinician a better knowledge and control of the best clinical course of action for individual patients.

Hematopoietic stem cell transplant

Hematopoietic stem cell transplant (HSCT) is utilized as a treatment modality of last resort for patients who have failed chemotherapy. It is also often used as first-line therapy for patients who have high-risk T-ALL that is not expected to respond well to chemotherapy. The role of HSCT in treating T-ALL is expected to increase as alternative donor sources become available. Alternative donor sources, including cord blood, are increasingly used for transplantation in children and adults with leukemia. A higher degree of mismatch is acceptable with cord blood units, and outcomes are comparable with those of allele-matched transplants.[117,118] Importantly, cord blood units can be obtained with a shorter waiting period and from a larger recipient pool, particularly for ethnic minorities who have a lower probability of having a suitably matched unrelated donor.[119]

HSCT is particularly applicable in cases of high-risk T-ALL. High-risk cases include those with poor initial response to induction therapy or high MRD, a stem cell-like immature T-ALL immunophenotype, high WBC count, or a t(4;11) translocation.

For example, in a large study of high-risk T-ALL in children comparing chemotherapy versus allogeneic HSCT, 5-year disease-free survival was 26.5% vs 56%, respectively.[120] Cases of Ph+ B-ALL would also be considered high-risk cases of ALL and eligible for first-line HSCT therapy. For instance, in one study of 267 children with Ph+ B-ALL, 5-year disease-free survival was 25% with chemotherapy alone versus 72% for patients receiving HSCT from a matched related donor.[121] In cases of successful remission induction followed by a subsequent relapse, HSCT would also be utilized if a second complete response (CR2) could be achieved using intensified salvage combination chemotherapy.

HSCT is usually more successful when using an allele-matched donor (allogeneic transplant) in comparison to autologous transplant from the patient's own bone marrow. In the LALA-94 trial, patients with high-risk ALL were allocated to allogeneic bone marrow transplantation if they had an HLA identical sibling or were randomized to autologous BMT or chemotherapy if they did not. Disease-free survival was 45% in patients with a matched donor versus 18% in those without.[122] A meta-analysis of this study and six others encompassing 1,274 patients showed a survival advantage for patients with an allogeneic stem cell donor that was augmented in high-risk patients. No benefit from autologous BMT was noted.[123]

An allogeneic transplant seeks to take advantage of the "graft versus leukemia" (GVL) effect, wherein if the patient experiences a relapse of T-ALL due to residual disease, the graft will recognize the relapsed T-ALL as foreign and destroy it. Allogeneic HSCT also carries with it the additional long-term benefit of being able to use T-cells harvested from the original donor in an infusion to "boost" the recipient's engrafted

immune system to destroy a refractory T-ALL relapse.[124] Unfortunately, the GVL effect is also often accompanied by "graft versus host disease" (GVHD), in which the allogeneic HSCT graft may recognize other healthy recipient tissues as foreign and seek to destroy them, resulting in undesirable long-term side effects. However, despite GVHD side-effects, many studies have shown that the long-term benefits of using allogeneic HSCT are superior to those using autologous transplant. Children undergoing HSCT on the average fare better than do adults. The only exceptions are infants who do not show benefit from allogeneic HSCT over combination chemotherapy alone. In fact, some showed worse outcomes in infants transplanted in first remission even after adjusting for presenting clinical features and waiting time to transplantation.[125,126]

Although many adult T-ALL patients benefit from allogeneic HSCT, still many are unable to tolerate the harsh myeloablative (MA) treatments necessary to prepare for the transplant, resulting in many cases of treatment-related mortality (TRM). This lack of tolerance for the prerequisite myeloablative therapy and consequent TRM increases as age increases. In consequence of this observed lack of tolerance for harsh preparative MA, many treatment centers are implementing a reduced intensity conditioning (RIC) pre-treatment regimen for older patients with T-ALL. The EBMT group has reported on a group of 97 patients with adult ALL, including one third of the patients in first CR with the majority in higher levels of CR or with refractory or persistent disease. The patients received a variety of RIC regimens and, with nearly 3 years of follow-up, the OS for the first CR patients was 52%. OS was 27% and 20%, respectively, for patients in second/third CR or with a more advanced disease.[127] Nevertheless, if a patient fails to

achieve a complete response after induction or salvage chemotherapy, HSCT is not likely to succeed and is not recommended in these cases.

Need for more targeted therapies in treating T-ALL

Long-term sequelae of T-ALL treatment

Thus far, most of the statistics cited in this document have focused on overall and disease-free survival in patients treated for T-ALL. However, these statistics do not take into consideration the long-term detrimental side effects of treatment for T-ALL. T-ALL is typically more difficult to treat than B-ALL, requiring harsher chemotherapy regimens with a concomitant increase in undesirable side-effects in both the short- and the long-term. These effects can be particularly detrimental for children treated for this disease. For instance, in comparison to their unaffected siblings, adult survivors of childhood cancers are 54 times more likely to have a major joint replacement, 15.1 times more likely to have congestive heart failure, and 14.8 times more likely to have a second malignancy, to name only a few effects (Table 1.7).

Although cure rates for T-ALL have improved dramatically in the past four decades, the means by which it has been accomplished has been for the most part intensification of the chemotherapy regimens used. Although this improvement in cure rates is welcome, such intensive chemotherapy comes at the cost of significant side effects, often continuing for years after treatment. And despite recent dramatic statistical improvements in cure rates, ~20% of pediatric and >50% of adult cases of T-ALL still cannot be cured. So the search for more targeted therapies that treat T-ALL more effectively while simultaneously reducing detrimental side-effects must be a research priority.

Goals of the dissertation

Although T-ALL treatment results have improved dramatically in the last 50 years, the improvement has come at the cost of increased side-effects of therapy. Hence, identification and development of more targeted therapies for treating T-ALL is the primary focus for this study. Questions to be asked and goals to be achieved by this study include the following:

1. Can zebrafish be utilized in an *in vivo* screen for compounds that show efficacy in treating T-ALL? As a vertebrate teleost, zebrafish (*Danio rerio)* have an immune system that is very similar to that of humans, including a thymus in which T-cells undergo a maturation process very similar to that of humans. Early zebrafish larvae are small enough to fit in a 96-well format, thus facilitating screening of thousands of compounds. In addition, transgenic zebrafish are available in which the T-cells have been genetically engineered to express eGFP, thus facilitating the observation of drug effects on T cell survival as well as T-ALL leukemogenesis and dissemination *in vivo*.

2. Can candidate compounds be identified that are effective in killing T-ALL while not exhibiting other toxic side-effects? To this end, candidate compounds identified will include those reproducibly exhibiting selective elimination of developing T-cells in larval zebrafish thymus while not sickening or killing the larvae. Furthermore, any candidate identified from the screen must not exhibit general cell cycle effects, as do traditional chemotherapy agents. Candidate compounds must also show lethality toward human T-ALL while still demonstrating a sufficient therapeutic window between the IC_{50} in human T-ALL cells compared to the IC_{50} determined for normal healthy peripheral

lymphocytes. Candidate compounds will also show efficacy in treating primary T-ALL patient samples.

3. If compounds can be identified from the screen that exhibit T-ALL specific lethality, what is/are the biochemical mechanism(s) of action employed by them? Numerous aberrantly activated molecular pathways have been implicated in T-ALL, including MAPK, JAK/STAT, NOTCH, Wnt, and PI3K/AKT/mTOR. Any T-ALL specific compounds identified in this screen may down-regulate one or more of these pathways. In addition, it is also possible that a candidate compound's activity may reveal a novel molecular mechanism heretofore unrecognized for its contribution to T-ALL leukemogenesis. In such a case, experiments would need to be designed and executed to characterize the biochemical behavior of such a pathway with the intent of identifying all druggable targets functioning within it.

4. Are the candidate compounds safe and effective in treating T-ALL *in vivo*? Multiple zebrafish models of spontaneous and induced (i.e., c-Myc) T-ALL development exist which could be utilized for this purpose. In addition, NOD-SCID mice may be utilized in a human xenograft model of T-ALL to determine mammalian response to drug candidate treatment. In addition to therapeutic response to treatment, maximum tolerated dose will be determined for candidate compounds along with endorgan toxicity and impact on hematological parameters *in vivo.*

References

1. Swerdlow SH, Campo E, Harris NL, et al. WHO Classification of Tumours of Haematopoietic and Lymphoid Tissues, 4th edn. (2008) IARC Press, Lyon.

2. Feng H, Stachura DL, White RM, et al. T-lymphoblastic lymphoma cells express high levels of BCL2, S1P1, and ICAM1, leading to a blockade of tumor cell intravasation. *Cancer Cell*. 2010; 18(4):353-66.

3. Uyttebroeck A, et al. Is there a difference in childhood T-cell acute lymphoblastic leukaemia and T-cell lymphoblastic lymphoma? *Leuk Lymphoma.* 2007; 48(9):1745–54.

4. de Leval L, Bisig B, Thielen C, et al. Molecular classification of T-cell lymphomas. *Crit Rev Oncol Hematol*. 2009; 72(2):125-43.

5. National Online SEER Database. http://seer.cancer.gov/statfacts/html/alyl. html. Accessed November 2, 2012.

6. National Cancer Institute. SEER Cancer Statistics Review, 1975–2006. Available at: http://seer.cancer.gov/csr/1975_2006/. Accessed January 23, 2009.

7. Plasschaert SL, Kamps WA, Vellenga E, et al. Prognosis in childhood and adult acute lymphoblastic leukaemia: a question of maturation? *Cancer Treatment Reviews.* 2004; 30:37–51.

8. Gurney JG, Severson RK, Davis S, et al. Incidence of cancer in children in the United States. Sex-, race-, and 1-year age-specific rates by histologic type. *Cancer.* 1995; 75(8):2186–95.

9. American Cancer Society. Cancer facts and figures 2008. Available at: http:// www.cancer.org. Accessed January 23, 2009.

10. Spector LG, Ross JA, Robison LL, et al. Epidemiology and etiology. In: Pui CH, editor. Childhood leukemias. New York: Cambridge University Press; 2006. p. 48–66.

11. Pui CH, Robison LL, Look AT. Acute lymphoblastic leukaemia. *Lancet*. 2008; 371: 1030-1043.

12. Fielding A. The treatment of adults with acute lymphoblastic leukemia. *Hematology Am Soc Hematol Educ Program*. 2008; 381-389.

13. Litzow MR. Evolving paradigms in the therapy of Philadelphia-chromosome-negative acute lymphoblastic leukemia in adults. *Hematology Am Soc Hematol Educ Program*. 2009: 362-70.

14. Pulte D, Gondos A, Brenner H. Improvement in survival in younger patients with acute lymphoblastic leukemia from the 1980s to the early 21st century. *Blood*. 2009; 113:1408-1411.

15. Cornelissen JJ, van der Holt B, Verhoef GE, et al. Myeloablative allogeneic versus autologous stem cell transplantation in adult patients with acute lymphoblastic leukemia in first remission: a prospective sibling donor versus no-donor comparison. *Blood.* 2009; 113: 1375–1382.

16. Harned TM, Gaynon P. Relapsed acute lymphoblastic leukemia: current status and future opportunities. *Curr Oncol Rep.* 2008; 10: 453–458.

17. Pui CH. Acute lymphoblastic leukemia. In: Pui CH, editor. Childhood leukemias. New York: Cambridge University Press; 2006; p. 439–72.

18. Plum J, De Smedt M, Leclercq G, et al. Interleukin-7 is a critical growth factor in early human T-cell development. *Blood.* 1996; 88: 4239–4245.

19. Graux C, Cools J, Michaux L, et al. Cytogenetics and molecular genetics of T-cell acute lymphoblastic leukemia: from thymocyte to lymphoblast. *Leukemia.* 2006; 20: 1496–510.

20. Klein L, Hinterberger M,Wirnsberger G, et al. Antigen presentation in the thymus for positive selection and central tolerance induction. *Nat Rev Immunol.* 2009; 9:833–44.

21. Murre C. Intertwining proteins in thymocyte development and cancer. *Nat Immunol.* 2000; 1:97–8.

22. Bene MC, Castoldi G, Knapp W, et al. Proposals for the immunological classification of acute leukemias. European group for the immunological characterization of leukemias (EGIL). *Leukemia.* 1995; 9(10):1783–6.

23. Asnafi V, Beldjord K, Libura M, et al. Age-related phenotypic and oncogenic differences in T-cell acute lymphoblastic leukemias may reflect thymic atrophy. *Blood.* 2004; 104(13):4173–80.

24. Aifantis I, Raetz E, Buonamici S. Molecular pathogenesis of T-cell leukaemia and lymphoma. *Nat Rev Immunol*. 2008 May; 8(5):380-90.

25. van Grotel M, Meijerink JP, van Wering ER, et al. Prognostic significance of molecular-cytogenetic abnormalities in pediatric T-ALL is not explained by immunophenotypic differences. *Leukemia*. 2008; 22(1):124–31.

26. Graux C, Cools J, Michaux L. Cytogenetics and molecular genetics of T-cell acute lymphoblastic leukemia: from thymocyte to lymphoblast. *Leukemia*. 2006; 20:1496–1510.

27. Bhojwani D, Howard SC, Pui CH. High-risk childhood acute lymphoblastic leukemia. *Clin Lymphoma Myeloma*. 2009; 9 Suppl 3:S222-30.

28. Krivtsov AV, Armstrong SA. 2007. MLL translocations, histone modifications and leukaemia stem-cell development. *Nat Rev Cancer*. 7:823–33.

29. Meyer C, Schneider B, Jakob S, Strehl S, et al. The MLL recombinome of acute leukemias. *Leukemia.* 2006; 20:777–84.

30. Bash RO, Hall S, Timmons CF, et al. Does activation of the TAL1 gene occur in a majority of patients with T-cell acute lymphoblastic leukemia? A pediatric oncology group study. *Blood.* 1995; 86:666–76.

31. Graux C, Cools J, Melotte C, et al. Fusion of NUP214 to ABL1 on amplified episomes in T-cell acute lymphoblastic leukemia. *Nat Genet.* 2004; 36:1084-9.

32. De Keersmaecker K, Graux C, Odero MD, et al. Fusion of EML1 to ABL1 in T cell acute lymphoblastic leukemia with cryptic t(9; 14)(q34; q32). *Blood.* 2005; 105:4849-52.

33. Sulong S, Moorman AV, Irving JA, et al. A comprehensive analysis of the CDKN2A gene in childhood acute lymphoblastic leukemia reveals genomic deletion, copy number neutral loss of heterozygosity, and association with specific cytogenetic subgroups. *Blood.* 2009; 113:100–7.

34. Van Vlierberghe P, van Grotel M, Beverloo HB, et al. The cryptic chromosomal deletion del(1 1)(p12p13) as a new activation mechanism of LMO2 in pediatric T-cell acute lymphoblastic leukemia. *Blood*. 2006; 108: 3520–9.

35. Mullighan CG, Collins-Underwood JR, Phillips LA, et al. Rearrangement of CRLF2 in B-progenitor- and Down syndrome-associated acute lymphoblastic leukemia. *Nat Genet.* 2009; 41:1243–6.

36. O'Neil J, Grim J, Strack P, et al. FBW7 mutations in leukemic cells mediate NOTCH pathway activation and resistance to gamma-secretase inhibitors. *J Exp Med.* 2007; 204: 1813–24.

37. Weng AP, Ferrando AA, Lee W, et al. Activating mutations of NOTCH1 in human T cell acute lymphoblastic leukemia. *Science.* 2004; 306:269–71.

38. Harrison CJ, Foroni L.Cytogenetics and molecular genetics of acute lymphoblastic leukemia. *Rev Clin Exp Hematol*. 2002; 6(2):91-113.

39. Kraszewska MD, Dawidowska M, Szczepański T, et al. T-cell acute lymphoblastic leukaemia: recent molecular biology findings. *Br J Haematol*. 2012; 156(3):303-15.

40. Ellisen LW, Bird J, West DC, et al. TAN-1, the human homolog of the Drosophila notch gene, is broken by chromosomal translocations in T lymphoblastic neoplasms. *Cell.*1991; 66:649–61.

41. Weng AP, Ferrando AA, Lee W, et al. Activating mutations of NOTCH1 in human T cell acute lymphoblastic leukemia. *Science*. 2004; 306:269–71.

42. O'Neil J, Grim J, Strack P, et al. FBW7 mutations in leukemic cells mediate NOTCH pathway activation and resistance to gamma-secretase inhibitors. *J Exp Med.* 2007; 204:1813–24.

43. Mavrakis KJ, Van Der Meulen J, Wolfe AL, et al. A cooperative microRNA-tumor suppressor gene network in acute T-cell lymphoblastic leukemia (T-ALL). *Nat Genet.* 2011; 43(7):673-8.

44. Roman-Gomez J, Cordeu L, Agirre X, et al. Epigenetic regulation of Wnt-signaling pathway in acute lymphoblastic leukemia. *Blood.* 2007; 109:3462–69.

45. Omura-Minamisawa M, Diccianni MB, Batova A, et al. Universal inactivation of both p16 and p15 but not downstream components is an essential event in the pathogenesis of T cell acute lymphoblastic leukemia. *Clin Cancer Res.* 2000; 6:1219–28.

46. Kraszewska MD, Dawidowska M, Szczepanski T, et al. T-cell acute lymphoblastic leukaemia: recent molecular biology findings. *British Journal of Haematology*. 2011; 156: 303–315.

47. Roman-Gomez J, Jimenez-Velasco A, Agirre X, et al. Lack of CpG island methylator phenotype defines a clinical subtype of T-cell acute lymphoblastic leukemia associated with good prognosis. *Journal of Clinical Oncology.* 2005; 23: 7043–7049.

48. Toyota M, Ahuja N, Ohe-Toyota M, et al. (1999) CpG island methylator phenotype in colorectal cancer. *Proceedings of the National Academy of Sciences of the United States of America*. 1999; 96: 8681–8686.

49. Roman-Gomez, J, Jimenez-Velasco A, Agirre X, et al. Lack of CpG island methylator phenotype defines a clinical subtype of T-cell acute lymphoblastic leukemia associated with good prognosis. *Journal of Clinical Oncology.* 2005; 23: 7043–7049.

50. Pui CH, Relling MV, Evans WE. Role of pharmacogenomics and pharmacodynamics in the treatment of acute lymphoblastic leukaemia. *Best Pract Res Clin Haematol.* 2002; 15(4):741–56.

51. Yang JJ, Cheng C, Yang W, et al. Genome-wide interrogation of germline genetic variation associated with treatment response in childhood acute lymphoblastic leukemia. *JAMA.* 2009; 301(4):393–403.

52. Faderl S, Jeha S, Kantarjian HM. The biology and therapy of adult acute lymphoblastic leukemia. *Cancer.* 2003; 98(7):1337–54.

53. Schultz KR, Pullen DJ, Sather HN, et al. Risk- and response-based classification of childhood B precursor acute lymphoblastic leukemia: a combined analysis of prognostic markers from the Pediatric Oncology Group (POG) and Children's Cancer Group (CCG). *Blood.* 2007; 109:926–35.

54. Carroll WL, Hunger SP, Borowitz MJ, et al. Risk-adapted therapy for children with acute lymphoblastic leukemia (ALL): the Children's Oncology Group (COG) approach. *Ann Hematol.* 2008; 87(suppl 1a):S42–S44.

55. Lugthart S, Cheok MH, den Boer ML, et al. Identification of genes associated with chemotherapy cross resistance and treatment response in childhood acute lymphoblastic leukemia. *Cancer Cell.* 2005; 7:375-386.

56. Golub TR, Slonim DK, Tamayo P, et al. Molecular classification of cancer: class discovery and class prediction by gene expression monitoring. *Science*. 1999; 286(5439):531-537.

57. Pui CH, Relling MV, Downing JR. Acute lymphoblastic leukemia. *N Engl J Med.* 2004; 350: 1535–1548.

58. Tissing WJ, Meijerink JP, den Boer ML, et al. Molecular determinants of glucocorticoid sensitivity and resistance in acute lymphoblastic leukemia. *Leukemia.* 2003; 17: 17–25.

59. Dordelmann M, Reiter A, Borkhardt A, et al. Prednisone response is the strongest predictor of treatment outcome in infant acute lymphoblastic leukemia. *Blood.* 1999; 94: 1209–1217.

60. Schrappe M, Arico M, Harbott J, et al. Philadelphia chromosome-positive (Ph+) childhood acute lymphoblastic leukemia: good initial steroid response allows early prediction of a favorable treatment outcome. *Blood.* 1998; 92: 2730–2741.

61. Klumper E, Pieters R, Veerman AJ, et al. In vitro cellular drug resistance in children with relapsed/refractory acute lymphoblastic leukemia. *Blood.* 1995; 86: 3861–3868.

62. Hongo T, Yajima S, Sakurai M, et al. In vitro drug sensitivity testing can predict induction failure and early relapse of childhood acute lymphoblastic leukemia. *Blood.* 1997; 89: 2959–2965.

63. Kaspers GJ, Wijnands JJ, Hartmann R, et al. Immunophenotypic cell lineage and in vitro cellular drug resistance in childhood relapsed acute lymphoblastic leukaemia. *Eur J Cancer.* 2005; 41: 1300–1303.

64. Inaba H, Pui CH. Glucocorticoid use in acute lymphoblastic leukaemia. *Lancet Oncol.* 2010; 11: 1096–106.

65. Meikle AW, Tyler FH. Potency and duration of action of glucocorticoids. Effects of hydrocortisone, prednisone and dexamethasone on human pituitary-adrenal function. *Am J Med.* 1977; 63: 200–07.

66. Rose LI, Saccar C. Choosing corticosteroid preparations. *Am Fam Physician.* 1978; 17: 198–204.

67. Kaspers GJ, Veerman AJ, Popp-Snijders C, et al. Comparison of the antileukemic activity in vitro of dexamethasone and prednisolone in childhood acute lymphoblastic leukemia. *Med Pediatr Oncol.* 1996; 27: 114–21.

68. Balis FM, Lester CM, Chrousos GP, Heideman RL, Poplack DG. Differences in cerebrospinal fluid penetration of corticosteroids: possible relationship to the prevention of meningeal leukemia. *J Clin Oncol.* 1987; 5: 202–07.

69. Jones B, Freeman AI, Shuster JJ, et al. Lower incidence of meningeal leukemia when prednisone is replaced by dexamethasone in the treatment of acute lymphocytic leukemia. *Med Pediatr Oncol.* 1991; 19: 269–75.

70. Veerman AJ, Hahlen K, Kamps WA, et al. High cure rate with a moderately intensive treatment regimen in non-high-risk childhood acute lymphoblastic leukemia. Results of protocol ALL VI from the Dutch Childhood Leukemia Study Group. *J Clin Oncol.* 1996; 14: 911–18.

71. van der Does-van den Berg A, van Wering ER, Suciu S, et al. Effectiveness of rubidomycin in induction therapy with vincristine, prednisone, and L-asparaginase for standard risk childhood acute lymphocytic leukemia: results of a Dutch phase III study (ALL V). A report on behalf of the Dutch Childhood Leukemia Study Group (DCLSG). *Am J Pediatr Hematol Oncol.* 1989; 11:125–33.

72. Schrappe M, Zimmermann M, Moricke A, et al. Dexamethasone in induction can eliminate one third of all relapses in childhood acute lymphoblastic leukemia (ALL): results of an international randomized trial in 3655 Patients (Trial AIEOP-BFM ALL 2000). 50th ASH Annual Meeting and Exposition, San Francisco, CA, Dec 6–9, 2008; 112: 7 (abstr).

73. Vrooman LM, Neuberg DS, Stevenson KE, et al. Dexamethasone and individualized asparaginase dosing are each associated with superior event-free survival in childhood acute lymphoblastic leukemia: results from DFCI-ALL Consortium Protocol 00-01. 51st ASH Annual Meeting and Exposition, New Orleans, LA, Dec 5–8, 2009; 114: 321 (abstr).

74. Silverman LB, Gelber RD, Dalton VK, et al. Improved outcome for children with acute lymphoblastic leukemia: results of Dana-Farber Consortium Protocol 91-01. *Blood.* 2001; 97: 1211–18.

75. Strauss AJ, Su JT, Dalton VM, et al. Bony morbidity in children treated for acute lymphoblastic leukemia. *J Clin Oncol.* 2001; 19: 3066–72.

76. Mitchell CD, Richards SM, Kinsey SE, et al. Benefit of dexamethasone compared with prednisolone for childhood acute lymphoblastic leukaemia: results of the UK Medical Research Council ALL97 randomized trial. *Br J Haematol.* 2005; 129: 734–45.

77. Wolkowitz OM. Prospective controlled studies of the behavioral and biological effects of exogenous corticosteroids. *Psychoneuroendocrinology.* 1994; 19: 233–55.

78. Waber DP, Carpentieri SC, Klar N, et al. Cognitive sequelae in children treated for acute lymphoblastic leukemia with dexamethasone or prednisone. *J Pediatr Hematol Oncol.* 2000; 22: 206–13.

79. Kadan-Lottick NS, Brouwers P, Breiger D, et al. A comparison of neurocognitive functioning in children previously randomized to dexamethasone or prednisone in the treatment of childhood acute lymphoblastic leukemia. *Blood.* 2009; 114: 1746–52.

80. Bostrom BC, Sensel MR, Sather HN, et al. Dexamethasone versus prednisone and daily oral versus weekly intravenous mercaptopurine for patients with standard-risk acute lymphoblastic leukemia: a report from the Children's Cancer Group. *Blood.* 2003; 101: 3809–17.

81. Druker BJ, Talpaz M, Resta DJ, et al: Efficacy and safety of a specific inhibitor of the BCR-ABL tyrosine kinase in chronic myeloid leukemia. *N Engl J Med.* 2001; 344:1031-1037.

82. Nagar B, Bornmann WG, Pellicena P, et al. Crystal structures of the kinase domain of c-Abl in complex with the small molecule inhibitors PD173955 and imatinib (STI-571). *Cancer Res.* 2002; 62:4236–43.

83. Schindler T, Bornmann W, Pellicena P, et al. Structural mechanism for STI-571 inhibition of abelson tyrosine kinase. *Science.* 2000; 289:1938–42.

84. Druker BJ. Imatinib as a paradigm of targeted therapies. *Adv Cancer Res.* 2004; 91:1-30, 2004.

85. Uckun FM, Nachman JB, Sather HN, et al. Clinical significance of Philadelphia chromosome positive pediatric acute lymphoblastic leukemia in the context of contemporary intensive therapies: a report from the Children's Cancer Group. *Cancer.* 1998; 83:2030–9.

86. Druker BJ, Sawyers CL, Kantarjian H, et al. Activity of a specific inhibitor of the BCR-ABL tyrosine kinase in the blast crisis of chronic myeloid leukemia and acute lymphoblastic leukemia with the Philadelphia chromosome. *N Engl J Med.* 2001; 344:1038–42.

87. Ottmann OG, Druker BJ, Sawyers CL, et al. A phase 2 study of imatinib in patients with relapsed or refractory Philadelphia chromosome-positive acute lymphoid leukemias. *Blood.* 2002; 100:1965-1971.

88. Armstrong SA, Look AT. Molecular genetics of acute lymphoblastic leukemia. *J Clin Oncol*. 2005; 23:6306–15.

89. Wassmann B, Pfeifer H, Goekbuget N, et al. Alternating versus concurrent schedules of imatinib and chemotherapy as front-line therapy for Philadelphia-positive acute lymphoblastic leukemia (Ph+ ALL). *Blood.* 2006; 108:1469–77.

90. Gorre ME, Mohammed M, Ellwood K, et al. Clinical resistance to STI-571 cancer therapy caused by BCR-ABL gene mutation or amplification. *Science.* 2001; 293:876–80.

91. Shah NP, Nicoll JM, Nagar B, et al. Multiple BCR-ABL kinase domain mutations confer polyclonal resistance to the tyrosine kinase inhibitor imatinib (STI571) in chronic phase and blast crisis chronic myeloid leukemia. *Cancer Cell.* 2002; 2:117–25.

92. Pfeifer H, Wassmann B, Pavlova A, et al. Kinase domain mutations of BCR-ABL frequently precede imatinib-based therapy and give rise to relapse in patients with de novo Philadelphia-positive acute lymphoblastic leukemia (Ph+ ALL). *Blood.* 2007; 110:727–34.

93. Hu Y, Liu Y, Pelletier S, et al. Requirement of Src kinases Lyn, Hck and Fgr for BCR-ABL1-induced B-lymphoblastic leukemia but not chronic myeloid leukemia. *Nat Genet.* 2004; 36:453–61.

94. Shah NP, Kantarjian HM, Kim DW, et al. Intermittent target inhibition with dasatinib 100 mg once daily preserves efficacy and improves tolerability in imatinib-resistant and -intolerant chronic-phase chronic myeloid leukemia. *J Clin Oncol.* 2008; 26:3204–12.

95. Porkka K, Koskenvesa P, Lundan T, et al. Dasatinib crosses the blood-brain barrier and is an efficient therapy for central nervous system Philadelphia chromosome-positive leukemia. *Blood.* 2008; 112:1005–12.

96. Deininger MW. Nilotinib. *Clin Cancer Res.* 2008; 14:4027–31.

97. Chiaretti S, Foà R.T-cell acute lymphoblastic leukemia. *Haematologica.* 2009; 94(2):160-2.

98. Hoffbrand AV, Moss PAH, Pettit JE. "Essential Haematology", Blackwell, 5th ed., 2006.

99. Lo NL, Cazzaniga G, Di Cataldo A, et al. Clonal stability in children with acute lymphoblastic leukemia (ALL) who relapsed five or more years after diagnosis. *Leukemia.* 1999; 13(2):190–5.

100. Chen W, Karandikar NJ, McKenna RW, et al. Stability of leukemia-associated immunophenotypes in precursor B-lymphoblastic leukemia/lymphoma: a single institution experience. *Am J Clin Pathol.* 2007; 127(1):39–46.

101. van Wering ER, Beishuizen A, Roeffen ET, et al. Immunophenotypic changes between diagnosis and relapse in childhood acute lymphoblastic leukemia. *Leukemia.* 1995; 9(9):1523–33.

102. Fielding AK, Richards SM, Chopra R, et al. Outcome of 609 adults after relapse of acute lymphoblastic leukemia (ALL); an MRC UKALL12/ECOG 2993 study. *Blood.* 2007; 109: 944–950.

103. Tavernier E, Boiron JM, Huguet F, et al. Outcome of treatment after first relapse in adults with acute lymphoblastic leukemia initially treated by the LALA-94 trial. *Leukemia*. 2007; 21:1907– 1914.

104. Hoelzer D, Gokbuget N, Ottmann O, et al. Acute lymphoblastic leukemia. *Hematology Am Soc Hematol Educ Program*. 2002; 162–192.

105. Oudot C, Auclerc MF, Levy V, et al. Prognostic factors for leukemic induction failure in children with acute lymphoblastic leukemia and outcome after salvage therapy: the FRALLE 93 study. *J Clin Oncol.* 2008; 26:1496–503.

106. Cave H, van der Werff ten Bosch J, Suciu S, et al. Clinical significance of minimal residual disease in childhood acute lymphoblastic leukemia. European Organization for Research and Treatment of Cancer—Childhood Leukemia Cooperative Group. *N Engl J Med.* 1998; 339:591-598.

107. Van Dongen JJM, Seriu T, Panzer-Grumayer ER, et al. Prognostic value of minimal residual disease in acute lymphoblastic leukaemia in childhood. *Lancet.* 1998; 352: 1731–1738.

108. Pui CH, Relling MV, Sandlund JT, et al. Rationale and design of Total Therapy Study XV for newly diagnosed childhood acute lymphoblastic leukemia. *Ann Hematol.* 2004; 83(Suppl 1):S124–6.

109. Nachman JB, Sather HN, Sensel MG, et al. Augmented post-induction therapy for children with high risk acute lymphoblastic leukemia and a slow response to initial therapy. *N Engl J Med.* 1998; 338:1663–71.

110. Szczepański T.Why and how to quantify minimal residual disease in acute lymphoblastic leukemia? *Leukemia*. 2007; 21(4):622-6.

111. Pongers-Willemse MJ, Seriu T, Stolz F, et al. Primers and protocols for standardized MRD detection in ALL using immunoglobulin and T cell receptor gene rearrangements and TAL1 deletions as PCR targets. Report of the BIOMED-1 Concerted Action: investigation of minimal residual disease in acute leukemia. *Leukemia.* 1999; 13: 110–118.

112. Van Dongen JJM, Langerak AW, Bruggemann M, et al. Design and standardization of PCR primers and protocols for detection of clonal immunoglobulin and T-cell receptor gene recombinations in suspect lymphoproliferations: report of the BIOMED-2 Concerted Action BMH4-CT98-3936. *Leukemia.* 2003; 17: 2257–2317.

113. Carroll WL, Bhojwani D, Min DJ, et al. Pediatric acute lymphoblastic leukemia. *Hematology Am Soc Hematol Educ Program*. 2003:102-31.

114. Szczepanski T, Willemse MJ, van Wering ER, et al. Precursor-B-ALL with DH-JH gene rearrangements have an immature immunogenotype with a high frequency of oligoclonality and hyperdiploidy of chromosome 14. *Leukemia.* 2001; 15: 1415–1423.

115. De Haas V, Verhagen OJ, von dem Borne AE, et al. Quantification of minimal residual disease in children with oligoclonal B-precursor acute lymphoblastic leukemia indicates that the clones that grow out during relapse already have the slowest rate of reduction during induction therapy. *Leukemia.* 2001; 15: 134–140.

116. Coustan-Smith E, Sancho J, Hancock ML, et al. Clinical importance of minimal residual disease in childhood acute lymphoblastic leukemia. *Blood*. 2000; 96(8):2691-2696.

117. Eapen M, Rubinstein P, Zhang MJ, et al. Outcomes of transplantation of unrelated donor umbilical cord blood and bone marrow in children with acute leukaemia: a comparison study. *Lancet.* 2007; 369:1947–54.

118. Kurtzberg J, Prasad VK, Carter SL, et al. Results of the Cord Blood Transplantation Study (COBLT): clinical outcomes of unrelated donor umbilical cord blood transplantation in pediatric patients with hematologic malignancies. *Blood.* 2008; 112:4318–27.

119. Schrauder A, Reiter A, Gadner H, et al. Superiority of allogeneic hematopoietic stem-cell transplantation compared with chemotherapy alone in high-risk childhood T-cell acute lymphoblastic leukemia: results from ALL-BFM 90 and 95. *J Clin Oncol.* 2006; 24:5742–9.

120. Balduzzi A, Valsecchi MG, Uderzo C, et al. Chemotherapy versus allogeneic transplantation for very high- risk childhood acute lymphoblastic leukaemia in first complete remission: comparison by genetic randomisation in an international prospective study. *Lancet.* 2005; 366:635–42.

121. Arico M, Valsecchi MG, Camitta B, et al. Outcome of treatment in children with Philadelphia chromosome-positive acute lymphoblastic leukemia. *N Engl J Med.* 2000; 342:998–1006.

122. Thomas X, Boiron JM, Huguet F, et al. Outcome of treatment in adults with acute lymphoblastic leukemia: analysis of the LALA-94 trial. *J Clin Oncol.* 2004; 22:4075-4086.

123. Yanada M, Matsuo K, Suzuki T, et al. Allogeneic hematopoietic stem cell transplantation as part of postremission therapy improves survival for adult patients with high-risk acute lymphoblastic leukemia: a metaanalysis. *Cancer.* 2006; 106:2657-2663.

124. Esperou H, Boiron JM, Cayuela JM, et al. A potential graft-versus-leukemia effect after allogeneic hematopoietic stem cell transplantation for patients with Philadelphia chromosome-positive acute lymphoblastic leukemia: results from the French Bone Marrow Transplantation Society. *Bone Marrow Transplant.* 2003; 31:909–18.

125. Pui CH, Gaynon PS, Boyett JM, et al. Outcome of treatment in childhood acute lymphoblastic leukaemia with rearrangements of the 11q23 chromosomal region. *Lancet.* 2002; 359:1909–15.

126. Graux C. Biology of acute lymphoblastic leukemia (ALL): Clinical and therapeutic relevance. *Transfusion and Apheresis Science* (2011) 44: 183–189.

127. Mohty M, Labopin M, Tabrizzi R, et al. Reduced intensity conditioning allogeneic stem cell transplantation for adult patients with acute lymphoblastic leukemia: a retrospective study from the European Group for Blood and Marrow Transplantation. *Haematologica.* 2008; 93:303-306.

128. Koch U, Radtke F. Mechanisms of T cell development and transformation. *Annu Rev Cell Dev Biol.* 2011; 27:539-62.

129. Graux C, Cools J, Michaux L, et al. Cytogenetics and molecular genetics of T-cell acute lymphoblastic leukemia: from thymocyte to lymphoblast. *Leukemia.* 2006; 9:1496-510.

130. Oeffinger KC, Mertens AC, Sklar CA, et al. Chronic health conditions in adult survivors of childhood cancer. *N Engl J Med*. 2006; 355(15):1572-82.

Table 1.1

WHO 2008 classification of T-cell neoplasms.
Adapted from de Leval et al. (2009).[4]

Category	Classifications	Subclassifications
Precursor T-cell neoplasms	Precursor T acute lymphoblastic leukemia (T-ALL/lymphoma, T-LBL)	
Mature T-cell neoplasms	Leukemic or disseminated	T_cell prolymphocytic leukemia
		T-cell large granular lymphocytic leukemia Adult T-cell lymphoma/leukemia (HTLV1-positive) Systemic EBV-positive T-cell lymphoproliferative disorders of childhood
	Extranodal-cutaneous	Mycosis fungoides Sezary syndrome Primary cutaneous CD30+ lymphoproliferative disorders Primary cutaneous anaplastic large cell lymphoma Lymphomatoid papulosis Subcutaneous panniculitis-like T-cell lympooma Primary cutaneous gamma-delta T-cell lymphoma Primary cutaneous aggressive epidermotropic CD8+ cytotoxic T-cell lymphoma Primary cutaneous small/medium CD4+ T-cell lymphoma
	Nodal	Angioimmunoblastic T-cell lyumphoma (AITL) Anaplastic large cell lymphoma, ALK-positive Anaplastic large cell lymphoma, ALK-negative Peripheral T-cell lymphoma, not otherwise specified (PTCL, NOS)

Table 1.2

Stages of T cell development correlate with specific locations in the thymus, distinct cell-surface phenotypes, requirements for Notch signals, and TCR rearrangement.
Adapted from Pui et al. (2002).[125]

Developmental stage	Cell surface phenotype	Location	Notch signal	TCRβ rearrangement	TCRα rearrangement
ETP	CD117hiCD44hiCD25−	CMJ	+++	Germline	Germline
DN1	CD24−/loCD27hi				
DN2a	CD117hiCD44hiCD25+	Cortex	+	Germline	Germline
	CD24hiCD27hi				
DN2b	CD117intCD44hiCD25+	Cortex	+	DJH	Germline
	CD24hiCD27int				
DN3a	CD117−/loCD44−/loCD25+	SCZ	+++	DJH,VDJH	Germline
	CD24hiCD27−/lo				
DN3b	CD117−/loCD44−/loCD25int	SCZ	+++	VDJ+	Germline
	CD24hiCD27hi				
DN4	CD117−/loCD44−/loCD25−/lo	SCZ	+	VDJ+	Germline
	CD24hiCD27hi				
DP	CD4+CD8+TCRβint	Cortex	–	VDJ+	VJ

Abbreviations: CMJ, corticomedullary junction; D, diverse; DN, double negative; DP, double positive; ETP, early thymic progenitor; H, heavy chain; J, joining; SCZ, subcapsular zone; TCR, T cell receptor; V, variable. The single + for Notch signal indicates Notch1 receptor expression; however, a specific function or requirement has not been described. The triple +++ for Notch signal indicates a requirement for Notch.

Table 1.3

EGIL classification system for T-ALL
Adapted from Bene et al. (1995).[22]

T-ALL Subtype	CD1a	CD2	cCD3	sCD3	CD4	CD5	CD7	CD8	CD34
Pro-T	-	-	+	-	-	-	+	-	+
Pre-T	-	+	+	-	-	±	-	-	±
Cortical T	+	+	+	-	+	±	+	+	-
Medullary T	-	+	+	+	±	±	+	±	-

Table 1.4

The TCR system for classifying T-ALL
Adapted from Asnafi et al. (2004).[23]

Stage:	Markers:
Immature (IM)	Cytoplasmic-beta$^-$ (Cytß$^-$), sCD3$^-$, TCRαß$^-$ or TCRγδ$^-$
Pre-αß	Cytß$^+$, sCD3$^-$, TCRαß$^-$ or TCRγδ$^-$
TCRαß	sCD3$^+$, TCRαß$^+$
TCRγδ	sCD3$^+$, TCRαß$^+$

Table 1.5

Most frequent genetic abnormalities in T-ALL
Adapted from Graux (2011).[126]

(Cyto) genetic changes:	Genes:	Remarks/prognosis:
TCR receptor genes translocations (14q11 & 7q34)		
t(10;14)(q24;q11)	TLX1;TCRA/D	Favorable
t(11;14)(p15;q11)	LMO1;TCR	
t(11;14(p13;q11)	LMO2;TCR	
t(1;14)(p32;q11)	TAL1;TCR	
inv(7)(p15q32)	HOXA;TCRB	
t(7;19)(q34;p13)	LYL1;TCRB	
t(5;14)(q35;q32)	TLX3;BCL11B	Poor?
Fusion genes		
del1(p32) interstitial	SIL-TAL1	
9(q34) episomes	NUP214-ABL1	
t(10;11)(p13;q14)	CALM-AF10	
t(11;19)(q23;p13)	MLL-ENL	
Deletion/amplification		
del(9)(p21)	CDKN2A	
del(6q)	Unknown	
dup(6)(q23)	MYB	
Mutations		
	NOTCH1/FBW7	Very frequent (>80%)
	JAK1, PTEN, RAS, FLT3, PHF6	

Table 1.6
Common fusion proteins in T-ALL
Adapted from Graux et al.(2006).[26]

	Involved gene(s)	Protein(s)	Normal thymic expression	Function of fusion gene or expressed oncogene	Frequency (%)	
					Children	Adults
Formation of fusion genes						
1p32 deletion (cryptic)	*SIL/*	Proline-rich extensin	Very early stages	Transcription factor	9–30	Decrease with age
	TAL1	bHLH type II				
t(10;11)(p13;q14) (often cryptic)	*CALM/*	ENTH motif containing	Ubiquitous		10	
	AF10	Zinc fingers/leucine zipper containing	Ubiquitous	Transcription factor		
t(11;19)(q23;p13)	*MLL/*	Mammalian homologue of *Drosophila trithorax*		Transcriptional regulator during embryogenesis and hematopoiesis	8 (all MLL)	
	ENL	Nuclear targeting sequence containing				
t(6;11)(q27;q23)	*MLL/*	Cfr supra		Cfr supra		
	AF6	GLGF motif containing				
t(10;11)(p13;q23)	*MLL/*	Cfr supra		Cfr supra		
	AF10	Zinc fingers/leucine zipper containing	Ubiquitous			
t(X;11)(q13;q23)	*MLL/*	Cfr supra		Cfr Supra		
	AFX1	Forkhead family				
t(4;11)(q21;q23)	*MLL/*	Cfr supra		Cfr Supra		
	AF4	Nuclear targeting sequence containing				
t(9;9)(q34;q34) (episomal or hsr)	*NUP214/*	Nuclear pore complex component			<6	
	ABL1	Intracellular tyrosine kinase	Yes	Signal transduction		
t(9;14)(q34;q32) (cryptic)	*EML1/*	Echinoderm microtubule-associated			<1	
	ABL1	Intracellular tyrosine kinase	Yes	Signal transduction		
t(9;12)(q34;p13)	*ETV6(TEL)/*	ETS DNA binding containing			<1	
	ABL1	Intracellular tyrosine kinase	Yes	Signal transduction		
t(9;12)(p24;p13)	*ETV6(TEL)/*	ETS DNA binding containing			<1	
	JAK2	Intracellular tyrosine kinase	Yes	Signal transduction		
t(9;22)(q34;q11)	*BCR/*	Serine-threonine kinase			<1	
	ABL1	Intracellular tyrosine kinase	Yes	Signal transduction		
t(4;11)(q21;p15)	*NUP98/*	Nuclear pore complex component			<1	
	RAP1GDS1	Cytoplasmic		?		

Table 1.7

Relative long-term side effect risks of adult survivors of childhood cancers
Adapted from Oeffinger et al. (2006).[130]

Condition	%Survivors (N = 10,397)	%Siblings (N = 3034)	Relative Risk (95% CI)
Major joint replacement	1.61	0.03	54.0 (7.6–386.3)
Congestive heart failure	1.24	0.10	15.1 (4.8–47.9)
Second malignant neoplasm	1.24	0.33	14.8 (7.2–30.4)
Cognitive dysfunction, severe	0.65	0.10	10.5 (2.6–43.0)
Coronary artery disease	1.11	0.20	10.4 (4.1–25.9)
Cerebrovascular accident	1.56	0.20	9.3 (4.1–21.2)
Renal failure or dialysis	0.52	0.07	8.9 (2.2–36.6)
Hearing loss not corrected by aid	1.96	0.36	6.3 (3.3–11.8)
Legally blind or loss of an eye	2.92	0.69	5.8 (3.5–9.5)
Ovarian failure	2.79	0.99	3.5 (2.7–5.2)

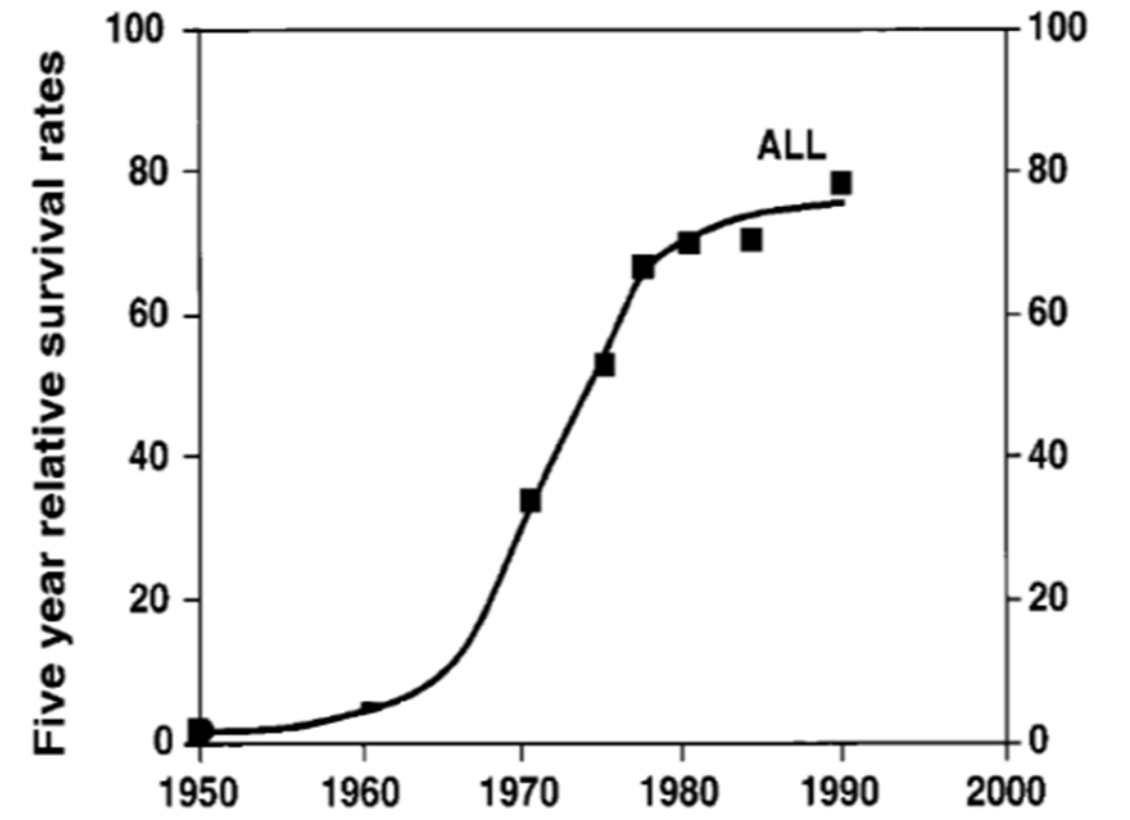

Figure 1.1. Five-year pediatric ALL survival rates over the past 60 years. Adapted from Koch et al. (2011).[128]

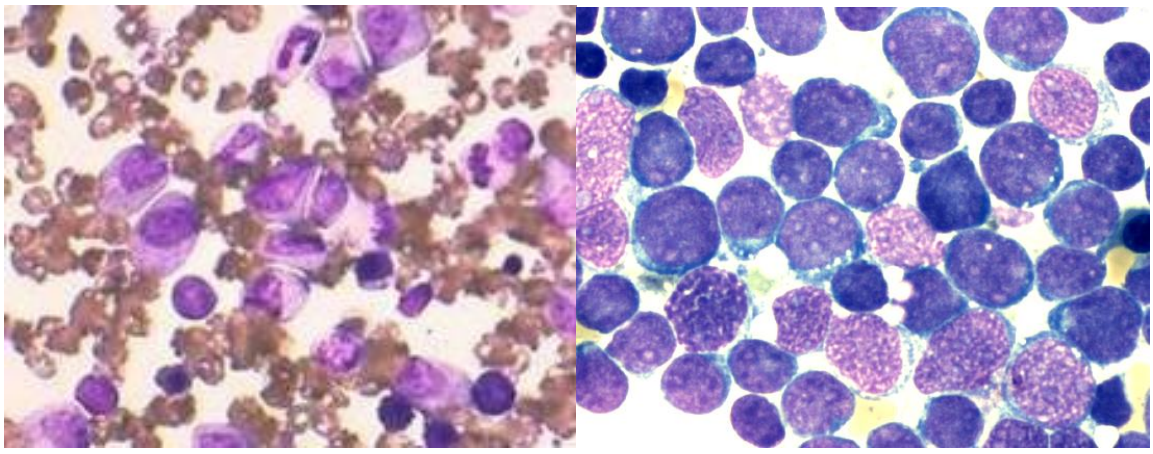

A. Normal healthy bone marrow **B.** Bone marrow from a T-ALL patient

Figure 1.2. Comparison of normal and T-ALL leukemic bone marrow. Adapted from Graux et al. (2006).[129]

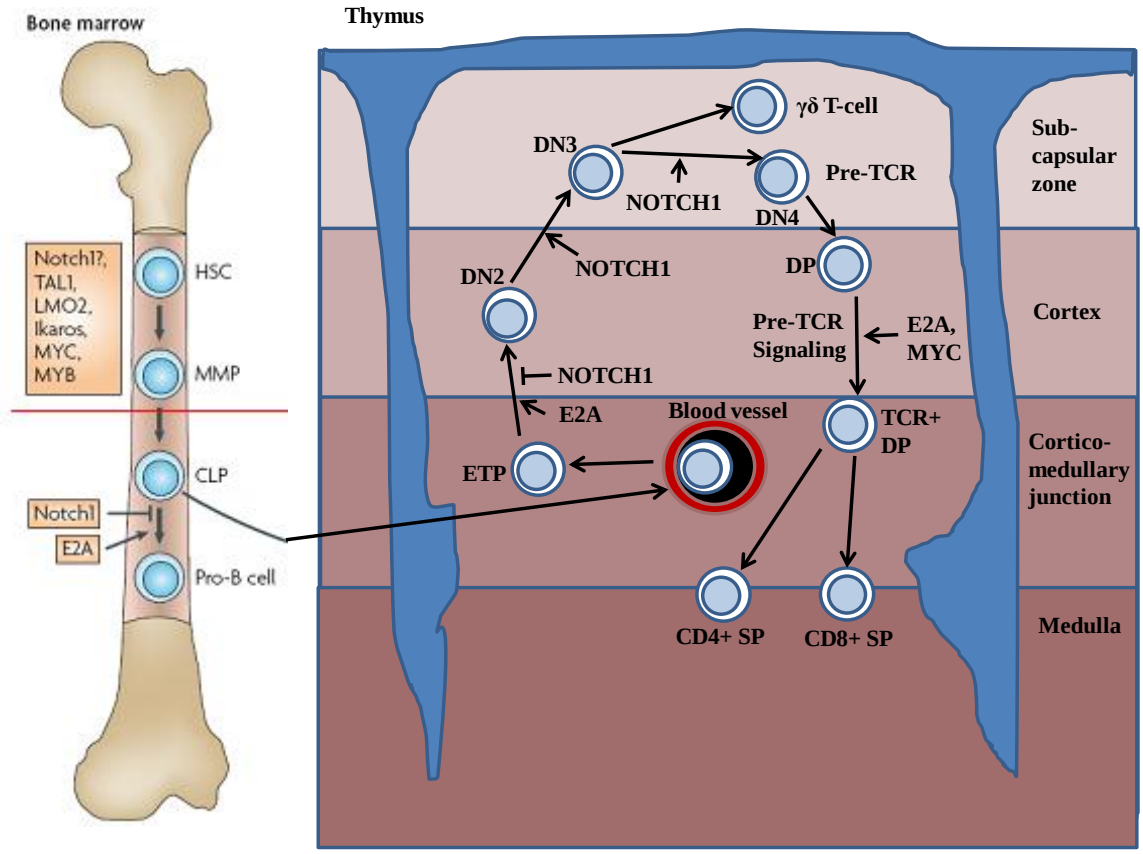

Figure 1.3. Stages of haematopoiesis and T‑cell development and T‑cell-leukaemia-related oncogenes. Bone-marrow haematopoietic stem cells (HSCs) exit the quiescent 'niche' and differentiate to become multipotent progenitors (MPPs). MPPs further commit to the lymphoid lineage generating common lymphoid progenitors (CLPs). Several progenitor subsets (including MPPs and CLPs) have been suggested to represent the progenitor of thymic pro‑T cells. These subsets migrate to the thymus (as early T‑cell-lineage progenitors (ETPs) and commit to the T‑cell lineage, progressing through the double negative (DN; CD4–CD8–) stages, DN2, DN3 and DN4. Upon successful recombination at the T‑cell receptor β (*TCRB*) locus, pre‑T cells acquire surface expression of the pre-TCR that promotes differentiation to the DN4 stage. Pre-TCR-selected cells reach the double positive (DP; CD4+CD8+) stage, at which point they are subjected to the processes of positive and negative selection. Selected cells then exit the thymus as single positive (SP) CD4+ or CD8+ T cells. The stages of differentiation at which oncogenes that are known to be associated with T‑cell acute lymphoblastic leukaemia and required in the bone marrow and thymus are also depicted. LMO2, LIM-only 2; TAL1, T-cell acute lymphocytic leukaemia 1. Adapted from Aifantis et al. (2008).[24]

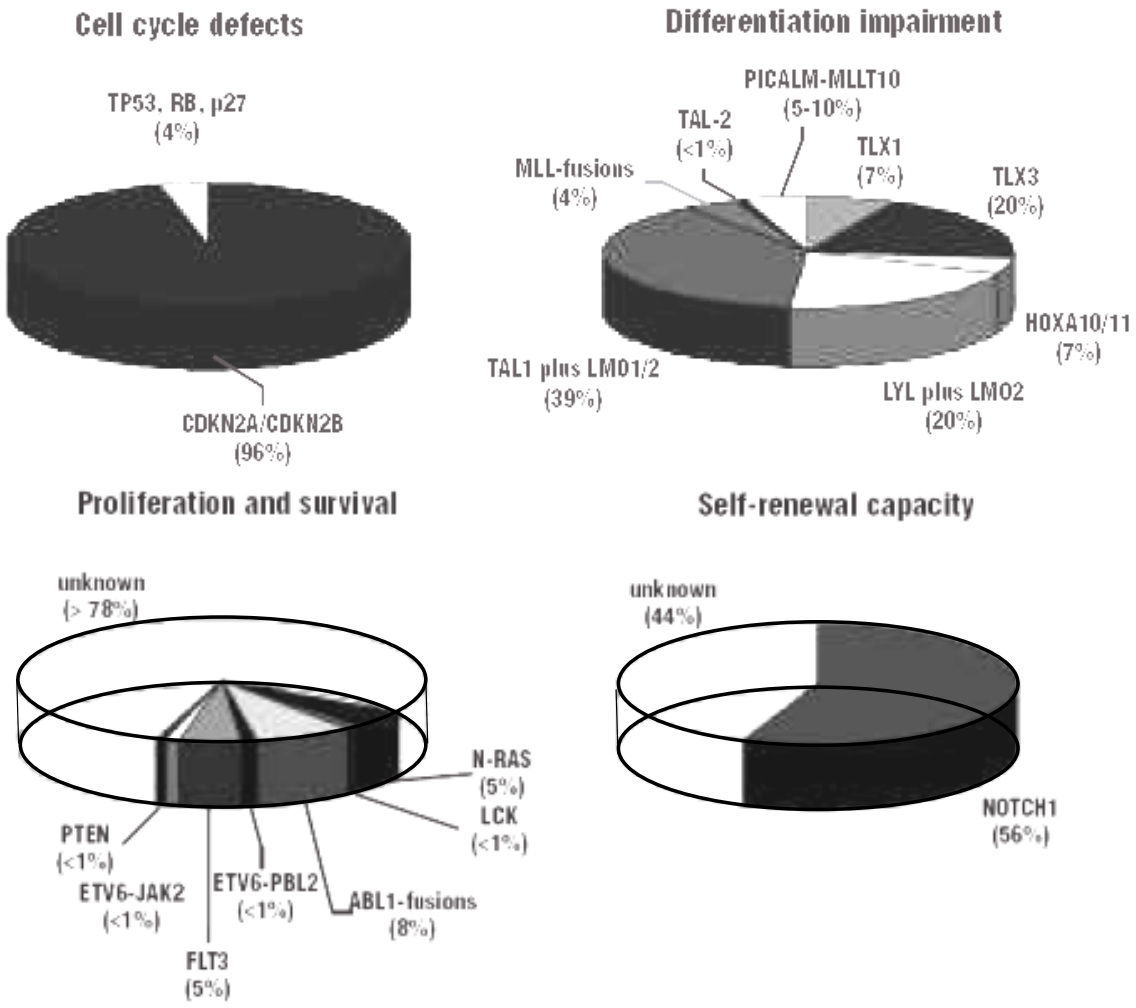

Figure 1.4. Functional classifications of common T-ALL mutations. Molecular analysis of T-ALL shows that four major classes of mutations are involved in the molecular pathogenesis of T-ALL. These four classes are represented by the four diagrams, in which the frequency of each of the different mutations is given. Adapted from Armstrong and Look (2005).[88]

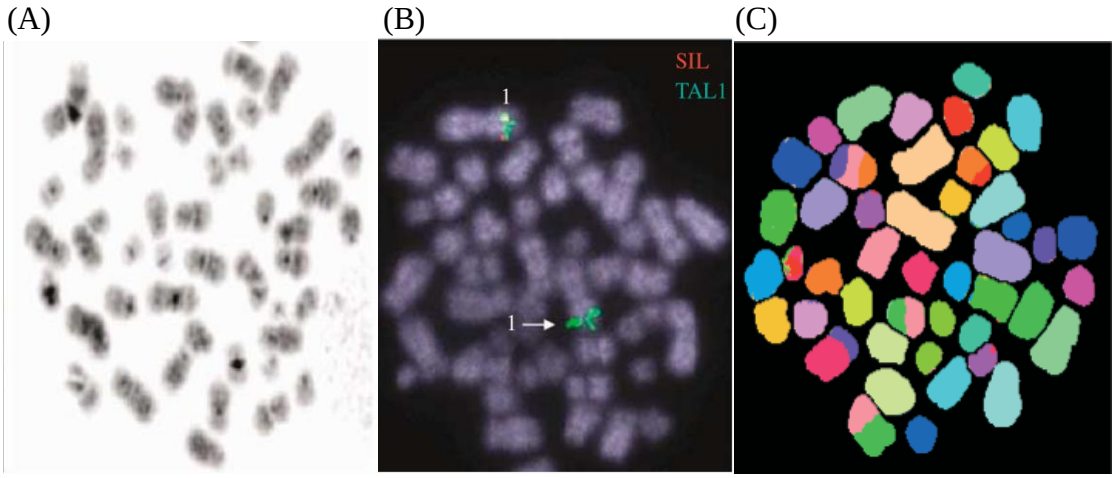

Figure 1.5. Classical karyotyping and FISH technique. (A) A typical G-banded karyotype. (B) Deletion of SIL resulting in SIL-TAL1 fusion gene, demonstrated with the SIL-TAL1 DNA probe (DAKOcytomation). The SIL probe (in red) is absent on del(1). Adapted from Graux et al. (2006).[132] (C) Multiple colour FISH (MFISH) of a highly abnormal metaphase taken from a child with ALL. The colour changes along the chromosomes indicate the locations and origins of chromosomal translocations. Adapted from Harrison et al. (2002).[38]

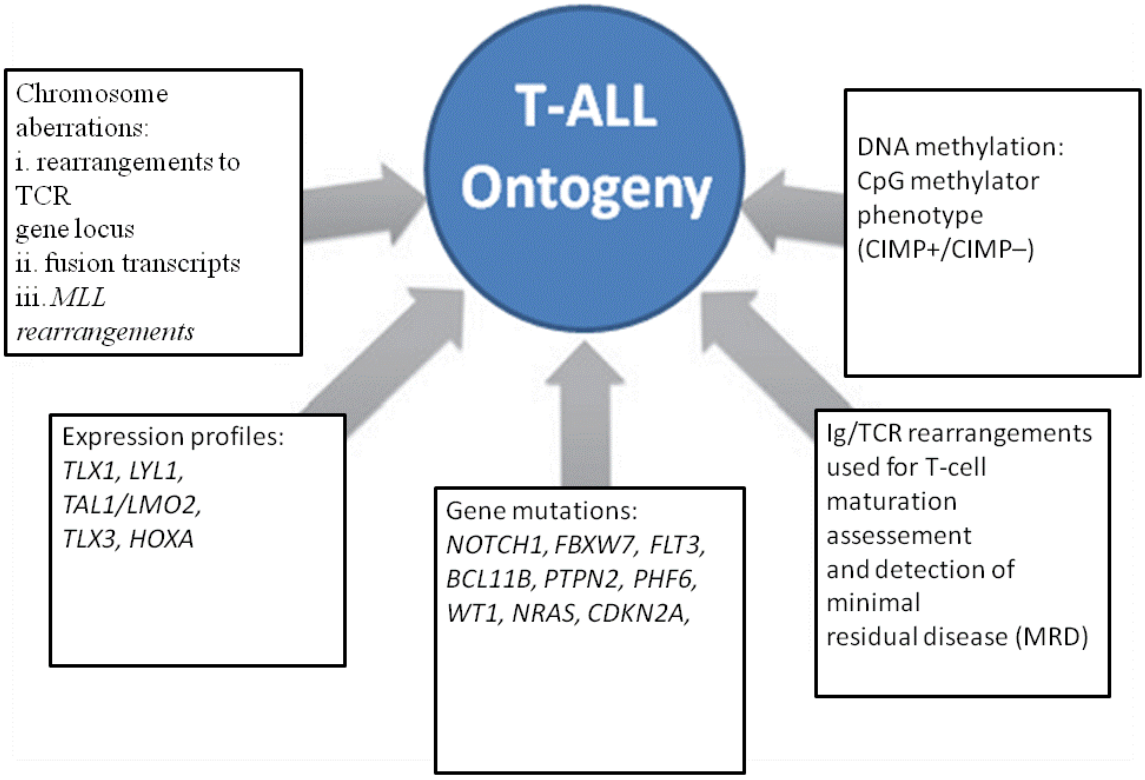

Figure 1.6. Schematic representation of molecular contributors to T-ALL ontogeny. Adapted from Kraszewska et al. (2012).[39]

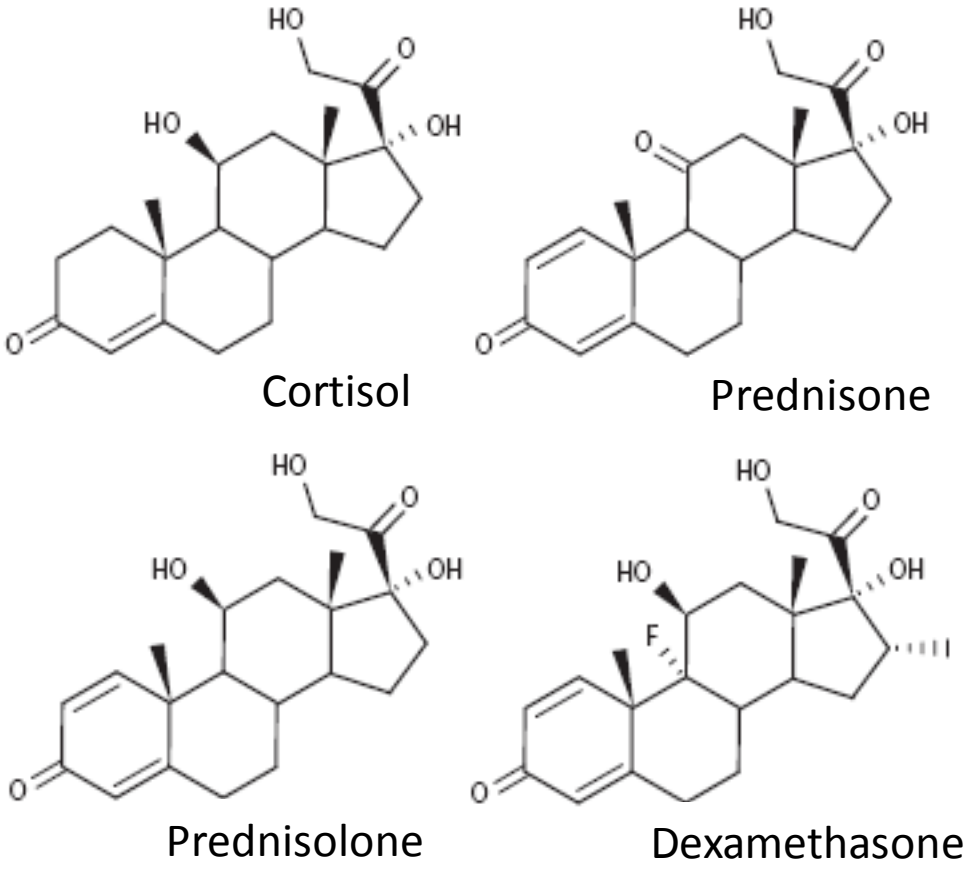

Figure 1.7. Chemical structures of cortisol and synthetic glucocorticoids prednisone, prednisolone, and dexamethasone. Adapted from Inaba and Pui (2010).[64]

CHAPTER 2

ABERRANT SIGNALING PATHWAYS IN T-ALL

Background

The last 50 years have seen remarkable progress in success rates for treating T-ALL. However, this remarkable progress has come about primarily through efforts in the clinic to intensify chemotherapy regimens. As a result, detrimental side effects have increased concomitantly with long-term remission percentages. Since intensity of untargeted chemotherapy intensity has been maximized in T-ALL therapy, further progress in treating refractory and relapsed cases must be achieved through alternative means. As a result, a primary focus in the field of T-ALL research has been to identify and characterize the biochemical pathways that are aberrantly activated in T-ALL leukemogenesis, and to discover mechanisms of resistance to chemotherapy. These research endeavors have the principal goal of identifying druggable targets, with the expectation that targeted therapy will achieve remission more efficiently and with fewer side effects than those observed with traditional chemotherapy.

Many of the chromosomal translocations and fusion proteins responsible for T-ALL have been characterized within the last 15 years. However, with rare exceptions such as p16 inactivation/deletion, no single chromosomal aberration has been found to be dominant in most cases of the disease. As a result, much research has focused on the common biochemical pathways downstream of these sporadic cytogenetic abnormalities

with the intent of finding common molecular pathways involved in a majority of T-ALL cases.

Ikaros' contribution to T-ALL leukemogenesis

Ikaros (Ik) is a transcriptional regulator expressed exclusively in the lymphoid system that is required for the development of all lymphoid lineages.[1] *Ikaros* is a member of the Kruppel transcription factor family characterized by the presence of zinc-finger domains located at their N- and C- termini. The N-terminal domain is involved in DNA binding, whereas the C-terminal domain is important for protein dimerization and stability. The *Ikaros* gene (*ZNFN1A1*) transcript is processed into a number of isoforms due to alternative splicing that regulates the expression of exons coding for the N-terminal DNA binding domain. Thus, all IKAROS proteins share a common C-terminal domain with two zinc-fingers attached to a domain with different combinations of one to four N-terminal zinc-fingers, each with distinct DNA binding capabilities and specificities. At least three N-terminal zinc-fingers are required for high affinity DNA binding to the motif GGGAA/T.[2]

Only the longer IKAROS isoforms that contain at least three N-terminal zinc fingers present high affinity to their specific DNA sequence, whereas the shorter IKAROS versions with fewer than three N-terminal zinc fingers cannot bind DNA with high affinity. Rather, they behave as dominant negative isoforms upon heterodimerization with IKAROS isoforms that have an intact DNA-binding domain.[3] The shorter, non DNA-binding IKAROS isoforms are normally expressed at low levels with respect to predominant long isoforms that are abundantly expressed throughout lymphocyte development. A mutation that results in the deletion of the N-terminal zinc-finger DNA

binding domain from the IKAROS proteins completely blocks lymphocyte development.[4,5]

Aberrant *Ikaros* function has been correlated with T-ALL leukemogenesis. Mice heterozygous for *Ikaros* mutations at birth show an apparently normal lymphoid cell distribution at birth. However, within a few months they develop a very aggressive form of lymphoblastic leukemia with a concomitant loss of heterozygosity, resulting in predominant synthesis of short IKAROS isoforms.[1,6] These data demonstrate that IKAROS functions as a tumor suppressor in the lymphoid system. In support of this model, loss of IKAROS activity has been associated with human leukemia. Loss of DNA-binding IKAROS isoforms and/or overexpression of the shorter dominant negative form of IKAROS was observed in nearly 100% of childhood and adolescent T-ALL cases examined in one study.[7-9] A current model suggests that the increase in expression of dominant negative IKAROS isoforms is a result of alternative splicing and not as a result of genomic alterations.

NOTCH1 contribution to T-ALL

NOTCH1 activity in T-cell hematopoiesis

The fundamental components of the NOTCH pathway include the Delta and Serrate family of ligands (Delta-like 1, 3, and 4; and Jagged 1 and 2), four distinct NOTCH receptors (NOTCH1-4) and the CBF1, Su(H), Lag-1(CSL) DNA-binding proteins.[10] All NOTCH receptors are class I transmembrane glycoproteins expressed at the cell surface as heterodimers. They consist of an N-terminal extracellular fragment and a C-terminal transmembrane-intracellular subunit. Of all the NOTCH receptors, only NOTCH1 has been found to play a role in T-ALL. The NOTCH1 receptor functions as a

ligand-activated transcription factor that directly transduces extracellular signals at the cell surface into changes in gene expression in the nucleus.[10] Activation of NOTCH receptors typically occurs via cell-cell contact and interaction of a NOTCH protein with a Delta-like or Jagged ligand expressed on the surface of a neighboring cell, typically a thymic epithelial cell (TEC) in T-cell ontogeny.

Two proteolytic events activate intracellular NOTCH1(ICN). First, an extracellular metalloprotease, typically ADAM10 or ADAM17, cleaves the receptor in the C-terminal portion of the heterodimerization (HD) domain (S2 cleavage). This generates a truncated protein with a short extracellular stub that is recognized and subsequently processed by the γ-secretase complex (S3 cleavage). Once released from the cell membrane, the ICN rapidly translocates to the nucleus, where it forms a transcriptional complex with the CSL DNA-binding protein. The ICN-CSL complex then activates gene transcription via recruitment of coactivators of the mastermind-like (MAML) family, whose transcriptional gene targets include hairy and enhancer of split 1 (HES1) and c-Myc (Figure 2.1).[11]

Importantly, transcriptional activation of NOTCH target genes is coupled with an active mechanism that ensures the rapid termination of NOTCH signaling. Recruitment of RNA polymerase II to the SCL-DNA binding transcription complex triggers phosphorylation of the PEST domain of the receptor, and its proteasomal degradation via the FBXW7-SCF ubiquitin ligase complex.[10]

NOTCH plays a critical role in T-cell ontogeny at multiple stages.[12] T-cell lineage specification is dependent on NOTCH, since ablation of NOTCH1 results in a complete block at the earliest stages of T-cell lymphopoiesis and lack of specification of the T-cell

lineage. Mice harboring a conditional deletion of NOTCH1 fail to develop T-cells and show ectopic B-cell development in the thymus. Conversely, mice expressing a constitutively active form of NOTCH1 show ectopic T-cell development in the bone marrow and fail to produce B lymphocytes.[12] Furthermore, NOTCH1 plays a role in progression through DN1, DN2, and DN3 stages of thymocyte maturation, regulates in part TCRB gene rearrangement and β-selection, and regulates the lineage decision between αβ and γδ fate.[12]

NOTCH1 pathway role in T-ALL leukemogenesis

Aberrant activation of NOTCH1 in T-ALL was first identified in 1991 in rare leukemia cases harboring the t(7;9)(q34;q34.3) translocation, which juxtaposes a truncated *NOTCH1* gene next to the *TCRB* locus (originally termed the TAN1 oncogene).[13,14] Thereafter occasional additional cases of the *NOTCH1* translocation were found in a small percentage of patients. However, because of the rarity of these translocations, the significance of these findings for the pathogenesis of T-ALL remained elusive until 2004, when Weng et al.[15] published a landmark study in which they identified activating mutations in *NOTCH1*, leading to high levels of NOTCH1 signaling in over 60% of human T-ALL cases. The most frequent hot spots for mutations in *NOTCH1* are exons 26 and 27, which encode the N- and C-terminal components of the heterodimerization (HD) domains, respectively.[15] These activating HD mutations are found in ~40% of human T-ALL. These HD mutations result in ligand hypersensitivity or ligand-independent NOTCH1 cleavage and thus activation by ADAM proteases and γ-secretase.[16]

A second type of *NOTCH1* mutation found in 20-25% of T-ALL is found in the intracellular PEST (Proline, Glutamate, Serine and Threonine rich) degron domain. The loss of the PEST domain results in increased levels of activated NOTCH1 due to impaired degradation of the activated receptor by the proteasome.[15,17] Similarly, 15% of T-ALL cases show mutations in *FBXW7*, which normally ubiquitylates the PEST degron domain. Either mutation can result in aberrant accumulation of intracellular NOTCH1 protein and hence over-activation of target genes' transcription.[17-19] Furthermore, FBXW7 is also responsible for ubiquitylating additional oncoproteins such as C-MYC, JUN, Cyclin E, and mTOR, for proteosomal degradation. As such, the biological consequences of FBXW7 inactivation may be broader than merely those of accumulation of NOTCH1 ICN, and may include increased cell metabolism, cell growth, and cell cycle progression.[20]

Gamma-secretase inhibitor treatment of T-ALL

The high frequency with which activating mutations in *NOTCH1* were observed initially generated much enthusiasm regarding the therapeutic potential of targeting this pathway in T-ALL. Given the requirement of γ-secretase cleavage for NOTCH1 activation, γ-secretase inhibitors (GSIs), already in use for treatment of Alzheimer's disease, were found to block oncogenic NOTCH1 signaling in T-ALL *in vitro.* [5,6,21] These results stimulated a phase I clinical trial of GSI MK-0752 for the treatment of relapsed T-ALL. However, despite some correlative data showing downreguation of NOTCH1 target genes in T-cell lymphoblasts, there were no objective clinical responses, and the effect on T-ALL blasts appeared to be cytostatic rather than cytolytic.[5,6]

Furthermore, many patients showed dose-limiting gastrointestinal toxicities from GSI treatment.[22] These dose-limiting gastrointestinal toxicities were not unexpected since inhibition of NOTCH signaling has been shown to induce cell cycle arrest and accumulation of mucus-secreting goblet cells in the intestinal epithelium.[23] However, the combination of glucocorticoid treatment with GSIs was much more efficient and exhibited a marked protective effect against GSI-induced intestinal toxicity in a mouse model of T-ALL, and may suggest that this may be a desirable and effective treatment combination modality for human T-ALL.[23]

The PI3K/AKT/mTOR pathway in T-ALL

Introduction

With the disappointing results seen in GSI treatment of T-ALL, research efforts turned to determining the reason(s) for T-ALL's resistance to GSI treatment. In a landmark study by Palomero et al. in 2007,[24] it was discovered that loss of PTEN in T-ALL conferred resistance to GSIs. Furthermore, it was determined that loss of PTEN resulted in upregulation of the PI3K/AKT/mTOR (P/A/mT) pathway, thus effectively transferring T-ALL's oncogene addiction from NOTCH1 to P/A/mT. The P/A/mT pathway is known to be upregulated in many forms of cancer, not solely in hematological malignancies. Upregulation of this pathway is correlated with poor prognosis in many cancers as well as premature aging and resistance to cancer therapy (Figure 2.2).[25]

PI3K is a heterodimeric protein with an 85KDa regulatory subunit and a 110KDa catalytic subunit.[26,27] Upon activation of a surface receptor tyrosine kinase, PI3K phosphorylates membrane phospholipids phosphatidylinositol 4-monophosphate (PIP) and phosphatidylinositol 4,5-diphosphate (PIP2) to generate phosphatidylinositol 3,4-

diphosphate (PIP2) and phosphatidylinositol 3,4,5-triphosphate (PIP3), respectively.[27-29] Through its pleckstrin homology (PH) domain, AKT interacts with PIP3, translocates to the cell membrane, and undergoes a conformational change that allows phosphorylation of AKT at T308 by PDK1, which itself is recruited to the membrane by PIP3 via its PH domain.[30,31] Full activation of AKT also requires phosphorylation at S473 by mTORC2.[32] However, mTORC1 is also activated by AKT indirectly by inhibition of the tuberous sclerosis complex 2 (TSC2).[33] Thus, AKT is both upstream and downstream of mTOR. Activation of the P/A/mT pathway affects cell survival, growth, proliferation, and transformation.[34,35,36] Negative regulation of P/A/mT activity is mediated by PTEN, a phosphatase that removes phosphate groups from PIP2 and PIP3, thus antagonizing activity of the P/A/mT pathway.[25] Each of these molecular entities in the P/A/mT pathway will be discussed in turn.

Phosphatidylinositide 3-kinase

The phosphatidylinositide 3-kinases (PI3Ks) are a family of lipid kinases that catalyze the phosphorylation of phosphotidylinositides at the 3'-hydroxyl group. Although three classes make up this family, only Class I PI3Ks have been shown to be coupled to extracellular stimuli.[35,37-39] This class can be subdivided in to Class IA kinases, which are activated by receptor-tyrosine kinases (RTKs), and Class IB kinases, which are regulated by G-protein-coupled receptors.[40] To date only Class IA enzymes have been clearly implicated in human cancers.[41,42]

Class IA PI3Ks are heterodimers consisting of a catalytic subunit (p110) and a regulatory subunit (p85). Three isoforms (p110α, p110β, and p110δ) are known for the catalytic subunit, which are encoded by the *PIK3CA, PIK3CB,* and *PIK3CD* genes,

respectively. Seven proteins (p85α, p85β, and p55γ and their splicing variants) comprise the regulatory subunits.[40,43] P85 keeps p110 in a stable but inactive state until, upon growth factor stimulation, p110 is recruited to the membrane. p100 is then activated at the membrane via the interaction of SH2 domains on p85 and phosphotyrosine motifs on the stimulated RTKs. The activated p110 catalytic subunit subsequently phosphorylates the D3 hydroxyl position of the inositol ring of PIP2, generating PIP3 at the membrane. PIP3 provides docking sites for activation of signaling proteins containing pleckstrin-homology (PH) domains,[44] including AKT and PDK1.

Activating mutations in the *PIK3CA* gene, which codes for the specific PI3K p110α catalytic subunit, have been found in many forms of cancer, making it one of the most frequently mutated oncoproteins in human cancer, along with *K-Ras* and *p53*.[45] Mutations in *PIK3CA* cluster in two "hotspot" regions: exon 9 encoding the beginning of the helical domain and exon 20 encoding the tail of the kinase domain.[46,47] The mutations found in these two regions of p110α encode single amino acid changes of E542K and E545K in the helical domain and H1047R in the kinase domain.[45,48] The E542K and E545K mutations in the helical domain are postulated to affect interactions with regulatory proteins, including p85, whereas the H1047R mutation in the kinase domain is postulated to affect specificity or affinity of p110α towards its substrates.[49] PI3K activity can also be upregulated by gene amplification as has been found to be the case in 40% of ovarian cancers.[50]

Phosphatase and tensin homolog deleted on chromosome 10 (PTEN)

PTEN, located on 10q23.3, is a dual lipid and protein phosphatase. Its primary function is to hydrolyze the 3' phosphate on PIP3, the product of PI3K activity, thus

producing PIP2,[51] and antagonizing the activity of PI3K.[52] Incidentally, SHIP-1 can also mimic the PIP3 phosphatase function of PTEN but does so by hydrolyzing the 5'phosphate of PIP3, whereas PTEN hydrolyzes the 3' phosphate.[53] Loss of PTEN function results in accumulation of PIP3, mimicking the effect of PI3K activation and triggering the activation of its downstream effectors, PDK1 and AKT.[54,55]

PTEN is a major tumor suppressor, frequently inactivated in human cancers.[56] However, PTEN does not fully conform to the formal definition of a tumor suppressor as it has been shown to be haploinsufficient in its tumor suppressor function.[57] PTEN gene mutations or deletions are associated with poor prognosis in T-ALL. Two mutations in PTEN's phosphatase domain abrogate tumor suppressor function: C124S abrogates both lipid and protein phosphatase activity, while G129E abrogates only lipid phosphatase activity.[58] However, relatively few primary T-ALL patient samples harbor PTEN gene mutations (5-27%), and they occur almost exclusively within exon 7.[59] Likewise, PTEN deletions are observed in no more than 9% of T-ALL cases.[59]

These data suggest the existence of other mechanisms whereby PTEN function is abrogated in T-ALL, as well as in other types of cancer, which has been verified in recent studies. Roman-Gomez et al. showed that PTEN promoter hypermethylation and consequent decrease in mRNA expression was reported in ~20% of T-ALL.[60] NOTCH1 also transcriptionally inhibits PTEN expression in T-ALL via up-regulation of HES1.[61] Furthermore, PTEN can also be regulated by miRNAs, and both miR-19 and miR-21 have been shown to be T-cell oncogenes by downregulating PTEN in T-ALL.[62,63]

PTEN can also be inactivated by several posttranslational mechanisms, including phosphorylation, ubiquitination, oxidation, and acetylation.[64] Specifically, RAK and CK2

have been shown to phosphorylate the C-terminus of PTEN and consequently both inactivate and stabilize PTEN protein. Thus, it is still entirely possible to have overactivation of the P/A/mT pathway despite the presence of even high levels of PTEN in T-ALL.[65,66]

AKT

The primary effector of the P/A/mT pathway is AKT (v-AKT thymoma retrovirus), also known as protein kinase B (PKB). It was originally discovered as the cellular homologue of the transforming retrovirus AKT8 and as a kinase with properties similar to protein kinases A and C.[26,28,29,67] AKT is a serine-threonine protein kinase that is expressed as three isoforms—AKT1, AKT2, and AKT3, encoded by the genes *PKBα, PKBβ,* and *PKBγ,* located at chromosomal loci 14q32, 19q13, and 1q44, respectively.[41,68] AKT1 and AKT2 are the isoforms with the highest expression in thymocytes.[69] The three isoforms share a similar structure. AKT contains an amino-terminal PH domain that serves to target the protein to the membrane for activation. Within its central region, AKT has a large serine-threonine kinase domain and is flanked on the C-terminus regulatory domain by hydrophobic and proline-rich regions.[26,67]

AKT is one of the most frequently upregulated kinases in human cancers,[70] and its over-expression is associated with a poor prognosis. AKT regulates cell survival, cell cycle progression, migration, proliferation, metabolism, tumor growth, and angiogenesis,[71,72] and as a result, AKT activity is strongly correlated with invasion and metastasis.[73] Furthermore, AKT activation is also found to correlate with resistance to chemotherapy and radiation therapy, and conversely, addition of AKT inhibitors to antitumor regimens renders cancer cells sensitive to chemotherapy.[74,75] AKT protects

cells from apoptosis by phosphorylation of pro-apoptotic substrates which are subsequently sequestered by the chaperone 14-3-3, which then sequesters them away from their target sites of action.[76] In addition, AKT has been shown to regulate HIF-1α and VEGF expression, which are both critical mediators of angiogenesis in cancer.[72,77]

Aberrant over-activation of AKT can occur by several different mechanisms, including amplification, over-expression, mutations in AKT, and/or alterations in AKT upstream regulators.[78] Upstream regulators of AKT activity include cytokines and growth factors such as VEGF, FGF, EGF, HGF, IGF and angiopoietin, along with their respective RTK cell surface receptors.[79,80]

A rare mutation in AKT that increases AKT activity is E17K. Though this mutation is seen in only a small percentage of cancers,[81] it has a significant impact on cellular function. The E17K mutation falls in the PH domain of the AKT protein, and hence alters the electrostatic interactions of AKT that allows it to form new hydrogen bonds with its natural phosphatidylinositol ligands.[81] This confers many different aberrant properties to the AKT protein, including an altered PH domain conformation, constitutive activation and constitutive association with the cell membrane. In confirmation of these observations, mutated AKT (E17K) has been shown to interact with c-Myc to induce leukemia in Eμ-Myc mice.[81] AKT can also be over-activated via gene amplification, though this phenomenon is not often observed in human cancers.[82,83]

Recruitment of AKT by PIP3 to the cell membrane results in a conformational change that exposes two crucial residues for phosphorylative activation. Full AKT activation requires phosphorylation of both of these two sites in the kinase domain, one in the “T-loop” at T308 (phosphorylated by PDK1) and the other in a hydrophobic motif

near the COOH terminus at S473.[84,85] Several kinases have been proposed to phosphorylate AKT at the S473 residue, including ILK, PKC, DNA-PK, and ATM. However, it is now generally thought that mTORC2 is primarily responsible for phosphorylation of AKT at S473 under most circumstances.[86] *In vitro* studies have established that AKT phosphorylated at only T308 is only 10% as catalytically active as AKT phosphoryated at both T308 and S473. Thus, phosphorylation of the hydrophobic motif controls both the activity and substrate specificity of AKT.[87,88]

After activation at the cell membrane, AKT is able to translocate to the cytoplasm and nucleus[28,29,89] where it phosphorylates a number of downstream targets for regulation of various cellular functions (Figure 2.2). So far over 100 AKT substrates have been identified,[33] of which about 40 have been characterized. AKT affects the activity of a number of critical transcriptional regulators including FOXO, CREB, E2F, NF-κB, Iκ-K, FKHR, HDM2, mTOR and MDM2.[90,91] These are all either direct or indirect substrates of AKT and each can regulate proliferation, survival, and epithelial-to-mesenchymal transition.[25] Besides transcription factors, AKT is able to target a number of other molecules to affect the survival state of the cell including BAD and GSK-3β.[92] GSK-3β regulates β-catenin protein stability. Thus, the P/A/mT pathway is connected to the Wnt/β-catenin pathway through GSK-3β. AKT also activates mTORC1 by phosphorylating and inactivating PRAS40, an inhibitor of mTORC1 activity.[28,29,93] AKT promotes the G1-S phase transition by blocking FOXO-mediated transcription of the cell-cycle inhibitor p27Kip1, and/or phosphorylating and inactivating p27Kip1 directly.[90,94]

AKT can also be down-regulated by means other than the expected PTEN- or SHIP-mediated dephosphoryation and inactivation of PIP3. The tumor suppressors PP2A

and PHLPP1/2 are known to inactivate AKT by dephosphorylating residues T308 and S473, respectively.[95] Loss of either PHLPP1 or PHLPP2 results in a striking 30-fold increase in the amplitude of AKT phosphorylation after agonist stimulation. There also is a striking increase in the duration of AKT phosphorylation after agonist-induced activation.[96] Inactivation of AKT results in G1 arrest since AKT normally phosphorylates and inactivates GSK-3β, a kinase that restricts G1 cell cycle progression through phosphorylation of cyclin D1 and cyclin E, targeting them for degradation.[97,98]

Mammalian target of rapamycin

The mammalian target of rapamycin (mTOR) is a 289KDa serine/threonine kinase.[99,100] It is considered to be a member of the PI3K-kinase-related kinase (PIKK) superfamily since its C-terminus has strong homology to the catalytic domain of PI3K.[101,102] mTOR is considered to be a master switch of cellular anabolic and catabolic processes since it regulates the rate of cell growth and proliferation via its ability to sense mitogen, energy, and nutrient levels.[103,104] Deregulation of the mTOR pathway is frequently observed in cancer as well as diabetes, and as a result, approximately 28% of human cancers are expected to be sensitive to mTOR inhibition.[105]

mTOR is found in two different signaling complexes: mTORC1 and mTORC2 (Figure 2.2). In each complex, mTOR is grouped with a different and distinct set of signaling proteins that confer upon it a distinct set of functions. mTORC1 consists of mTOR, mLST8/GβL, and raptor along with two negative regulatory proteins, PRAS40 and DEPTOR.[106] mTORC1's main functions are to regulate cell growth, proliferation, and survival by sensing mitogen, energy, and nutrient signals.[107] mTORC2 consists of mTOR, mLST8, mSin1, rictor, and DEPTOR.[108,109] mTORC2 regulates the actin

cytoskeleton by mediating the phosphorylation state of protein kinase PKCα, and modulates cell survival in response to growth factors by phosphorylating AKT at S473.[86,110]

mTOR can be activated by multiple signaling means. It can be activated by upstream signals, including growth factors, such as insulin and type I insulin-like growth factor (IGF-1), energy, stress, and nutrients.[107] In response to growth factor ligand binding, IGFR is activated and in turn phosphorylates the insulin receptor substrates 1-4 (IRS1-4) which then trigger multiple downstream signal transduction pathways, such as PI3K and hence AKT.[111] AKT in turn modulates mTOR activity by at least three means. First, AKT phosphorylates and inactivates TSC2, which combined with TSC1 antagonize mTOR activity through GTP hydrolysis and inactivation of RHEB, which is an mTOR activator.[112] Second, AKT can activate mTOR through phosphorylation and inactivation of PRAS40, a negative regulator of mTOR activity.[29] Lastly, AKT can activate mTOR directly upon insulin stimulation through phosphorylation of the S2448 residue of mTOR.[113]

In mammals, the two best-characterized downstream phosphorylation targets of mTOR are p70S6K and 4E-BP1. In mammalian cells, p70S6K is activated by PDK1 via phosphorylation at T229.[114,115] mTOR further activates p70S6K by phosphorylating residues S371 and T389.[116,117] P70S6K is known as the major ribosomal protein S6 kinase in mammalian cells and is a key player in the control of cell growth and proliferation.[118] Activated p70S6K is suggested to regulate protein synthesis through phosphorylation of the 40S ribosomal protein S6, which is postulated to increase the translational efficiency of mRNA transcripts with a 5'-terminal oligopolypirymidine (5'-

TOP).[119] A negative feedback loop from p70S6K to the PI3K pathway has also been identified. This inhibition occurs as a result of direct phosphorylation and inactivation of IRS by p70S6K,[120,121] hence down-regulating activity of the PI3K pathway.

4E-BP1 is the other well-characterized downstream phosphorylation target of mTORC1 and is a repressor of the translation initiation factor eIF4E. Hypo-phosphorylated 4E-BP1 binds tightly to eIF4E, the mRNA cap-binding protein, and represses cap-dependent translation by blocking the binding of eIF4E to eIF4G. In response to sufficient growth signals and adequate nutrients, mTOR-mediated phosphorylation of 4E-BP1 at multiple sites induces the dissociation of 4E-BP1 from eIF4E, allowing eIF4E to bind eIF4G.[122,123] eIF4G then serves as a scaffolding protein for the assembly of other initiation factors including eIF4A, which together recruit the 40S ribosome to the 5' end of the mRNA to commence protein translation.[124]

The Ras/Raf/MEK/ERK (MAPK) pathway

Mitogen-activated protein kinases (MAPK) are a family of evolutionarily conserved pro-directed serine-threonine kinases, which play a central role in transducing extracellular cues into a variety of intracellular responses including the modulation of cell proliferation, differentiation, and apoptosis.[125] The ERK subfamily is comprised not only of the widely studied ERK1 and ERK2, but also the more recently identified ERK5.[126] In normal thymocytes, TCR controls positive selection by modulating ERK activity.[127]

There is evidence that ERKs may contribute to T-ALL biology.[128] Aberrant activation of the TAL1 protein by phosphorylation via ERK1 has been described in the human T-ALL cell line Jurkat.[129] Furthermore, activation of ERK1/2 has been observed in T-ALL cells on stimulation with IL-7. In contrast, normal T-cells do not appear to

activate ERK1/2 in response to IL-7.[130-132] Ras can also be activated by growth factor receptor tyrosine kinases, such as insulin receptor (IR), via intermediates like insulin receptor substrate (IRS) proteins that bind growth factor receptor bound protein 2.[132,133] Ras:GTP then recruits Raf to the membrane where it becomes activated, likely via a Src-family tyrosine kinase.[134]

Both Ras and Raf are members of multigene families. There are three Ras members (K-, N-, and H-Ras)[132] and three Raf members (B-, C-, and A-Raf).[134] Raf is responsible for serine/threonine (S/T) phosphorylation of mitogen-activated protein kinase kinase-1 (MEK1).[135] Activated MEK1 then phosphorylates ERK1/2 at specific T and Y residues.[136] Activated ERK1/2 can translocate to the nucleus and phosphorylate many downstream phosphorylation substrates, including p90Rsk1, which can activate the cAMP-response element binding protein (CREB) transcription factor,[137] Elk-1, Fos, and Gata-1.[28,138-140]

Activating mutations of Ras and Raf occur frequently in both solid and hematological malignancies, leading to aberrant activation of their downstream targets MEK1/2 and ERK1/2.[141] Mutations that lead to expression of constitutively active Ras proteins have been observed in approximately 20-30% of human cancers.[132] The majority of RAS mutations in humans occur in K-RAS which is followed by N-RAS,[132,142] making K-Ras one of the two most frequently mutated oncogenes observed in cancer along with *PIK3CA*.[143] It is thought that B-Raf is the most important kinase in the MAPK cascade,[144] and the most frequent mutation detected in the BRAF gene is V600E in its activation domain.[145] Often point mutations in RAS genes result in increased Ras activity that frequently perturbs the Raf/MEK/ERK as well as the P/A/mT pathways.[132,146-148]

mTOR is also activated by mitogenic signals through activation of the Ras/Raf/MEK/ERK pathway. Phosphorylation of TSC2 by ERK promotes dissociation of the TSC1/2 complex from RHEB and hence attenuates TSC2-mediated inhibition of mTOR.[149,150] Moreover, the MAPK-activated kinase, p90Rsk1 also interacts with and phosphorylates TSC2 at a regulatory site leading to inhibition of the tumor suppressor function of the TSC1/2 complex and subsequent activation of mTORC1 signaling.[151] Furthermore, activated GTP-bound RAS proteins are capable of activating the PI3K pathway directly by binding to the p110 catalytic subunit.

In cancers bearing mutant RTKs or oncogenes such as RAS that activate both the RAF/MAPK and PI3K pathways, blocking the PI3K pathway can actually upregulate signaling of the RAF-MAPK pathway because the two pathways have cross-inhibitory effects.[152] RAF-MAPK signaling can in turn drive tumor growth, counteracting the effect of the PI3K pathway inhibition, suggesting that rapalogs may also induce activation of the MAPK pathway.[153,154] It was recently shown that mTORC1 inhibition led to the activation of MAPK in a PI3K-dependent manner, providing another example of such signaling feedback loops and crosstalk.[153]

JAK/STAT

The Janus kinase/signal transducer and activator of transcription (JAK/STAT) pathway is one more effector of T-ALL leukemogenesis that deserves discussion. It plays an important role in biological processes such as apoptosis, differentiation, proliferation and cellular immune responses, mediated by growth factors and cytokines.[155] Binding of cytokines results in cell surface receptor oligomerization and activation of the JAK family of tyrosine kinases.[156] Activated JAKs then phosphorylate the cytoplasmic domain

of the receptor, thereby creating docking sites for STATs, which are phosphorylated by JAKs and consequently dimerize and migrate to the nucleus where they regulate gene transcription.[156]

JAK1 mutations have been observed in 18.4% of adult cases of T-ALL and are associated with advanced age at diagnosis, poor response to therapy, and overall poor prognosis.[157] In pediatric T-ALL, the genetic juxtaposition between *JAK2* and *TEL* results from the t(9;12)(p24;p13) chromosomal translocation and generates a constitutively active TEL-JAK2 protein.[158] TEL-Jak2 transgenic mice develop fatal leukemia, with invasion of non-hematopoietic organs by leukemic T-cells,[158] further supporting the proposition that *TEL-Jak2* is an oncogene *in vivo.* Moreover, the expression of a tyrosine-phosphorylated TEL-Jak2 protein correlates with activation of STAT1 and STAT5 in leukemic tissues.[158] STATs are frequently overexpressed and hyperactivated by alterations in such upstream signaling pathways, participating in oncogenesis through up-regulation of genes encoding apoptosis inhibitors such as Mcl-1 and Bcl-x as well as cell cycle regulators such as cyclin D1/D2 and c-Myc.[159]

PI3K/AKT/mTOR pathway inhibitors

A primary focus of this study was the impact that a novel small molecule inhibitor, Lenaldekar (LDK), has on hematologic malignancies (See Chapter 4). As LDK was found to exert this impact in part through modulation of the PI3K/AKT/mTOR (P/A/mTOR) pathway, this portion of the thesis will be devoted to addressing P/A/mTOR inhibitors currently in clinical use and/or development.

mTOR inhibitors

The first discovered and best characterized mTOR inhibitor is rapamycin (sirolimus). It was originally isolated from the bacterium *Streptomyces hygroscopicus* found in a soil sample from Easter Island (also called Rapa Nui in the native tongue). Named rapamycin after the island where it was first discovered, it initially showed antifungal potential, particularly against *Candida albicans.*[160] Rapamycin works by binding to FKBP12, an intracellular chaperone. The rapamycin/FKBP12 complex affects mTORC1 activity and stability through an allosteric mechanism, binding to a surface of mTOR distant from the active site.[161] In most cellular systems, rapamycin delays cell-cycle progression through G1 phase arrest, but rarely has cytotoxic effects as a single agent, although rapamycin can synergize with chemotherapeutics in some settings.[162,163]

Rapamycin was originally utilized as an immunosuppressive agent in organ transplant patients. However, its anti-proliferative properties prompted its testing for anti-neoplastic activity. Because rapamycin is extremely insoluble in aqueous solution, other chemical variations of rapamycin have been developed with better pharmaceutical properties, including temsirolimus (CCI-779), everolimus (RAD001) and deforolimus (AP23573), collectively referred to as "rapalogs." These rapalogs have been tested extensively in clinical trials against various types of cancers. Encouraging results came from studies in renal cell carcinoma in which CCI-779 and RAD001 improved overall survival among patients with metastatic renal cell carcinoma (RCC)[164] and hence received FDA approval for treatment of RCC. However, rapalogs have failed to show any appreciable single agent activity in most other tumor types.[165]

The existence of feedback loops counteracting the action of rapalogs may be a source of rapalog resistance in cancer.[166] Inhibition of mTORC1 by a rapalog blocks the p70S6K-mediated negative feedback loop on IRS-1. This in turn leads to hyperactivation of PI3K signaling and increases phosphorylation of AKT at Ser437[166] as well as mTORC2. Because the rapamycin/FKBP12 complex does not bind mTORC2, mTORC2 was initially thought to be immune from rapamycin effects. However, prolonged treatment with rapamycin can decrease mTORC2 activity by disrupting *de novo* assembly of the mTORC2 complex. This disruption happens via sequestration of the intracellular pool of mTOR protein in a complex with rapamycin-FKBP12,[167] although rapamycin-mediated inhibition of mTORC2 appears to be somewhat cell-type specific.[168]

The evidence for rapamycin-resistant mTORC1 and mTORC2 activity has prompted the development of pan-mTOR inhibitors that target the ATP binding site of the mTOR kinase domain, thus inhibiting both mTOR complexes.[163,169] Furthermore, as a member of the PI3K superfamily of kinases, the kinase domain of mTOR shows strong homology to that of PI3K. Hence, the first class of ATP site-competitive mTOR inhibitors were found to cross-inhibit PI3Ks as well.[170,171] Another advantage of pan-mTOR/PI3K compounds is that they eliminate the feedback activation of PI3K/AKT signaling through p70S6K.[172,173] Preclinical compounds in this "pan PI3K/mTOR" class of inhibitors include PI-103, Ku-0063794, Torin-1, and WYE-354.[174] Originally, despite the improved anti-neoplastic activity, global inhibition of mTOR was expected to be accompanied by greater toxicity in normal tissues. Yet contradictory to these predictions, preclinical studies in a mouse model argue that full inhibition of mTORC1 and mTORC2 could be well tolerated in adult tissues.[161,174]

PI3K/AKT inhibitors

Activation of the PI3K signaling pathway contributes to cell proliferation, survival, and motility as well as to angiogenesis, all of which are responsible for the important aspects of tumorigenesis. Considering the impact that hyperactivation of the PI3K/AKT pathway exerts on cancer development and resistance to cancer treatment modalities, enormous efforts have been undertaken to identify and develop inhibitors that down-regulate the activity of this pathway (Table 2.1). Among other effects, inhibition of PI3K has been found to suppress angiogenesis and proliferation.[175,176]

The PI3K inhibitors wortmannin and LY294002 are commonly used to inhibit cancer cell proliferation and tumor growth and to sensitize tumor cells to chemotherapy and radiation *in vitro*. Wortmannin is a natural product isolated from *Penicillium wortmannin* and binds irreversibly to PI3K by covalent modifications. LY294002 is a synthetic drug small molecule that reversibly targets PI3K family members. However, both wortmannin and LY294002 show little or no selectivity for individual PI3K isoforms and have considerable toxicity in animals,[177,178] and the poor solubility and high toxicity of these inhibitors limit their clinical applicability. To overcome these shortcomings, derivatives of LY294002 and wortmannin are being developed. PX-866, a wortmannin derivative, has more potent and less toxic effects than wortmannin.[179] In addition, LY294002 derivatives TGX115 and TGX126 have been developed and have greater water solubility, lower toxicity, improved pharmacodynamics, and more specific PI3K selectivity.[180,181]

AKT is a major downstream target of the PI3K pathway and, like PI3K, is known to be involved in tumor growth and angiogenesis. Perifosine is the best characterized

AKT inhibitor. It is a lipid-based phosphatidylinositol analogue that targets the pleckstrin homology domain of AKT that prevents both AKT and PDK1 from binding to PIP3 and undergoing membrane translocation and activation.[182] Perifosine has been shown to inhibit the growth of several different solid tumors and has been shown to overcome cancer cell resistance to chemotherapeutic drugs and radiation therapy.[75] Furthermore, perifosine induces apoptosis in chemoresistant CCRF-CEM T-ALL cells[183] and, combined with etoposide, induces cell death in a synergistic manner in Jurkat cells.[184] Moreover, novel AKT inhibitor A443654 leads to rapid cell death of T-ALL cell lines Jurkat, CCRF-CEM, and MOLT-4 as well as primary patient samples.[185]

Because of the hyperactivation of AKT via feedback loops from mTOR inhibition, dual PI3K/mTOR inhibitors have been synthesized. The first dual PI3K/mTOR small molecule to become available was PI-103, a small molecule of the pyridofuropyrimidine class.[186] As PI-103 targets both class IA PI3Ks (at p110α) as well as mTOR, it does not lead to AKT activation, which is seen with mTOR-only inhibitors. PI-103 possesses strong cytotoxic activity against T-ALL cell lines and lymphoblasts derived from T-ALL patients, accompanied by dephosphorylation of AKT and its downstream target GSK-3β. Also, mTOR downstream targets, p70S6K and 4E-BP1 are dephosphorylated in response to PI-103 treatment.[187] BEZ235 is another example of a dual PI3K/mTOR inhibitor. BEZ235 is an imidazoquinazoline derivative that inhibits multiple class I PI3K isoforms and mTOR kinase activity by binding to the ATP binding pocket.[188,189] However, despite extensive development of such P/A/mT pathway inhibitors, clinical challenges still exist regarding their usability for treatment of human cancers.

Due to the genetic instability of most human cancers, it can be expected that any targeted therapy when used as a single agent will ultimately be overwhelmed by resistance development. However, the development of targeted therapies with minimal side effects would hopefully enable the combinatorial use of drugs with non-overlapping toxicities to effectively treat and eradicate the disease. Furthermore, a single agent with dual specificity may have the added advantage of being less likely to induce drug resistance than mono-specific agents. Clinical resistance to a kinase inhibitor often arises through second-site mutations in the targeted kinase. Targeting two kinases simultaneously greatly diminishes the possibility of resistance. Of course, this assumes that both kinases are essential for tumor survival and/or growth.

However, one necessary precaution with dual inhibitor activity is that the role of PI3K and mTOR in a wide range of normal biological processes also means that dual PI3K/mTOR inhibitors are also likely to be associated with increased toxicity.[172] For example, in a comparison of the mTOR-kinase only inhibitor PP242 and the dual PI3K/mTOR inhibitor PI-103, the latter was found to have a much narrower therapeutic range.[174] Furthermore, early clinical results have found common side effects of these inhibitors, including diarrhea, nausea, vomiting, and fatigue, as is already found in traditional chemotherapy regimens. Moreover, it is still possible that a tumor could develop resistance to even dual PI3K/mTOR inhibition by upregulating the MAPK pathway. Thus, combination therapy with both PI3K/mTOR and/or MAPK inhibitors may be necessary in some cases, but only to the extent that the combined side effects and toxicities of dual treatment are clinically tolerable. Clinicians would also need to know

the individual aberrant activation profile of a patient's tumor sample in order to inform the treatment decision.

References

1. Georgopoulos K, Moore DD, Derfler B. Ikaros, an early lymphoid-specific transcription factor and a putative mediator for T cell commitment. *Science.* 1992; 258:808–812.

2. Molnar A, Georgopoulos K. The Ikaros gene encodes a family of functionally diverse zinc finger DNA-binding proteins. *Mol Cell Biol.* 1994; 14:8292-303.

3. Sun L, Liu A, Georgopoulos K. Zinc finger-mediated protein interactions modulate Ikaros activity, a molecular control of lymphocyte development. *Embo J.* 1996; 15:5358-69.

4. Georgopoulos K, Bigby M, Wang JH, et al. The Ikaros gene is required for the development of all lymphoid lineages. *Cell.* 1994; 79:143-56.

5. Nichogiannopoulou A, Trevisan M, Neben S, et al. Defects in hemopoietic stem cell activity in Ikaros mutant mice. *J Exp Med.* 1999; 190:1201-14.

6. Winandy S, Wu P, Georgopoulos K. A dominant mutation in the Ikaros gene leads to rapid development of leukemia and lymphoma. *Cell.* 1995; 83:289-99.

7. Sun L, Crotty ML, Sensel M, et al. Expression of dominant-negative Ikaros isoforms in T-cell acute lymphoblastic leukemia. *Clin Cancer Res.* 1999; 5:2112–2120.

8. Sun L, Goodman PA, Wood CM, et al. Expression of aberrantly spliced oncogenic ikaros isoforms in childhood acute lymphoblastic leukemia. *J Clin Oncol.* 1999; 17:3753–3766.

9. Sun L, Heerema N, Crotty L, et al. Expression of dominant-negative and mutant isoforms of the antileukemic transcription factor Ikaros in infant acute lymphoblastic leukemia. *Proc Natl Acad Sci USA.*1999; 96:680–685.

10. Aster JC, Pear WS, Blacklow SC. Notch signaling in leukemia. *Annu Rev Pathol.* 2008; 3:587-613.

11. Palomero T, Ferrando AA. Oncogenic NOTCH1 Control of MYC and PI3K: Challenges and Opportunities for Anti-NOTCH1 Therapy in T-Cell Acute Lymphoblastic Leukemias and Lymphomas. *Clin Cancer Res.* 2008; 14:5314-5317.

12. Tanigaki K, Honjo T. Regulation of lymphocyte development by Notch signaling. *Nat Immunol.* 2007; 8:451-456.

13. Ellisen LW, Bird J, West DC, et al. TAN-1, the human homolog of the Drosophila notch gene, is broken by chromosomal translocations in T lymphoblastic neoplasms. *Cell.* 1991; 66:649-661.

14. Palomero T, Barnes KC, Real PJ, et al. CUTLL1, a novel human T-cell lymphoma cell line with t(7; 9) rearrangement, aberrant NOTCH1 activation and high sensitivity to gamma-secretase inhibitors. *Leukemia.* 2006; 20:1279-1287.

15. Weng AP, Ferrando AA, Lee W, et al. Activating mutations of NOTCH1 in human T cell acute lymphoblastic leukemia. *Science*. 2004; 306:269-271.

16. Malecki MJ, Sanchez-Irizarry C, Mitchell JL, et al. Leukemia-associated mutations within the NOTCH1 heterodimerization domain fall into at least two distinct mechanistic classes. *Mol Cell Biol.* 2006; 26:4642-4651.

17. Thompson BJ, Buonamici S, Sulis ML, et al. The SCFFBW7 ubiquitin ligase complex as a tumor suppressor in T cell leukemia. *J Exp Med.* 2007; 204:1825-1835.

18. O'Neil J, Grim J, Strack P, et al. FBW7 mutations in leukemic cells mediate NOTCH pathway activation and resistance to gamma-secretase inhibitors. *J Exp Med.* 2007; 204:1813-1824.

19. Asnafi V, Buzyn A, Le Noir S, et al. NOTCH1/FBXW7 mutation identifies a large subgroup with favorable outcome in adult T-cell acute lymphoblastic leukemia (T-ALL): a Group for Research on Adult Acute Lymphoblastic Leukemia (GRAALL) study. *Blood.* 2009; 113:3918-3924.

20. Minella AC, Clurman BE. Mechanisms of tumor suppression by the SCF(Fbw7). *Cell Cycle.* 2005; 4:1356-1359.

21. Palomero T, Lim WK, Odom DT, et al. NOTCH1 directly regulates c-MYC and activates a feed-forward-loop transcriptional network promoting leukemic cell growth. *Proc Natl Acad Sci U S A.* 2006; 103:18261-18266.

22. Deangelo D, Stone R, Silverman L, et al. A phase I clinical trial of the notch inhibitor MK-0752 in patients with T-cell acute lymphoblastic leukemia/ lymphoma (T-ALL) and other leukemias. *J Clin Oncol*. 2006; 24:6585.

23. Real PJ, Tosello V, Palomero T, et al. Gamma-secretase inhibitors reverse glucocorticoid resistance in T cell acute lymphoblastic leukemia. *Nat Med.* 2009; 15:50-58.

24. Palomero T, Sulis ML, Cortina M, et al.Mutational loss of PTEN induces resistance to NOTCH1 inhibition in T-cell leukemia. *Nat Med.* 2007 Oct; 13(10):1203-10.

25. Steelman LS, Chappell WH, Abrams SL, et al. Roles of the Raf/MEK/ERK and PI3K/PTEN/Akt/mTOR pathways in controlling growth and sensitivity to therapy-implications for cancer and aging. *Aging*. 2011 Mar; 3(3):192-222.

26. Zhao L, Vogt PK. Hot-spot mutations in p110alpha of phosphatidylinositol 3-kinase (pI3K): differential interactions with the regulatory subunit p85 and with RAS. *Cell Cycle.* 2010; 9:596-600.

27. Franke TF, Kaplan DR, Cantley LC, et al. Direct regulation of the Akt proto-oncogene product by phosphatidylinositol-3,4- bisphosphate. *Science*. 1997; 275:665-668.

28. Martelli AM, Evangelisti C, Chiarini F, et al. The phosphatidylinositol 3-kinase/Akt/mTOR signaling network as a therapeutic target in acute myelogenous leukemia patients. *Oncotarget.* 2010; 1:89-103.

29. Martelli AM, Evangelisti C, Chiarini F, et al. The emerging role of the phosphatiylinositol 3-kinase/Akt/mammalian target of rapamycin signaling network in normal myelopoiesis and leukemogensis. *Biochim Biophys Act.* 2010; 1803:991-1002.

30. Lawlor MA, Alessi DR. PKB/Akt: a key mediator of cell proliferation, survival and insulin responses? *J Cell Sci.* 2001; 114:2903-10.

31. Coffer PJ, Jin J, Woodgett JR. Protein kinase B (c-Akt): a multifunctional mediator of phosphatidylinositol 3-kinase activation. *Biochem J.* 1998; 335 :1-13.

32. Hresko RC, Mueckler M. mTOR.RICTOR is the Ser473 kinase for Akt/protein kinase B in 3T3-L1 adipocytes. *J Biol Chem.* 2005; 280:40406-40416.

33. Manning BD, Cantley LC. AKT/PKB signaling: navigating downstream. *Cell.* 2007; 129:1261–1274.

34. Cantley LC. The phosphoinositide 3-kinase pathway. *Science.* 2002; 296:1655-7.

35. Bader AG, Kang S, Zhao L, et al. Oncogenic PI3K deregulates transcription and translation. *Nat Rev Cancer.* 2005; 5:921-9.

36. Vu C, Fruman DA. Target of Rapamycin Signaling in Leukemia and Lymphoma. *Clin Cancer Res.* 2010; 16:5374-5380.

37. Fruman DA, Meyers RE, Cantley LC. Phosphoinositide kinases. *Annu Rev Biochem.* 1998; 67:481-507.

38. Vanhaesebroeck B, Waterfield MD. Signaling by distinct classes of phosphoinositide 3-kinases. *Exp Cell Res.* 1999; 253:239-54.

39. Deane JA, Fruman DA. Phosphoinositide 3-kinase: Diverse roles in immune cell activation. *Annu Rev Immunol.* 2004; 22:563-98.

40. Blume-Jensen P, Hunter T. Oncogenic kinase signalling. *Nature.* 2001; 411:355-65.

41. Vivanco I, Sawyers CL. The phosphatidylinositol 3-Kinase AKT pathway in human cancer. *Nat Rev Cancer.* 2002; 2:489-501.

42. Samuels Y, Wang Z, Bardelli A, et al. High frequency of mutations of the PIK3CA gene in human cancers. *Science.* 2004; 304:554.

43. Abell K, Watson CJ. The Jak/Stat pathway: A novel way to regulate PI3K activity. *Cell Cycle.* 2005; 4:897-900.

44. Corvera S, Czech MP. Direct targets of phosphoinositide 3-kinase products in membrane traffic and signal transduction. *Trends Cell Biol.* 1998; 8:442-6.

45. Kang S, Bader AG, Vogt PK. Phosphatidylinositol 3-kinase mutations identified in human cancer are oncogenic. *Proc Natl Acad Sci USA.* 2005; 102:802-7.

46. Saal LH, Holm K, Maurer M, et al. PIK3CA mutations correlate with hormone receptors, node metastasis, and ERBB2, and are mutually exclusive with PTEN loss in human breast carcinoma. *Cancer Res.* 2005; 65:2554-9.

47. Campbell IG, Russell SE, Choong DY, et al. Mutation of the PIK3CA gene in ovarian and breast cancer. *Cancer Res.* 2004; 64:7678-81.

48. Kang S, Bader AG, Zhao L, et al. Mutated PI 3-kinases: Cancer targets on a silver platter. *Cell Cycle.* 2005; 4:578-81.

49. Eng C. PTEN: one gene, many syndromes. *Hum Mutat.* 2003; 22: 183–198.

50. Shatyesteh L, Lu Y, Kuo WL, et al. PIK3CA is implicated as an oncogene in ovarian cancer. *Nat Genet.* 1999; 21:99-102.

51. Maehama,T. et al. The tumor suppressor, PTEN/MMAC1, dephosphorylates the lipid second messenger, phosphatidylinositol 3,4,5- trisphosphate. *J Biol Chem*. 1998; 273: 13375–13378.

52. Leevers S J, Vanhaesebroeck B, Waterfield M D. Signalling through phosphoinositide 3-kinases: the lipids take centre stage. *Curr Opin Cell Biol*. 1999; 11: 219- 225.

53. Luo JM, Yoshida H, Komura S, et al. Possible dominant-negative mutation of the SHIP gene in acute myeloid leukemia. *Leukemia.* 2003; 17:1-8.

54. Stokoe D. Pten. *Curr Biol.* 2001; 11:R502.

55. Dahia PL. PTEN, a unique tumor suppressor gene. *Endocr Relat Cancer.* 2000; 7:115–129.

56. Sansal I, Sellers WR. The biology and clinical relevance of the PTEN tumor suppressor pathway. *J Clin Oncol.* 2004; 22:2954–63.

57. Alimonti A, Carracedo A, Clohessy JG, et al. Subtle variations in Pten dose determine cancer susceptibility. *Nat Genet.* 2010; 42:454–8.

58. Liaw D, Marsh DJ, Li J, et al. Germline mutations of the PTEN gene in Cowden disease, an inherited breast and thyroid cancer syndrome. *Nat Genet* .1997; 16:64–7.

59. Gutierrez A, Sanda T, Grebliunaite R, et al. High frequency of PTEN, PI3K, and AKT abnormalities in T-cell acute lymphoblastic leukemia. *Blood.* 2009; 114:647–50.

60. Roman-Gomez J, Jimenez-Velasco A, Agirre X, et al. Lack of CpG island methylator phenotype defines a clinical subtype of T-cell acute lymphoblastic leukemia associated with good prognosis. *J Clin Oncol.* 2005; 23:7043–9.

61. Silva A, Jotta PY, Silveira AB, et al. Regulation of PTEN by CK2 and Notch1 in primary T-cell acute lymphoblastic leukemia: rationale for combined use of CK2- and gamma-secretase inhibitors. *Haematologica.* 2010; 95:674–8.

62. Mavrakis KJ, Wolfe AL, Oricchio E, et al. Genome-wide RNA-mediated interference screen identifies miR-19 targets in Notch-induced T-cell acute lymphoblastic leukaemia. *Nat Cell Biol.* 2010; 12:372–9.

63. Rodriguez-Viciana P, Warne PH, Dhand R, et al. Phosphatidylinositol-3-OH kinase as a direct target of Ras. *Nature.* 1994; 370: 527–532.

64. Tamguney T, Stokoe D. New insights into PTEN. *J Cell Sci.* 2007; 120:4071–9.

65. Miller SJ, Lou DY, Seldin DC, et al. Direct identification of PTEN phosphorylation sites. *FEBS Lett.* 2002; 528:145–53.

66. Yim EK, Peng G, Dai H, et al. Rak functions as a tumor suppressor by regulating PTEN protein stability and function. *Cancer Cell.* 2009; 15:304–14.

67. Coffer PJ, Woodgett JR. Molecular cloning and characterisation of a novel putative protein-serine kinase related to the cAMP-dependent and protein kinase C families. *Eur J Biochem.* 1991; 201:475-481.

68. Scheid MP, Woodgett JR. PKB/AKT: functional insights from genetic models. *Nature Rev Mol Cell Biol*. 2001; 2:760–768.

69. Juntilla MM, Wofford JA, Birnbaum MJ, et al. Akt1 and Akt2 are required for ab thymocyte survival and differentiation. *Proc Natl Acad Sci USA.* 2007; 104:12105–12110.

70. Altomare DA, Testa JR. Perturbations of the AKT signaling pathway in human cancer. *Oncogene.* 2005; 24:7455-64.

71. Duronio V, Scheid MP, Ettinger S. Downstream signalling events regulated by phosphatidylinositol 3-kinase activity. *Cell Signal.* 1998; 10 233–239.

72. Jiang BH , Zheng JZ, Aoki M, et al. Phosphatidylinositol 3-kinase signaling mediates angiogenesis and expression of vascular endothelial growth factor in endothelial cells. *Proc Natl Acad Sci U S A* 2000; 97: 1749–1753.

73. Qiao M, Sheng S, Pardee AB. Metastasis and AKT activation. *Cell Cycle*. 2008 Oct; 7(19):2991-6.

74. Brognard J , Clark AS, Ni Y, et al. Akt/protein kinase B is constitutively active in non-small cell lung cancer cells and promotes cellular survival and resistance to chemotherapy and radiation. *Cancer Res*. 2001; 61 3986–3997.

75. Martelli AM , Tazzari PL, Tabellini G, et al. A new selective AKT pharmacological inhibitor reduces resistance to chemotherapeutic drugs, TRAIL, all-transretinoic acid, and ionizing radiation of human leukemia cells. *Leukemia.* 2003; 17:794–1805.

76. Datta SR, Brunet A, Greenberg ME. Cellular survival: a play in three Akts. *Genes Dev.* 1999; 13:2905–27.

77. Skinner HD, Zheng JZ, Fang J, et al. Vascular endothelial growth factor transcriptional activation is mediated by hypoxiainducible factor 1alpha, HDM2, and p70S6K1 in response to phosphatidylinositol 3-kinase/AKT signaling. *J Biol Chem*. 2004; 279: 45643–45651.

78. Bellacosa A, Kumar CC, Di Cristofano A, et al. Activation of AKT kinases in cancer: implications for therapeutic targeting. *Adv Cancer Res.* 2005; 94:29-86.

79. Carmeliet P , Lampugnani MG, Moons L, et al. Targeted deficiency or cytosolic truncation of the VE-cadherin gene in mice impairs VEGF-mediated endothelial survival and angiogenesis. *Cell.* 1999; 98:147–157.

80. Burgering BM , Coffer PJ. Protein kinase B (c-Akt) in phosphatidylinositol- 3-OH kinase signal transduction. *Nature.* 1995; 376: 599–602.

81. Carpten JD, Faber AL, Horn C, et al. A transforming mutation in the pleckstrin homology domain of AKT1 in cancer. *Nature*. 2007; 448:439-444.

82. Bellacosa A, DeFeo D, Godwin AK, et al. Molecular alterations of the Akt oncogene in breast cancer. *Int J Cancer.* 1995; 64:280-285.

83. Davies MA, Stemke-Hale K, Tellez C, et al. A novel Akt3 mutation in melanoma tumours and cell lines. *Brit J Cancer*. 2008; 99:1265-1268.

84. Troussard AA, Mawji NM, Ong C, et al. Conditional knock-out of integrin-linked kinase demonstrates an essential role in protein kinase B/Akt activation. *J Biol Chem*. 2003; 278:22374–8.

85. Feng J, Park J, Cron P, et al. Identification of a PKB/Akt hydrophobic motif Ser-473 kinase as DNA-dependent protein kinase. *J Biol Chem.* 2004; 279:41189–96.

86. Sarbassov DD, Guertin DA, Ali SM, et al. Phosphorylation and regulation of Akt/PKB by the rictor-mTOR complex. *Science.* 2005; 307:1098–1101.

87. Alessi DR, et al. Mechanism of activation of protein kinase B by insulin and IGF-1. *EMBO J*. 1996; 15: 6541–6551.

88. Guertin DA, et al. Ablation in mice of the mTORC components raptor, rictor, or mLST8 reveals that mTORC2 is required for signaling to Akt-FOXO and PKCalpha, but not S6K1. *Dev Cell.* 2006; 11:859–871.

89. Lee JT, Steelman LS, Chappell WH, et al. Akt Inactivates ERK causing decreased response to chemotherapeutic drugs in advanced CaP cells. *Cell Cycle*. 2008; 7:631-636.

90. Stephens L, Williams R, Hawkins P. Phosphoinositide 3-kinases as drug targets in cancer. *Curr Opin Pharmacol*. 2005; 5:357–365.

91. Engelman JA, Luo J, Cantley LC, The evolution of phosphatidylinositol 3-kinases as regulators of growth and metabolism. *Nat Rev Genet.* 2006; 7: 606–619.

92. Cross DA, Alessi DR, Cohen P, et al. Inhibition of glycogen synthase kinase-3 by insulin mediated by protein kinase B. *Nature*. 1995; 378:785-789.

93. Tamburini J, Green AS, Chapuis N, et al. Targeting translation in acute myeloid leukemia: a new paradigm for therapy? *Cell Cycle*. 2009; 8:3893- 3899.

94. Jiang BH, Liu LZ. Role of mTOR in anticancer drug resistance: perspectives for improved drug treatment. *Drug Resist Updat*. 2008 Jun; 11(3):63-76.

95. Gao T, Furnari F, Newton AC. PHLPP: a phosphatase that directly dephosphorylates Akt, promotes apoptosis, and suppresses tumor growth. *Mol Cell*. 2005; 18(1):13-24.

96. Brognard J, et al. PHLPP and a second isoform, PHLPP2, differentially attenuate the amplitude of Akt signaling by regulating distinct Akt isoforms. *Mol Cell.* 2007; 25: 917–931.

97. Diehl JA, Cheng M, Roussel MF, et al. Glycogen synthase kinase-3beta regulates cyclin D1 proteolysis and subcellular localization. *Genes Dev.* 1998; 12:3499-511.

98. Welcker M, Singer J, Loeb KR, et al. Multisite phosphorylation by Cdk2 and GSK3 controls cyclin E degradation. *Mol Cell.* 2003; 12:381-92.

99. Brown EJ, Albers MW, Shin TB, et al. A mammalian protein targeted by G1-arresting rapamycin-receptor complex. *Nature.* 1994; 369:756–758.

100. Chiu MI, Katz H, Berlin V. RAPT1, a mammalian homolog of yeast Tor, interacts with the FKBP12/ rapamycin complex. *Proc Natl Acad Sci USA*.1994; 91:12574–12578.

101. Keith CT, Schreiber SL. PIK-related kinases: DNA repair, recombination, and cell cycle checkpoints. *Science.* 1995; 270:50–51.

102. Kunz J, Henriquez R, Schneider U, et al. Target of rapamycin in yeast, TOR2, is an essential phosphatidylinositol kinase homolog required for G1 progression. *Cell.* 1993; 73:585–596.

103. Dennis PB, Jaeschke A, Saitoh M, et al. Mammalian TOR: a homeostatic ATP sensor. *Science.* 2001; 294:1102–1105.

104. Inoki K, Zhu T, Guan KL. TSC2 mediates cellular energy response to control cell growth and survival. *Cell.* 2003; 115:577–590.

105. Xu G, Zhang W, Bertram P, et al. Pharmacogenomic profiling of the PI3K/PTENAKT- mTOR pathway in common human tumors. *Int J Oncol.* 2004; 24:893–900.

106. Hara K, Maruki Y, Long X, et al. Raptor, a binding partner of target of rapamycin (TOR), mediates TOR action. *Cell.* 2002; 110:177– 189.

107. Fingar DC, Blenis J. Target of rapamycin (TOR): an integrator of nutrient and growth factor signals and coordinator of cell growth and cell cycle progression. *Oncogene.* 2004; 23:3151–3171.

108. Jacinto E, Loewith R, Schmidt A, et al. Mammalian TOR complex 2 controls the actin cytoskeleton and is rapamycin insensitive. *Nat Cell Biol.* 2004; 6:1122–1128.

109. Sarbassov DD, Ali SM, Kim DH, et al. Rictor, a novel binding partner of mTOR, defines a rapamycin-insensitive and raptorindependent pathway that regulates the cytoskeleton. *Curr Biol.* 2004; 14:1296–1302.

110. Park S, Chapuis N, Tamburini J, et al.Role of the PI3K/AKT and mTOR signaling pathways in acute myeloid leukemia. *Haematologica*. 2010 May; 95(5):819-28.

111. Valentinis B, Baserga R. IGF-I receptor signalling in transformation and differentiation. *Mol Pathol.* 2001; 54:133–137.

112. Inoki K, Li Y, Zhu T, et al. TSC2 is phosphorylated and inhibited by Akt and suppresses mTOR signalling. *Nat Cell Biol.* 2002; 4:648–657.

113. Nave BT, Ouwens M, Withers DJ, et al. *Biochem J.* 1999; 344 (Pt 2): 427.

114. Alessi DR, Kozlowski MT, Weng QP, et al. 3-Phosphoinositide-dependent protein kinase 1 (PDK1) phosphorylates and activates the p70 S6 kinase in vivo and in vitro. *Curr Biol.* 1998; 8:69–81.

115. Pullen N, Dennis PB, Andjelkovic M, et al. Phosphorylation and activation of p70s6k by PDK1. *Science.* 1998; 279:707–710.

116. Saitoh M, Pullen N, Brennan P, et al. Regulation of an activated S6 kinase 1 variant reveals a novel mammalian target of rapamycin phosphorylation site. *J Biol Chem.* 2002; 277:20104–20112.

117. Isotani S, Hara K, Tokunaga C, et al. Immunopurified mammalian target of rapamycin phosphorylates and activates p70 S6 kinase alpha in vitro. *J Biol Chem.* 1999; 274:34493–34498.

118. Montagne J, Stewart MJ, Stocker H, et al. Drosophila S6 kinase: a regulator of cell size. *Science.* 1999; 285:2126–2129.

119. Jefferies HB, Reinhard C, Kozma SC, et alG. Rapamycin selectively represses translation of the "polypyrimidine tract" mRNA family. *Proc Natl Acad Sci USA.* 1994; 91:4441–4445.

120. Petroulakis E, Mamane Y, Le Bacquer O, et al. mTOR signaling: implications for cancer and anticancer therapy. *Br J Cancer.* 2006; 94: 195-199.

121. Um SH, Frigerio F, Watanabe M, et al. Absence of S6K1 protects against age- and diet-induced obesity while enhancing insulin sensitivity. *Nature.* 2004; 431: 200-205.

122. Pause A, Belsham GJ, Gingras AC, et al. Insulin dependent stimulation of protein synthesis by phosphorylation of a regulator of 5'-cap function. *Nature.* 1994; 371:762–767.

123. Marcotrigiano J, Gingras AC, Sonenberg N, et al. Cap-dependent translation initiation in eukaryotes is regulated by a molecular mimic of eIF4G. *Mol Cell.* 1999; 3:707–716.

124. Gingras AC, Raught B, Sonenberg N. eIF4 initiation factors: effectors of mRNA recruitment to ribosomes and regulators of translation. *Annu Rev Biochem.* 1999; 68:913–963.

125. Lewis TS, Shapiro PS, Ahn NG. Signal transduction through MAP kinase cascades. *Adv Cancer Res.* 1998; 74: 49-139.

126. Nishimoto S, Nishida E. MAPK signalling: ERK5 versus ERK1/2. *EMBO Rep*. 2006; 7: 782-786.

127. McNeil LK, Starr TK, Hogquist KA. A requirement for sustained ERK signaling during thymocyte positive selection in vivo. *Proc Natl Acad Sci USA.* 2005; 102: 13574–13579.

128. Palomero T, Sulis ML, Cortina M, et al. Mutational loss of PTEN induces resistance to NOTCH1 inhibition in T-cell leukemia. *Nat Med*. 2007 Oct; 13(10):1203-10.

129. Cheng JT, Cobb MH, Baer R. Phosphorylation of the TAL1 oncoprotein by the extracellular-signal-regulated protein kinase ERK1. *Mol Cell Biol.* 1993; 13: 801-808.

130. Barata JT, Cardoso AA, Boussiotis VA. Interleukin-7 in T-cell acute lymphoblastic leukemia: an extrinsic factor supporting leukemogenesis? *Leuk Lymphoma.* 2005; 46: 483-495.

131. McCubrey JA, Steelman LS, Abrams SL, et al. Targeting Survival Cascades Induced by Activation of Raf/Raf/ MEK/ERK, PI3K/PTEN/Akt/mTOR and Jak/STAT pathways for effective leukemia therapy. *Leukemia*. 2008; 22:708- 722.

132. Downward J. Targeting Ras signaling pathways in cancer therapy. *Nature Reviews Cancer*. 2003; 3:11-22.

133. Hayashi K, Shibata K, Morita T, et al. Insulin receptor substrate-1/SHP-2 interaction, a phenotypedependent switching machinery of insulin-like growth factor-I signaling in vascular smooth muscle cells. *J Biol Chem*. 2004; 279:40807-40818.

134. Marais R, Light Y, Paterson HF, et al. Ras recruits Raf-1 to the plasma membrane for activation by tyrosine phosphorylation. *EMBO J.* 1995; 14:3136-145.

135. McCubrey JA, Steelman LS, Abrams SL, et al. Emerging Raf inhibitors. *Exp Opin Emerging Drugs.* 2009; 14:633-648.

136. Lefloch R, Pouyssegur J, Lenormand P. Total ERK1/2 activity regulates cell proliferation. *Cell Cycle.* 2009; 8:705-711.

137. Xing J, Ginty DD, Greenberg ME. Coupling of the Ras-MAPK pathway to gene activation by Rsk2, a growth factor regulated CREB kinase. *Science*. 1996; 273:959-963.

138. Balan V, Leicht DT, Zhu J, et al. Identification of novel in vivo Raf-1 phosphorylation sites mediating positive feedback Raf-1 regulation by extracellular signal-regulated kinase. *Mol Biol Cell*. 2006; 17:1141-1153.

139. Davis RJ. Transcriptional regulation by MAP kinases. *Mol Reprod Dev*. 1995; 42:459-467.

140. Korotchkina LG, Leontieva OV, Bukreeva EI, et al. The choice between p53-induced senescence and quiescence is determined in part by the mTOR pathway. *Aging*. 2010; 2:344-352.

141. Sebolt-Leopold JS, Herrera R. Targeting the mitogen-activated protein kinase cascade to treat cancer. *Nat Rev Cancer*. 2004; 4:937–947.

142. Bacher U, Haferlach T, Schoch C, et al. Implications of NRAS mutations in AML: a study of 2502 patients. *Blood*. 2006; 107:3847-3853.

143. Bos JL. Ras oncogenes in human cancer: a review. *Cancer Research.* 1989; 49:4682-9.

144. Wan PT, Garnett MJ, Roe SM, et al. Mechanism of activation of the RAFERK signaling pathway by oncogenic mutations of B-RAF. *Cell.* 2004; 116:855-867.

145. Davies H, Bignell GR, Cox C, et al. Mutations of the BRAF gene in human cancer. *Nature*. 2002; 417:949-954.

146. Johnson SM, Grosshans H, Shingara J, et al. RAS is regulated by the let-7 microRNA family. *Cell.* 2005; 120: 635–647.

147. Repasky GA, Chenette EJ, Der CJ, Renewing the conspiracy theory debate: does Raf function alone to mediate Ras oncogenesis? *Trends Cell Biol*. 2004; 14: 639–647.

148. Castro AF, Rebhun JF, Clark GG, et al. Rheb binds TSC2 and promotes S6 kinase activation in a rapamycinand farnesylation-dependent manner. *J Biol Chem*. 2003; 278:32493–32496.

149. Han S , Santos TM, Puga A, et al. Phosphorylation of tuberin as a novel mechanism for somatic inactivation of the tuberous sclerosis complex proteins in brain lesions. *Cancer Res*. 2004; 64(3):812-16.

150. Ma L, Chen Z, Erdjument-Bromage HP, et al. Phosphorylation and functional inactivation of TSC2 by Erk implications for tuberous sclerosis and cancer pathogenesis. *Cell.* 2005; 121(2): 179.

151. Roux PP, Ballif BA, Anjum R, et al. Tumor-promoting phorbol esters and activated Ras inactivate the tuberous sclerosis tumor suppressor complex via p90 ribosomal S6 kinase. *Proc Natl Acad Sci U S A.* 2004; 101:13489–94.

152. Jun T, Gjoerup O, Roberts TM. Tangled webs: evidence of cross-talk between c-Raf-1 and Akt. *Sci STKE.* 1999; PE1.

153. Carracedo A, Ma L, Teruya-Feldstein J, et al. Inhibition of mTORC1 leads to MAPK pathway activation through a PI3K-dependent feedback loop in human cancer. *J Clin Invest.* 2008; 118: 3065–3074.

154. Li J, Liu J, Song J, et al. mTORC1 inhibition increases neurotensin secretion and gene expression through activation of the MEK/ERK/c-Jun pathway in the human endocrine cell line BON. *Am J Physiol Cell Physiol*. 2011.

155. Dreesen O, Brivanlou AH. Signaling pathways in cancer and embryonic stem cells. *Stem Cell Rev.* 2007; 3:7-17.

156. Valentino L, Pierre J. JAK/STAT signal transduction: regulators and implication in hematological malignancies. *Biochem Pharmacol.* 2006; 71: 713-721.

157. Flex E, Petrangeli V, Stella L, et al. Somatically acquired JAK1 mutations in adult acute lymphoblastic leukemia. *J Exp Med.* 2008; 205: 751–758.

158. Carron C, Cormier F, Janin A, et al. TEL-JAK2 transgenic mice develop T-cell leukemia. *Blood.* 2000; 95: 3891-3899.

159. Sinibaldi D, Wharton W, Turkson J, et al. Induction of p21WAF1/CIP1 and cyclin D1 expression by the Src oncoprotein in mouse fibroblasts: role of activated STAT3 signaling. *Oncogene.* 2000; 19: 5419-5427.

160. Alvarado Y , Mita MM, Vemulapalli S, et al. Clinical activity of mammalian target of rapamycin inhibitors in solid tumors. *Target Oncol.* 2011; 6: 69–94.

161. Guertin DA, Sabatini DM. The pharmacology of mTOR inhibition. *Sci Signal.* 2009; 2:24.

162. Abraham RT, Eng CH. Mammalian target of rapamycin as a therapeutic target in oncology. *Expert Opin Ther Targets.* 2008; 12:209–22.

163. Janes MR, Fruman DA. Targeting TOR dependence in cancer. *Oncotarget*. 2010; 1:69–76.

164. Hudes G, Carducci M, Tomczak P, et al. Temsirolimus, interferon alfa, or both for advanced renalcell carcinoma. *The New England Journal of Medicine.* 2007; 356:2271–81.

165. LoPiccolo J, Blumenthal GM, Bernstein WB, et al. Targeting the PI3K/Akt/ mTOR pathway: effective combinations and clinical considerations. *Drug Resist Updat.* 2008; 11:32–50.

166. Efeyan A, Sabatini DM. MTOR and cancer: many loops in one pathway. *Curr Opin Cell Biol.* 2010; 22:169–176.

167. Sarbassov DD, Ali SM, Sengupta S, et al. Prolonged rapamycin treatment inhibits mTORC2 assembly and Akt/PKB. *Mol Cell.* 2006; 22: 159–68.

168. Zeng Z, Sarbassov dos D, Samudio IJ, et al. Rapamycin derivatives reduce mTORC2 signaling and inhibit AKT activation in AML. *Blood.* 2007; 109:3509–12.

169. Shor B, Gibbons JJ, Abraham RT, et al. Targeting mTOR globally in cancer: thinking beyond rapamycin. *Cell Cycle.* 2009; 8:3831–7.

170. Garcia-Echeverria C, Sellers WR. Drug discovery approaches targeting the PI3K/Akt pathway in cancer. *Oncogen*e. 2008; 27: 5511–26.

171. Yap TA, Garrett MD, Walton MI, et al. Targeting the PI3K-AKT-mTOR pathway: progress, pitfalls, and promises. *Curr Opin Pharmacol.* 2008; 8:393–412.

172. Zoncu R, Efeyan A, Sabatini DM. MTOR: from growth signal integration to cancer, diabetes and ageing. *Nat Rev Mol Cell Biol*. 2011; 12:21–35.

173. Yu K, Toral-Barza L, Shi C, et al. Biochemical, cellular, and in vivo activity of novel ATP-competitive and selective inhibitors of the mammalian target of rapamycin. *Cancer Res*. 2009; 69: 6232–6240.

174. Janes MR, Limon JJ, So L, et al. Effective and selective targeting of leukemia cells using a TORC1/2 kinase inhibitor. *Nat Med.* 2010; 16: 205–13.

175. Arbiser JL, Kau T, Konar M, et al. Solenopsin, the alkaloidal component of the fire ant (Solenopsis invicta), is a naturally occurring inhibitor of phosphatidylinositol-3-kinase signaling and angiogenesis. *Blood.* 2007; 109: 560–565.

176. Xia C, Meng Q, Cao Z, et al. Regulation of angiogenesis and tumor growth by p110 alpha and AKT1 via VEGF expression. *J Cell Physiol*. 2006; 209: 56–66.

177. Epling-Burnette PK, Liu JH, Catlett-Falcone R, et al. Inhibition of STAT3 signaling leads to apoptosis of leukemic large granular lymphocytes and decreased Mcl-1 expression. *J Clin Invest.* 2001; 107: 351–362.

178. Eriksen KW, Kaltoft K, Mikkelsen G, et al. Constitutive STAT3-activation in Sezary syndrome: tyrphostin AG490 inhibits STAT3-activation, interleukin-2 receptor expression and growth of leukemic Sezary cells. *Leukemia.* 2001; 15: 787–793.

179. Ihle NT, Paine-Murrieta G, Berggren MI, et al. The phosphatidylinositol-3- kinase inhibitor PX-866 overcomes resistance to the epidermal growth factor receptor inhibitor gefitinib in A-549 human non-small cell lung cancer xenografts. *Mol Cancer Ther*. 2005; 4:1349–1357.

180. Ward SG, Finan P. Isoform-specific phosphoinositide 3 -kinase inhibitors as therapeutic agents. *Curr Opin Pharmacol.* 2003 Aug; 3(4):426-34.

181. Granville CA , Memmott RM, Gills JJ, et al. Handicapping the race to develop inhibitors of the phosphoinositide 3-kinase/Akt/mammalian target of rapamycin pathway. *Clin Cancer Res*. 2006; 12:679–689.

182. Hilgard P, et al. D-21266, a new heterocyclic alkylphospholipid with antitumour activity. *Eur J Cancer.* 1997; 33:442–446.

183. Chiarini F, Del Sole M, Mongiorgi S, et al. The novel Akt inhibitor, perifosine, induces caspase-dependent apoptosis and downregulates P-glycoprotein expression in multidrug-resistant human T-acute leukemia cells by a JNK-dependent mechanism. *Leukemia*. 2008; 22: 1106–1116.

184. Nyakern M, Cappellini A, Mantovani I, et al. Synergistic induction of apoptosis in human leukemia T cells by the Akt inhibitor perifosine and etoposide through activation of intrinsic and Fas-mediated extrinsic cell death pathways. *Mol Cancer Ther.* 2006; 5: 1559–1570.

185. Fala F, Blalock WL, Tazzari PL, et al. Proapoptotic activity and chemo-sensitizing effect of the novel Akt inhibitor (2S)-1-(1H-Indol-3-yl)-3-[5-(3-methyl-2H-indazol-5-yl)- pyridin-3-yl]oxypropan2-ami ne (A443654) in T-cell acute lymphoblastic leukemia. *Mol Pharmacol.* 2008; 74: 884–895.

186. Fan QW, Knight ZA, Goldenberg DD, et al. A dual PI3 kinase/mTOR inhibitor reveals emergent efficacy in glioma. *Cancer Cell.* 2006; 9: 341–349.

187. Chiarini F, Fala F, Tazzari PL, et al. Dual inhibition of class IA phosphatidylinositol 3-kinase and mammalian target of rapamycin as a new therapeutic option for T-cell acute lymphoblastic leukemia. *Cancer Res.* 2009; 69: 3520–3528.

188. Maira SM, et al. Identification and characterization of NVP-BEZ235, a new orally available dual phosphatidylinositol 3-kinase/mammalian target of rapamycin inhibitor with potent in vivo antitumor activity. *Mol Cancer Ther*. 2008; 7:1851–1863 .

189. Liu P, Cheng H, Roberts TM, et al.Targeting the phosphoinositide 3-kinase pathway in cancer. *Nat Rev Drug Discov*. 2009; Aug; 8(8):627-44.

Table 2.1

Summary of drugs targeting the PI3K pathway in clinical trials for cancer treatment. Adapted from Liu et al. (2009).[189]

Agent	Target	Sponsor	Phase	Cancer type or condition
PI3K inhibitors:				
BEZ235	Class I PI3K/mTOR	Novartis	Phase I–II	Advanced solid tumors; advanced breast cancer
BGT226	Class I PI3K/ mTOR	Novartis	Phase I–II	Solid tumors; advanced breast cancer; Cowden's syndrome
BKM120	Class I PI3K	Novartis	Phase I	Solid tumors
GDC0941	Class I PI3K	Genentech	Phase I	Advanced solid tumors; non‐Hodgkin's lymphoma
SF1126	Pan‐PI3K/ mTOR	Semafore	Phase I	Advanced solid tumors
GSK1059615	Pan‐PI3K	GlaxoSmith Kline	Phase I	Advanced solid tumors; metastatic breast cancer; endometrial cancer; lymphoma
AKT inhibitors:				
Perifosine (akaKRX‐0401)	AKT	Keryx	Phase I–II	Solid tumors; multiple myeloma; ovarian cancer; soft‐tissue sarcoma; malignant melanoma
MK2206	AKT	Merck	Phase I	Advanced solid tumors
VQD‐002	AKT	VioQuest	Phase I	Haematological malignancies; leukaemia; NSC lung cancer
XL418	AKT and S6K	Exelixis	Phase I	Solid tumors
mTOR inhibitors:				
Rapamycin/ sirolmus (Rapamune)	mTORC1	Wyeth	Phase I–II Approved	Solid tumors; metastatic breast cancer; myeloid leukaemia Advanced renal cell carcinoma
Temsirolimus (CCI‐779/ Torisel)	mTORC1	Wyeth	Phase I–III Approved	Solid tumors; MM; ovarian and endometrial cancer; mantle cell lymphoma; brain tumors; NSCLC; melanoma Advanced renal cell carcinoma
Everolimus (RAD001/ Afinitor)	mTORC1	Novartis	Phase I–III Approved	Solid tumors; HCC; bladder, head and neck cancer; glioma/astrocytoma; prostate cancer; brain tumors; gastric, breast and pancreatic cancer Soft‐tissue and bone sarcomas
AZD8055	mTORC1 and mTORC2	AstraZeneca	Phase I–II	Solid tumors; endometrial carcinoma; Lymphoma

mTOR, mammalian target of rapamycin; mTORC1, mTOR complex 1; PI3K, phosphoinositide 3‐kinase; S6K1, ribosomal protein S6 kinase 1 (also known as p70S6K). *Information presented is compiled from company websites and from www.clinicaltrials.gov and www.fda.gov. ‡The trial has been suspended due to low drug exposure.

Figure 2.1. Schematic representation of the NOTCH1 signaling pathway and transcriptional networks promoting leukemic cell growth downstream of oncogenic NOTCH1. The two subunits of the mature NOTCH1 receptor are generated by cleavage by a furin protease in the trans-Golgi network soon after translation of NOTCH1 precursor protein. The extracellular subunit responsible for ligand-receptor interaction and the transmembrane subunit responsible for triggering transcription activation interact by their respective heterodimerization (HD) domains. Upon binding to its ligands (BD-like 1, 3, and 4; Jagged 1 and 2B), the transmembrane portion of NOTCH1 is sequentially cleaved by ADAM proteases and then by the γ-secretase complex. This final proteolytic cleavage liberates the active intracellular fragment of NOTCH1, which translocates to the nucleus and activates the expression of target genes by forming a ternary complex with the CSL DNA binding protein and the MAML1 transcriptional coactivator. Small-molecule inhibitors of the γ-secretase block NOTCH1 activation by retaining the receptor at the membrane. NOTCH1 promotes cell growth by transcriptional up-regulation of genes involved in anabolic pathways and also by transcriptional up-regulation of MYC. In addition, NOTCH1 induces the expression of HES1, a transcriptional repressor that promotes the up-regulation of the PI3K-AKT signaling pathway by transcriptional down-regulation of PTEN. Termination of NOTCH1 signaling is mediated by phosphorylation-coupled degradation of the activated receptor in the proteasome via FBXW7-SCF.[2]

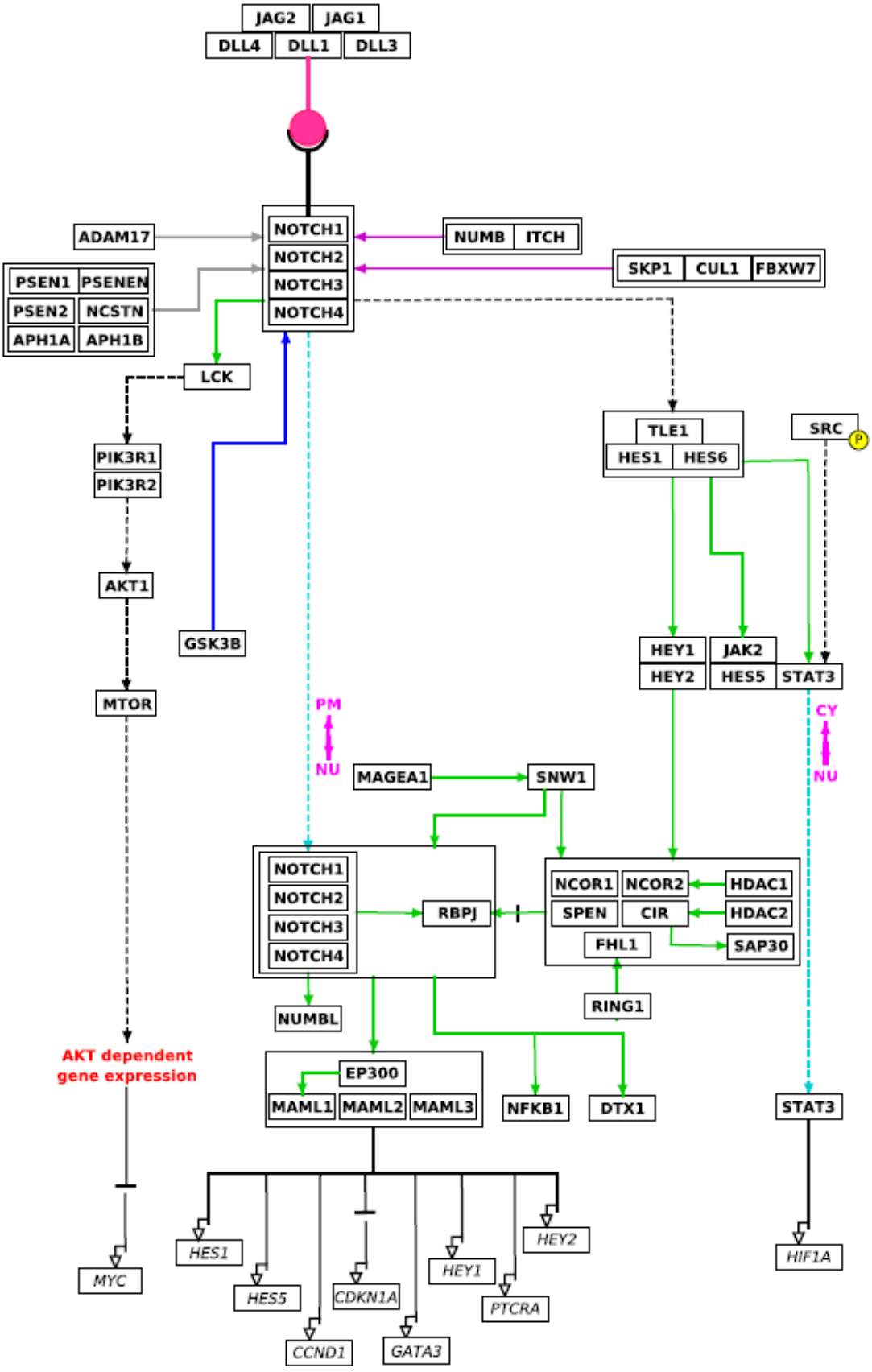
JAG2
JAG1
DLL4
DLL1
DLL3
ADAM17
NOTCH1
NOTCH2
NOTCH3
NOTCH4
NUMB
ITCH
SKP1
CUL1
FBXW7
PSEN1
PSENEN
PSEN2
NCSTN
APH1A
APH1B
LCK
PIK3R1
PIK3R2
AKT1
GSK3B
MTOR
TLE1
HES1
HES6
SRC
HEY1
HEY2
JAK2
HES5
STAT3
PM
NU
CY
NU
MAGEA1
SNW1
NOTCH1
NOTCH2
NOTCH3
NOTCH4
RBPJ
NCOR1
NCOR2
SPEN
CIR
FHL1
HDAC1
HDAC2
SAP30
RING1
NUMBL
AKT dependent
gene expression
EP300
MAML1
MAML2
MAML3
NFKB1
DTX1
STAT3
HES1
HES5
CCND1
CDKN1A
GATA3
HEY1
PTCRA
HEY2
MYC
HIF1A

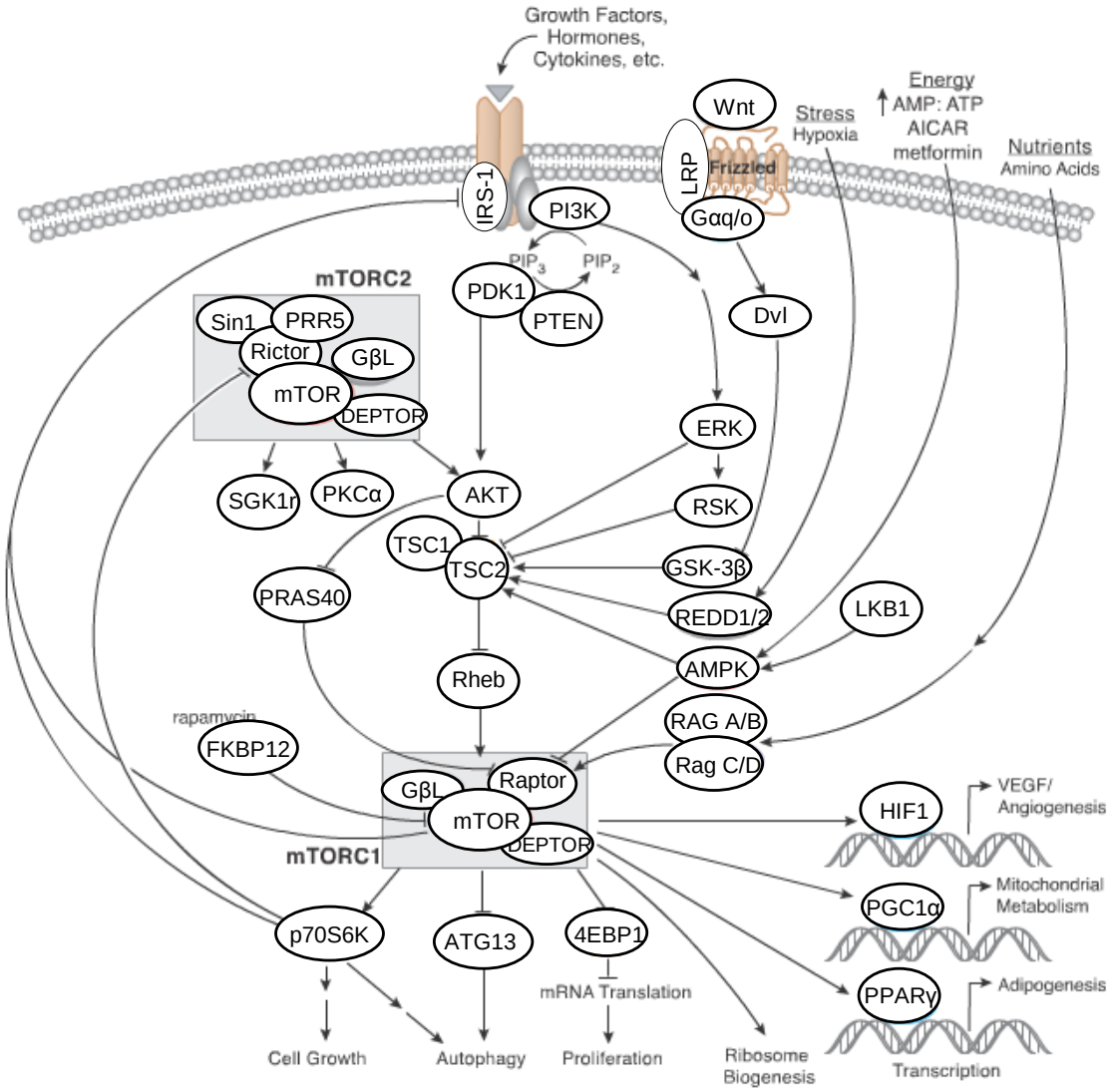

Figure 2.2. Diagram of key features of the PI3K/AKT/mTOR signaling network. The lipid kinase PI3K is activated downstream of oncogenic receptors or intracellular proteins in various hematological diseases, with examples shown. PI3K produces second messagers phosphatidylinositol-3,4-diphosphate (PIP2) and phosphatidylinositol-3,4,5-triphosphate (PIP3), which activates PDK1 and Akt. The mTOR serine-threonine kinase is present in two distinct multiprotein complexes, termed mTORC1 and mTORC2. Key substrates are shown, and their activities are either increased (pointed arrows) or decreased (block arrows) by mTOR-mediated phosphorylation. (Adapted from Vu and Fruman 2010[36]).

CHAPTER 3

ZEBRAFISH AS A MODEL ORGANISM FOR NORMAL AND MALIGNANT HEMATOPOIESIS

Historical background

The zebrafish (*Danio rerio*) is a small tropical fish, popular in home aquariums, that has become a powerful animal model system for understanding the genetic basis of vertebrate development. The initial interest in zebrafish as a model system goes back to the early 1970s when George Streisinger selected zebrafish larvae to develop the first vertebrate assay enabling forward genetic screening.[1] During the subsequent 20 years, zebrafish were almost exclusively used for studying developmental biology and organ development in particular. This resulted in the characterization of an exceptionally large number of genes involved in vertebrate pathways, which contributed to the establishment of zebrafish as a relevant model for human disease and pharmaceutical research.[2,3]

Early studies

In more recent decades, the zebrafish has developed into an important model organism for biomedical research. Although the main focus of zebrafish research had traditionally been on developmental biology, keeping and monitoring zebrafish in the lab led to the observation and identification of diseases similar to those in humans, such as cancer, which subsequently became a subject for study.[4] In 1993, two large–scale ENU-

based mutagenesis screens in zebrafish were simultaneously performed at the Massachusetts General Hospital (Boston, MA) and the Max-Planck Institute (Tübingen, Germany), which resulted in the identification of thousands of mutants exhibiting a vast array of developmental phenotypes.[3,5] Since then, the zebrafish has increasingly become a model of human disease, since mutants have been found with mutations in the orthologs of human disease genes.

Zebrafish have contributed to hematologic research for more than 50 years. Interest in zebrafish embryology dates to the 1930s,[6] and they have long been used for zoology and toxicology research.[7] However, their developmental hematology only entered the literature in 1963 with the second appearance of zebrafish in the journal *Nature*, as a representative teleost fish with an intraembryonic origin for blood.[8] Then the first descriptions of zebrafish blood cell morphology appeared in the 1970s.[9-11] The modern phase of zebrafish hematology research, driven by genetic experimental approaches, started just over 10 years ago with the collection of zebrafish mutants with hematopoietic defects, mostly recognized for their anemia.[12-14]

Zebrafish disease model strengths

Zebrafish exhibit a number of characteristics that make it an exceptionally strong model organism for scientific research. Their small size (<5 cm as adults) means that more zebrafish can be housed in a smaller space and with far less maintenance expense than other mammalian models, such as mice. Furthermore, zebrafish have high fecundity, with a single mating pair producing up to 100 transparent eggs twice per week. Thereafter fertilization and embryogenesis take place *ex vivo*, thus facilitating *in vitro* fertilization as well as developmental observation from as early as the single-cell stage.

Embryos remain translucent for several days, allowing unprecedented visualization of the development and function of somatic systems. Moreover, cells can be tracked either with specific probes using whole mount *in situ* (WISH) in fixed embryos, or followed in realtime in live transgenic fish in which fluorochromes have been used to tag cells.

The zebrafish is a vertebrate with complex organs and represents a blueprint for all vertebrate organogenesis. Rapid organogenesis is a strength of zebrafish as an experimental organism with most organs becoming fully functional within 3-5 days post-fertilization (dpf). This rapid organogenesis coupled with transparent embryos for several days after fertilization make the zebrafish uniquely qualified among experimental organisms for studies in vertebrate organ development and function (Figure 3.1A).[15,16]

The zebrafish genome is also sequenced with multiple genetic markers and gene chips are already available commercially. For these reasons, large zebrafish screens can be carried out speedily and at relatively low cost to dissect the molecular basis of developmental pathways as well as the phenotypic analysis of embryogenesis and organogenesis *in vivo*.

The zebrafish is amenable to forward genetic screens on a scale that is not feasible in any other vertebrate models.[17] There is a high degree of genetic conservation between man and other vertebrates despite millions of years of divergent evolution.[18-19] Invertebrate models are generally unable to recapitulate the pathogenesis of many human diseases. By contrast, the zebrafish system allows forward genetic approaches in a vertebrate that can manifest the pathologies of human diseases. In addition, the establishment of transgenic lines expressing fluorochromes, such as green fluorescent protein (GFP), in specific developing tissues,[20,21] makes the transparent developing

zebrafish particularly amenable to *in vivo* studies of neoplastic progression, metastasis, and remission.

Zebrafish are also highly amenable to reverse genetic studies (reviewed in Refs. 22,23). Key reverse genetic techniques for functionally studying genes of interest in zebrafish include transient gene over-expression and knockdown, stable transgenesis,[24] and recovering stable mutated alleles by the TILLING method (Targeting Induced Local Lesions in Genomes).[25] Zebrafish mutants can also be obtained from catalogued libraries of insertional mutants.[26]

Because fertilization and development occur *ex utero* in zebrafish, alternative chemical means may be used to phenocopy the impact of mutagenesis, but within a much shorter and less expensive experimental timeframe. For instance, antisense morpholinos are routinely used to knock down target protein expression in zebrafish embryos by micro-injection at the one-cell stage. Antisense morpholinos block either mRNA splicing or translation, both of which lead to loss of expression of the targeted gene. Morpholino-mediated knock down is transient,[27] lasting for only up to 3-4 days.[28] However, due to rapid organogenesis, this is often sufficient time to phenocopy mutants with mutations in the corresponding target genes during early development.[29]

Transgenic zebrafish generation via ZFN, TILLING and TALEN mutagenesis

The development of zebrafish models that accurately phenocopy human congenital diseases requires the generation of tailor-made mutations in the orthologs of human disease genes. Targeted knockout approaches and the engineering of genes carrying predetermined mutations has been very successful in mice, but are not feasible in zebrafish due to the inability to grow embryonic stem cells. A step forward towards

recovering mutations in a gene of interest has been the introduction of TILLING (Targeted Induced Local Lesions IN Genomes) methodology.[30-32] This reverse genetics strategy utilizes the screening of chemically mutagenized genomes by resequencing and TILLING to identify mutations in specific genes. More recently, zinc-finger nuclease (ZFN) technology has been developed that offers the possibility to engineer mutations in specific zebrafish genes.[33,34] The technique employs zinc-finger nucleases, chimeric molecules consisting of a DNA binding zinc-finger domain and the FokI restriction endonuclease, to induce targeted mutations in any gene of interest. This technique offers the possibility of a rational and straightforward strategy to engineer precise models of human inherited diseases in zebrafish.

Alternatively, a more recent technology has emerged, referred to as "TALEN" (Transcription Activator-Like Effector Nuclease). TALENs, which comprise an engineered array of transcription activator-like effector repeats fused to the nonspecific FokI cleavage domain, introduce targeted double-stranded breaks in human cells at specific targeted DNA sequences with high efficiency. Repair of these double-stranded breaks by normal DNA repair mechanisms, such as nonhomologous end-joining or homologous recombination, enables introduction of alterations at or near the site of the break.[35]

The same TALEN technology has recently been applied to zebrafish embryos via microinjection of TALEN constructs at the one-cell stage. This has resulted in the efficient introduction of small insertions or deletions (indels) at cleavage sites in endogenous zebrafish genes. These indels frequently result in frameshift knockout mutations that can be passed through the germ line to create mutant fish. Thus the ability

to use both ZFNs and TALENs should enable any researcher to rapidly and easily create targeted mutations in any zebrafish gene of interest.[36,37]

In zebrafish, the application of chemical genetics to dissect biological processes has also become an attractive alternative to mutagenesis screens due to its technical simplicity, inexpensive reagents, and low startup costs. It also offers a new approach in that it is reversible and adjustable, allowing dosing adjustments to be made. In a zebrafish chemical genetic screen, small molecule inhibitors may be added directly to fish water in a 48- or 96-well format and used to block a specific protein function (Figure 3.1B). In vertebrates, only fish and amphibians are amenable to chemical genetic screens carried out in this format.[38,39]

Zebrafish disease model limitations

One of the more obvious zebrafish disease model limitations is the lack of a respiratory system as found in mammals. Hence, diseases of the mammalian respiratory system cannot be recapitulated in zebrafish. Another limitation of the zebrafish system is that the blood-brain barrier of the larval zebrafish is not fully formed until 10dpf. Therefore, the assessment of CNS-mediated effects in larvae may erroneously identify compounds that are excluded from the brain in older fish and in mammals. Furthermore, the larval zebrafish is a rapidly-developing system, which may not be appropriate for modeling the effects of compounds on adults.[40]

The zebrafish also lacks an extended history of disease model experimentation. Unlike many mammalian models that have been used for decades, the zebrafish cannot benefit from a large reservoir of historical data establishing the system's validity and

limitations. Lack of antibodies to surface proteins and difficulty of establishing cell cultures are two additional limitations.[41]

Zebrafish cancer models

Throughout its research history, zebrafish have mostly been used for developmental studies. However, while keeping zebrafish in the laboratory environment, researchers noticed different diseases developing in adult fish, including cancer. Human disease models for drug efficacy screening have also been developed in zebrafish across a wide range of disease areas, including cardiovascular disease, infection, inflammation and metabolic diseases.[42] Studies on zebrafish cancer revealed that zebrafish spontaneously develop many types of tumors.[43-46] This led to enthusiasm that the development of zebrafish cancer models could enable researchers to exploit them to conduct modifier screens. Such modifier screens could combine the ability to model human cancer pathologies with the capacity for powerful forward genetic analysis in this organism.[47]

Zebrafish oncogenesis induction

Because zebrafish in the wild develop cancer relatively infrequently, researchers sought to accelerate the tumorigenesis process through various means. There are three principal ways that cancer can be experimentally induced in zebrafish: (i) carcinogen treatment; (ii) transgenesis; and (iii) genetic predisposition achieved by induced mutations or insertions.[47] Researchers have appreciated the relative ease of treating fish with carcinogens because the chemicals can be dissolved or suspended in water and the

animals can be exposed for longer time periods.[48,49] Historically, fish had already been used as a model for toxicological and carcinogenesis assays.[50,51]

While it is difficult to document the extent of spontaneous fish tumorigenesis in the wild, upon exposure to aqueous carcinogen treatments they can develop a wide range of benign and malignant tumors. Interestingly, many of these fish cancers histologically resemble human tumors, suggesting the conservation of genetic mechanisms underlying the pathogenic changes associated with malignancy.[52-54] In support of this, fish have many orthologs of the oncogenes and tumor suppressor genes that have been identified in mouse and humans, including multiple *Myc*, *Ras*, and *Notch* family members, *β-catenin*, *p53*, *Mdm2*, *Bcl-2*, and *Bcl-xL*. Strong amino acid similarities and functional studies suggest the conservation of these proteins with their mammalian counterparts.[55-57] Of note also is the fact that teleosts, including zebrafish, lack *ARF*, which in mammals functions as a tumor suppressor gene via regulation of p53 activity.[58]

Zebrafish transgenesis

The largest number of studies on cancer development in zebrafish at this point come from transgenic zebrafish expressing mammalian oncogenes. This approach takes advantage of the ability to inject foreign DNA into one-cell-stage zebrafish embryos.[4] Generating stable transgenic zebrafish is efficiently done with *Tol2* transposons.[59] Because constitutive expression of a transgenic mammalian oncogene often results in lethality before achieving sexual maturity, several approaches, such as the cre-*loxP* and Gal4-*UAS* systems, have been developed to control the spatial and temporal expression of transgenes.[60,61]

Fluorescence was also very elegantly used for tracking recombination events in *cre/lox*-regulated systems in whole fish. In a zebrafish model of T-ALL, a floxed *dsRED* gene between the *rag2* promoter and *EGFP-mMyc* transgene resulted in dsRED expression in thymocytes. Directed activation of CRE recombination resulted in a switch to enhanced green fluorescent protein (EGFP) expression in the same cells.[62,63]

Zebrafish mutagenesis

Despite the availability of technology to generate cancer-prone transgenic zebrafish, cancer remains a disease that requires the simultaneous loss or mutation of multiple genes in the same cell. For this reason, transgenic cancer zebrafish lines still require time to accumulate additional mutations or a "boost" of carcinogen treatment in order to generate sufficient numbers of cancer-bearing fish to be experimentally useful and statistically meaningful. For instance, a nonsense mutation in zebrafish *Apc* was found to result in less than 30% of heterozygous fish spontaneously developing liver and intestinal tumors from 15 months of age onward. However, treatment of *Apc* heterozygotes with 7,12-dimethylbenz [a]anthracene enhanced tumorigenesis, resulting in intestinal, hepatic, and pancreatic tumors, with frequencies 3- to 4-fold higher at 6-12 months of age than treated wild-types. Furthermore, the tumors displayed activated *Wnt* signaling, indicating that the genetic pathway is conserved.[64]

Cancer transplantation

Different groups have also experimented with direct transplantation of mammalian cancer cells into zebrafish embryos. This creates an *in vivo* system in which the advantages of cultured human cancer cells are combined with those of transparent

zebrafish embryos in which development can be followed in real time.[65] This visualization advantage is further enhanced in part by the development of a zebrafish line that lacks all types of pigmentation named "*casper*."[66] However, the visualization of fluorescently-tagged proteins and cells can still often be very much feasible even without abolition of pigment due to the relatively small size of zebrafish adults, depending on what anatomical site and at what developmental stage the animal is visualized.[65,67]

For instance, in another elegant study, researchers used i.p. injection to introduce fluorescently labeled human breast cancer cells into 1-month-old zebrafish. They used the transplanted cells in combination with three-dimensional modeling to show how the human cells interact with vessels and invade in tissues. The experiment showed that expression of vascular endothelial growth factor induces openings in vessel walls that can be used for invasion.[68]

Zebrafish as a model for human hematopoiesis

The primary purpose of this work was to use the zebrafish as an experimental organism to identify and characterize novel compounds with potential for targeted efficacy in treating human T-cell acute lymphoblastic leukemia (T-ALL). In order for such a purpose to be achieved, a large degree of structural, genetic and functional homology must exist between human and zebrafish in their respective hematopoietic systems in order for findings in the zebrafish model to be translatable to human T-ALL. The organization of the genome and the genetic pathways controlling signal transduction and hematopoietic development appear to be highly conserved between zebrafish and humans.[19] This evolutionary conservation of hematopoietic development means that

zebrafish can be exploited to elucidate human hematopoietic mechanisms, both healthy and malignant, as well as treatment modalities with the potential to address them.

Although the first circulating blood cells are visible by 24 hours postfertilization (hpf) during zebrafish development, the processes required for hematopoietic stem cell (HSC) generation are already underway from 5hpf, when gastrulation takes place. During the gastrula period, embryos develop three germ layers – ectoderm, mesoderm and endoderm. Among these three germ layers, blood and angioblasts (endothelial progenitors) originate from the mesoderm.[69,70]

Primitive and definitive hematopoiesis

As in other vertebrates, there are two major waves of hematopoiesis in zebrafish (Figure 3.2). The first wave, primitive hematopoiesis, originates in the yolk sac in mammals and birds, and in the intermediate cell mass (ICM) in zebrafish, specifically the anterior lateral plate mesoderm (ALM) and the posterior lateral plate mesoderm (PLM). At early somitogenesis stages, the ALM gives rise to a transient hemangioblast population that differentiates into myeloid and endothelial cells. In its turn, the PLM gives rise to a second population of hemangioblasts that differentiate into erythroid and endothelial cells.[71,72] Red blood cells do not differentiate in the PLM. Instead the erythroid derivatives of the PLM migrate to the midline to differentiate in the intermediate cell mass.[73] However, this primitive wave is only transient, and the successive definitive wave starts intraembryonically.

The second wave of hematopoiesis, definitive hematopoiesis, initiates in the zebrafish embryo from 30hpf. This wave gives rise to hematopoietic stem cells (HSCs), which generate all blood cell types in the later embryo and throughout adult life,

including erythroid (erythrocyte), myeloid (macrophage, neutrophil, monocyte) and lymphoid cells (B and T).[74] HSCs can also reconstitute hematopoietic lineages in clinical or experimental settings when transplanted into a host lacking HSCs. Apart from megakaryocytes and natural killer (NK) cells, all other differentiated blood lineages have been found and characterized in zebrafish embryos and/or adults, and they exhibit a high degree of conservation in both molecular and cellular features when compared to their counterparts in mammals.[75]

In vertebrate embryos, the first definitive HSCs arise primarily from the aorta-gonad-mesonephros (AGM) region and express *runx1* and *c-myb* transcription factors.[76,77] From 48hpf, these *c-myb+* cells appear in the posterior part of the embryo, known as the caudal hematopoietic tissue (CHT).[78, 79] The structure of the CHT highly resembles that of kidney marrow and fetal liver, its equivalent in mammals, as it has many sinusoids that slow down the blood flow, and this could help seeding of HSCs.[79] The *c-myb+* cells later appear in the thymus from 3dpf and in the pronephros from 4dpf.[2]

In the adult zebrafish, the kidney serves as the main hematopoietic organ,[80] and its function is equivalent to that of the bone marrow in mammals. T cell progenitors develop initially within the kidney marrow and then migrate to the thymus where they undergo differentiation.[81] Kidney marrow generates adult hematopoietic cells throughout the life of a zebrafish. The development of T cells and the thymus in zebrafish is remarkably similar to that of mammals with the main exception that the zebrafish thymus remains as two discrete bilateral structures in connection with pharyngeal endoderm.[82]

Zebrafish and human hematopoiesis homology

However, despite differences in physiological location of the hematopoietic niche, the gene programs utilized in each tissue are well conserved across species.[83] A high degree of conservation in transcription factors and the sequence of their functional domains translate into a high degree of functional conservation. As in mammals, the basic helix-loop-helix transcription factor *tal1(scl)* and its partner *lmo2* sit at the apex of hematopoietic and endothelial development.[84-86] *Gata1* and *spi1(pu.1)* have conserved lineage-specific erythroid and myeloid fate-specifying roles.[87] *Runx1* and *cmyb* retain their connection with definitive hematopoiesis.[77,88] Detailed analyses of the staggered temporal expression of hematopoietic transcription factors imply a conserved regulatory hierarchy.[86,89] Probing the transcriptional regulation of hematopoiesis in zebrafish is hence informative for mammalian hematopoiesis. Furthermore, zebrafish have proven to be a useful heterologous model for examining human disease-associated transcription factor mutations and their fusion proteins.[77,90]

Zebrafish T cell-specific developmental genes have also been cloned and show strong homologies to mammalian counterparts with similar expression and functional profiles. They include *ikaros, lck, GATA-3 rag-1, and rag-2.*[91-93] Intracellular cytokine signaling pathways also appear to be conserved. There are zebrafish orthologs of JAK kinases,[94-97] STAT molecules,[98-100] and SOCS negative regulators.[101-103] Descriptive and functional data point to their involvement in cytokine and growth factor signaling pathways mediating conserved biologic responses.[95,104] Furthermore, zebrafish possess all the major proteins of the coagulation system, including both vitamin K-dependent procoagulant factors, anticoagulant factors, and the fibrinolytic pathway.[105]

Despite the similarities between zebrafish and human hematopoiesis, differences between them do exist which must be considered before undertaking experimental conception and design. While the antibody-based, adaptive immune system is present in all jawed vertebrates (gnathostomes),[106] zebrafish differ considerably with regard to the presence of major lymphoid tissues.[91,107] Bone marrow, gut-associated lymphoid nodules (Peyer's patches), and primitive lymph nodes are absent from zebrafish. In the absence of lymph nodes, antigen-presenting cells (APCs) and lymphocytes interact in the only truly secondary lymphoid organ of zebrafish – the spleen, a site where dendritic cells (DCs) reside.[108] The liver and gut can also serve as surrogate lymphoid organs.[109]

There are also significant differences in immunoglobulin gene organization, gene usage, and gene number of immunoglobulin genes.[110] Furthermore, zebrafish express a new immunoglobulin heavy chain subtype, immunoglobulin Z, which does not have a counterpart in mammals.[111] Moreover, immunoglobulin isotype class switching is a process that has its earliest evolutionary roots in amphibians and therefore does not occur in fishes.[91,112] Additional limitations of the zebrafish model in hematology research are summarized in Table 3.1.[113]

Zebrafish as a model for human leukemia

Malignant hematologic diseases, including acute leukemia and myelodysplastic and myeloproliferative disorders, have been modeled in zebrafish, which recapitulate many features found in analogous human leukemias (Table 3.2).[114] The development of lymphoblastic leukemia zebrafish models was facilitated by the early availability of lymphocyte-specific promoters, such as *rag2*, providing appropriately selective spatiotemporal regulation for expressing oncogenes in lymphoid cells.[115] These

transgenic zebrafish were generated by injecting cDNA constructs into embryos at the one-cell stage, resulting in the tissue-specific expression of the oncogene when integrated into the genome.

Zebrafish models of T-ALL

The first zebrafish model of T-ALL involved expression of the mouse *Myc* gene tagged with eGFP under control of the *rag2* promoter.[116] The stable transgenic *rag2-EGFP-mMyc* zebrafish lines developed T-cell leukemia with a mean latency of 22 days post-fertilization (dpf) and a mean survival of 82 dpf.[39] At the molecular level, mMyc-induced leukemias are similar to a subtype of human T-ALL expressing both *scl* and *lmo2*. In human patients, this subgroup represents the most common and most treatment-resistant form of this disease.[117] Furthermore, combining *bcl2* over-expression with the enforced *Myc* expression generated a transplantable leukemia with increased resistance to γ-irradiation-induced apoptosis.[118]

However, though effective in generating a visible form of T-ALL in zebrafish, the induction of leukemia in this model was so efficient that the majority of the injected animals died before reaching sexual maturity, thus hampering the ability to maintain a stable line.[54] To solve this problem, a conditional Cre-*loxP* system was subsequently introduced in the form of double transgenics expressing *rag2:loxP-dsred-loxPGFP*-MYC and heat-shock-inducible Cre recombinase (*hsp70*:cre). In this model, T-cell lymphoblastic lymphoma was efficiently induced after heat-shock induction and T-cell lymphoblastic leukemia (T-LBL) rapidly progressed to T-ALL.[55] Establishing inducible T-ALL models allows tumor-prone transgenic lines to be propagated disease-free and to only exhibit the neoplastic phenotype when desired. This strategy also allows for analysis

of the temporal effects of both transgene expression and inactivation on the tumor phenotype.[39]

The second T-ALL model was created by introducing the human T-ALL oncogene, *Notch1*, into zebrafish under control of the *rag2* promoter, fused to eGFP for easy visualization of T-cells. Transgenic animals begin to show expansion of fluorescence in the thymic region at about 5 months of age with progression to widespread dissemination similar to that seen in the *mMyc* model. Similar to that seen in the *rag2:EGFP*-mMyc model, crossing *rag2:Notch1* model animals to a *rag2*-Bcl2-expressing fish leads to a significant decrease in disease latency.[118,119]

More recently, Gutierrez et al. (2011)[120] sought to generate a model in which Myc activity could be modulated in established tumor cells. To this end, they generated stable transgenic zebrafish expressing *rag2:Myc-ER.* In this model the zebrafish *rag2* promoter drives expression of a fusion transgene consisting of human *MYC* fused to the ligand-binding domain of a modified estrogen receptor. This modified estrogen receptor is post-translationally induced by 4-hydroxytamoxifen (4HT) treatment but not by endogenous estrogens.[120] In this manner, they generated a conditional zebrafish model of T-ALL in which 4HT treatment induces MYC activation and disease, and withdrawal of 4HT results in T-ALL apoptosis and tumor regression.[120]

To characterize a heritable predisposition to T-ALL, Frazer et al. (2009)[121] pioneered a phenotype-driven forward-genetic screen in zebrafish. Using transgenic WIK fish with T-lymphocyte-specific expression of eGFP (WIK *lck:eGFP),*[121] they performed chemical ENU mutagenesis, screened animals for GFP+ tumors, and identified multiple lines with a heritable predisposition to T-cell malignancy. They reported three such

zebrafish lines of heritable T-cell malignancy. Two are reported as having dominant inheritance: *shrek (srk)* and *hulk (hlk)*, and the third exhibits recessive inheritance: *oscar the grouch (otg)*. Each line faithfully recapitulates human T-ALL and T-cell lymphoblastic lymphoma (T-LBL) in onset, invasion pattern, and morphology. Furthermore, their neoplastic cells are clonal and transplantable.[114]

Zebrafish models of B-cell acute lymphoblastic leukemia (B-ALL)

The only current zebrafish model of B-ALL is a transgenic fish expressing the *ETV6-RUNX1(TEL-AML1)* fusion oncogene. This oncogene is associated with t(12;21) pediatric B-cell acute lymphoblastic leukemia, but does not result in ALL when driven from the *rag2* promoter. However, when expressed ubiquitously, an ALL-like disease with the phenotypic features of B-ALL is observed at low levels of penetrance.[122] Gene expression profiling in diseased animals is consistent with childhood CD10+ pre-B cell ALL.[122]

Zebrafish models of acute myeloid leukemia (AML)

Myeloid leukemia has also been modeled in zebrafish. The AML1-ETO (AE) translocation (also known as RUNX1-RUNX1T1) is the most common chromosomal translocation in acute myeloid leukemia. However, as in earlier T-ALL models, ubiquitous over-expression of the oncogenic AE protein in zebrafish embryos leads to early lethality and thus requires inducible expression by the heat shock promoter in transgenic fish (*hsp70:AML1-ETO).*[123,124]

Zebrafish utility in drug screening

In addition to its power in forward genetic screens, the zebrafish is now emerging as a new model for drug discovery.[31] The high degree of sequence structure conservation between the proteins of zebrafish and humans increases the likelihood that bioactive compounds recovered in zebrafish chemical screens will retain activity and specificity for preclinical studies in mice and eventually for clinical studies in humans. In recent years, zebrafish have been used for evaluating the toxicity of pharmaceutical agents.[125] In zebrafish larvae, an *in vivo* toxicology assessment has the advantage that it can be achieved in a week, a much shorter time frame than that required when performing comparable mammalian assays. In addition, much larger numbers of compounds can be tested in zebrafish than what can be feasibly tested in mice.

The potential of zebrafish to be used as a vertebrate model for chemical screens was first assessed by Peterson and colleagues.[126] They used wild-type zebrafish embryos to screen for chemical modifiers of development using a strategy analogous to genetic screens, where mutations are identified that affect development of different organ systems. In their screen, 1,100 synthetic small molecules were randomly chosen from the DIVERSet library (ChemBridge Corp.) and added to the embryos. The effects of the individual compounds on the embryos' morphology and physiology were examined visually under the dissection microscope. From this screen, 2% of the compounds cause lethality, and 1% caused specific phenotypes leading to the identification of compounds that affect development of the central nervous system, the cardiovascular system, pigmentation, and the ear.

Many of the advantages of utilizing zebrafish in compound screening stem from its small size (5cm for an adult and 5mm for 7dpf larvae), combined with high fecundity, which enable medium-to high-throughput screening. Small size also means that only milligrams of compound are needed for screening in 96-well plates as the larvae can live in as little as 50μL of fluid. Both of these factors contribute to relatively low costs for high-throughput zebrafish screening. Furthermore, zebrafish fertilization and embryonic development are external and rapid, with most organ systems becoming functional within 3-5 dpf when the larvae are still small enough to grow in 96-well format. At that age, the zebrafish larvae are not fetal but are closer to the juvenile state in that the nervous system is mature, vital organs are functioning and tissue architecture is fully developed at the time of the assays. Rapid development *in vitro* also means that small molecule compounds can be added with precise timing, allowing pinpointing of the exact temporal requirement for the target protein.[126]

Another very important advantage in zebrafish drug screening is the fact that the zebrafish larvae are whole vertebrate organisms with many of the same organ systems as humans and other mammals, including a cardiovascular system, immune system, and kidneys, relevant to human biology and physiology. Screening large panels of chemical compounds for specific effects in cell culture is a well-established strategy for drug discovery. However, many biological processes cannot be reproduced in cultured cells and often the three-dimensional environment of cells determines their function. Moreover, metabolism of the compounds may be profoundly different in whole organisms, and may be required for conversion into active drug form. Conventional *in*

vitro cell-based chemical screens would fail to identify drugs that require metabolic activation within an organism.

Furthermore, "hit" compounds have to be cell-permeable, devoid of obvious toxicities, effective, and possess favorable pharmacodynamic and pharmacokinetic profiles. Drug discovery in the whole organism, therefore, combines screening and animal testing in one step. While slower than *in vitro* assessment, compared with cell-based drug screening, a whole-animal model substantially reduces the likelihood of encountering common issues that arise during late stages of drug development, such as drug toxicity and off-target side effects. This is particularly relevant in testing potential new chemotherapeutic agents, where toxicity often limits efficacy.[127] Therefore, one would like to screen large numbers of small molecule compounds with high throughput for biological activity in whole organisms as early in the screening process as possible. This now has become feasible using zebrafish embryos. Until recently zebrafish has remained the only vertebrate model used for large-scale chemical screens. However, *Xenopus* exhibits many of the same desirable drug screening traits as zebrafish and is now being used in some drug screening applications (Table 3.3).[34]

Finally, chemical screening is facilitated by the fact that zebrafish are reasonably tolerant to dimethylsulphoxide (DMSO), generally used in such screening efforts. Compounds of chemical libraries are usually stored as stock solutions in DMSO, which also serves as a vehicle to improve solubility of the compounds in the aqueous solutions used to culture embryos.[128] Zebrafish embryos are surprisingly tolerant to a range of DMSO concentrations.[129,130] A final concentration of 1% DMSO is compatible with normal development in zebrafish, which allows compounds to be screened at a wide

range of concentrations in embryos and larvae. High tolerability for DMSO also enables matrix pooling in compound screening where multiple compounds are aliquoted into a single test well with larvae, thus greatly accelerating throughput.[131,132] The strategy is, however, primarily suitable for synthetic, combinatorial libraries as many compounds will have no biological activity. In contrast, pooling of compounds from collected bioactive libraries is undesirable as this leads to a very high rate of toxicity.[133]

Lack of need for known molecular target

Conventional *in vitro* drug screens often focus on identifying specific inhibitors of an established molecular target. For example, imatinib (Gleevec®) was designed to target the ABL kinase, blocking signal transduction pathways downstream of the BCR-ABL fusion kinase in chronic myeloid leukemias.[31] By contrast, reversion of a disease phenotype in the zebrafish does not require the *a priori* knowledge of gene targets. This allows the identification of drugs that disrupt novel pathways or affect the interactions of complex molecular signaling cascades that can contribute to disease states.[134] Furthermore, zebrafish drug screens can be used to establish a rapid and reliable readout for novel drug compounds' impact *in vivo*. Taken together, chemical zebrafish screens promise to provide a rapid, alternative approach to identify lead compounds for diseases whose underlying biology and pathological mechanisms are not well understood.

Further therapeutic development to optimize for specificity will, however, benefit from identification of the molecular targets and understanding of the mode of action of the recovered lead compounds.[30] The use of tagged compounds (i.e., biotin tag) facilitates identification of their molecular targets.[135] However, a drawback of the tagged library is that the tag may block biological activity of the compound.[135] Comparison of two drug

screens suggests that tagging the compounds leads to a dramatic reduction in the number of compounds that are biologically active. In a screen of untagged compounds, ~3% induced a phenotype[126] vs. 0.07% (1 out of 1536) of the same compounds with a tag.[135] Moreover, the untagged compounds were biologically active at low concentrations (~1μM),[126] while a relatively high concentration of the tagged compounds was required to induce a phenotype (50μM).[135] Moreover, once identified, candidate molecular targets should be confirmed and validated by independent means such as by morpholino-mediated knock down of the target, or, if available, by detailed analysis of a mutant with a mutation in the target gene.

Use of genetically modified zebrafish for drug screening

One promising use of drug screens in the zebrafish is to employ genetically modified zebrafish embryos. Mutants from either the phenotype-driven forward mutagenesis screen or from reverse genetic TILLING may be used as well as transgenic fish (over-) expressing a gene of interest. Over the last few years, several zebrafish mutants have been isolated that mimic human disease, such as polycystic kidney disease, heart disease, and anemias.[23,34,136] These genetically modified fish may be screened with large panels of drugs for reversion of the phenotype. Mutants in disease genes that display an embryonic phenotype, as well as transgenic lines with an embryonic phenotype may be used for these drug screens. The targets of the chemical compounds will include factors downstream of the mutant gene and may include an (over-) expressed transgene as well. These types of screens provide a direct means to screen for chemical compounds that act in disease pathways.[137] Such chemical suppressors of a disease

process in a whole, vertebrate organism would represent potential lead compounds for drug development.

The feasibility of this approach was first demonstrated by the identification of a novel class of compounds capable of suppressing the gridlock mutation.[138] Gridlock mutants have a hypomorphic mutation in the *hey2* gene, a hairy/enhancer of split-related basic helix-loop-helix transcription factor, leading to the malformation of the dorsal aorta preventing blood circulation to the trunk and tail.[139] Coarctation of the aorta is a common human congenital cardiovascular malformation that is morphologically similar to the gridlock mutant.[140] After screening a diverse library of 5,000 drug-like compounds, two structurally related compounds were identified that completely rescued *gridlock* mutants in a dose-dependent manner to develop a normal vasculature without causing additional developmental defects.[138] The mechanism of action is unknown, but the more potent compound, GS4012, induced expression of vascular endothelial growth factor (VEGF). In support of this notion, over-expression of VEGF is sufficient to rescue the gridlock mutation and, similar to VEGF, GS4012 promotes human endothelial tube formation *in vitro.*[138]

Forward chemical genetic screens

One of the first forward chemical genetic screens was aimed at identifying new pathways modulating definitive hematopoietic stem cell formation during zebrafish embryogenesis.[141] In this screen, North et al. found that prostaglandin E2 (PGE2) increased HSC number. PGE2 interacts with the Wnt signaling pathway to regulate HSCs through cAMPPKA-mediated β-catenin phosphorylation.[142] A stable derivative of PGE2 (dmPGE2) increases the frequency of long-term repopulating HSCs in irradiated murine

bone marrow, strongly suggesting a therapeutic potential.[141] As another prostaglandin-relevant example, Yeh and colleagues utilized the transgenic *hsp70:AML1-ETO* (AE) zebrafish line and screened for compounds that suppressed the inducible erythropoiesis-to-granulopoiesis conversion.[143] They found that chemicals that inhibit PGE2 or β-catenin pathways block the capacity of AEs to redirect hematopoiesis, a strategy that could potentially provide therapeutic benefits in AML patients. These two independent screens collectively demonstrate the crucial roles of PGE2 and β-catenin interaction in normal and leukemic hematopoiesis.

In another example of a chemical suppressor screen in zebrafish, Stern and colleagues screened a chemical library using the recessive cell cycle mutant crash & burn (*crb*), a homozygous lethal mutation of the *bmyb* gene that has an increased number of mitotic cells as detected by pH3 antibody staining.[132] Screening of a 16,320-compound library resulted in the identification of one compound, named persynthamide, which suppressed the phenotype of the *crb* mutant. Because of its ability to suppress a specific cell cycle defect in *crb* mutants without affecting wild-type embryos, persynthamide might be a useful anticancer agent.

Conclusion

In summary, the zebrafish as a model organism for scientific research offers a unique combination of opportunity and convenience unequalled currently by any other experimental organism. Because of its small size and fecundity, its maintenance is less expensive than other mammalian models such as mice. Furthermore, *ex vivo* development of transparent eggs and embryos combined with rapid organogenesis offer a very powerful model for studying and manipulating developmental processes. Moreover, as a

vertebrate, its physiology and genome exhibit a high degree of homology with that of humans such that many human diseases can be recapitulated in the zebrafish model. This also means that any remedy found for such a disease in zebrafish is likely to translate to having a similar remedial impact in human patients with the same disease.

The primary purpose of this work was to use a transgenic *lck*:eGFP zebrafish to screen for and characterize novel compounds with the ability to eliminate immature T-cell progenitors developing in the thymus, and thus also eliminate immature, developmentally-arrested leukemic blasts. The zebrafish offers unique opportunities for conducting such a large-scale drug screen due to the ease of creating transgenic reporter animals, small size and rapid development, along with an immune system which is remarkably similar to that of humans, including the ability to develop leukemia. Furthermore, a zebrafish *in vivo* drug screening platform also provides the context of an entire vertebrate organism capable of simultaneously testing for efficacy, bioavailability, and lack of systemic toxicity in the same screening. For these reasons, it is likely that the zebrafish will continue to be a powerful and effective tool for hematological research.

References

1. Streisinger G, Walker C, Dower N, et al. Production of clones of homozygous diploid zebra fish (Brachydanio rerio). *Nature.* 1981; 291: 293–296.

2. Alestrom P, Holter JL, Nourizadeh-Lillabadi R. Zebrafish in functional genomics and aquatic biomedicine. *Trends Biotechnol*. 2006; 24: 15–21.

3. Driever W, Solnica-Krezel L, Schier AF, et al. A genetic screen for mutations affecting embryogenesis in zebrafish. *Development.* 1996; 123: 37–46.

4. Feitsma H, Cuppen E. Zebrafish as a cancer model. *Mol Cancer Res*. 2008; May; 6(5):685-94.

5. Haffter P, Granato M, Brand M, et al. The identification of genes with unique and essential functions in the development of the zebrafish, Danio rerio. *Development.* 1996; 123:1-36.

6. Roosen-Runge E. Observations of the early development of the zebra fish, Brachydanio rerio. *Anat Rec.*1937; 70(Suppl 1):103.

7. Laale HW. The biology and use of zebrafish, Brachydanio rerio, in fisheries research: a literature review. *J Fish Biol.* 1977; 10:121-173.

8. Colle-Vandevelde A. Blood anlage in Teleosti. *Nature.* 1963; 198:1223.

9. Rieb JP. La Circulation Sanguine Chez L'Embryon De Brachydanio Rerio. *Ann Embryol Morphogenese.* 1973; 6:43-54.

10. Johnson RA, Hart NH, Powell D. Studies on the morphology of blood cells in the fresh water teleost, Brachydanio rerio. *Bull N Y Acad Sci*. 1973; 18:20-21.

11. Al-Adhami MA, Kunz YW. Ontogenesis of haematopoietic sites in Brachydanio rerio (Hamilton- Buchanan). *Dev Growth Differ.* 1977; 19:171-179.

12. Stainier DY, Weinstein BM, Detrich HW , et al. Cloche, an early acting zebrafish gene, is required by both the endothelial and hematopoietic lineages. *Development.* 1995; 121:3141-3150.

13. Weinstein BM, Schier AF, Abdelilah S, et al. Hematopoietic mutations in the zebrafish. *Development.* 1996; 123:303-309.

14. Ransom DG, Haffter P, Odenthal J, et al. Characterization of zebrafish mutants with defects in embryonic hematopoiesis. *Development.* 1996; 123: 311-319.

15. Dodd A, Curtis PM, Williams LC, et al. Zebrafish: bridging the gap between development and disease. *Hum Mol Genet.* 2000; 16:2443–2449.

16. Zon LI. Zebrafish: a new model for human disease. *Genome Res*. 1999; 9:99–100.

17. Patton EE, and Zon LI. The art and design of genetic screens: zebrafish. *Nat Rev Genet*. 2001; 2: 956-966.

18. Liu TX, Zhou Y, Kanki JP, et al. Evolutionary conservation of zebrafish linkage group 14 with frequently deleted regions of human chromosome 5 in myeloid malignancies. *Proc Natl Acad Sci* USA. 2002; 99:6136-6141.

19. Postlethwait JH, Woods IG, Ngo-Hazelett P, et al. Zebrafish comparative genomics and the origins of vertebrate chromosomes. *Genome Res.* 2000; 10:1890-1902.

20. Long Q, Meng A, Wang H, et al. GATA-1 expression pattern can be recapitulated in living transgenic zebrafish using GFP reporter gene. *Development.* 1997; 124:4105-4111.

21. Jessen JR, Jessen TN, Vogel SS, et al. Concurrent expression of recombination activating genes 1 and 2 in zebrafish olfactory sensory neurons. *Genesis.* 2001; 29:156-162.

22. de Jong JL, Zon LI. Use of the zebrafish system to study primitive and definitive hematopoiesis. *Annu Rev Genet.* 2005; 39:481-501.

23. Lieschke GJ, Currie PD. Animal models of human disease: zebrafish swim into view. *Nat Rev Genet.* 2007; 8:353-367.

24. Udvadia AJ, Linney E. Windows into development: historic, current, and future perspectives on transgenic zebrafish. *Dev Biol.* 2003; 256:1-17.

25. Wienholds E, Schulte-Merker S, Walderich B, et al. Target-selected inactivation of the zebrafish rag1 gene. *Science.* 2002; 297:99-102.

26. Wang D, Jao LE, Zheng N, et al. Efficient genome- wide mutagenesis of zebrafish genes by retroviral insertions. *Proc Natl Acad Sci U S A.* 2007; 104:12428-12433.

27. Nasevicius A, and Ekker SC. Effective targeted gene ‘knockdown’ in zebrafish. *Nat Genet*. 2000; 26:216–220.

28. Van der Sar A, Zivkovic D, and den Hertog J. Eye defects in receptor protein-tyrosine phosphatase alpha knock-down zebrafish. *Dev Dyn.* 2002; 223:292–297.

29. Genesis Morpholino gene knock down issue. *Genesis.* 2001; 30:89–200.

30. Moens CB, Donn TM, Wolf-Saxon ER, et al. Reverse genetics in zebrafish by TILLING. *Brief Funct Genomic Proteomic.* 2008; 7:454–459.

31. Stemple DL. TILLING: a highthroughput harvest for functional genomics. *Nat Rev Genet.* 2004; 5:145–150.

32. Wienholds E, van Eeden F, Kosters M, et al. Efficient target-selected mutagenesis in zebrafish. *Genome Res.* 2003; 13: 2700–2707.

33. Doyon Y, McCammon JM, Miller JC, et al. Heritable targeted gene disruption in zebrafish using designed zinc-finger nucleases. *Nat Biotechnol*. 2008; 26:702–708.

34. Meng X, Noyes MB, Zhu LJ, et al. Targeted gene inactivation in zebrafish using engineered zincfinger nucleases. *Nat Biotechnol*. 2008; 26:695– 701.

35. Miller JC, Tan S, Qiao G, et al. A TALE nuclease architecture for efficient genome editing. *Nat Biotechnol.* 2011 Feb; 29(2):143-8.

36. Sander JD, Cade L, Khayter C, et al. Targeted gene disruption in somatic zebrafish cells using engineered TALENs. *Nat Biotechnol.* 2011 Aug 5; 29(8):697-8.

37. Huang P, Xiao A, Zhou M, et al. Heritable gene targeting in zebrafish using customized TALENs. *Nat Biotechnol.* 2011 Aug 5; 29(8):699-700.

38. Wheeler GN, Brändli AW. Simple vertebrate models for chemical genetics and drug discovery screens: lessons from zebrafish and Xenopus. *Dev Dyn.* 2009 Jun; 238(6):1287-308.

39. Barros TP, Alderton WK, Reynolds HM, et al. Zebrafish: an emerging technology for in vivo pharmacological assessment to identify potential safety liabilities in early drug discovery. *Br J Pharmacol.* 2008 Aug; 154(7):1400-13.

40. Barros TP, Alderton WK, Reynolds HM, et al. Zebrafish: an emerging technology for *in vivo* pharmacological assessment to identify potential safety liabilities in early drug discovery. *Br J Pharmacol*. 2008 August; 154(7): 1400–1413.

41. Meeker ND, Trede NS. Immunology and zebrafish: Spawning new models of human disease. *Developmental and Comparative Immunology.* 2008; 32, 745–757.

42. Zon LI, Peterson RT. In vivo drug discovery in the zebrafish. *Nat Rev Drug Discov.* 2005; 4: 35–44.

43. Kent ML, Bishop-Stewart JK, Matthews JL, et al. Pseudocapillaria tomentosa, a nematode pathogen, and associated neoplasms of zebrafish (Danio rerio) kept in research colonies. *Comp Med.* 2002; 52:354 – 8.

44. Kent ML, Spitsbergen JM, Matthews JM, et al. Diseases of zebrafish in research facilities. *Zebrafish International Resource Center.* 2002 Sept. Available from: http://zebrafish.org/zirc/health/diseaseManual.php. Accessed November 5, 2012.

45. Matthews JL. Common diseases of laboratory zebrafish. *Methods Cell Biol.* 2004; 77:617 – 43.

46. Smolowitz R, Hanley J, Richmond H. A three-year retrospective study of abdominal tumors in zebrafish maintained in an aquatic laboratory animal facility. *Biol Bull.* 2002; 203:265 – 6.

47. Berghmans S, Jette C, Langenau D, et al. Making waves in cancer research: new models in the zebrafish. *Biotechniques.* 2005 Aug; 39(2):227-37.

48. Khudoley VV. Use of aquarium fish, Danio rerio and Poecilia reticulata, as test species for evaluation of nitrosamine carcinogenicity. *Natl Cancer Inst Monogr.* 1984; 65:65 – 70.

49. Pliss GB, Khudoley VV. Tumor induction by carcinogenic agents in aquarium fish. *J Natl Cancer Inst.* 1975; 55:129 – 36.

50. Stern HM and Zon LI. Cancer genetics and drug discovery in the zebrafish. *Nat Rev Cancer.* 2003; 3:533-539.

51. Walter RB and Kazianis S. Xiphophorus interspecies hybrids as genetic models of induced neoplasia. *Ilar J.* 2001; 42:299-321.

52. Langheinrich U, Hennen E, Stott G, et al. Zebrafish as a model organism for the identification and characterization of drugs and genes affecting p53 signaling. *Curr Biol*. 2002; 12:2023-2028.

53. Schreiber-Agus N, Horner J, Torres R, et al. Zebra fish myc family and max genes: differential expression and oncogenic activity throughout vertebrate evolution. *Mol Cell Biol*. 1993; 13:2765-2775.

54. Liu TX, Howlett NG, Deng M, et al. Knockdown of zebrafish Fancd2 causes developmental abnormalities via p53-dependent apoptosis. *Dev Cell.* 2003; 5:903-914.

55. Langheinrich U, Hennen E, Stott G, et al. Zebrafish as a model organism for the identification and characterization of drugs and genes affecting p53 signaling. *Curr Biol*. 2002; 12:2023-2028.

56. Schreiber-Agus N, Horner J, Torres R, et al. Zebra fish myc family and max genes: differential expression and oncogenic activity throughout vertebrate evolution. *Mol Cell Biol*. 1993; 13:2765-2775.

57. Liu TX, Howlett NG, Deng M, et al. Knockdown of zebrafish Fancd2 causes developmental abnormalities via p53-dependent apoptosis. *Dev Cell.* 2003; 5:903-914.

58. Gilley J and Fried M. One INK4 gene and no ARF at the Fugu equivalent of the human INK4A/ARF/INK4B tumour suppressor locus. *Oncogene.* 2001; 20:7447 – 7452.

59. Kawakami K. Tol2: a versatile gene transfer vector in vertebrates. *Genome Biol*. 2007; Suppl. 1, S7.

60. Halpern ME, Rhee J, Goll MG, et al. Gal4/UAS transgenic tools and their application to zebrafish. *Zebrafish.* 2008; 5:97-110.

61. Mosimann C, Kaufman CK, Li P, et al. Ubiquitous transgene expression and Cre-based recombination driven by the ubiquitin promoter in zebrafish. *Development.* 2011; 138:169-177.

62. Langenau DM, Feng H, Berghmans S, et al. Cre/lox-regulated transgenic zebrafish model with conditional myc-induced T cell acute lymphoblastic leukemia. *Proc Natl Acad Sci U S A.* 2005; 102: 6068 – 73.

63. Feng H, Langenau DM, Madge JA, et al. Heat-shock induction of T-cell lymphoma/leukaemia in conditional Cre/lox-regulated transgenic zebrafish. *Br J Haematol.* 2007; 138:169 – 75.

64. Haramis AP, Hurlstone A, van der Velden Y, et al. Adenomatous polyposis coli-deficient zebrafish are susceptible to digestive tract neoplasia. *EMBO Rep.* 2006; 7:444 – 9.

65. Lee LM, Seftor EA, Bonde G, et al. The fate of human malignant melanoma cells transplanted into zebrafish embryos: assessment of migration and cell division in the absence of tumor formation. *Dev Dyn.* 2005; 233:1560 – 70.

66. White RM, Sessa A, Burke C, et al. Transparent adult zebrafish as a tool for in vivo transplantation Analysis. *Cell Stem Cell*. 2008 February 7; 2(2): 183–189.

67. Topczewska JM, Postovit LM, Margaryan NV, et al. Embryonic and tumorigenic pathways converge via Nodal signaling: role in melanoma aggressiveness. *Nat Med.* 2006; 12:925 – 32.

68. Stoletov K, Montel V, Lester RD, et al. High-resolution imaging of the dynamic tumor cell vascular interface in transparent zebrafish. *Proc Natl Acad Sci U S A.* 2007; 104:17406 – 11.

69. Kimmel CB, Warga RM, Schilling TF. Origin and organization of the zebrafish fate map. *Development.* 1990; 108: 581-594.

70. Warga RM, Nusslein-Volhard C. Origin and development of the zebrafish endoderm. *Development.* 1999; 126: 827-838.

71. Hogan BM, Layton JE, Pyati UJ, et al. Specification of the primitive myeloid precursor pool requires signaling through Alk8 in zebrafish. *Curr Biol.* 2006; 16: 506-511.

72. Galloway JL, Zon LI. Ontogeny of hematopoiesis: examining the emergence of hematopoietic cells in the vertebrate embryo. *Curr Top Dev Biol.* 2003; 53: 139-158.

73. Hogan BM, Layton JE, Pyati UJ, et al. Specification of the primitive myeloid precursor pool requires signaling through Alk8 in zebrafish. *Curr Biol.* 2006; 16: 506-511.

74. Galloway JL, Zon LI. Ontogeny of hematopoiesis: Examining the emergence of hematopoietic cells in the vertebrate embryo. *Curr Top Dev Biol.* 2003; 53:139-58.

75. Meeker ND, Trede NS. Immunology and zebrafish: spawning new models of human disease. *Dev Comp Immunol*. 2008; 32(7):745-57.

76. Burns CE, DeblasioO T, Zhou Y, et al. Isolation and characterization of runxa and runxb, zebrafish members of the runt family of transcriptional regulators. *Exp Hematol.* 2002; 30: 1381-1389.

77. Kalev-Zylinska ML, Horsfield JA, Flores MV, et al. Runx1 is required for zebrafish blood and vessel development and expression of a human RUNX1-CBF2T1 transgene advances a model for studies of leukemogenesis. *Development.* 2002; 129:2015-2030.

78. Jin H, Xu J, Wen Z. Migratory path of definitive hematopoietic stem/progenitor cells during zebrafish development. *Blood.* 2007; 109: 5208-5214.

79. Murayama E, Kissa K, Zapata A, et al. Tracing hematopoietic precursor migration to successive hematopoietic organs during zebrafish development. *Immunity.* 2006; 25:963–75.

80. Willett CE, Cortes A, Zuasti A, et al. Early hematopoiesis and developing lymphoid organs in the zebrafish. *Dev Dyn.* 1999; 214: 323-336.

81. Murayama E, Kissa K, Zapata A, et al. Tracing hematopoietic precursor migration to successive hematopoietic organs during zebrafish development. *Immunity.* 2006; 25:963–75.

82. Lam SH, Chua HL, Gong Z, et al. Morphologic transformation of the thymus in developing zebrafish. *Dev Dyn.* 2002; 225:87–94.

83. Lord AM, North TE, Zon LI. Prostaglandin E2: making more of your marrow. *Cell Cycle*. 2007 Dec 15; 6(24):3054-7.

84. Liao EC, Paw BH, Oates AC, et al. SCL/Tal-1 transcription factor acts downstream of cloche to specify hematopoietic and vascular progenitors in zebrafish. *Genes Dev*. 1998; 12:621-626.

85. Gering M, Rodaway AR, Gottgens B, et al. The SCL gene specifies haemangioblast development from early mesoderm. *EMBO J.* 1998; 17:4029-4045.

86. Patterson LJ, Gering M, Patient R. Scl is required for dorsal aorta as well as blood formation in zebrafish embryos. *Blood.* 2005; 105:3502-3511.

87. Rhodes J, Hagen A, Hsu K, et al. Interplay of pu.1 and gata1 determines myelo-erythroid progenitor cell fate in zebrafish. *Dev Cell*. 2005; 8:97-108.

88. Thompson MA, Ransom DG, Pratt SJ, et al. The cloche and spadetail genes differentially affect hematopoiesis and vasculogenesis. *Dev Biol*. 1998; 197:248-269.

89. Patterson LJ, Gering M, Eckfeldt CE, et al. The transcription factors Scl and Lmo2 act together during development of the hemangioblast in zebrafish. *Blood.* 2007; 109:2389-2398.

90. Gering M, Yamada Y, Rabbitts TH, et al. Lmo2 and Scl/Tal1 convert non-axial mesoderm into haemangioblasts which differentiate into endothelial cells in the absence of Gata1. *Development.* 2003; 130:6187-6199.

91. Traver D, Herbomel P, Patton EE, et al. The zebrafish as a model organism to study development of the immune system. *Adv Immunol*. 2003; 81: 253–330.

92. Schorpp M, Bialecki M, Diekhoff D, et al. Conserved functions of ikaros in vertebrate lymphocyte development: genetic evidence for distinct larval and adult phases of T cell development and two lineages of B cells in zebrafish. *J Immunol.* 2006; 177: 2463–76.

93. Lam SH, Chua HL, Gong Z, et al. Development and maturation of the immune system in zebrafish, Danio rerio: a gene expression profiling, in situ hybridization and immunological study. *Dev Comp Immunol.* 2004; 28:9–28.

94. Conway G, Margoliath A, Wong-Madden S, et al. Jak1 kinase is required for cell migrations and anterior specification in zebrafish embryos. *Proc Natl Acad Sci U S A.* 1997; 94: 3082-3087.

95. Oates AC, Brownlie A, Pratt SJ, et al. Gene duplication of zebrafish JAK2 homologs is accompanied by divergent embryonic expression patterns: only jak2a is expressed during erythropoiesis. *Blood*. 1999; 94:2622-2636.

96. ZFIN:The zebrafish model organism database. http://zfin.org/cgi-bin/webdriver?MIval aamarkerview. apg&OID ZDB-GENE-070725–4. Accessed October 1, 2007.

97. Lieschke GJ. Zebrafish: an emerging genetic model for the study of cytokines and hematopoiesis in the era of functional genomics. *Int J Hematol.* 2001; 73:23-31.

98. Oates AC, Wollberg P, Pratt SJ, et al. Zebrafish stat3 is expressed in restricted tissues during embryogenesis and stat1 rescues cytokine signaling in a STAT1-deficient human cell line. *Dev Dyn*. 1999; 215:352-370.

99. Thisse B, Heyer V, Lux A, et al. Spatial and temporal expression of the zebrafish genome by large-scale in situ hybridization screening. *Methods Cell Biol.* 2004; 77:505-519.

100. Lewis RS, Ward AC. Conservation, duplication and divergence of the zebrafish stat5 genes. *Gene.* 2004; 338:65-74.

101. Jin HJ, Xiang LX, Shao JZ. Identification and characterization of suppressor of cytokine signaling 1 (SOCS-1) homologues in teleost fish. *Immunogenetics.* 2007; 59:673-686.

102. Jin HJ, Shao JZ, Xiang LX. Identification and characterization of suppressor of cytokine signaling 3 (SOCS-3) homologues in teleost fish. *Mol Immunol.* 2007; 44:1042-1051.

103. ZFIN: the zebrafish model organism database http://zfin.org/cgi-bin/webdriver?MIval aamarkerselect. apg&marker_type GENE& query_results t&input_name socs&compare contains&WINSIZE 20. Accessed October 1, 2007.

104. Ma ACH, Ward AC, Liang R, et al. The role of jak2a in zebrafish hematopoiesis. *Blood*. 2007; 110:1824-1830.

105. Hanumanthaiah R, Day K, Jagadeeswaran P. Comprehensive analysis of blood coagulation pathways in teleostei: evolution of coagulation factor genes and identification of zebrafish factor VIIi. *Blood Cells Mol Dis.* 2002; 29:57-68.

106. Klein J, Nikolaidis N. The descent of the antibody-based immune system by gradual evolution. *Proc Natl Acad Sci USA.* 2005; 102:169–174.

107. Du Pasquier L, Schwager J, Flajnik MF. The immune system of Xenopus. *Annu Rev Immunol.* 1989; 7:251–275.

108. Lugo-Villarino G, Balla KM, Stachura DL, et al. Identification of dendritic antigen-presenting cells in the zebrafish. *Proc Natl Acad Sci USA.* 2010; 107:15850-15855.

109. Hofmann J, Greter M, Du Pasquier L, et al. B-cells need a proper house, whereas T-cells are happy in a cave: the dependence of lymphocytes on secondary lymphoid tissues during evolution. *Trends Immunol*. 2010; 31, 144-153.

110. Du Pasquier L. The immune system of invertebrates and vertebrates. *Comp Biochem Physiol B Biochem Mol Biol.* 2001; 129:1–15.

111. Danilova N, Bussmann J, Jekosch K, et al. The immunoglobulin heavy-chain locus in zebrafish: identification and expression of a previously unknown isotype, immunoglobulin Z. *Nat Immunol.* 2005; 6:295–302.

112. Jing L, Zon LI. Zebrafish as a model for normal and malignant hematopoiesis. *Dis Model Mech.* 2011 Jul; 4(4):433-8.

113. Carradice D, Lieschke GJ. Zebrafish in hematology: sushi or science? *Blood.* 2008 Apr 1; 111(7):3331-42.

114. Rudner LA, Brown KH, Dobrinski KP, et al. Shared acquired genomic changes in zebrafish and human T-ALL. *Oncogene.* 2011; 30(41):4289-96.

115. Willett CE, Cherry JJ, Steiner LA. Characterization and expression of the recombination activating genes (rag1 and rag2) of zebrafish. *Immunogenetics.* 1997; 45:394-404.

116. Langenau DM, Traver D, Ferrando AA, et al. Myc-induced T cell leukemia in transgenic zebrafish. *Science.* 2003; 299: 887-890.

117. Ferrando AA, Neuberg DS, Staunton J, et al. Gene expression signatures define novel oncogenic pathways in T cell acute lymphoblastic leukemia. *Cancer Cell.* 2002; 1:75-87.

118. Langenau DM, Jette C, Berghmans S, et al. Suppression of apoptosis by bcl-2 overexpression in lymphoid cells of transgenic zebrafish. *Blood.* 2005; 105:3278-3285.

119. Chen J, Jette C, Kanki JP, et al. Notch1-induced T-cell leukemia in transgenic zebrafish. *Leukemia.* 2007; 21:462–71.

120. Littlewood TD, Hancock DC, Danielian PS, et al. A modified oestrogen receptor ligand-binding domain as an improved switch for the regulation of heterologous proteins. *Nucleic Acids Res*. 1995; 23:1686–1690.

121. Langenau DM, Ferrando AA, Traver D, et al. In vivo tracking of T cell development, ablation, and engraftment in transgenic zebrafish. *Proc Natl Acad Sci USA.* 2004; 101: 7369–7374.

122. Sabaawy HE, Azuma M, Embree LJ, et al. TELAML1 transgenic zebrafish model of precursor B cell acute lymphoblastic leukemia. *Proc Natl Acad Sci U S A*. 2006; 103:15166-15171.

123. Yeh JR, Munson KM, ChaoYL, et al. AML1-ETO reprograms hematopoietic cell fate by downregulating scl expression. *Development.* 2008; 135, 401-410.

124. Bretaud S, Lee S, Guo S. Sensitivity of zebrafish to environmental toxins implicated in Parkinson's disease. *Neurotoxicol Teratol.* 2004; 26: 857–864.

125. Hill AJ, Teraoka H, Heideman W, et al. Zebrafish as a model vertebrate for investigating chemical toxicity. *Toxicol Sci.* 2005; 86: 6–19.

126. Peterson RT, Link BA, Dowling JE, et al. Small molecule developmental screens reveal the logic and timing of vertebrate development. *Proc Natl Acad Sci USA.* 2000; 97:12965–12969.

127. Bowman TV and Zon LI. Swimming into the future of drug discovery: in vivo chemical screens in zebrafish. *ACS Chem. Biol*. 2008; 5: 159-161.

128. Rombough P. Gills are needed for ionoregulation before they are needed for O(2) uptake in developing zebrafish, Danio rerio. *J Exp Biol.* 2002; 205: 1787–1794.

129. Brandli AW. Prospects for the Xenopus embryo model in therapeutics technologies. *Chimia.* 2004; 58:694–702.

130. Chan J, Serluca FC. Chemical approaches to angiogenesis. *Methods Cell Biol.* 2004; 76:475–487.

131. Murphey RD, Stern HM, Straub CT, et al. A chemical genetic screen for cell cycle inhibitors in zebrafish embryos. *Chem Biol Drug Des.* 2006; 68:213–219.

132. Stern HM, Murphey RD, Shepard JL, et al. Small molecules that delay S phase suppress a zebrafish bmyb mutant. *Nat Chem Biol.* 2005; 1:366 –370.

133. Murphey RD, Zon LI. Small molecule screening in the zebrafish. *Methods.* 2006; 39: 255–261.

134. Butcher EC, Berg EL, Kunkel EJ. Systems biology in drug discovery. *Nat Biotechnol.* 2004; 22:1253–9.

135. Khersonsky SM, Jung DW, Kang TW, et al. Facilitated forward chemical genetics using a tagged triazine library and zebrafish embryo screening. *J Am Chem Soc*. 2003; 125:11804–11805.

136. Shin JT, Fishman MC. From Zebrafish to human: modular medical models. *Annu Rev Genomics Hum Genet.* 2002; 3:311–340.

137. den Hertog J. Chemical genetics: Drug screens in Zebrafish. *Biosci Rep*. 2005 Oct-Dec; 25(5-6):289-97.

138. Peterson RT, Shaw SY, Peterson TA, et al. Chemical suppression of a genetic mutation in a zebrafish model of aortic coarctation. *Nat Biotechnol.* 2004; 22:595–599.

139. Zhong TP, Rosenberg M, Mohideen MA, et al. gridlock, an HLH gene required for assembly of the aorta in zebrafish. *Science.* 2000; 287:1820 –1824.

140. Towbin JA, McQuinn TC. Gridlock: a model for coarctation of the aorta? *Nat Med.* 1995; 1:1141–1142.

141. North TE, Goessling W, Walkley CR, et al. Prostaglandin E2 regulates vertebrate haematopoietic stem cell homeostasis. *Nature.* 2007; 447:1007–1011.

142. Goessling W, North TE, Loewer S, et al. Genetic interaction of PGE2 and Wnt signaling regulates developmental specification of stem cells and regeneration. *Cell.* 2009; 136:1136-1147.

143. Yeh JR, Munson KM, Elagib KE, et al. Discovering chemical modifiers of oncogene-regulated hematopoietic differentiation. *Nat Chem Biol.* 2009; 5:236-243.

Table 3.1

Limitations of the zebrafish model in hematology research
Adapted from Carradice and Lieschke (2008).[113]

Area of research	Problem	Possible solution(s)
Anatomy	Different morphology of blood cells, eg, erythrocytes and thrombocytes are nucleated	Abstraction in experimental design, ie, seeing similarity rather than difference and learning from difference
	Different gross anatomy, eg, what is the equivalent of the marrow stroma?	Improving depth of understanding of zebrafish physiology and anatomy will likely narrow rather than widen the apparent gaps
Physiology	Lack of cell markers/antibodies	Partially addressed by rapidly expanding toolbox of fluorescently labeled cell compartments, but generation of a repertoire of zebrafish antibodies is highly desirable
	Lack of hematopoietic cell lines	Not currently addressed
	Lack of in vitro differentiation system (hematopoietic cell culture assays)	Identification and purification of zebrafish hematopoietic growth factors with optimization of zebrafish cell culture techniques
	Lack of inbred strains, eg, for transplantation studies; to facilitate gene mapping	Limited attempts to generate inbred lines which retain hybrid vigor
Genetics	Genetic divergence between fish and humans	Completion of zebrafish genome sequencing project will provide more information about missing genes, but some genetic diseases will prove difficult to model due to genome duplication and divergent evolution
		Despite divergence in gene structure and function, zebrafish bioassays for human gene activity can still have validity
	No technique for targeted gene modification by homologous recombination	TILLING (Targeting Induced Local Lesions In Genomes) allows off the shelf ordering of mutants in any gene of interest
		Library of characterized insertional mutants; random retroviral insertions disrupt the function of genes and tag the insertion site within the genome
		Transient knockdown of any gene easily achieved using morpholino antisense oligonucleotides (stable mutant line is preferable because of the possibility of nonspecific/off target morpholino effects)
	Limited options for conditional transgenesis or gene modification	Temperature sensitive alleles *hsp70* (heat shock) promoter Gal4-UAS transgenic approaches, Cre-recombinase or transposon-mediated recombination

Table 3.2

Zebrafish models of human leukemia

Adapted from Carradice and Lieschke (2008)[113] and Rudner et al. (2011).[114]

Disease	Zebrafish model	Model type	Phenotype
T cell leukemia	Mouse Myc overexpression	Conditional and traditional transgenic Tg(*rag2* :*LoxP-DsRED2-LoxP-EGFP-mMyc*)	Leukemia and tissue tumours
	Activated human NOTCH –1 overexpression	Transgenic Tg(*rag2:ICN1-EGFP*)	T cell leukemia and tissue infiltration
	Heritable oncogene overexpression and/or tumor suppressor down-regulation via ENU mutagenesis	Spontaneous leukemogenesis with variable penetration	T-cell leukemia and tissue infiltration
Acute myeloid leukemia t(8;21)	Human *RUNX1-RUNX1T1* (*AML1-ETO*) overexpression	Transient over-expression using mRNA injection	Early maturation block, cellular dysplasia, cerebral hemorrhages
Precursor B-acute lymphoblastic leukemia t(12;21)	Human *ETV6-RUNX1* (*TEL-AML1*) overexpression	Transgenic Tg(*XEF/XBA:EGFP-ETV6-RUNX1*)	Lymphoid leukemia
Myeloproliferative disorders	Activated *jak2a* overexpression	Transient overexpression CA-*jak2a*	Increase in *gata1* expressing erythrocytes
	Activated human *KRAS* overexpression	Conditional transgenic Tg(β-*actin:LoxP-EGFP-LoxP-KRASG12D*)	Myeloid precursor expansion, erythroid maturation block
Follicular lymphoma (t14;18)	*bcl2* overexpression	Transgenic Tg(*rag2:EGFP-bcl2*)	Lymphocytosis, resistance to γ irradiation and dexamethasone

Table 3.3

Summary of chemical library screens performed in zebrafish and *Xenopus*
Adapted from Wheeler and Brändli (2009).[38]

Library name	Source	Compounds screened	Conc.	Organism (Genotype)	Phenotypic readout
DIVERSet E	ChemBridge	1,100	10 μg/ml	Zebrafish (wild type)	Central nervous system, ear, cardiovascular system, pigmentation
1,3-dioxane library	Schreiber laboratory	1,300	60 μM	Zebrafish (wild type)	Embryogenesis
Compounds with biaryl containing medium rings	Schreiber laboratory	1,412	10μM	Zebrafish (wild type)	Embryogenesis
Trisubstituted triazines	Chang laboratory	109	10 μM	Zebrafish (wild type)	Embryogenesis
Tagged trisubstituted triazines	Chang laboratory	1,536	50 μM	Zebrafish (wild type)	Brain, Eye
Bioactive small molecules	Various suppliers	100	1,10 & 100μg/ml	Zebrafish (wild type)	Heart rate
DIVERSet E	ChemBridge	5,000	2 μg/ml	Zebrafish (wild type)	Erythropoiesis
DIVERSet E	ChemBridge	5,000 & 7,000	2 μg/ml	Zebrafish (*grl* mutant)	Suppression of vascular defect
Expanded 1,3 dioxane library	Schreiber laboratory	384	5-10 μM	Zebrafish (wild type)	Embryogenesis, organogenesis
Tagged trisubstituted triazines	Chang laboratory	1,536	10 μM	Zebrafish (wild type)	Pigmentation
DIVERSet E	ChemBridge	16,320	5 μg/ml (20 μM)	Zebrafish (*crb* mutant)	Suppression of mitotic defects
DIVERSet E	ChemBridge	16,320	20 μM	Zebrafish (wild type)	Suppression of mitotic defects
NINDS Custom Collection	NIH/NINDS	1,040	5 μg/ml (20 μM)	Zebrafish (wild type)	Haematopoiesis
Spectrum Collection	MicroSource	2,000	25 μM	Zebrafish (caudal fin amputation)	Inhibition of regeneration
LOPAC1280	Sigma Aldrich	1,280	30 μM	Zebrafish (transgenic VEGFR2: GRCFP)	Angiogenesis
DIVERSet E Collection	ChemBridge	5,580	10 μM	Zebrafish (wild type)	Dorsalization
DIVERSet E	ChemBridge	5,760	5 μg/ml (20 μM)	Zebrafish (wild type)	Organogenesis
a) Diversity set	NCI	1,990	20 & 40 μM	*Xenopus laevis* (wild type)	Pigmentation
LOPAC1280	Sigma Aldrich	1,280	20 μM	*Xenopus laevis* (wild type)	Blood vasculature, lymphatics
DIVERSet	ChemBridge	26,400	10 μM	Zebrafish (lck:eGFP)	Elimination of thymus fluorescence without systemic toxicity

A.

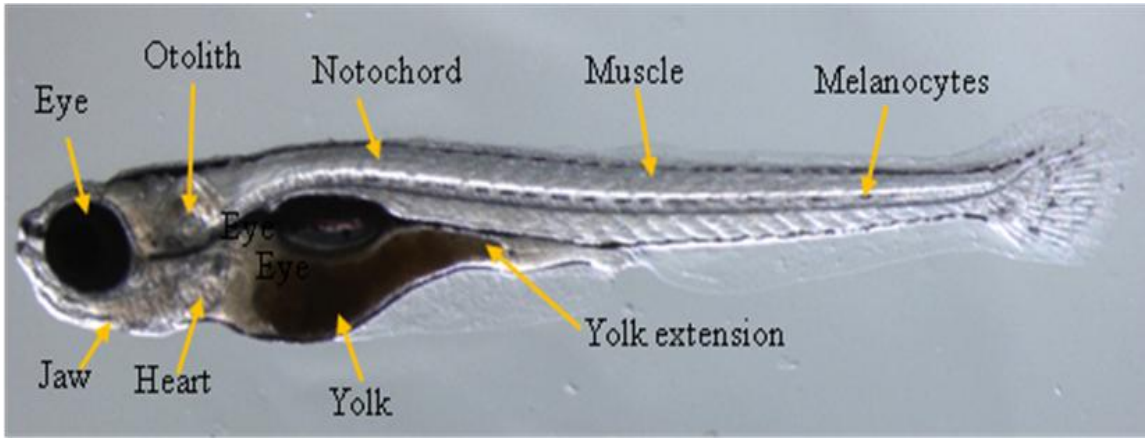

B.

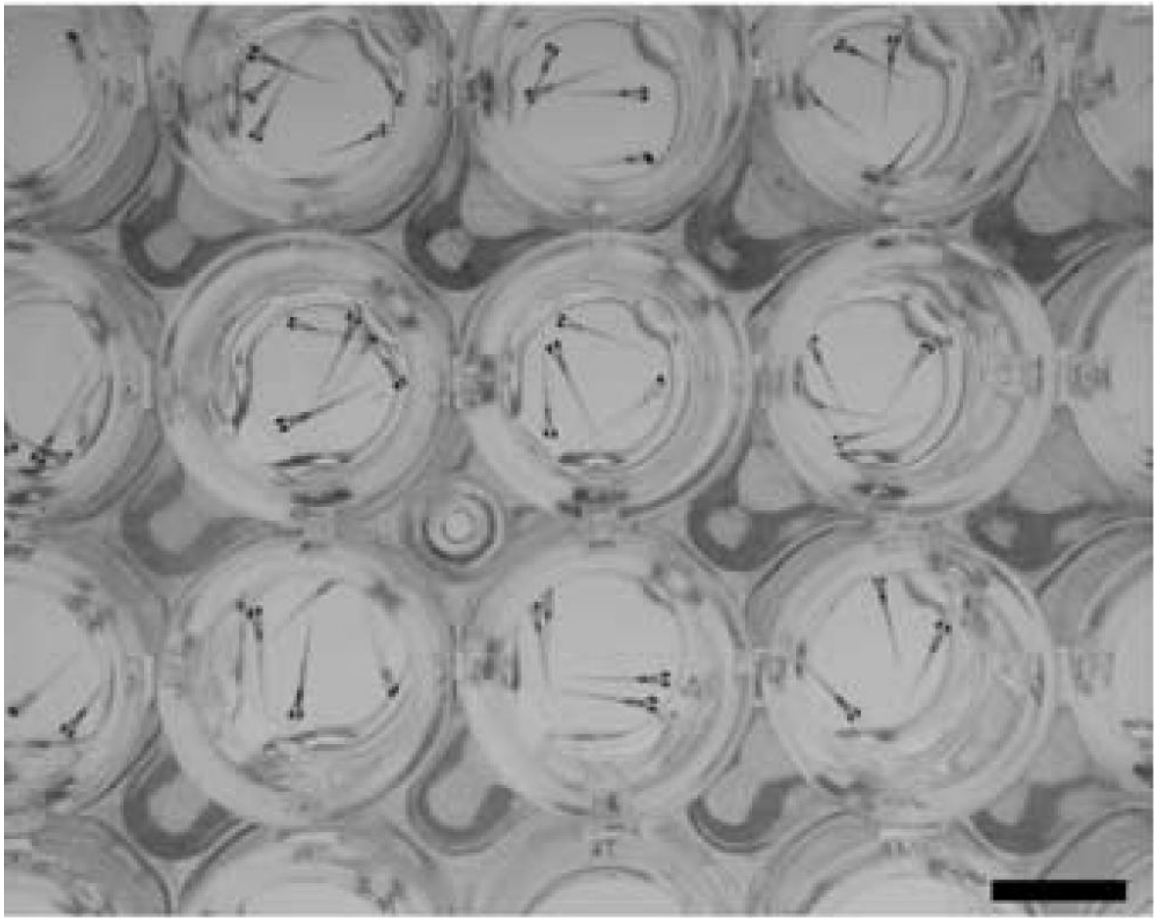

Figure 3.1 Zebrafish larva at 3-7dpf. (A) Organs such as the heart are clearly visible due to the optical clarity of the larva at this age. (B) Zebrafish larvae at 7dpf in a 96-well plate. Bar 5mm. Adapted from Barros et al. (2008).[39]

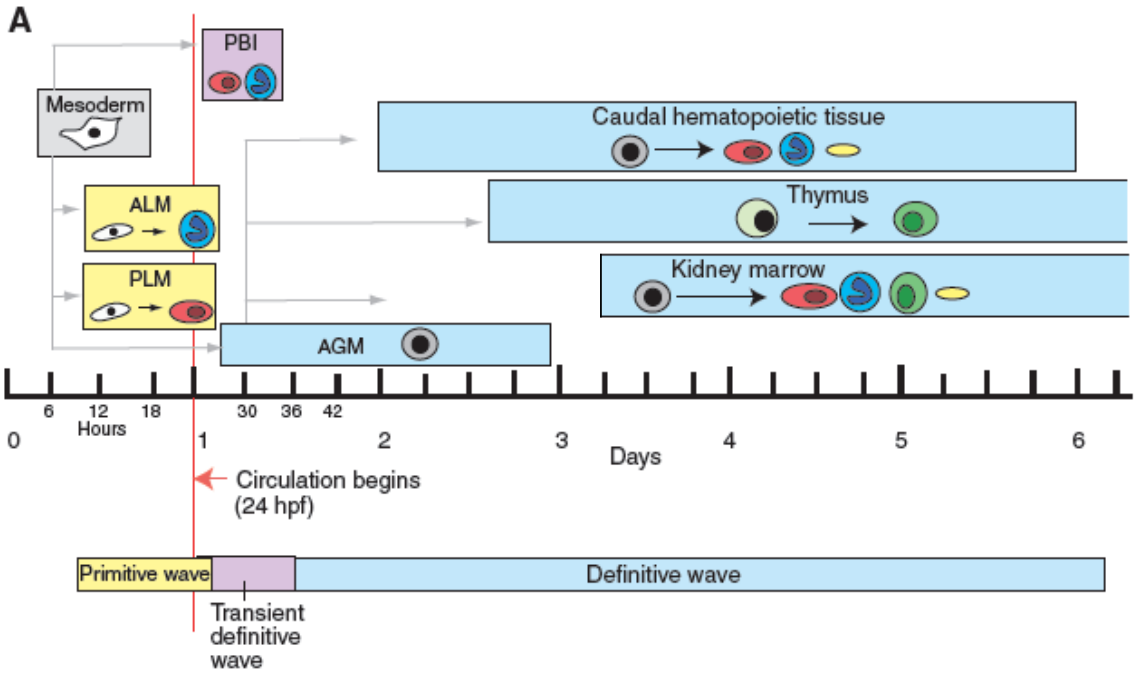

Figure 3.2. The ontogeny of hematopoiesis in zebrafish. Hematopoiesis in zebrafish occurs in consecutive waves. Embryonic primitive hematopoiesis (yellow) starts at around 11 hours post fertilization (hpf) when hemangioblasts (which have the potential to become either endothelial vascular cells or hematopoietic cells, shown in white) appear in the anterior lateral mesoderm (ALM) and posterior lateral mesoderm (PLM), which collectively are analogous to the blood islands in the mammalian yolk sac. Hemangioblasts in the PLM later converge medially to form the intermediate cell mass (ICM; not shown), where primitive erythrocytes (red) predominantly arise. The ALM, which later becomes the rostral blood island (RBI; not shown), is the major site for primitive myeloid cells (blue). At around 24 hpf, embryonic erythrocytes enter circulation. As circulation begins, hematopoiesis within the ICM gradually diminishes. A transient definitive wave (pink) initiates shortly after multi-lineage erythromyeloid progenitors appear in the posterior blood island (PBI). Starting from 26 hpf, definitive HSCs (gray) emerge from hemogenic endothelial cells of the dorsal aorta in the aorta-gonad-mesonephros (AGM) region. Shortly thereafter, HSCs migrate to and seed the caudal hematopoietic tissue at 48 hpf, which is an expansion of the PBI and acts as a transient hematopoietic site that gives rise to erythroid, myeloid and thromboid (yellow) cells. The caudal hematopoietic tissue is equivalent to mouse fetal liver or placenta. HSCs from the AGM region colonize kidney around 48 hpf. Kidney marrow, which is functionally similar to mammalian bone marrow, gives rise to all blood lineages, including erythroid, myeloid, thromboid and lymphoid (green) cells for the larval and adult zebrafish. At around 54 hpf, common lymphoid progenitor (CLP) cells from the AGM region seed the thymus, which is the site for maturation of lymphoid T cells. Adapted from Jing and Zon (2011).[112]

CHAPTER 4

ZEBRAFISH SCREEN IDENTIFIES NOVEL COMPOUND WITH SELECTIVE TOXICITY AGAINST LEUKEMIA

This research was originally published in *Blood.* Suzanne Ridges,[a] Will L. Heaton,[a] Deepa Joshi,[a] Nikolaus S. Trede,[a,b] et al. Zebrafish screen identifies novel compound with selective toxicity against leukemia. *Blood.* 2012; 119: 5621-5631.

a: Huntsman Cancer Institute, b: Department of Pediatrics, University of Utah, Salt Lake City, UT 84112, USA

Corresponding author: Dr. Nikolaus S. Trede

Investigator, The Huntsman Cancer Institute

University of Utah

2000 Circle of Hope

Salt Lake City, UT 84112, USA

Office: 1-801-585-0199

FAX: 1-801-581-8547

nikolaus.trede@hci.utah.edu

blood

2012 119: 5621-5631
Prepublished online April 9, 2012;
doi:10.1182/blood-2011-12-398818

Zebrafish screen identifies novel compound with selective toxicity against leukemia

Suzanne Ridges, Will L. Heaton, Deepa Joshi, Henry Choi, Anna Eiring, Lance Batchelor, Priya Choudhry, Elizabeth J. Manos, Hossein Sofla, Ali Sanati, Seth Welborn, Archana Agarwal, Gerald J. Spangrude, Rodney R. Miles, James E. Cox, J. Kimble Frazer, Michael Deininger, Kaveri Balan, Matthew Sigman, Markus Müschen, Tatiana Perova, Radia Johnson, Bertrand Montpellier, Cynthia J. Guidos, David A. Jones and Nikolaus S. Trede

Blood (print ISSN 0006-4971, online ISSN 1528-0020), is published weekly by the American Society of Hematology, 2021 L St, NW, Suite 900, Washington DC 20036.

Plenary paper

Zebrafish screen identifies novel compound with selective toxicity against leukemia

*Suzanne Ridges,[1] *Will L. Heaton,[1] *Deepa Joshi,[1] Henry Choi,[1] Anna Eiring,[1] Lance Batchelor,[1] Priya Choudhry,[1] Elizabeth J. Manos,[1] Hossein Sofla,[1] Ali Sanati,[1] Seth Welborn,[1] Archana Agarwal,[2] Gerald J. Spangrude,[2] Rodney R. Miles,[2] James E. Cox,[3] J. Kimble Frazer,[1,4] Michael Deininger,[1,5] Kaveri Balan,[6] Matthew Sigman,[6] Markus Müschen,[7] Tatiana Perova,[8,9] Radia Johnson,[8,10] Bertrand Montpellier,[8] Cynthia J. Guidos,[8-10] David A. Jones,[1] and Nikolaus S. Trede[1,4]

[1]Department of Oncological Sciences, Huntsman Cancer Institute, [2]Department of Pathology, [3]Metabolomics Core Facility, and Departments of [4]Pediatrics, [5]Hematology, and [6]Chemistry, University of Utah, Salt Lake City, UT; [7]Leukemia and Lymphoma Program, Norris Comprehensive Cancer Center, University of Southern California, Los Angeles, CA; [8]Program in Developmental and Stem Cell Biology, Hospital for Sick Children Research Institute, Toronto, ON; and Departments of [9]Medical Biophysics and [10]Immunology, University of Toronto, Toronto, ON

To detect targeted antileukemia agents we have designed a novel, high-content in vivo screen using genetically engineered, T-cell reporting zebrafish. We exploited the developmental similarities between normal and malignant T lymphoblasts to screen a small molecule library for activity against immature T cells with a simple visual readout in zebrafish larvae. After screening 26 400 molecules, we identified Lenaldekar (LDK), a compound that eliminates immature T cells in developing zebrafish without affecting the cell cycle in other cell types. LDK is well tolerated in vertebrates and induces long-term remission in adult zebrafish with cMYC-induced T-cell acute lymphoblastic leukemia (T-ALL). LDK causes dephosphorylation of members of the PI3 kinase/AKT/mTOR pathway and delays sensitive cells in late mitosis. Among human cancers, LDK selectively affects survival of hematopoietic malignancy lines and primary leukemias, including therapy-refractory B-ALL and chronic myelogenous leukemia samples, and inhibits growth of human T-ALL xenografts. This work demonstrates the utility of our method using zebrafish for antineoplastic candidate drug identification and suggests a new approach for targeted leukemia therapy. Although our efforts focused on leukemia therapy, this screening approach has broad implications as it can be translated to other cancer types involving malignant degeneration of developmentally arrested cells. (*Blood*. 2012;119(24):5621-5631)

Introduction

The yearly incidence in the US for all leukemia types, including acute lymphoblastic leukemia (ALL), acute myeloid leukemia (AML), and chronic myelogenous leukemia (CML), was estimated at more than 40 000 men and women in 2010, with a yearly death rate of 50%.[1] More than 2000 cases of ALL are diagnosed in US children every year, making it the most common childhood cancer.[2] T-cell ALL (T-ALL) represents approximately 15% and 25% of pediatric and adult ALL cases, respectively.[3] Although leukemia treatment has become increasingly efficient over the past 50 years, mortality from ALL is still 20% for children and more than 40% for adults, and T-ALL has been more difficult to treat than B-cell ALL (B-ALL).[4] Currently, research efforts are devoted to molecular-based risk stratification of patients and the development of targeted therapies to limit side effects[5-7] and to increase treatment efficacy.

Development of targeted cancer therapies typically requires knowledge of the molecular target.[8] In the absence thereof, an alternative approach may use a robust readout designed to screen large numbers of compounds for specific effects[9] against the malignant cell type in question. More than 50% of patients with T-ALL have deregulated NOTCH1,[10] and in a recent study 47% had mutations in the PI3 kinase/AKT/mTOR (P/A/mT) pathway.[11] NOTCH1 signaling requires proteolytic cleavage by γ-secretase and other proteases[12] to release the intracytoplasmic domain, providing several potential targets for therapeutic intervention. Targeted treatment approaches for T-ALL using γ-secretase inhibitors (GSIs), although appearing a priori promising, have been disappointing,[13] possibly through pre-existing or newly acquired mutations in phosphatase and tensin homolog (PTEN) that render many T-ALL cell lines AKT-addicted.[14] However, others found that even in the absence of PTEN, primary murine and human T-ALL samples remain sensitive to NOTCH inhibition.[15] Overall, gain-of-function mutations in the NOTCH1 and P/A/mT pathways are strongly selected for in human T-ALL. This has raised interest in clinically useful, nontoxic inhibitors of the P/A/mT pathway[13] for leukemia and other cancers,[16] and makes combined treatment approaches (anti-NOTCH, anti-P/A/mT) attractive.[17]

Small molecule screens can be carried out in vitro either using biochemical assays or cell lines. Although often successful in providing "hits," these approaches lack the biologic context of an entire vertebrate organism, and identified active compounds often fail when applied in vivo because of poor bioavailability or toxicity. Although mice are an integral component of preclinical drug development, their use for high-throughput drug screening is fiscally prohibitive. Small animal models are therefore needed. For

Submitted December 19, 2011; accepted March 11, 2012. Prepublished online as *Blood* First Edition paper, April 9, 2012; DOI 10.1182/blood-2011-12-398818.

*S.R., W.L.H., and D.J. contributed equally to this work.

There is an Inside *Blood* commentary on this article in this issue.

The online version of this article contains a data supplement.

The publication costs of this article were defrayed in part by page charge payment. Therefore, and solely to indicate this fact, this article is hereby marked "advertisement" in accordance with 18 USC section 1734.

anti–T-ALL drug development, the zebrafish (*Danio rerio*) appears particularly well-suited because its adaptive immune system is similar to that of humans,[18] T-ALL models have been established,[19,20] and its use for in vivo drug discovery is advantageous (reviewed by Langenau et al[21]).

We have previously shown that dexamethasone, widely used for treatment of T-ALL, can eliminate immature T cells from the thymus of zebrafish larvae carrying the T-cell specific *p56^{lck}-promoter*:enhanced green fluorescence protein (*lck*:EGFP) transgene.[21] In a novel zebrafish screen we searched a small molecule library for compounds that similarly eliminate immature T cells from 5 days post fertilization (dpf) *lck*:EGFP larvae, reasoning that active compounds may also eliminate developmentally arrested, immature T-ALL blasts. One compound we identified, with previously unknown biologic activity, is active against immature normal and cMYC-transformed leukemic T cells in adult zebrafish[20] and has selective activity against human leukemia lines. We named the compound Lenaldekar (LDK; 1H-indole-3-carbaldehyde 8-quinolinylhydrazone). LDK is well tolerated in mice, has favorable pharmacokinetics, and slows the in vivo growth of human T-ALL in murine xenografts. Importantly, LDK is active against primary human leukemia cells, including T315I mutated, BCR-ABL positive, therapy-refractory B-ALL and CML samples. We show that in all sensitive cells LDK has 2 independent activities: delay in late mitosis and inhibition of the P/A/mT pathway, probably by an indirect route. LDK-resistant cells tested to date lack mitotic delay, suggesting that both activities of LDK may be required for cytotoxicity and providing a possible mechanistic basis for its selectivity. We propose that LDK's unique activity offers a new, targeted approach to leukemia treatment.

Methods

Zebrafish and mouse studies

Animal studies were performed according to the University of Utah animal protocol guidelines under protocol numbers 11-07006 (zebrafish) and 09-11001 and 09-11002 (mouse).

Zebrafish drug screen

The transgenic *p56^{lck}*:EGFP zebrafish line (*lck*:EGFP) was previously described.[21] *lck*:EGFP transgenic zebrafish were bred and eggs collected and raised in E3 water 5 to 6 dpf. Larvae were then aliquoted 3 per well in a 96-well format in 300 μL E3 fish water. Compounds for screening from the ChemBridge DIVERSet Library (ChemBridge) were added to each well of the duplicate plates at a final concentration of 10μM. Zebrafish larvae were examined after 2 days of incubation in compounds and scored for thymus fluorescence via Nikon Eclipse E600 imaging system by 2 operators. Scores ("unchanged," "moderate," or "strong reduction" of fluorescence emitted from T cells in thymus compared with diluent treated controls) were compared and reconciled. Initial "hits" were retested and subjected to a dose-response assay at 1, 5, 10, and 25μM. Initially, 112 compounds scored as "hits." Of these, 21 compounds that reproducibly caused "strong reduction" in thymus fluorescence without obvious larval toxicity ≤ 10μM were retained for further evaluation.

Zebrafish embryo cell cycle analysis

Dechorionated embryos were incubated with compounds at 4 hours postfertilization (hpf). At 24 hpf, larvae were dissociated, stained with propidium iodide (PI), and analyzed for cell cycle status[38] using the ModFit LT Version 3.1 software (Verity Software House).

Leukemic zebrafish experiments

rag2. cMYC-ER zebrafish[22] were crossed with *lck*:EGFP zebrafish and leukemic adults were identified via fluorescence microscopy for T-ALL dissemination. Leukemic adults were treated either with vehicle or LDK on a 2-day-on, 1-day-off treatment regimen with daily water changes. Treatment was discontinued after 14 days. Tumor response was monitored twice weekly using the Olympus MVX10 Imaging System.

Tissue sections and staining

Fish were fixed in paraformaldehyde (4% in PBS), and sequential 4-micron-thick sections were either stained with H&E or with anti-GFP antibody (B-2; Santa Cruz Biotechnology) at 1:400 dilution with hematoxylin counterstaining.

Mouse xenograft experiments

Male nonobese diabetic (NOD)–severe combined immunodeficiency (SCID) mice were injected with 500 000 Matrigel (BD Bioscience) embedded CCRF-CEM-Luc cells per flank. After 3 days, mice were injected intraperitoneally twice daily with vehicle only (5% cremophor-EL, 5% N,N-dimethylacetamide, and 0.7% NaCl in ddH_2O at pH 6.0) or LDK (16 mg/kg) and monitored weekly for tumor progression using Xenogen IVIS 100 Imaging System (Caliper Life Sciences) and Living Image Version 2.50 software (Caliper Life Sciences). *P* values were calculated using Wilcoxon rank sum test.

Primary human leukemia samples

De-identified primary human patient samples were obtained under the University of Utah IRB protocol no. 10924. B-ALL samples (see Figure 5A-D) were cocultured with OP9 feeder cells. For CML specimens, frozen CD34$^+$ cells from peripheral blood (PB) of CML-CP (chronic phase) patients (n = 2) were cultured overnight in Iscove modified Dulbecco medium (IMDM) plus 30% FBS and 2mM L-glutamine supplemented with IL-3 (20 ng/mL), IL-6 (20 ng/mL), Flt-3 ligand (100 ng/mL), and kit ligand (100 ng/mL; StemCell Technologies). The CD34$^+$ fraction was isolated using the CD34 MultiSort kit (Miltenyi Biotec). For Ph$^+$ALL specimens, frozen mononuclear patient cells from PB were cultured overnight in IMDM plus 30% FBS and 2mM L-glutamine supplemented IL-7 (10 ng/mL; Peprotech) and treated as indicated.

Results

Zebrafish screen identifies compounds targeted to immature T cells

Our previous studies revealed that dexamethasone, known for its toxicity against human lymphoblasts, also eliminates immature T cells in the thymus of zebrafish larvae.[21] We reasoned that among the molecules identified in a drug screen for their activity against immature T cells in zebrafish, we would find novel compounds with the potential to eradicate human T-ALL cells. The use of the transgenic *lck*:EGFP line that fluorescently labels all T cells facilitates rapid assessment of a compound's effect on T-cell survival in a 96-well format by fluorescence microscopy.[21] Based on these considerations, 3 *lck*:EGFP transgenic zebrafish at 5 dpf were placed in each well of a 96-well plate and incubated for 2 days with compounds at 10μM from the ChemBridge DIVERSet library (Figure 1A-C). On retesting of 112 primary "hits" (among the 26 400 compounds screened) with strong reduction of EGFP-positive immature T cells in the thymus of zebrafish larvae, 21 were retained as candidates (supplemental Table 1, available on the *Blood* Web site; see the Supplemental Materials link at the top of the online article). To ascertain that these "hits," contrary to

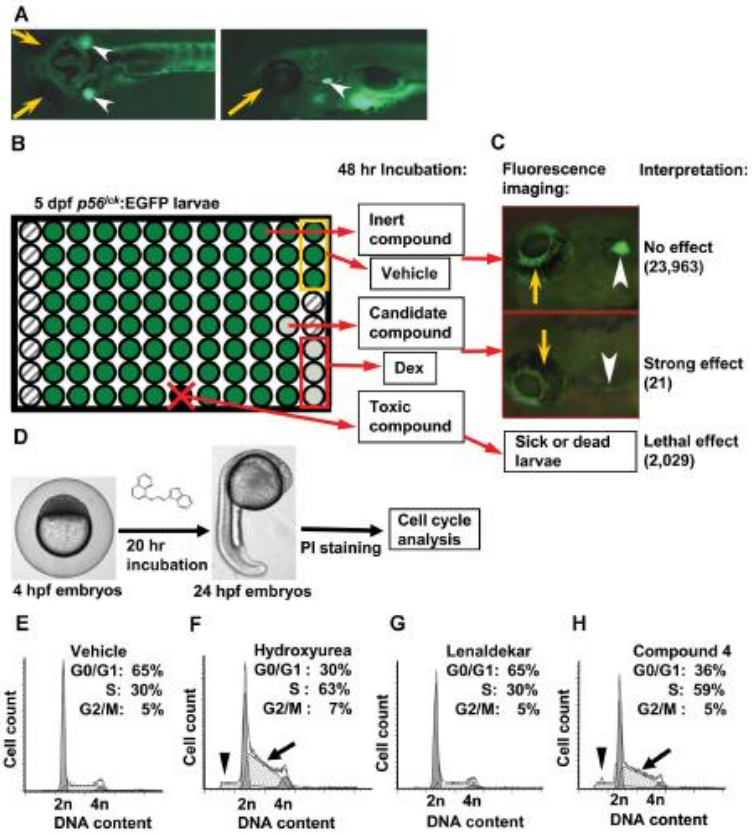

Figure 1. Zebrafish drug screen identifies anti–T-cell compounds. Zebrafish larvae carrying the T-cell specific *lck*:EGFP transgene were used for screening of a small molecule library for anti–T-cell effect. (A) Dorsal (left) and lateral (right) views of 5 days post fertilization (dpf) normal healthy *lck*:EGFP larva (yellow arrow indicates eye; and arrowhead, thymus). (B) Three 5-dpf larvae per well in 96-well format were treated with compounds, DMSO (vehicle, yellow box) and dexamethasone (Dex; positive control, red box). Fluorescence emission was evaluated after 48 hours: no effect/normal fluorescence (dark green), strong effect (light green), toxic effect (black well/red x), and empty well (hatched). (C) Examples of strong (bottom) and no effect (top). Of 26 400 compounds screened, 387 compounds with weak reduction of thymus fluorescence were also identified. (D) Twenty-one compounds with strong effect on survival of immature T cells were tested for cell cycle effects in nonlymphoid cells. Four hours postfertilization (hpf) zebrafish larvae were incubated in candidate compounds for 20 hours, dissociated into single-cell suspensions, stained with propidium iodide (PI) and subjected to flow cytometry. (E) Representative cell cycle profile for DMSO vehicle-treated embryos. (F) Hydroxyurea-treated embryos show S-phase arrest (arrow) as well as sub-G_1 peak (arrowhead). (G) Lenaldekar (5μM) shows a cell cycle profile similar to that of control embryos. (H) Compound 4 shows S-phase arrest (arrow) and sub-G_1 peak (arrowhead); 2n indicates G_0/G_1 phase; 4n, G_2/M phase; and between 2n and 4n, S phase. (A-C) Images were acquired at room temperature using Olympus MVX10 microscope with MV PLAPO 1× lens (Olympus). Camera used was Diagnostic Instruments model 14.2 Color Mosaic Insight FireWire SPOT. Acquisition software used was SPOT Atlas Version 4.6 software, 2000 ms exposure with no binning, $\gamma = 1.0$. Fluorescence excitation light source was EXFO X-Cite Series 120. (D) Microscope used was Nikon Eclipse E800 with Nikon Plan APO 4× lens at room temperature. Camera used was CRI Nuance multispectral imaging system model N-MSI-420-FL. SPOT Advanced Version 4.6 acquisition software was used.

conventional chemotherapy, did not affect the cell cycle in all cell types, we incubated each with 20 zebrafish embryos at 4 hours postfertilization (hpf) and performed cell cycle analysis on cells isolated from whole embryos at 24 hpf (Figure 1D). Sixteen of the 21 compounds caused detectable cell cycle delays in S-phase or G_0/G_1 (supplemental Table 1) and some caused a sub-G_1 peak, indicative of cytotoxicity. The remaining 5 compounds had no effect on the cell cycle, caused no cytotoxicity (Figure 1E-H) and thus met criteria for drugs targeted to immature zebrafish T cells.

Lenaldekar induces apoptosis selectively in human leukemic blasts

Testing these 5 molecules by thiazolyl blue tetrazolium bromide (MTT) assay in the Jurkat T-ALL line (Figure 2A), one compound that we named LDK (Figure 2B) was the most potent with an IC_{50} consistently between 0.8 and −1.3μM, measured by both MTT (Figure 2A,D-F,H) and trypan blue exclusion test (Figure 2C). LDK was equally effective against the other 4 human T-ALL lines

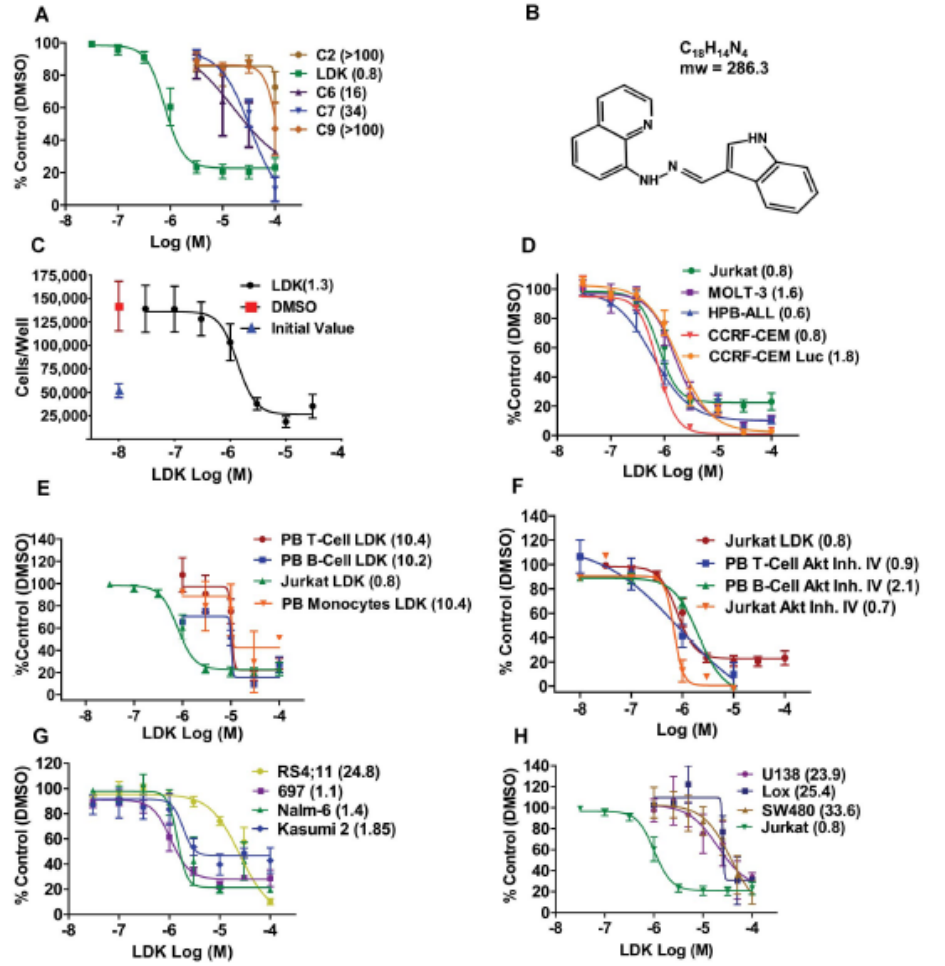

Figure 2. LDK is active against malignant lymphoblasts. IC_{50} values (μM) of indicated treatments by MTT assay after 48-hour incubation are shown in parentheses. (A) Among 5 hit compounds without general cell cycle effects, only Lenaldekar (LDK) had low micromolar activity against human Jurkat T-ALL (IC_{50} = 0.8μM). (B) LDK chemical structure (1H-indole-3-carbaldehyde quinolin-8-yl-hydrazone). (C) Trypan blue exclusion assay for LDK-treated Jurkat cells. (D) LDK dose-response for 5 human T-ALL lines. (E) LDK dose-response for PBTCs (stimulated with IL-2 30 U/mL), PB B cells (stimulated with IL-10 100 ng/mL), and PB monocytes from healthy human donors, compared with Jurkat. (F) Dose-response for LDK compared with AKT Inhibitor IV for Jurkat, PBTCs, and PB B cells. (G) LDK dose-response for 4 human B-ALL lines. (H) Jurkat T-ALL response to LDK in comparison to glioblastoma (U138), melanoma (Lox), and colon cancer (SW480). (A-H) n ≥ 3, error bars = SEM.

we tested (Figure 2D). LDK was more potent than GSI IX at inhibiting growth of 4 primary murine T-ALL lines harboring mutant NOTCH1, derived from *Atm*-deficient mice,[23] regardless of PTEN status (supplemental Figure 1). However, the IC_{50} of LDK in IL-2 stimulated peripheral blood T cells (PBTCs), B cells, and monocytes from healthy donors was 10-fold higher than in lymphoblasts (Figure 2E). AKT is an important enzyme in the survival of T-ALL cells and developing, immature thymocytes. We therefore chose an AKT inhibitor to test whether such a molecule would affect the survival of PBTCs. Interestingly, AKT inhibitor IV, equipotent to LDK against lymphoblastic cells, readily killed PBTCs (Figure 2F), which suggests that the lack of LDK activity against PBTCs was not based on general resistance to cell death in our assay system, and indicates a superior therapeutic window compared with a known AKT inhibitor. LDK was active against 3 B-ALL lines with an IC_{50} of 1 to 2μM, but higher concentrations (IC_{50} of ~ 25μM) were required against the RS4;11 line (Figure 2G). The IC_{50}s of 8 epithelial cancer cell lines tested ranged from

20 to 100μM, significantly higher than those for lymphoblastic lines, (Figure 2H, data not shown). To interrogate the apparent selectivity for lymphoid lineage malignancies, we tested LDK for efficacy against the NCI60 cell line panel. The 6 hematologic malignancy lines in this panel, including the multiple myeloma line RPMI-8226, the AML line HL-60, and the CML-derived line K-562, had IC_{50} values of 0.16 to 2.3μM, within the range of the T and B-ALL lines we had previously tested (supplemental Figure 2A). By contrast, the majority of the remaining 54 epithelial cancer lines had IC_{50} values more than 10-fold above the hematologic malignancy lines.

We next explored whether LDK killed Jurkat cells by apoptosis, the predominant form of cell death after drug treatment. Indeed, LDK at 1μM induced apoptosis in Jurkat cells, measured both by flow cytometry (supplemental Figure 2B), by Western blot (supplemental Figure 2C), and by activated caspase 3 staining (supplemental Figure 2D). LDK at 10μM caused only minimal visible toxicity in developing zebrafish embryos and larvae (supplemental Table 2).

LDK has in vivo activity in a zebrafish T-ALL model

We next tested whether LDK had anti–T-ALL activity in vivo. Affected adult individuals from the human cMYC-expressing line of zebrafish, crossed onto the *lck*:EGFP background (Figure 3A), were incubated with LDK at 250nM for 14 days on a 2-days-on/1-day-off treatment regimen. EGFP emission from T lymphoblasts was captured by fluorescence microscopy. Eighty-five percent of treated fish responded to LDK with a marked reduction of fluorescence extent and intensity (Figure 3B) and the remaining 15% of LDK-treated fish showed stable tumor burden (data not shown). To ascertain that fluorescence reduction was because of elimination of T-ALL cells, treated fish were sectioned and compared with untreated siblings. H&E staining of sections demonstrated a marked reduction in cells infiltrating nonlymphoid tissues such as skin and was mirrored by a decrease in EGFP-positive cells (Figure 3C) in treated individuals. This indicates that decrease in GFP intensity in LDK-treated zebrafish was because of absence of T lymphoblasts and not to quenching of the EGFP signal. By contrast, 100% of vehicle treated fish showed tumor progression and all succumbed to disease by day 40 (Figure 3B-D). Remarkably, despite the short course of treatment, the majority of LDK-treated fish maintained long-term remission (Figure 3D).

LDK is active against human T-ALL in murine xenografts

For in vivo efficacy testing in mammals, we intended to use luciferase-transduced Jurkat cells, but found that they did not engraft well into NOD/SCID mice (data not shown), as has been previously reported.[24] We therefore turned to luciferase-transduced CCRF-CEM T-ALL cells that had IC_{50} values (Figure 2D) similar to Jurkat cells, and engrafted better in NOD/SCID mice.[24] Other characteristics of CCRF-CEM cells were also similar to Jurkat cells (supplemental Figure 6). We embedded 5×10^5 cells in Matrigel and transplanted them into each flank of NOD/SCID mice.[25] Three days after xenografting, and then weekly for 4 weeks, mice were injected with luciferin and luminescence was measured. After the first measurement, mice were separated into 2 groups, one receiving diluent only, the other LDK at 16 mg/kg intraperitoneally twice daily. Luminescence was significantly lower in LDK-treated individuals on weeks 2, 3, and 4 (Figure 3E-F), resulting in a greater than 4-fold difference at the end of treatment. Furthermore, the average weight of the mice in each group was not statistically different at any time point, indicating lack of gastrointestinal toxicity of LDK (Figure 3G).

LDK leads to inhibition of the P/A/mT pathway

Next we wanted to identify the biologic pathway modulated by LDK. Our screening rationale predicted a pathway on which both immature developing T cells and developmentally arrested, immature T lymphoblasts are critically dependent. An obvious candidate is the P/A/mT pathway that is important for survival of immature T cells.[26] In addition, the recent detection of high-frequency abnormalities in the P/A/mT pathway in T-ALL[11] explains their exquisite sensitivity to inhibition of this pathway.[27] Western blot experiments showed that LDK, but not dexamethasone (data not shown), led to diminished phosphorylation of AKT on both T308 and S473 (Figure 4A). Similarly, LDK led to dephosphorylation of mTOR and of p70S6 kinase (S6K), a direct mTOR target (Figure 4B-C). Decreased AKT and mTOR phosphorylation was first detectable 1 hour after incubation with LDK at 2.5 and 5μM, respectively (supplemental Figure 3A), close to the IC_{50} in Jurkat cells. To determine the effects of LDK on AKT's phosphorylation dynamics, we examined LDK's ability to prevent serum-induced phosphorylation of serum-starved cells. Among T-ALL lines tested, CCRF-CEM showed the most robust decrease in AKT phosphorylation after 72 hours of serum starvation. The known PI3K inhibitor Ly294002 blocked any rephosphorylation of AKT with a 15- or 30-minute preincubation time (supplemental Figure 3B). LDK, on the other hand, did not block serum-induced AKT phosphorylation even after 30 minutes of preincubation and showed reduction of AKT phosphorylation first at 15 minutes after serum-stimulation (supplemental Figure 3B). We have also examined phosphorylation dynamics of S473 and have obtained identical results to T308 (data not shown).

To test whether P/A/mT pathway inhibition was selective and a general feature of LDK's activity in lymphoblastic cells, we assessed murine B-cell lines Ramos and BaF3 by Phosflow analysis.[28] Growth factor–independent Ramos cells have baseline hyperphosphorylated SRC and S6 ribosomal protein (S6; supplemental Figure 3C). As expected, the tyrosine kinase inhibitor dasatinib reduced SRC phosphorylation to background levels but did not affect S6 phosphorylation. Conversely, LDK did not affect pSRC but reduced S6 phosphorylation close to background levels (supplemental Figure 3C). The IL-3 dependent pro-B cell line BaF3 shows increased phosphorylation of signal transducer and activator of transcription (STAT)3 and S6 after IL-3 stimulation (supplemental Figure 3D). As expected, JAK Inhibitor I reduced IL-3–induced phosphorylation of both STAT3 and S6 to background levels. In contrast, LDK prevented IL-3–induced phosphorylation of S6 but not of STAT3 (supplemental Figure 3D). Furthermore, LDK did not affect IL-3–induced phosphorylation of STAT5, ERK1/2, or p38 in BaF3 cells (data not shown). These findings support selective action of LDK on the P/A/mT signaling pathway in lymphoblastic lines.

Next we wanted to determine whether inhibition of the P/A/mT pathway was required for LDK's cytotoxic activity. For this we modified a myristoylated form of AKT (myr-AKT, a kind gift from Dr S. Grant) that targets AKT to the plasma membrane, by introducing phosphomimetic aspartic acid residues at T308 and S473. We introduced this constitutively active form of AKT (myr-AKT-DD) into Jurkat cells. Expression and activity of the construct was demonstrated by Western blot (supplemental Figure 4A). Whereas native Jurkat cells responded to LDK treatment with PARP cleavage and marked decrease in viability, constitutively

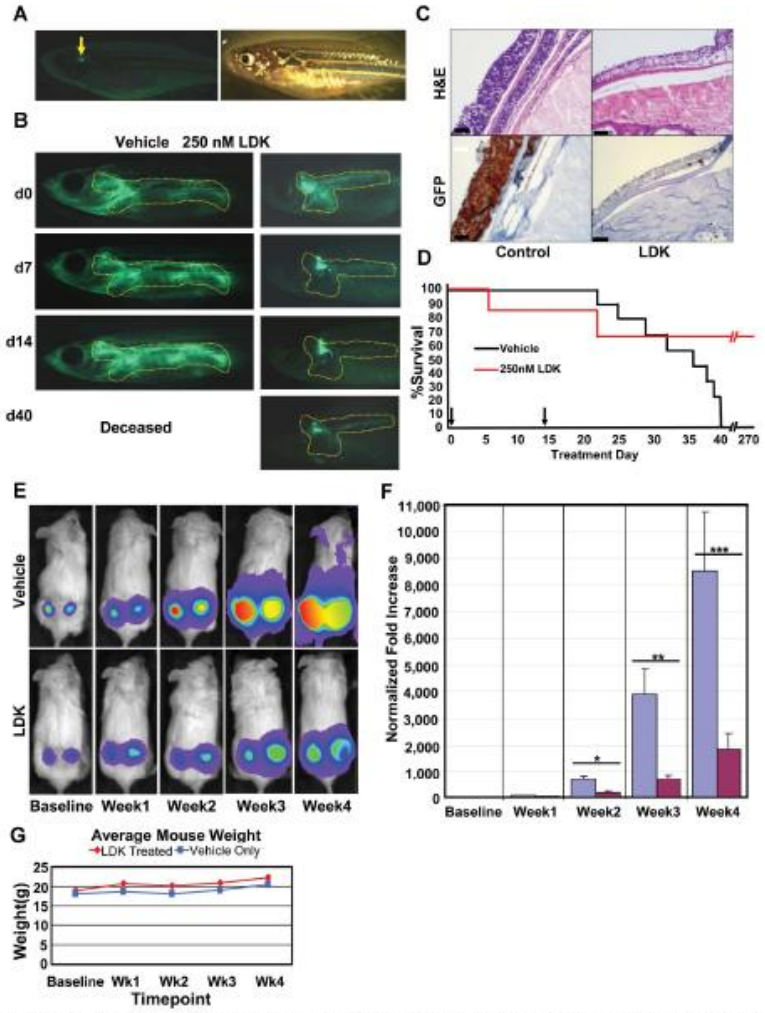

Figure 3. LDK treatment inhibits tumor progression in 2 in vivo models of T-ALL. (A-D) Adult *rag2*:cMYC-ER*lck*EGFP transgenic zebrafish with T-cell leukemia infiltration (outline) were treated with DMSO vehicle (n = 10) or 250nM LDK (n = 20) dissolved in E3 fish water over a 2-week period. As continuous exposure to LDK had toxic side effects, fish were subjected to a well-tolerated 2-day on drug/1-day off drug treatment regimen before being taken off drug altogether after day 14. (A) Fluorescence (left) and bright field (right) imaging of normal healthy adult *rag2*:cMYC-ER*lck*EGFP transgenic fish (arrow indicates normal T-cell fluorescence in thymus). (B) Treatment outcome of leukemic zebrafish incubated in DMSO vehicle only or 250nM LDK. One representative fish shown per treatment. (C) Vehicle control (left panels) and LDK treated (right panels) leukemic fish were sectioned and stained with H&E (top panels) as well as immunohistochemistry staining for GFP (bottom panels). Scale bars, 10 μm. (D) Kaplan-Meier survival plot shows superior survival of LDK-treated fish. Although all vehicle-treated fish (10/10) had expired by day 40, 67% of LDK-treated fish (13/20) were alive at day 270 (256 days after treatment). Three LDK-treated fish expired of unknown causes. Arrows indicate start and end time points of treatment. (E-G) LDK treatment inhibits tumor growth in a mouse xenograft model of T-ALL. Thirty male NOD-SCID mice were injected in each flank with 5×10^6 luciferase-transduced CCRF-CEM T-ALL cells. Cells were then allowed to engraft for 3 days before first bioluminescence measurement. The mice were then divided into 2 groups of 15 mice each and treated twice daily via intraperitoneal injection with either LDK (16 mg/kg) or vehicle only. Bioluminescence was assessed weekly with a CCD camera. (E) Representative pictures for tumor progression in vehicle control (top) versus LDK-treated (bottom) mice. (F) Increase in tumor bioluminescence of vehicle and LDK-treated mice, normalized to baseline. (*P = .0265, **P = .0006, ***P = .0304). (G) Average weight of LDK-treated (red line) versus vehicle only (blue line) treated mice. Error bars = SEM. (A-B) Images were acquired at room temperature using the Olympus MVX10 microscope with MV PLAPO 1× lens (Olympus). Camera used was Diagnostic Instruments model 14.2 Color Mosaic Insight FireWire SPOT. SPOT Atlas Version 4.6 acquisition software was used, 2000 ms exposure with no binning, $\gamma = 1.0$. Fluorescence excitation light source was EXFO X-Cite Series 120. (C) Images were obtained using automated immunostainer (BenchMark XT; Ventana Medical Systems) followed by iView DAB detection (Ventana Medical Systems). (E) Mouse images and tumor emittance data were collected at 37°C using the XENOGEN IVIS 100 imaging system (Caliper Life Sciences) with Spectral Instruments 600 Series camera controller. Mouse images were processed and analyzed for quantitative emittance using Living Image Version 2.50.2 software (Caliper Life Sciences).

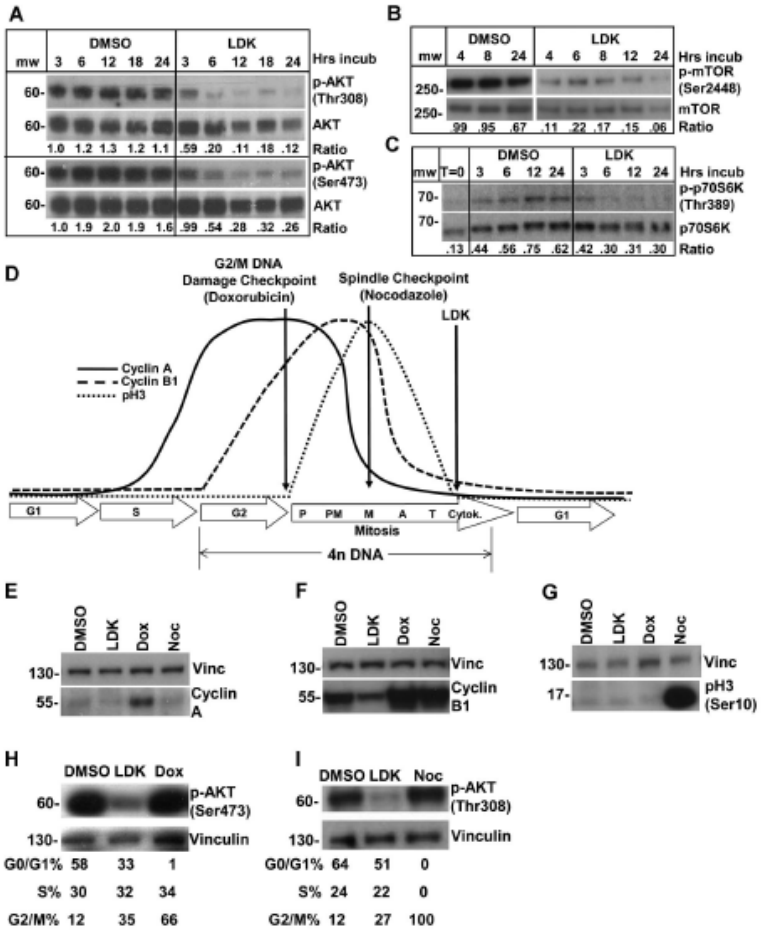

Figure 4. LDK down-regulates phosphorylation of targets in the PI3K/AKT/mTOR pathway and causes late mitosis arrest in treated cells. (A-C) Jurkat cells were treated with 10μM LDK for the indicated durations then probed for phospho as well as total proteins by Western blot. Densitometric ratio of phospho to total protein is indicated below the paired panels. (A) LDK treatment reduces phosphorylation of AKT at Thr308 and Ser473. (B) LDK treatment reduces phosphorylation of mTOR. (C) LDK treatment reduces serum-induced phosphorylation of mTOR downstream target, p70S6 kinase, at 6 hours of treatment. Note that LDK did not prevent serum-induced phosphorylation of p70S6K at 3 hours. (cropped, noncontiguous sections of same gels are shown for panels A-C). (D-G) Western blot assessment of LDK-treated Jurkat cells indicates that the G_2/M block occurs after anaphase. (D) Schematic of cyclin A and B1 as well as phospho-histone H3 (pH3) temporal expression patterns observed during the mammalian cell cycle. (E-G) Western blot assessment of LDK (10μM) treated cells indicates that neither cyclin A, cyclin B1, nor pH3 accumulate in treated cells. Treatment durations were 24 hours for E and 16 hours for panels F and G. Dox indicates 100nM doxorubicin; Noc, 1μM nocodazole; and dox and noc, positive control. (H-I) Western blot assessment of Jurkat cells treated with the inhibitors doxorubicin and nocodazole indicates that these inhibitors do not cause dephosphorylation of AKT. (E-I) Vinc indicates vinculin loading control, noncontiguous sections of same gel. Western blots were scanned at room temperature using Epson Expression 1680 scanner and software, 16-bit grayscale acquisition, 300 dpi resolution. Image processing was done using Adobe Photoshop 9.0.2.

active AKT caused almost complete inhibition of PARP cleavage and increased LDK's IC_{50} 3-fold (supplemental Figure 4A-C). Although these data suggest that inhibition of the P/A/mT pathway is at least partially required for LDK's cytotoxic activity in Jurkat cells it does not address whether LDK's action on the P/A/mT pathway is direct or indirect.

To answer this question, we sought to identify enzymes whose activity LDK may be modulating. Using purified protein substrates for in vitro kinase assays we tested 33 enzymes, including members of the P/A/mT pathway and serine/threonine and tyrosine kinases that may act on the P/A/mT pathway. Whereas the nonspecific kinase inhibitor staurosporine at 1μM potently inhibited the

majority of these enzymes, high doses of LDK (25μM) were required to achieve a mild (20%-30%) reduction in activity of 2 tyrosine and 2 serine/threonine kinases (supplemental Table 3), and inhibited the remainder of the tested enzymes less than 20%. To confirm these data we have also tested 451 different kinases, including lipid and atypical kinase families (KINOME*Scan*). Remarkably, LDK at 1μM did not inhibit any of the kinases to a significant degree (< 35% of control activity, data not shown). Taken together, these data suggest that unlike staurosporine, LDK is not a nonspecific kinase inhibitor. Rather, it potently induces inhibition of the P/A/mT pathway in lymphoblasts, probably by acting on an as of yet unidentified upstream target.

LDK induces cell cycle delay in late mitosis

In most cells, conventional P/A/mT inhibitors, such as wortmannin, delay the cell cycle in G_0/G_1 (supplemental Table 4). Surprisingly, in 4 LDK-sensitive (Ls) lines (Jurkat, CCRF-CEM, 697 and Nalm-6) LDK induced G_2/M delay, whereas the LDK-resistant (Lr) line RS4;11 was delayed in G_0/G_1 (supplemental Table 4). A time-course in Jurkat cells showed that G_2/M delay was detectable by 4 hours after LDK treatment (supplemental Figure 5), and subsequently cells progressively accumulated in G_2/M. To determine the specific timing of the LDK induced G_2/M delay, we analyzed the expression of cyclin A, cyclin B1, and phospho(Ser10)-histone H3 (pH3), whose levels are all highly regulated (Figure 4D) within the mammalian cell cycle.[29,30] Whereas the relative expression of these 3 proteins in Jurkat cells accurately described doxorubicin-induced G_2 delay and nocodazole-induced metaphase delay, LDK treatment showed a very different profile, indicating an accumulation of cells in late mitosis (Figure 4E-G).

Taken together our results suggest that LDK has 2 activities in Ls cells: indirect inhibition of the P/A/mT pathway and cell cycle delay in late mitosis. We asked whether these 2 activities are dependent on each other. As P/A/mT inhibition with wortmannin does not lead to mitosis delay in the T and B-ALL lines we tested (supplemental Table 4), we probed whether, conversely, G_2/M delay could cause reduced AKT phosphorylation. We induced G_2 delay with doxorubicin and mitosis delay using nocodazole. Neither G_2 nor M delay reduced phosphorylation of AKT in Jurkat cells (Figures 4H-I). We therefore conclude that LDK has 2 independent activities in Ls cells and that inhibition of the P/A/mT pathway is not a mere consequence of ill health of LDK-treated cells.

Favorable pharmacokinetics and lack of endorgan toxicity in LDK-treated mice

We tested serum concentrations of LDK after 14 days of twice daily intraperitoneal application of LDK at 16, 80, and 200 mg/kg. Serum concentrations, measured 24 hours after the last intraperitoneal LDK application, were proportional to the applied doses (supplemental Figure 7A-B). Determination of pharmacokinetic properties of LDK in mice revealed a plasma elimination half-life of ~ 2 hours after both single oral and intravenous administration (supplemental Figure 7C). In toxicology studies, mice were treated with LDK by gavage at doses up to 45 mg/kg for 14 days. Mice remained healthy, did not show weight loss even at the highest dose, and serum protein, renal, and liver function tests were not significantly influenced by LDK treatment, regardless of dose (data not shown). Pathologic examination of kidneys and livers of diluent and 45 mg/kg LDK-treated animals showed no toxic effects (supplemental Figure 7D). LDK-treated individuals showed no significant difference compared with diluent-only treated mice in PB counts, spleen, and thymus differential cell counts (supplemental Figure 8A-C). We observed a 10% drop in the percentage of CD8 single-positive T lymphocytes in the thymus that may be a reflection of the particular sensitivity of immature, intermediate, CD8 single-positive thymocytes to AKT inhibition.[31] Total numbers of thymocytes and overall size of thymi were reduced by approximately 50% (data not shown).

LDK kills the majority of primary human leukemia cells

To interrogate the clinical relevance of our data, we asked whether LDK had activity against primary human leukemia samples. We tested several primary B-ALL samples either grown directly in culture (supplemental Figure 9, supplemental Table 6) or on OP9 stromal cells (Figure 5A-D, supplemental Table 5) including treatment-refractory, relapsed BCR-ABL B-ALL and T315I-mutated BCR-ABL positive B-ALL samples. We found that proliferation was strongly inhibited in 85% of patient B-ALL samples and that they exhibited G_2/M delay, similar to Jurkat cells (Figure 5). As the NCI60 data indicated that LDK might have activity against CML, we also tested 2 primary samples from patients with imatinib-resistant CML, one with wild-type BCR-ABL, the other with the T315I mutation. Colony assays demonstrated strong activity of LDK against both samples, whereas high doses of imatinib had only mild effects (Figure 5E). Finally, we tested 3 primary imatinib-resistant Ph^+ B-ALL samples for viability in the presence of LDK (Figure 5F). Samples 11-008 and 11-032 are paired diagnosis and relapse samples, with the relapse sample showing decreased sensitivity to LDK treatment. By contrast, LDK did not compromise health of normal bone marrow mononuclear cells at concentrations up to 3μM (Figure 5G). Similarly, the IC_{50} of proliferating human CD34 positive cord blood cells was 8-fold higher than leukemia cells (Figure 5H), supporting LDK's therapeutic window we had observed with normal PB mononuclear cells (Figure 2E). In sum, LDK was active against the majority of primary human leukemia samples, and led to G_2/M delay in Ls cells.

Discussion

The screen described herein represents the first successful and unbiased approach using zebrafish larvae to identify molecules with potency against a human cancer from a small molecule library containing compounds with unknown activity. Zebrafish have been increasingly used to screen for bioactive compounds with possible clinical relevance. For example, a screen of 2000 well-characterized compounds (Spectrum Library, MicroSource Discovery System) revealed PGE2 as a stimulator of hematopoietic stem cell growth,[32] a finding that is now being translated into clinical trials (L. Zon, personal e-mail communication, December 13, 2011). In another screen of the Spectrum Library for active compounds in a zebrafish model of acute myeloid leukemia (AML), Yeh et al identified a new role for COX-2 and β-catenin in AML1-ETO–induced AML.[33] More recently, a screen of the Spectrum Library for chemical suppressors of neural crest development revealed a class of dihydroorotate dehydrogenase inhibitors that not only almost completely abrogate neural crest development in zebrafish but also markedly decrease melanoma growth both in vitro and in mouse xenograft studies.[34]

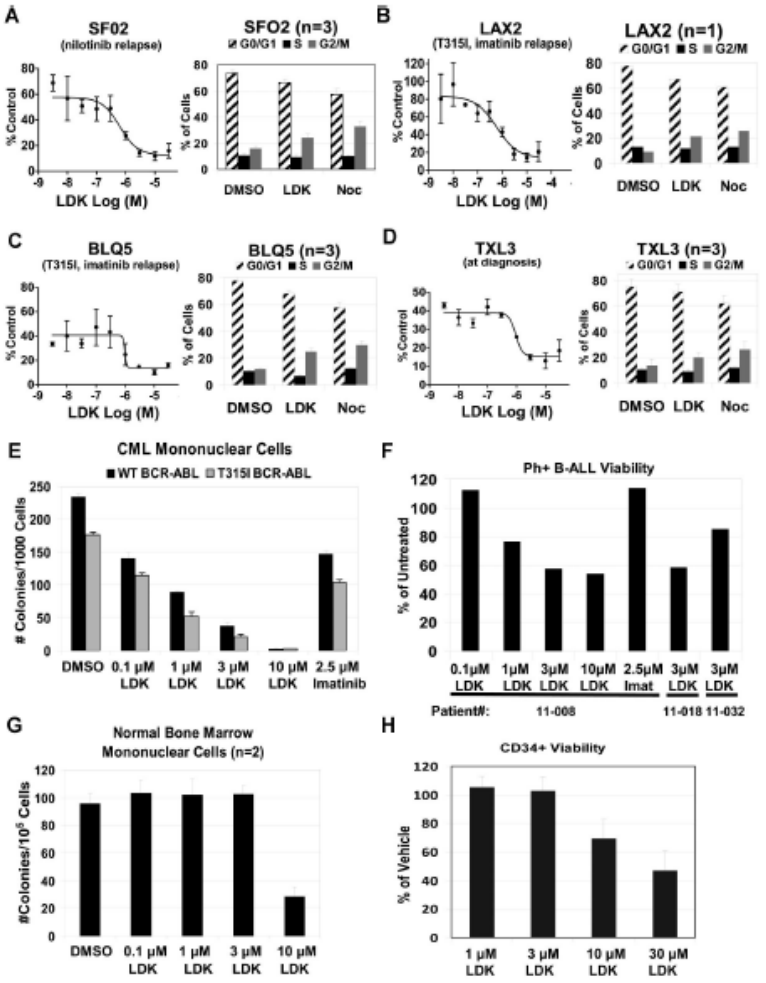

Figure 5. LDK is active against primary patient samples without toxicity to hematopoietic progenitors. (A-D) LDK decreases viability and induces G_2/M block in primary Ph+ B-ALL patient samples. Left side of each panel shows MTT test of LDK dose-response viability assay at 48 hours incubation, n = 3, error bars = SD. Right side of each panel shows cell cycle profile for primary patient samples treated for 12 hours with DMSO, 10µM LDK, and 3µM nocodazole, n values as indicated, error bars = SEM. (E-H) LDK decreases viability of Ph+ CML and B-ALL primary leukemias without toxicity to hematopoietic stem/progenitor cells (HSPCs). (E) Cytokine-dependent methylcellulose colony formation (mean ± SD) of CML-CP (CP indicates chronic phase) with wild-type BCR-ABL (patient ID no. 10-003, black bars) and T315I mutated BCR-ABL (patient ID no. 11-007, gray bars), either untreated or treated with the indicated inhibitors. (F) Trypan blue viability assay of mononuclear cells from 3 Ph+ B-ALL patient samples treated with the indicated inhibitors. Samples 11-008 and 11-032 are paired samples from the same patient at diagnosis and relapse, respectively. (G) Cytokine-dependent methylcellulose colony formation (mean ± SD) of normal bone marrow mononuclear cells, treated with either DMSO or LDK at the indicated concentrations. (H) MTT viability assay of CD34+ HSPCs from human cord blood, treated with LDK at the indicated concentrations, relative to vehicle control. Error bars = SD Additional primary patient sample characteristics may be found in supplemental Table 5.

Drug screening in zebrafish offers the obvious advantage of being conducted within the context of an entire vertebrate organism, including intact, heterologous cell-cell interactions (eg, thymocyte-thymic epithelial cells or hematopoietic stem cell–stromal cells). As our results demonstrate, such a screen can identify relatively nontoxic compounds with selective bioactivity in human cells. However, there are also clear limitations in how far we can extrapolate results from zebrafish drug screening to mammals. For example, zebrafish screens may have relevance for bioavailability as demonstrated by LDK. However, there are 3 routes of absorption

in fishes after immersion in compound (gastrointestinal, gill, and skin), compared with only one after oral application in mammals, and only the gill route is not available in zebrafish larvae at 5 dpf when we carried out the screen. In addition, the exposure to drug is constant and only restricted by stability in water during immersion, a different scenario from the intermittent oral dosing in mammals. Therefore, bioavailability in fishes may not accurately predict the same in mammals. Finally, targets may have diverged during evolution so that compounds that are active in zebrafish may not exhibit the desired effect in mammalian cells. This may be the case for the 4 compounds that had specific activity in zebrafish but did not kill Jurkat cells in our screen (Figure 2A).

Screening of large numbers of compounds is not practical in adult leukemic zebrafish. However, contrary to the AML model,[35] currently no zebrafish T-ALL models exist that manifest early in development to allow screening of thousands of compounds. We developed a 2-pronged screening strategy to identify targeted, nontoxic, antileukemia compounds in zebrafish larvae from a large chemical library. First, we reasoned that given their similar developmental stage, immature T cells and leukemic T lymphoblasts share similar pathways or biologic processes on which both critically depend. Consequently, compounds that eliminate the former may also kill the latter. Our rationale was supported by our previous finding that dexamethasone, a mainstay of anti-ALL treatment, eliminated immature T cells from the thymus of developing zebrafish larvae.[21] Our data that killing of immature zebrafish T cells and malignant human T-ALL lines by LDK involves indirect inhibition of the P/A/mT pathway (see below) bolstered our rationale as both types of cells critically depend on AKT activity for survival.[14,26,36] Second, we sought to identify active molecules that are devoid of general toxicity. The capacity to interfere with the cell cycle of dividing cells underpins the efficacy and toxicity of most chemotherapeutic agents. Despite species-specific variations, cell cycle regulation is highly conserved throughout metazoan evolution[37] and modulators of the cell cycle identified in zebrafish are active in mammals and vice versa.[38,39] We therefore reasoned that nontargeted compounds that are generally toxic to mammalian cells could be detected and eliminated by screening for cell cycle effects in developing zebrafish embryos (Figure 1D-H). Our finding that LDK has little toxicity in developing and adult zebrafish, mice, and nonmalignant human cells corroborates the rationale for our screening algorithm.

The P/A/mT pathway has become an attractive target for drug development[16] and molecules have been identified that inhibit 1[40,41] or 2[27,42,43] components of the pathway. The targets of these inhibitors are either the 3 enzymes themselves or kinases that activate the pathway, as for example PDK1[44] and mTORC2.[45] These inhibitors act against a wide range of tumor cell lines that depend on P/A/mT signaling.[46] LDK induces decreased phosphorylation state in members of the P/A/mT pathway and has potent activity against leukemias. Several lines of evidence indicate that LDK exerts an indirect effect on the P/A/mT pathway. First, extensive in vitro kinase assays clearly show that LDK does not significantly inhibit any of the members of the P/A/mT pathway. Second, in our serum starvation experiments, LDK exhibited markedly delayed activity on AKT phosphorylation compared with the PI3K inhibitor Ly294002. Third, LDK lacks activity against several AKT-dependent tumor lines, including glioblastoma and melanoma that are readily killed by AKT inhibitors. We therefore conclude that LDK's action on the P/A/mT pathway is indirect.

What is the underpinning of LDK's leukemia selectivity? Although the molecular basis of LDK resistance versus sensitivity remains the subject of future investigations, selective antileukemia activity could be explained by several mechanisms. These include a hematopoietic cell-restricted target (Figure 2, supplemental Figure 2), unique sensitivity of lymphocytes[47] to LDK's action, or differential drug metabolism by resistant versus sensitive lines.[48] Finally, the 2 activities of LDK may have to coincide for cytotoxicity. For example, hematopoietic cells can overcome cell cycle arrest in G_2/M through growth factor-stimulated activation of the P/A/mT pathway.[49] Thus, LDK's ability to induce G_2/M delay while simultaneously blocking the P/A/mT pathway, even after growth factor stimulation (supplemental Figure 3D), appears particularly significant. A requirement for dual activity is bolstered by our observation that in RS4;11 cells failure of LDK-mediated G_2/M delay correlates with resistance (Figure 2G, supplemental Table 4). We have shown that LDK's 2 activities, P/A/mT inhibition and late mitosis delay, are independent of each other (Figure 4H-I), but whether LDK accomplishes selectivity by interfering with single or multiple targets must be addressed in future studies.

In our study, LDK was active as monotherapy against all T-ALL lines tested and 85% of primary leukemia samples, regardless of PTEN status, resistance to glucocorticoids or other antileukemia compounds that may compromise patient treatment. Furthermore, with our dosing regimen LDK lacks endorgan (supplemental Figure 7D) and hematopoietic toxicity (Figures 2E and 5G-H, supplemental Figure 8). Thus LDK is an attractive, nontoxic compound that will form the basis of future endeavors to bring leukemia-selective treatments to the bedside.

Acknowledgments

The authors wish to acknowledge Ira Kraft, Jon Beck, Rupeng Zhuo, Kalavathy Ramachandran, and Bradley Demarest for expert technical assistance. Histology and immunohistochemistry were performed at the ARUP Institute for Clinical and Experimental Pathology with the technical assistance of Sheryl Tripp. Cell lines and fish strains were a kind gift of Joshua Schiffman, Randy Jensen, and Doug Grossman (University of Utah, Salt Lake City, UT); Adolfo Ferrando (Columbia University, New York, NY); and Andrew Kung, Alejandro Gutierrez, and Thomas Look (Dana-Farber Cancer Institute, Boston, MA). Dr Steven Grant (Virginia Commonwealth University Medical Center, Richmond, VA) provided the myr-AKT plasmid.

N.S.T. was supported by The Dana Foundation, The William Lawrence-Blanche Hughes Foundation, The Alex's Lemonade Stand Foundation, and the Huntsman Cancer Foundation. C.J.G. was supported by a grant from Genome Canada Competition III through the Ontario Genomics Institute. Core facilities of the Huntsman Cancer Institute, supported by National Cancer Institute grant P30 CA042014, and the University of Utah, supporting the CZAR zebrafish research core facility, also contributed to this work.

Authorship

Contribution: S.R., W.L.H., D.J., and N.S.T. conceived the experiments; H.C., P.C., H.S., A.S., E.J.M., and D.A.J. designed and carried out the zebrafish screen; D.A.J. carried out cell cycle analysis and toxicity studies on zebrafish embryos and larvae; D.A.J., W.L.H., and S.W. performed MTT assays, cell cycle, and antiactivated caspase 3 assay; K.B. and M.S. synthesized LDK; L.B. and J.K.F. conceived and carried out in vivo testing of LDK in

adult leukemic zebrafish; A.A., R.R.M., and G.J.S. carried out pathologic and biochemical evaluation of LDK-treated mice and zebrafish; J.E.C. developed the LC/MS assay to measure LDK concentrations; T.P., R.J., B.M., and C.J.G. conceived and performed Phosflow analysis, and efficacy testing of LDK in murine T-ALL lines and in primary human leukemias; A.E., M.M., M.D., and W.L.H. conceived and performed further experiments on primary human leukemia cells; and N.S.T. wrote the paper.

Conflict-of-interest disclosure: The authors declare no competing financial interests.

The current affiliation for M.M. is Department of Laboratory Medicine, University of California, San Francisco, San Francisco, CA 94143.

Correspondence: Nikolaus Sebastian Trede, The Huntsman Cancer Institute, University of Utah, 2000 Circle of Hope, Salt Lake City, UT 84112; e-mail: nikolaus.trede@hci.utah.edu.

References

1. National Cancer Institute, Surveillance Epidemiology and End Result. Stat Fact Sheets: Leukemia. Available at http://www.seer.cancer.gov/statfacts/html/leuks.html. Accessed December 10, 2011.
2. Smith MA, Gloeckler Ries LA, Gurney JG, Ross JA. Leukemia. SEER Pediatric Monograph. Available at seer.cancer.gov/publications/childhood/leukemia.pdf. National Cancer Institute. Accessed December 10, 2011.
3. Pui CH, Relling MV, Downing JR. Acute lymphoblastic leukemia. *N Engl J Med*. 2004;350(15):1535-1548.
4. Goldberg JM, Silverman LB, Levy DE, et al. Childhood T-cell acute lymphoblastic leukemia: the Dana-Farber Cancer Institute acute lymphoblastic leukemia consortium experience. *J Clin Oncol*. 2003;21(19):3616-3622.
5. Armstrong SA, Look AT. Molecular genetics of acute lymphoblastic leukemia. *J Clin Oncol*. 2005;23(26):6306-6315.
6. Ferrando AA, Look AT. Clinical implications of recurring chromosomal and associated molecular abnormalities in acute lymphoblastic leukemia. *Semin Hematol*. 2000;37(4):381-395.
7. Yeoh EJ, Ross ME, Shurtleff SA, et al. Classification, subtype discovery, and prediction of outcome in pediatric acute lymphoblastic leukemia by gene expression profiling. *Cancer Cell*. 2002;1(2):133-143.
8. Druker BJ, Tamura S, Buchdunger E, et al. Effects of a selective inhibitor of the Abl tyrosine kinase on the growth of Bcr-Abl positive cells. *Nat Med*. 1996;2(5):561-566.
9. Smith A. Screening for drug discovery: the leading question. *Nature*. 2002;418(6896):453-459.
10. Weng AP, Ferrando AA, Lee W, et al. Activating mutations of NOTCH1 in human T cell acute lymphoblastic leukemia. *Science*. 2004;306(5694):269-271.
11. Gutierrez A, Sanda T, Grebliunaite R, et al. High frequency of PTEN, PI3K, and AKT abnormalities in T-cell acute lymphoblastic leukemia. *Blood*. 2009;114(3):647-650.
12. Lai EC. Notch cleavage: Nicastrin helps Presenilin make the final cut. *Curr Biol*. 2002;12(6):R200-202.
13. Palomero T, Dominguez M, Ferrando AA. The role of the PTEN/AKT Pathway in NOTCH1-induced leukemia. *Cell Cycle*. 2008;7(9):965-970.
14. Palomero T, Sulis ML, Cortina M, et al. Mutational loss of PTEN induces resistance to NOTCH1 inhibition in T-cell leukemia. *Nat Med*. 2007;13(10):1203-1210.
15. Medyouf H, Gao X, Armstrong F, et al. Acute T-cell leukemias remain dependent on Notch signaling despite PTEN and INK4A/ARF loss. *Blood*. 2010;115(6):1175-1184.
16. Yap TA, Garrett MD, Walton MI, et al. Targeting the PI3K-AKT-mTOR pathway: progress, pitfalls, and promises. *Curr Opin Pharmacol*. 2008;8(4):393-412.
17. Cullion K, Draheim KM, Hermance N, et al. Targeting the Notch1 and mTOR pathways in a mouse T-ALL model. *Blood*. 2009;113(24):6172-6181.
18. Meeker ND, Trede NS. Immunology and zebrafish: spawning new models of human disease. *Dev Comp Immunol*. 2008;32(7):745-757.
19. Frazer JK, Meeker ND, Rudner L, et al. Heritable T-cell malignancy models established in a zebrafish phenotypic screen. *Leukemia*. 2009;23(10):1825-1835.
20. Langenau DM, Traver D, Ferrando AA, et al. Myc-induced T cell leukemia in transgenic zebrafish. *Science*. 2003;299(5608):887-890.
21. Langenau DM, Ferrando AA, Traver D, et al. In vivo tracking of T cell development, ablation, and engraftment in transgenic zebrafish. *Proc Natl Acad Sci U S A*. 2004;101(19):7369-7374.
22. Gutierrez A, Grebliunaite R, Feng H, et al. Pten mediates Myc oncogene dependence in a conditional zebrafish model of T cell acute lymphoblastic leukemia. *J Exp Med*. 2011;208(9):1595-1603.
23. Barlow C, Hirotsune S, Paylor R, et al. Atm-deficient mice: a paradigm of ataxia telangiectasia. *Cell*. 1996;86(1):159-171.
24. Fusetti L, Pruneri G, Gobbi A, et al. Human myeloid and lymphoid malignancies in the non-obese diabetic/severe combined immunodeficiency mouse model: frequency of apoptotic cells in solid tumors and efficiency and speed of engraftment correlate with vascular endothelial growth factor production. *Cancer Res*. 2000;60(9):2527-2534.
25. Masiero M, Minuzzo S, Pusceddu I, et al. Notch3-mediated regulation of MKP-1 levels promotes survival of T acute lymphoblastic leukemia cells. *Leukemia*. 2011;25(4):588-596.
26. Jones RG, Parsons M, Bonnard M, et al. Protein kinase B regulates T lymphocyte survival, nuclear factor kappaB activation, and Bcl-X(L) levels in vivo. *J Exp Med*. 2000;191(10):1721-1734.
27. Chiarini F, Fala F, Tazzari PL, et al. Dual inhibition of class IA phosphatidylinositol 3-kinase and mammalian target of rapamycin as a new therapeutic option for T-cell acute lymphoblastic leukemia. *Cancer Res*. 2009;69(8):3520-3528.
28. Sachs K, Perez O, Pe'er D, et al. Causal protein-signaling networks derived from multiparameter single-cell data. *Science*. 2005;308(5721):523-529.
29. McManus KJ, Hendzel MJ. The relationship between histone H3 phosphorylation and acetylation throughout the mammalian cell cycle. *Biochem Cell Biol*. 2006;84(4):640-657.
30. Morgan D. *The Cell Cycle*. London, United Kingdom: Oxford University Press; 2007.
31. Juntilla MM, Koretzky GA. Critical roles of the PI3K/Akt signaling pathway in T cell development. *Immunol Lett*. 2008;116(2):104-110.
32. North TE, Goessling W, Walkley CR, et al. Prostaglandin E2 regulates vertebrate haematopoietic stem cell homeostasis. *Nature*. 2007;447(7147):1007-1011.
33. Yeh JR, Munson KM, Elagib KE, et al. Discovering chemical modifiers of oncogene-regulated hematopoietic differentiation. *Nat Chem Biol*. 2009;5(4):236-243.
34. White RM, Cech J, Ratanasirintrawoot S, et al. DHODH modulates transcriptional elongation in the neural crest and melanoma. *Nature*. 2011;471(7339):518-522.
35. Yeh JR, Munson KM, Chao YL, et al. AML1-ETO reprograms hematopoietic cell fate by downregulating scl expression. *Development*. 2008;135(2):401-410.
36. Huo J, Xu S, Lam KP. Fas apoptosis inhibitory molecule regulates T cell receptor-mediated apoptosis of thymocytes by modulating Akt activation and Nur77 expression. *J Biol Chem*. 2010;285(16):11827-11835.
37. DePamphilis ML, Blow JJ, Ghosh S, et al. Regulating the licensing of DNA replication origins in metazoa. *Curr Opin Cell Biol*. 2006;18(3):231-239.
38. Murphey RD, Stern HM, Straub CT, et al. A chemical genetic screen for cell cycle inhibitors in zebrafish embryos. *Chem Biol Drug Des*. 2006;68(4):213-219.
39. Stern HM, Murphey RD, Shepard JL, et al. Small molecules that delay S phase suppress a zebrafish bmyb mutant. *Nat Chem Biol*. 2005;1(7):366-370.
40. Feldman RI, Wu JM, Polokoff MA, et al. Novel small molecule inhibitors of 3-phosphoinositide-dependent kinase-1. *J Biol Chem*. 2005;280(20):19867-19874.
41. Martelli AM, Tazzari PL, Tabellini G, et al. A new selective AKT pharmacological inhibitor reduces resistance to chemotherapeutic drugs, TRAIL, all-trans-retinoic acid, and ionizing radiation of human leukemia cells. *Leukemia*. 2003;17(9):1794-1805.
42. Fan QW, Knight ZA, Goldenberg DD, et al. A dual PI3 kinase/mTOR inhibitor reveals emergent efficacy in glioma. *Cancer Cell*. 2006;9(5):341-349.
43. Janes MR, Limon JJ, So L, et al. Effective and selective targeting of leukemia cells using a TORC1/2 kinase inhibitor. *Nat Med*. 2010;16(2):205-213.
44. Mora A, Komander D, van Aalten DM, et al. PDK1, the master regulator of AGC kinase signal transduction. *Semin Cell Dev Biol*. 2004;15(2):161-170.
45. Sarbassov DD, Guertin DA, Ali SM, et al. Phosphorylation and regulation of Akt/PKB by the rictor-mTOR complex. *Science*. 2005;307(5712):1098-1101.
46. Serra V, Markman B, Scaltriti M, et al. NVP-BEZ235, a dual PI3K/mTOR inhibitor, prevents PI3K signaling and inhibits the growth of cancer cells with activating PI3K mutations. *Cancer Res*. 2008;68(19):8022-8030.
47. Carson DA, Kaye J, Matsumoto S, et al. Biochemical basis for the enhanced toxicity of deoxyribonucleosides toward malignant human T cell lines. *Proc Natl Acad Sci U S A*. 1979;76(5):2430-2433.
48. Higgins CF. Multiple molecular mechanisms for multidrug resistance transporters. *Nature*. 2007;446(7137):749-757.
49. Henry MK, Lynch JT, Eapen AK, et al. DNA damage-induced cell-cycle arrest of hematopoietic cells is overridden by activation of the PI-3 kinase/Akt signaling pathway. *Blood*. 2001;98(3):934-941.

Supplemental Figure 1. LDK decreases viability of primary murine T-ALL cells. Four murine samples derived from primary T-ALL arising in *Atm*$^{-/-}$ mice and expressing high levels of PEST-truncated activated NOTCH1 were evaluated for growth inhibition in response to Lenaldekar (LDK). Two T-ALL cell lines are PTEN- (1975, 3496) and two are PTEN+ (2317, 6658). Cells were cultured for 24 or 48 hours with Interleukin-7 (10ng/ml) and treated with DMSO vehicle, gamma-secretase inhibitor IX (GSI-IX) or LDK (10μM). After 24 and 48 hours, cell viability was quantified using the Cell Titre Blue Assay and expressed as percent relative to vehicle treatment at each time point. Experiment was repeated, one representative experiment is shown.

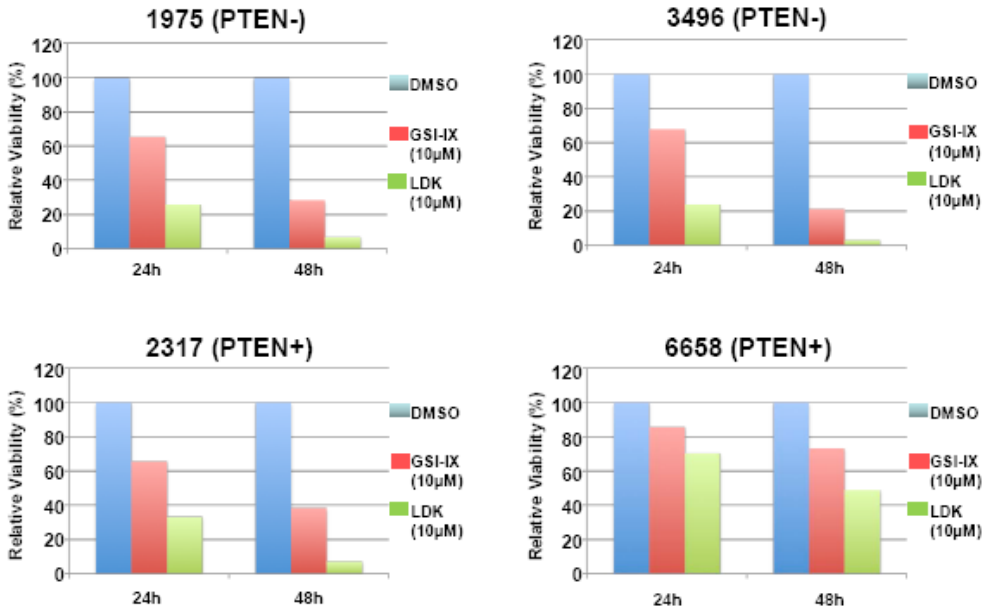

Supplemental Figure 2. LDK has selective activity against hematological malignancies and induces apoptosis in Jurkat cells. (A) LDK was submitted to the NCI for dose-response testing on the NCI60 panel of cancer cell lines. Results are shown as the IC_{50} for each cell line (Red = high sensitivity/low IC_{50}, Yellow/orange = medium sensitivity/medium IC_{50}, Green = Low sensitivity/high IC_{50}). Results are organized by cancer cell type with names of cell lines tested shown below their IC_{50} listings in the same order. (B) Annexin V-FITC/Propidium Iodide staining of Jurkat cells incubated for 24 hours with DMSO, 1μM LDK, or 5μM Camptothecin. (C) Caspase activation demonstrated by PARP cleavage (arrow) by 8 hours of incubation in 1μM LDK. (D = DMSO vehicle. Vinculin loading control. Non-contiguous sections of same gel). (D) LDK induction of apoptosis demonstrated by activated Caspase-3 immunostaining of Jurkat cells incubated for 16 hrs in DMSO, 1μM LDK, or 5μM Camptothecin. Scale bars = 2μm. For panel C, Western blots were scanned at room temperature using the Epson Expression 1680 scanner and software (Long Beach, CA), 16-bit grayscale acquisition, 600 dpi resolution. Image processing was done utilizing Adobe Photoshop software v9.0.2 (San Jose, CA). For panel D, fluorescence microscope used was Nikon Eclipse E600 (Melville, NY) using Nikon Plan Fluor 40X objective lens (Melville, NY) at room temperature. Fluorochromes used were DAPI and Alexa Fluor 568 goat anti-rabbit IgG secondary antibody (Invitrogen, Grand Island, NY). Camera used was Nuance CRI model N-MSI-420-FL (Hopkinton, MA). Image capture was done using IP Lab software version 4.0 (Becton, Dickinson, Sparks, MD), with image presentation processed using Image J version 1.43U (NIH, Bethesda, MD).

A

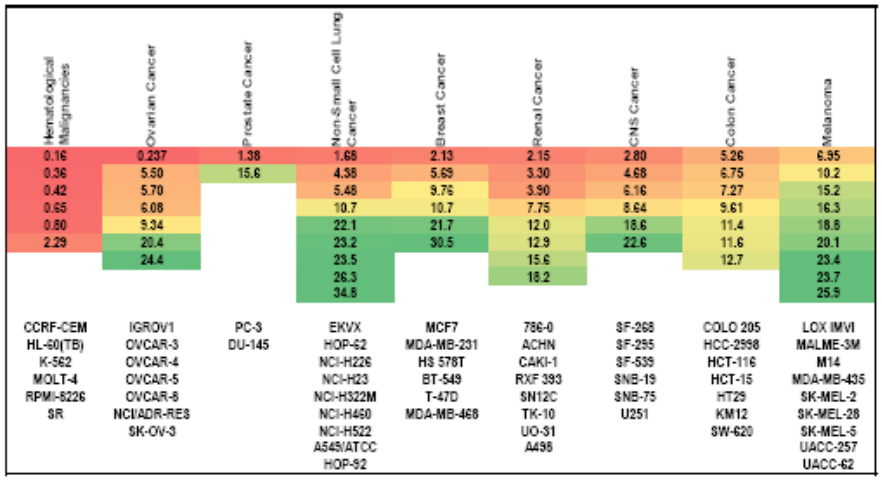

B

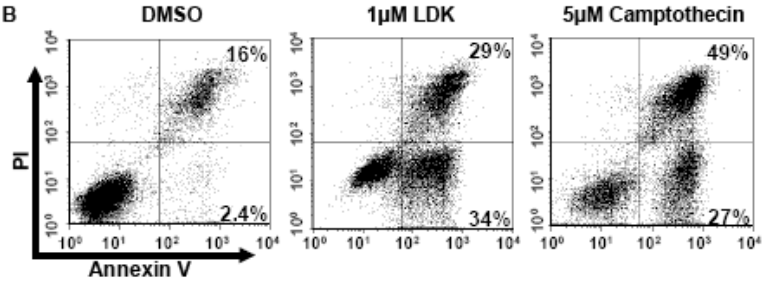

C

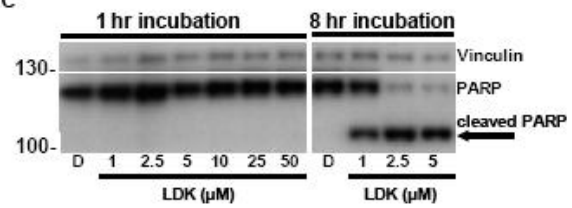

D

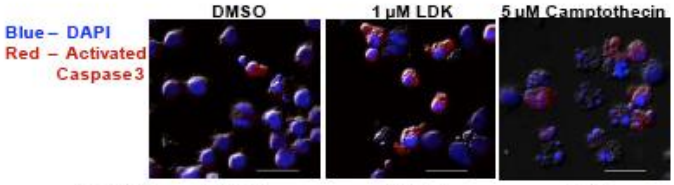

Normal:	96.9%	68.8%	41.0%
Apoptotic: (Caspase 3+)	0.2%	23.8%	11.8%
Apoptotic: (Caspase 3-)	2.9%	7.5%	47.2%

Supplemental Figure 3. LDK-mediated reduction of AKT and mTOR phosphorylation. (A), Dose-response of Jurkat cells to LDK treatment for one or eight hours of incubation. Phosphorylation of AKT at Thr308 and mTOR at Ser2448 was assessed by Western blot. Same blot was stripped and re-probed with antibodies for total mTOR and AKT. Densitometric ratios were normalized to 1 and 8 hours' DMSO treatment. D = DMSO. Non-contiguous sections of same gels are shown. (B) Assessment of LDK's ability to prevent serum-induced phosphorylation of serum-starved cells. CCRF-CEM T-ALL cells were serum-starved for 72 hours then pre-treated for 30 min with DMSO, LDK (10μM) or known PI3K inhibitor Ly294002 (Ly)(10μM) before addition of serum to cell media. Ly blocked any re-phosphorylation of AKT. LDK did not block serum-induced AKT re-phosphorylation and showed reduction of AKT phosphorylation first at 15 minutes post serum-stimulation. (C-D) Phosflow analysis of B-ALL line Ramos and pro-B cell line BaF3. (C) Effect of Dasatinib (top panels) and LDK (lower panels) on SRC (Y418, left panel) and S6 (S235/236, right panels) phosphorylation in B-ALL line Ramos. (D) Effects of JAK Inhibitor I (top panels) and LDK (lower panels) on STAT3 (Ser727, left panels) and S6 (S235/236, right panels) phosphorylation in pro-B cell line BaF3. For panels A and B, Western blots were scanned at room temperature using the Epson Expression 1680 scanner and software (Long Beach, CA), 16-bit grayscale acquisition, 600 dpi resolution. Image processing and densitometry was done utilizing Adobe Photoshop software v9.0.2 (San Jose, CA).

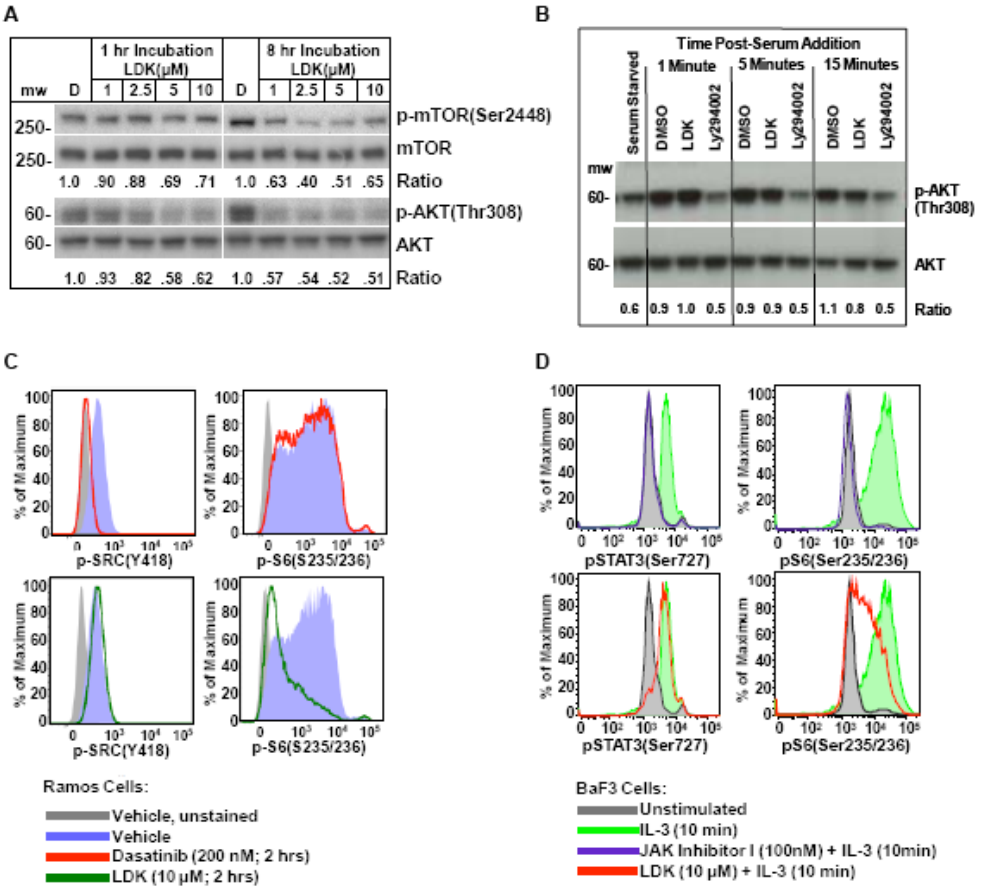

Supplemental Figure 4. LDK does not target the AKT pathway directly, but AKT inhibition is required for its toxicity in Jurkat cells. (A-C) Assessment of constitutively active myristoylated, double phosphomimetic (T308D/S473D) AKT (myr-AKT-DD) rescue of Jurkat cells from LDK treatment. (A) Western blot shows expression of myr-AKT-DD, including upregulation of AKT phosphorylation target GSK-3β, and reduction of LDK-mediated apoptosis, as indicated by reduction in cleaved PARP. (Dox = doxycycline). (B) Annexin-V/PI assessment indicates a reduction of apoptosis in LDK-treated (1μM) Jurkat (myr-AKT-DD) cells compared to Jurkat cells, relative to vehicle-treated cells. (n=3, error bars = s.e.m.) (C) Constitutively active AKT increases LDK's IC_{50} in Jurkat cells three-fold (double arrow) as determined by 24hr MTT viability assay. For panel A, Western blot was scanned at room temperature using the Epson Expression 1680 scanner and software (Long Beach, CA), 16-bit grayscale acquisition, 600 dpi resolution. Image processing and densitometry was done utilizing Adobe Photoshop software v9.0.2 (San Jose, CA).

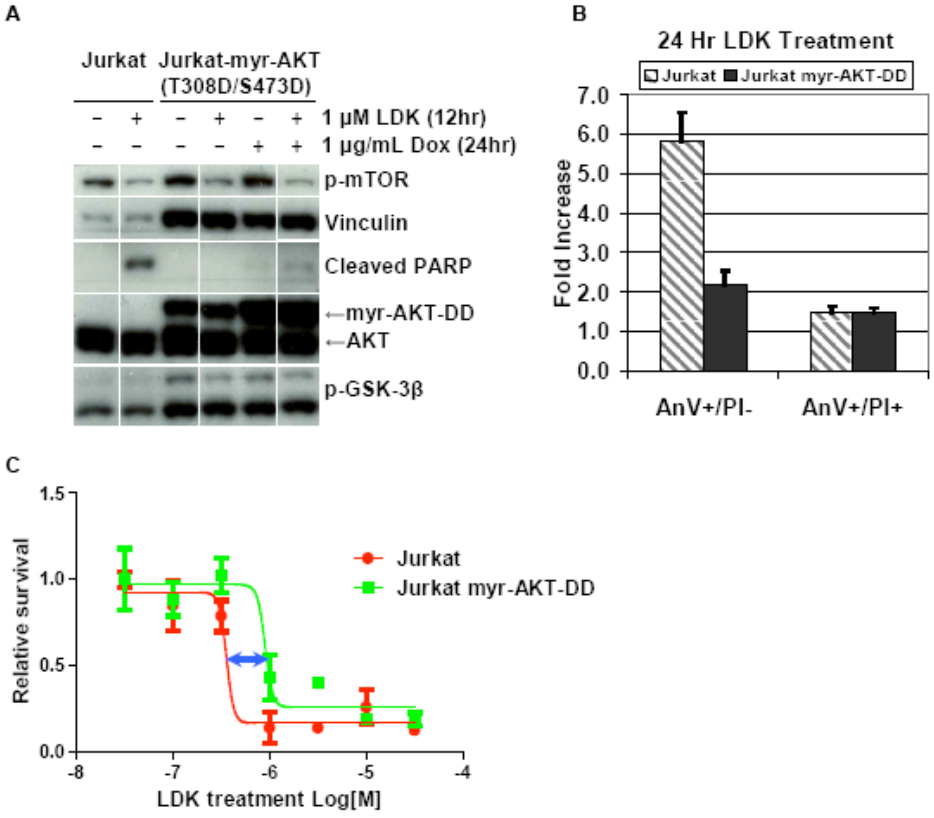

Supplemental Figure 5. Time-course of LDK treatment shows progressive accumulation of cells in G2/M. Jurkat T-ALL cells were treated with DMSO vehicle, LDK (10μM), or Wortmannin (1μM) and cell cycle percentages were assessed over a 4-24 hour time period via flow cytometry. Wortmannin, a known inhibitor of the PI3K/AKT/mTOR pathway, shows accumulation in G0/G1 while LDK causes a progressive accumulation in G2/M.

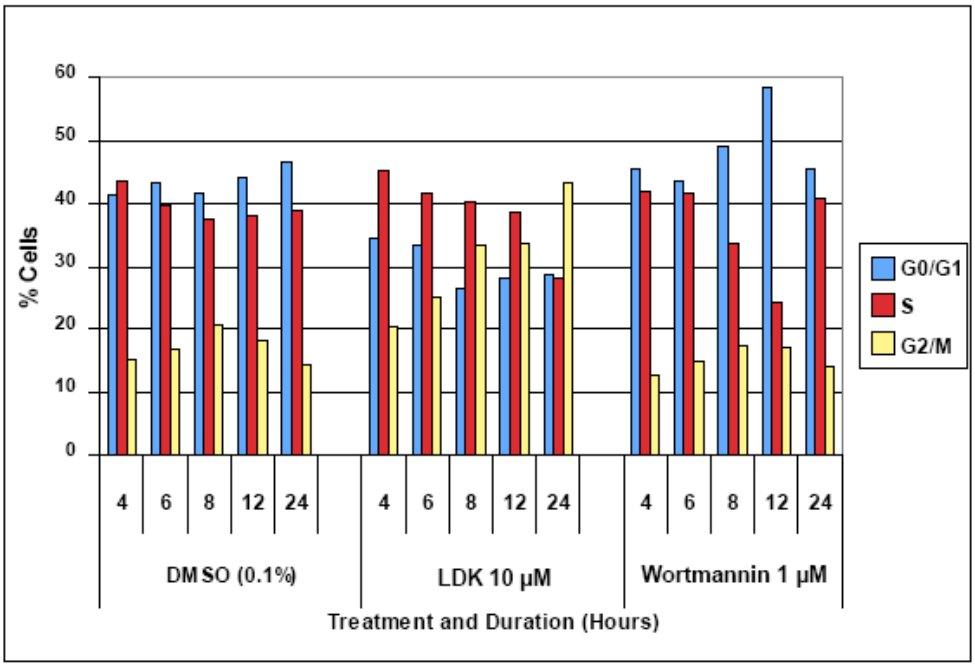

Supplemental Figure 6. LDK treatment results in de-phosphorylation of AKT and G2/M delay in the T-ALL cell line CCRF-CEM. (A) CCRF-CEM cells were incubated for 12 hours with no treatment, DMSO (0.1%), LDK (10μM), Nocodazole (3μM), or Wortmannin (1μM) then probed via Western blot for AKT phosphorylation. Total AKT and Vinculin = loading controls, cropped non-contiguous sections of same gel. (B) CCRF-CEM cells were treated for 12 hours with LDK (10μM), Wortmannin (1μM), or Nocodazole (3μM) then stained with PI and assessed for cell cycle status via flow cytometry. For panel A, Western blots were scanned using Epson Expression 1680 scanner and software, 16-bit grayscale acquisition, 600 dpi resolution. Image processing and densitometry was done utilizing Adobe Photoshop software v9.0.2. For panel A, Western blot was scanned at room temperature using the Epson Expression 1680 scanner and software (Long Beach, CA), 16-bit grayscale acquisition, 600 dpi resolution. Image processing and densitometry was done utilizing Adobe Photoshop software v9.0.2 (San Jose, CA).

A

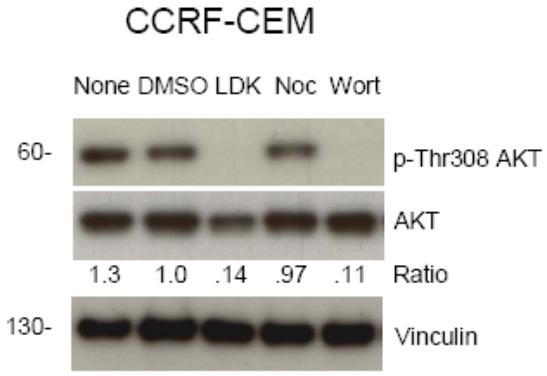

B

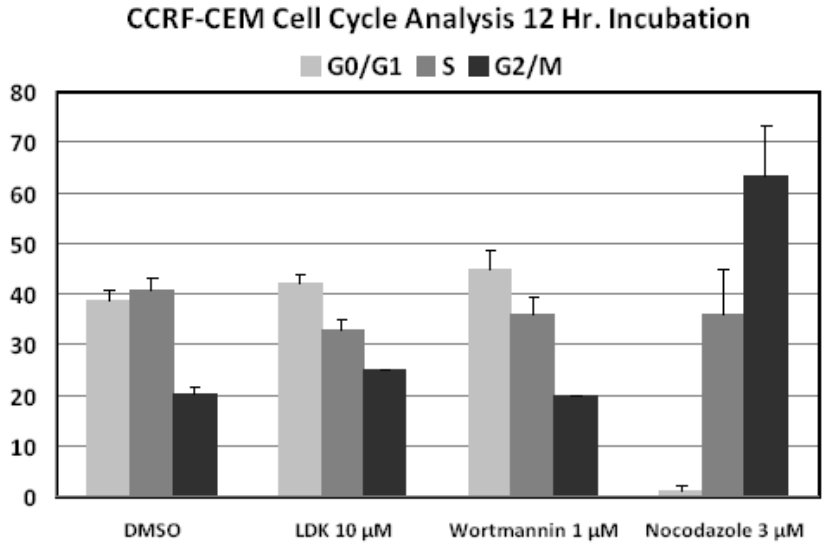

Supplemental Figure 7. Pharmacokinetics and lack of toxicity of LDK in mice. (A) LC/MS standard calibration curve for LDK detection. (B) Four groups of five male NOD-SCID mice each were injected IP b.i.d for two weeks with either vehicle or LDK at 16, 80, or 200mg/kg. After the two-week course of treatment, LDK serum levels were determined 24 hours following last treatment by liquid chromatography followed by mass spectroscopy (LC/MS). One representative serum sample per treatment level is shown. (C) Plasma concentration-time profile (mean ± s.d,; n=3) of LDK in male Swiss Albino mice following single intravenous (IV) (3mg/kg) or oral (PO) (15mg/kg) administration was determined by mass spectroscopy. Single-dose half-life of LDK was 1.7h for IV and 2h for oral administration. (D) LDK shows lack of endorgan toxicity in treated mice. Kidney and liver H&E sections were taken after 2-week treatment course from vehicle- and LDK-treated mice (45mg/kg, oral, b.i.d.) and evaluated for endorgan toxicity. Representative histological sections are shown. Scale bars = 100µm. For panel D, hematoxylin - eosin stained tissue sections were reviewed with an Olympus 4E/19753 microscope (Center Valley, PA) using lens of S Plan 10. The image was acquired using digital camera Olympus DP71 (Center Valley, PA) and was processed with DP controller.

A

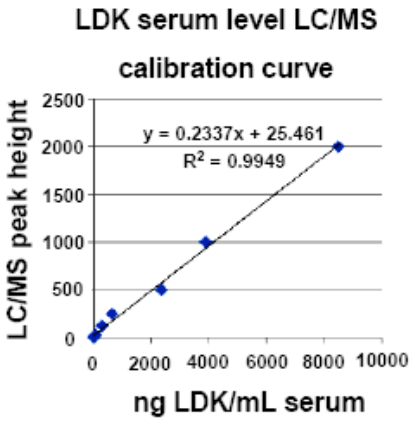

B

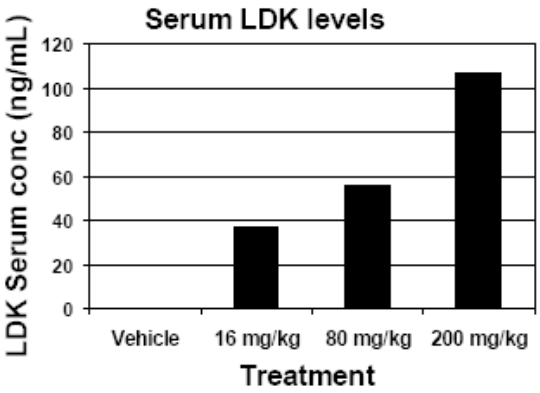

C

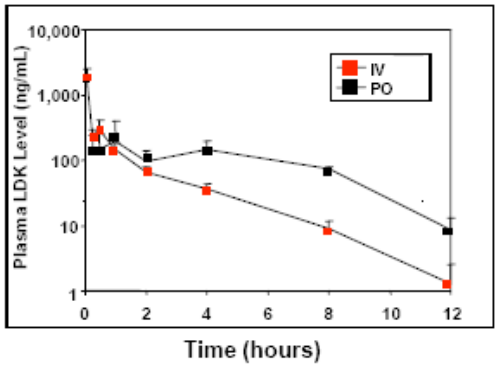

D

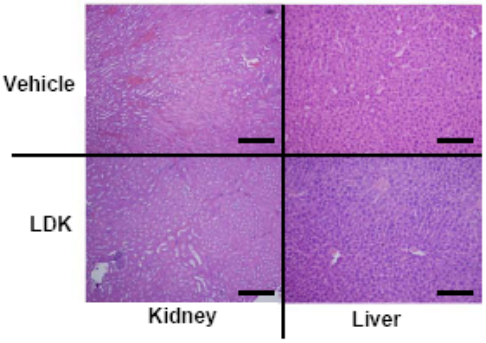

Supplemental Figure 8. LDK treatment shows no significant toxicity in complete blood count, thymus, or spleen cell counts. LDK-treated individuals (indicated doses were given orally b.i.d.) showed no significant difference when compared to diluent-only treated mice (tested on day 2) in (A) peripheral blood counts, (B) thymus and (C) spleen differential cell counts. There was a 10% drop in the percentage of CD8 single positive T lymphocytes in the thymus. Total numbers of thymocytes and overall size of thymi were reduced approximately 50%. Each data point represents average of three mice sacrificed on the indicated time point and dose. Blue bars = treatment day 2, Red bars = treatment day 14, Error bars = SD.

A

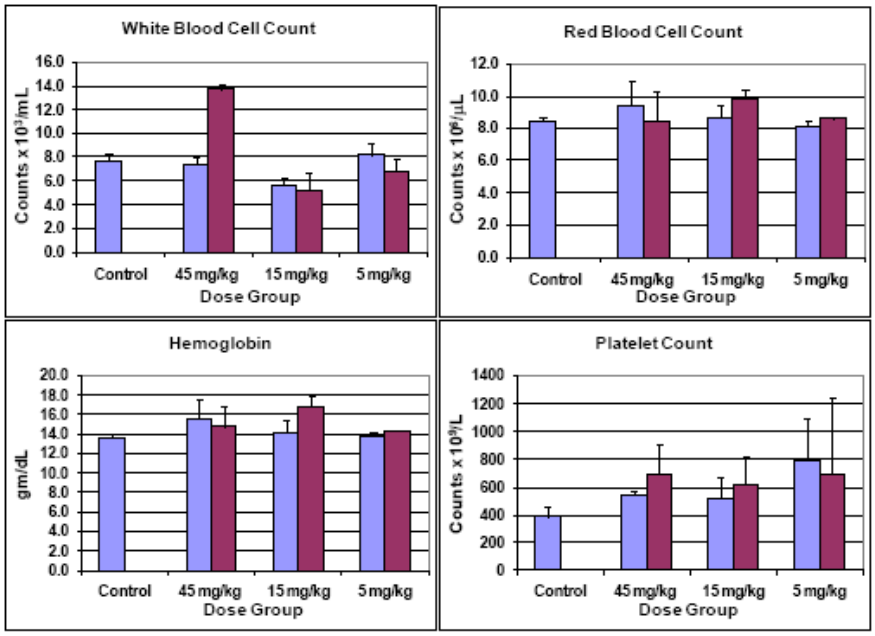

B

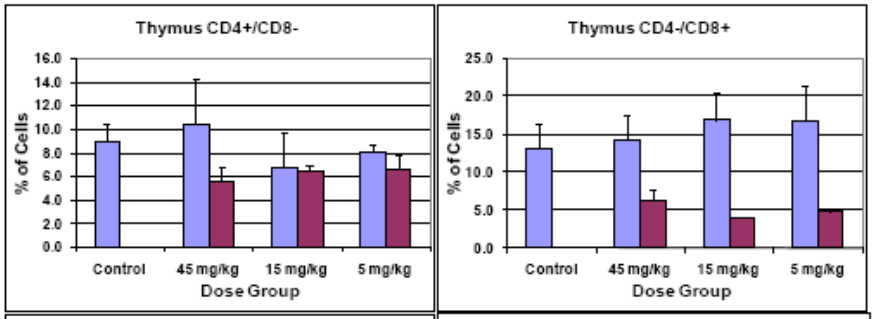
Thymus CD4+/CD8-
% of Cells
16.0
14.0
12.0
10.0
8.0
6.0
4.0
2.0
0.0
Control
45 mg/kg
15 mg/kg
5 mg/kg
Dose Group

Thymus CD4-/CD8+
% of Cells
25.0
20.0
15.0
10.0
5.0
0.0
Control
45 mg/kg
15 mg/kg
5 mg/kg
Dose Group

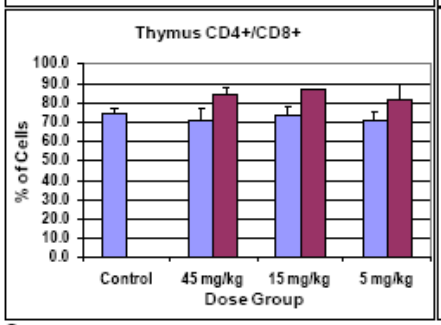
Thymus CD4+/CD8+
% of Cells
100.0
90.0
80.0
70.0
60.0
50.0
40.0
30.0
20.0
10.0
0.0
Control
45 mg/kg
15 mg/kg
5 mg/kg
Dose Group

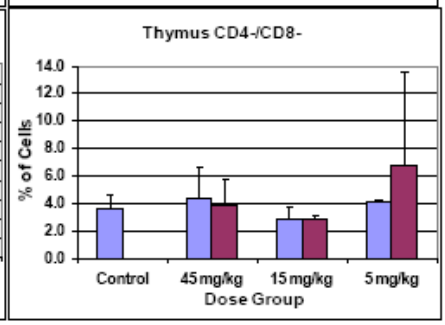
Thymus CD4-/CD8-
% of Cells
14.0
12.0
10.0
8.0
6.0
4.0
2.0
0.0
Control
45 mg/kg
15 mg/kg
5 mg/kg
Dose Group

C

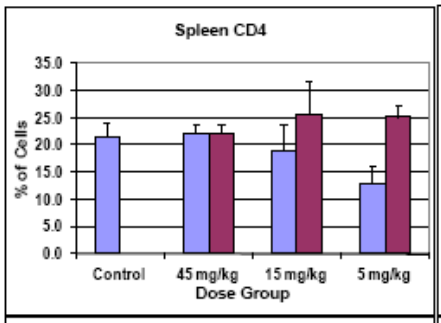
Spleen CD4
% of Cells
35.0
30.0
25.0
20.0
15.0
10.0
5.0
0.0
Control
45 mg/kg
15 mg/kg
5 mg/kg
Dose Group

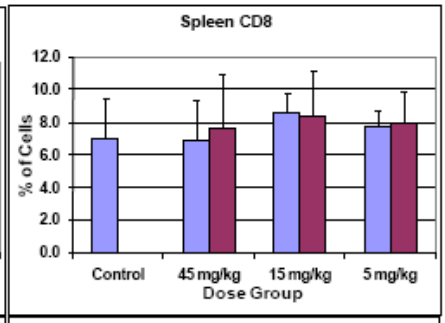
Spleen CD8
% of Cells
12.0
10.0
8.0
6.0
4.0
2.0
0.0
Control
45 mg/kg
15 mg/kg
5 mg/kg
Dose Group

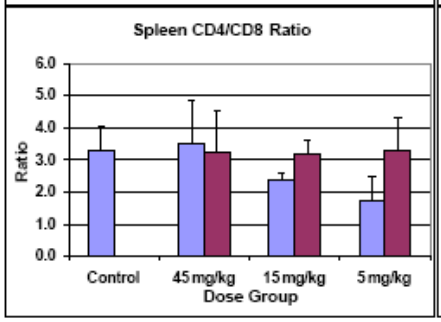
Spleen CD4/CD8 Ratio
Ratio
6.0
5.0
4.0
3.0
2.0
1.0
0.0
Control
45 mg/kg
15 mg/kg
5 mg/kg
Dose Group

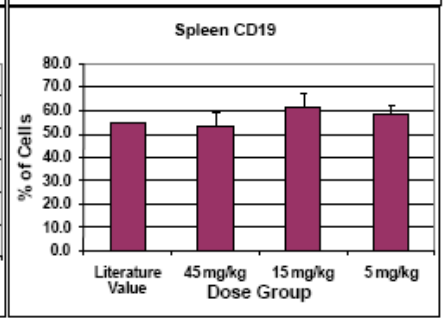
Spleen CD19
% of Cells
80.0
70.0
60.0
50.0
40.0
30.0
20.0
10.0
0.0
Literature Value
45 mg/kg
15 mg/kg
5 mg/kg
Dose Group

10

Supplemental Figure 9. Response of a collection of primary patient B-ALL samples to LDK treatment. (A-J) Ten primary human B-ALL cell samples were treated with LDK and the PI3K inhibitor LY294002 then assessed for viability via DPM measurement. Left panels – dose response of primary B-ALL sample viability after 48 hrs incubation in LDK. Right panels – dose response of primary B-ALL patient samples to treatment with LY294002. (n values as noted, error bars = s.e.m.) Full descriptions of patient samples may be found in Supplemental Table 6.

A

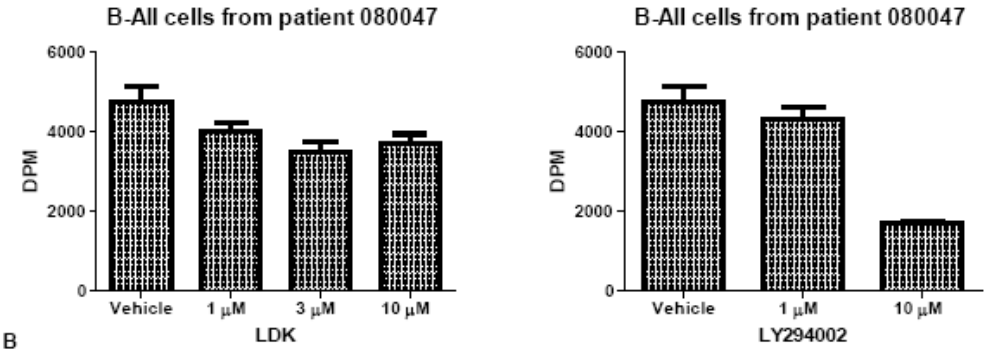

B

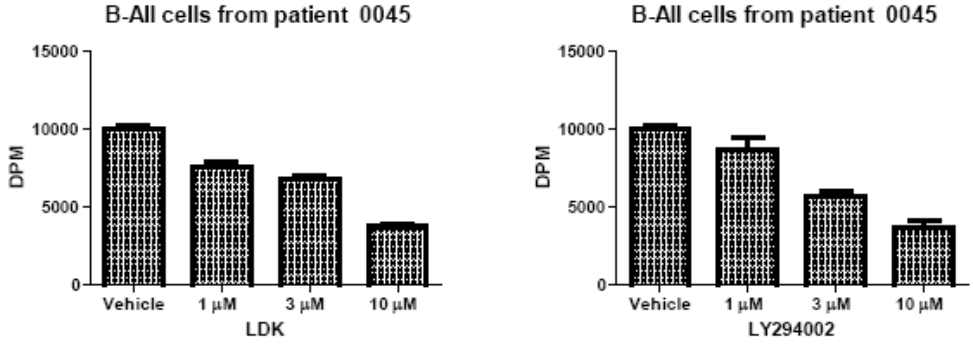

C

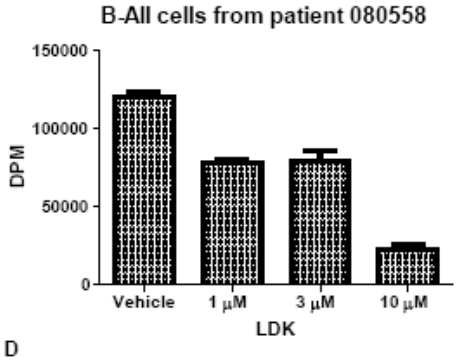
B-All cells from patient 080558
DPM
150000
100000
50000
0
Vehicle
1 μM
3 μM
10 μM
LDK

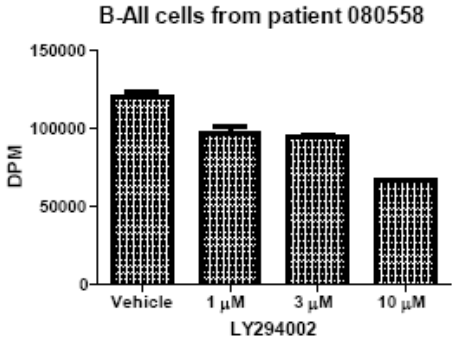
B-All cells from patient 080558
DPM
150000
100000
50000
0
Vehicle
1 μM
3 μM
10 μM
LY294002

D

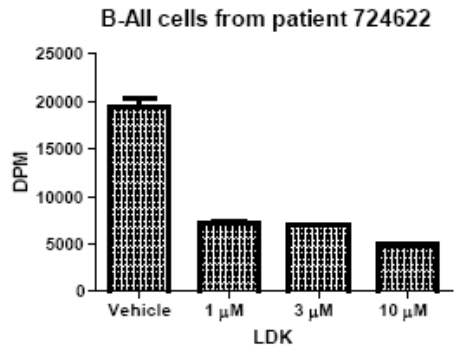
B-All cells from patient 724622
DPM
25000
20000
15000
10000
5000
0
Vehicle
1 μM
3 μM
10 μM
LDK

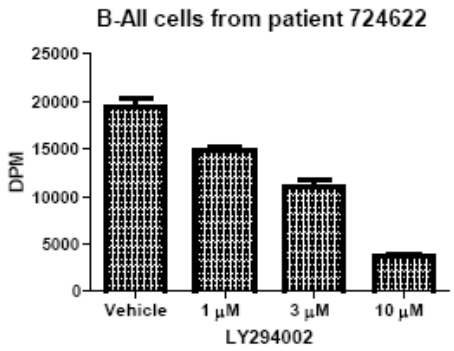
B-All cells from patient 724622
DPM
25000
20000
15000
10000
5000
0
Vehicle
1 μM
3 μM
10 μM
LY294002

E

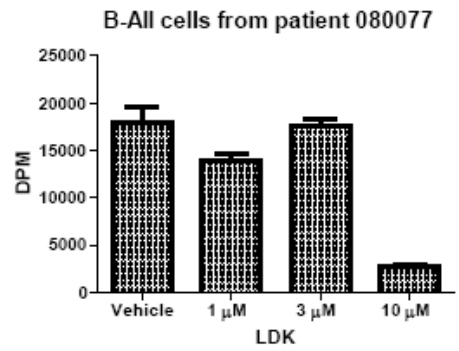
B-All cells from patient 080077
DPM
25000
20000
15000
10000
5000
0
Vehicle
1 μM
3 μM
10 μM
LDK

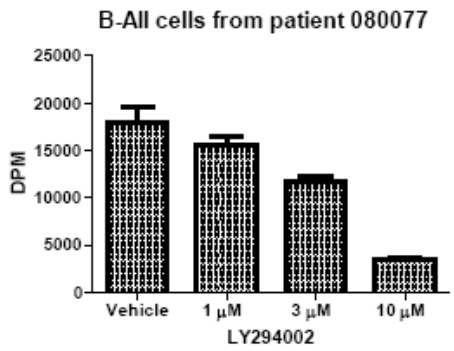
B-All cells from patient 080077
DPM
25000
20000
15000
10000
5000
0
Vehicle
1 μM
3 μM
10 μM
LY294002

12

F

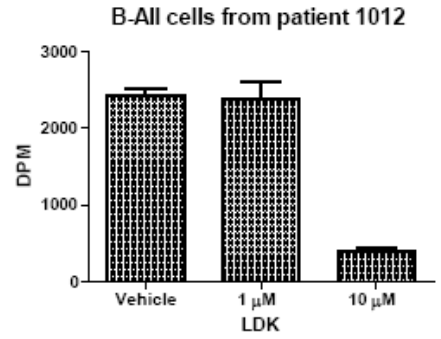
B-All cells from patient 1012
DPM
3000
2000
1000
0
Vehicle
1 μM
10 μM
LDK

G

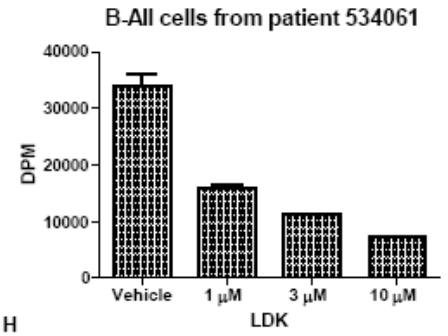
B-All cells from patient 534061
DPM
40000
30000
20000
10000
0
Vehicle
1 μM
3 μM
10 μM
LDK

H

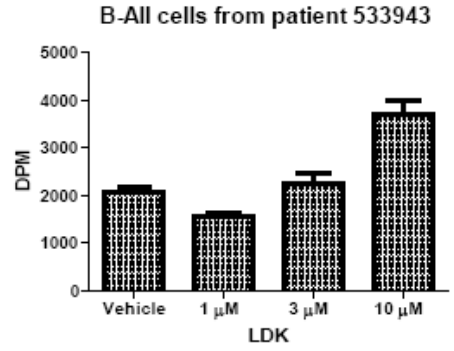
B-All cells from patient 533943
DPM
5000
4000
3000
2000
1000
0
Vehicle
1 μM
3 μM
10 μM
LDK

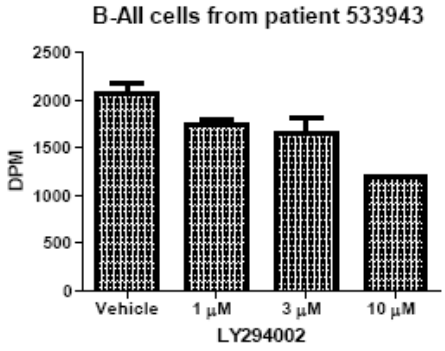
B-All cells from patient 533943
DPM
2500
2000
1500
1000
500
0
Vehicle
1 μM
3 μM
10 μM
LY294002

13

I

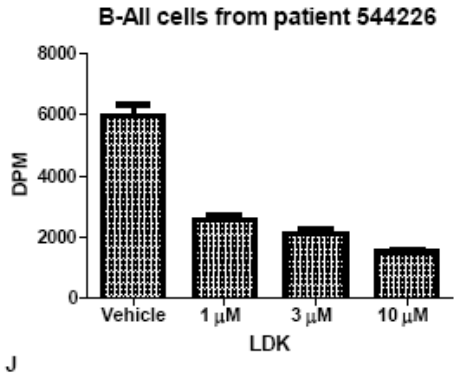
B-All cells from patient 544226
DPM
8000
6000
4000
2000
0
Vehicle
1 μM
3 μM
10 μM
LDK

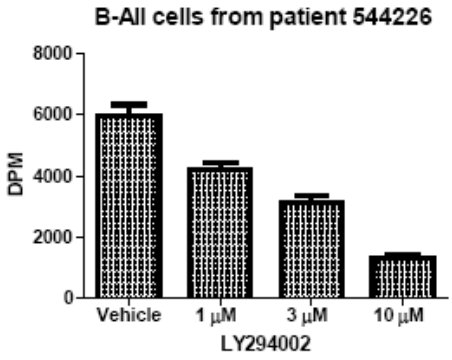
B-All cells from patient 544226
DPM
8000
6000
4000
2000
0
Vehicle
1 μM
3 μM
10 μM
LY294002

J

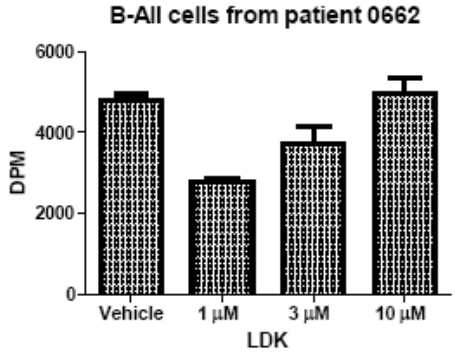
B-All cells from patient 0662
DPM
6000
4000
2000
0
Vehicle
1 μM
3 μM
10 μM
LDK

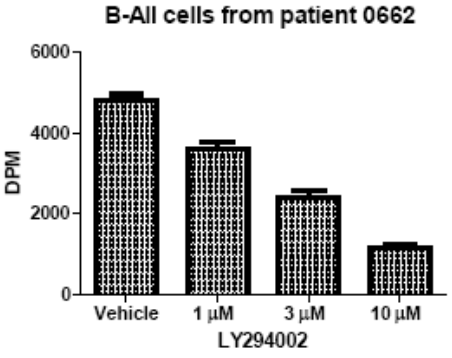
B-All cells from patient 0662
DPM
6000
4000
2000
0
Vehicle
1 μM
3 μM
10 μM
LY294002

14

Supplemental Table 1. Cell cycle effects of 21 candidate compounds on zebrafish embryos. The 21 compounds with strong effects on survival of immature zebrafish T cells were assessed for their impact on the cell cycle of non-lymphoid zebrafish cells between 4 and 24 hpf. (N = No, Y = Yes, None = No effect, S = S-phase, G0/G1 = G0/G1 phase).

Strong Effect Compound Number:	Sub G1 Peak?	Delay:
1	Y	S
2	N	None
3 (LDK)	N	None
4	Y	S
5	Y	S
6	N	None
7	N	None
8	Y	S
9	N	None
10	N	G0/G1
11	N	G0/G1
12	N	G0/G1
13	N	G0/G1
14	N	G0/G1 & S
15	Y	G0/G1
16	N	G0/G1
17	N	S
18	N	G0/G1
19	Y	G0/G1
20	Y	G0/G1
21	N	G0/G1

Supplemental Table 2. LDK has minimal impact on zebrafish embryonic and larval development.
Larvae were inspected after 48 hrs treatment by light microscopy and health and development was assessed. Toxicity was ranked: Grade I – no effect, Grade II – mild edema, Grade III – sick, impaired behavior, Grade IV – lethal. (hpf = hours post-fertilization).

Age at beginning of treatment	Toxicity Ranking after 48 hrs of treatment		
	Untreated	Vehicle	LDK 10μM
24 hpf	Grade I- 96% Grade II- None Grade III- None Grade IV- 4%	Grade I- 66% Grade II- None Grade III- None Grade IV- 34%	Grade I- 35% Grade II- 35% Grade III- None Grade IV- 30%
48 hpf	Grade I- 96% Grade II- None Grade III- None Grade IV- 4%	Grade I- 88% Grade II- None Grade III- None Grade IV-12%	Grade I- ~74% Grade II- ~10% Grade III- None Grade IV- 16%
72 hpf	Grade I- 97% Grade II- None Grade III- None Grade IV- 3%	Grade I- 93% Grade II- None Grade III- None Grade IV- 7%	Grade I- ~80% Grade II- ~10% Grade III- None Grade IV- 10%
96 hpf	Grade I- 97% Grade II- None Grade III- None Grade IV- 3%	Grade I- 90% Grade II- None Grade III- None Grade IV- 10%	Grade I- ~73% Grade II- ~10% Grade III- None Grade IV- 17%
120 hpf	Grade I- 90% Grade II- None Grade III- None Grade IV- 10%	Grade I- 84% Grade II- None Grade III- None Grade IV- 16%	Grade I- 78% Grade II- None Grade III- 8% Grade IV- 14%

Supplemental Table 3. LDK is not a general kinase inhibitor. 33 kinases/phosphatases were selected for assessment of LDK activity *in vitro*. Four increasing concentrations of LDK were used per kinase or phosphatase and change in activity level was measured. The non-selective kinase inhibitor staurosporine was used as a positive control. Experiments conducted by SignalChem (Richmond, BC).

Target	%Activity change (0.2 μM LDK)	%Activity change (1 μM LDK)	%Activity change (5 μM LDK)	%Activity change (25 μM LDK)	%Activity change (1 μM Staurosporine)
AKT1	-6	-2	-9	-20	-93
AKT2	0	-7	-14	-22	-93
AKT3	0	6	-1	-1	-85
AMPK(A1/B1/G1)	-3	2	1	-1	-93
PTPRC (CD45)	1	2	-3	-6	1
c-KIT	0	1	-3	-7	-95
CAMK1	2	4	3	-1	-89
CSK	-1	-5	-6	-13	-53
ERK1	1	-1	-3	-1	-32
FAK	2	3	5	4	-97
FYN A	-3	-1	-4	-7	-92
GSK-3β	-6	-8	-15	-17	-91
HCK	-2	-6	-10	-14	-99
ITK	-2	3	2	1	-100
JNK1	-4	-3	0	2	-40
JNK2	0	-2	-6	0	-32
LCK	3	3	-2	-4	-76
LYN A	0	0	-5	-10	-96
MEK1	0	0	-11	-16	-72
p38α	3	1	1	-7	-6
p38δ	1	1	0	0	-9
PI3K (p110α/p85α)	-1	-3	-8	-9	-16
PI3K (p110β/p85α)	6	0	-4	-5	-26
PDK1	-3	-5	-2	-4	-86
PIM1	-5	-9	-18	-25	-100
PKCγ	-1	-3	-6	-8	-93
PKCθ	-3	-7	-3	-5	-99
PKCζ	1	1	1	-8	-68
SRC	-1	-11	-15	-18	-87
SYK	-1	-1	-6	-11	-95
TEC	-2	-8	-7	-11	-92
YES1	-4	-4	-7	-28	-98
ZAP70	1	2	-2	-5	-99

Supplemental Table 4. LDK treatment results in G2/M arrest for sensitive T-ALL and B-ALL cell lines. T-ALL (Jurkat, CCRF-CEM) and B-ALL (697, Nalm-6, and RS4;11) cell lines were treated with either DMSO vehicle only, LDK, or Wortmannin. All LDK-sensitive cell lines (Jurkat, CCRF-CEM, 697, Nalm-6) show G2/M accumulation upon treatment with LDK, whereas the LDK-resistant B-ALL cell line RS4;11 shows accumulation in G0/G1 upon treatment with LDK. Wortmannin, a known inhibitor of the PI3K pathway, causes G0/G1 accumulation in all lines tested with the exception of 697. Cell cycle percentages shown are average of three separate experiments ± s.d.

Cell Line	Treatment	% Cells / Phase		
		G0 / G1	S	G2 / M
Jurkat	DMSO (0.1%)	47 ± 2	38 ± 1	15 ± 1
	LDK 10 μM	44 ± 3	28 ± 2	28 ± 2
	Wortmannin 1 μM	59 ± 2	27 ± 1	15 ± 2
CCRF-CEM	DMSO (0.1%)	39 ± 2	41 ± 2	20 ± 1
	LDK 10 μM	42 ± 2	33 ± 2	25 ± 0
	Wortmannin 1 μM	45 ± 4	36 ± 4	20 ± 0
697	DMSO (0.1%)	42 ± 3	35 ± 6	23 ± 3
	LDK 10 μM	32 ± 4	30 ± 11	39 ± 7
	Wortmannin 1 μM	42 ± 6	34 ± 7	24 ± 1
Nalm-6	DMSO (0.1%)	44 ± 2	45 ± 2	11 ± 1
	LDK 10 μM	44 ± 4	32 ± 1	24 ± 6
	Wortmannin 1 μM	56 ± 2	33 ± 2	10 ± 1
RS4;11	DMSO (0.1%)	49 ± 1	43 ± 2	8 ± 4
	LDK 10 μM	65 ± 3	27 ± 3	9 ± 1
	Wortmannin 1 μM	67 ± 5	27 ± 5	6 ± 1

Supplemental Table 5. Characteristics of primary BCR-ABL translocated B-ALL and CML patient samples and growth inhibition by LDK treatment.

Sample ID (Type)	Gender / Age	Cytogenetics	BCR-ABL1	BCR-ABL1 mutation	Cell Isolation / Clinical Course	MTT Assay LDK IC_{60}
LAX2 (Ph+ B-ALL)	m/38	t(9;22)(q34;q11)	p210	T315I	Relapse (on Imatinib)	0.814 µM
SFO2 (Ph+ B-ALL)	m/7 m/8	t(9;22)(q34;q11)	p210	unmutated	Diagnosis and Relapse (on Nilotinib)	0.762 µM
BLQ5 (Ph+ B-ALL)	f	FISH der(9), der(22)	p190	T315I	Relapse (on Imatinib)	0.939 µM
TXL3 (Ph+ B-ALL)	N/A	t(9;22)(q34;q11)	p210	unmutated	Diagnosis	0.888 µM
ICN1 (Ph+ B-ALL)	N/A	t(9;22)(q34;q11)	p210	unmutated	Diagnosis	0.795 µM

Sample ID	Leukemia Type	Age at Diagnosis	Gender	Cytogenetics	Source (BM or PB)	BCR-ABL1 mutation	Prognosis/ Outcome
10-003	Ph+ CML	43	M	BCR-ABL	PB	Unmutated	Alive
11-007	Ph+ CML	N/A	F	BCR-ABL (T315I)	PB	(T315I)	Alive
11-008	Ph+ B-ALL	62	M	Complex Karyotype	PB	Complex Karyotype	Alive
11-018	Ph+ B-ALL	N/A	M	BCR-ABL	PB	Unmutated	Alive
11-032	Ph+ B-ALL	62	M	Complex Karyotype	PB	Complex Karyotype	Alive

Supplemental Table 6. Characteristics of primary B-ALL patient samples and LDK-mediated inhibition of proliferation.

Sample ID	Age at Diagnosis	Gender	PB WBC Count (109)	Source (BM or PB)	Cytogenetics	Prognosis / Outcome
80047	55	Female	129	PB	MLL rearrangent	Alive
45	67	Female	79	PB	BCR-ABL	Deceased
80558	46	Female	22	PB	BCR-ABL (p190)	Alive
724622	46	Male	135	PB	BCR-ABL	Deceased
80077	21	Male	5	BM	t(2;3)	Deceased
534061	44	Male	N/A	N/A	N/A	Deceased
533943	25	Male	N/A	N/A	N/A	Deceased
544226	57	Female	N/A	N/A	N/A	Deceased
662	30	Male	89	PB	xy del. 17 (p11.2)	Deceased
1012	16	Male	9	BM	Normal	Alive

Sample ID	LDK			Ly294002		
	1 µM	3 µM	10 µM	1 µM	3 µM	10 µM
80047	16 ± 4	27 ± 6	23 ± 5	10 ± 6	N/A	65 ± 1
45	24 ± 4	32 ± 2	63 ± 3	13 ± 7	43 ± 3	63 ± 5
80558	35 ± 2	34 ±6	81 ± 3	19 ± 3	21 ± 1	44 ± 0
724622	63 ± 1	64 ± 1	75 ± 1	24 ± 2	44 ± 4	81 ± 1
80077	22 ± 3	2 ± 4	85 ± 2	13 ± 6	35 ± 3	81 ± 1
534061	54 ± 2	67 ± 1	79 ± 1	N/A	N/A	N/A
533943	25 ± 4	-8 ± 11	-78 ± 15	16 ± 3	20 ± 8	43 ±1
544226	58 ± 3	65 ± 3	75 ± 2	30 ± 4	48 ± 4	79 ± 2
662	42 ± 2	22 ± 9	-4 ± 8	25 ± 4	50 ± 4	76 ± 2
1012	2 ± 9	N/A	84 ± 2	N/A	N/A	N/A

Percent inhibition +/- s.e.m., normalized to vehicle control

Supplemental Methods

Cell lines and cell culture

All cells were cultured in media containing 100U/mL Penicillin (Invitrogen) and 100µg/mL Streptomycin (Invitrogen) and incubated at 37°C and 5% CO_2. T-ALL cell lines Jurkat, MOLT-3, HPB-ALL and CCRF-CEM were grown in RPMI 1640 media (Invitrogen) supplemented with 10% FBS (Atlanta Biologicals, Lawrenceville, GA). CCRF-CEM-Luc was grown in the presence of 0.3 mg/mL Geneticin. The T-ALL cell lines HPB-ALL and CCRF-CEM-Luc were a kind gift of Adolfo Ferrando (Columbia University, New York, NY). B-ALL cell lines 697, Nalm-6, Kasumi-2, and RS4;11 were grown in RPMI 1640 media supplemented with 20% FBS. RS4;11 was a kind gift of Andrew Kung (DFCI, Boston, MA). U138 (glioblastoma), Lox (melanoma), and SW480 (colon cancer) were grown in DMEM media supplemented with 10% FBS and 2mM L-glutamine. All cell lines were cultured in media containing 100U/mL Penicillin (Invitrogen) and 100µg/mL Streptomycin (Invitrogen) and incubated at 37°C and 5% CO_2.

***In vitro* drug treatment**

Lenaldekar was initially obtained from the ChemBridge DIVERSet® library (ChemBridge, San Diego, CA). Subsequently LDK was manufactured by the University of Utah Chemistry Department (M.S., K.B.) using the following components: hydroxyquinoline (Sigma-Aldrich), hydrazine hydrate (Sigma-Aldrich), and indole-3-carboxaldehyde (Sigma-Aldrich). Camptothecin, Nocodazole, imatinib, γ-secretase inhibitor IX, dexamethasone, LY294002, UCN-01 and Wortmannin were obtained from Sigma-Aldrich. AKT Inhibitor IV and Doxorubicin were obtained from Calbiochem. Taxol was obtained from VWR (Radnor, PA). Drugs were dissolved in 100% DMSO then diluted for experimentation such that the final concentration of DMSO did not exceed 0.1%.

MTT assays

Cells were plated in 96-well plates at a density of 25,000 cells per well for RS4;11, 100,000 cells per well for peripheral blood T-cells, and 50,000 cells per well for all other cell types. Cells were exposed to treatment conditions for the indicated durations at 37°C and 5% CO_2 then incubated with thiazolyl blue tetrazolium bromide (MTT) reagent (Sigma-Aldrich Corp., St. Louis, MO) for an additional 3 hours. Each well was washed one time with HBSS then DMSO was added to dissolve the formazan crystals. Absorbance values were then

measured at 570nm with a Bio-Rad microplate spectrophotometer (Bio-Rad, Hercules, CA). The absorbance values were background subtracted and normalized to vehicle (DMSO) treated values. Concentration response curves were generated using non-linear regression with the GraphPad Prism® software package (GraphPad Software, Inc., La Jolla, CA) to generate IC_{50} values.

Viability of $Atm^{-/-}$ mouse primary T-ALL cell lines

A detailed characterization of these lines will be published elsewhere. Briefly, IL-7-dependent cell lines were established from primary T-ALLs arising in *Atm*$^{-/-}$ mice. Expression of PTEN and activated NOTCH1 in the primary T-ALLs was evaluated by western blotting. Cells were cultured for 24 and 48 hours in IL-7 with 10μM γ-secretase inhibitor IX (Calbiochem, Gibbstown, NJ), LDK, or DMSO vehicle. Cell viability was determined using the Cell Titre Blue® Cell Viability Assay (Promega, Madison, WI) following the manufacturer's instructions.

Peripheral blood T- and B-Cell isolation

All cells were cultured in media containing 100U/mL Penicillin (Invitrogen) and 100μg/mL Streptomycin (Invitrogen) and incubated at 37°C and 5% CO_2. Blood was drawn into BD Vacutainer K2 EDTA blood collection tubes (Becton Dickinson). Blood was diluted in an equal volume of PBS, layered over lymphocyte separation medium (Cellgro, Manassas, VA), and centrifuged at 1400 rpm for 20 minutes. The mononuclear lymphocyte layer was transferred to a new tube, diluted with PBS, and centrifuged to pellet the lymphocytes. The lymphocyte pellet was diluted in 5 mL of RPMI 1640 media supplemented with 20% FBS, 100U/mL penicillin, and 100μg/mL streptomycin; transferred to a T25 cell culture flask, and incubated overnight at 37°C and 5% CO_2. The following day media was removed by centrifugation and cells were suspended at a density of 1×10^8 cells/mL. B-cells were isolated using the EasySep CD19 positive selection kit from StemCell Technologies (Vancouver, BC). Isolated B-Cells were cultured in media with 100ng/mL Interleukin-10 (Prospec, East Brunswick, NJ) for experimental procedures. The remaining cell suspension was then subject to T-Cell isolation using the EasySep CD3 positive selection kit from StemCell Technologies. Isolated T-Cells were cultured in media with 30IU/mL Interleukin-2 (Hoffman-La Roche Inc., Nutley, NJ) for subsequent experimental procedures.

***In vitro* apoptosis assay**

Jurkat cells were treated with DMSO vehicle (0.1%), 1μM LDK or 5μM Camptothecin for 24 hours then stained with propidium iodide and Annexin V-FITC (BD Pharmingen) according to the manufacturer's instructions. Apoptosis was determined via flow cytometry in a FACScan analyzer (Becton Dickinson).

Western blot analysis

Cells were treated with the indicated compounds, pelleted and washed with cold PBS. Protein was extracted via 10 min incubation on ice in cell lysis buffer (25mM TRIS pH 7.4, 150mM NaCl, 1mM $CaCl_2$, 1% Triton X-100) with phosphatase (Sigma-Aldrich) and protease (Sigma-Aldrich) inhibitors. Protein density was determined via Bio-Rad Protein assay. Proteins were separated via gel electrophoresis on SDS-PAGE gels (Invitrogen). Protein was then transferred to PVDF membrane and the membrane incubated in milk block (5% non-fat dry milk powder in 1% PBS-T) for either 1 hour at room temperature or overnight at 4°C. Membranes were then incubated for either 1-3 hours at room temperature or over night at 4°C in primary antibody diluted in primary antibody dilution buffer (5% BSA, 0.1% Tween 20 and 0.01% NaN_3 in PBS, filtered at 0.45μm). Primary antibodies purchased from Cell Signaling included PARP, AKT, p-AKT(Ser473), p-AKT(Thr308), mTOR, p-mTOR(Ser2448), PTEN, p70S6K, p-p70S6K(Thr389), Cyclin A and Cyclin B1. Phospho-Histone H3 antibody was purchased from Santa Cruz Biotechnology (Santa Cruz, CA). Actin primary antibody was purchased from ImmunO MP Biomedicals (Solon, OH). Vinculin antibody was purchased from Sigma. All primary antibodies were utilized at a 1:1,000 dilution ratio in primary antibody dilution buffer with the exceptions of vinculin (1:5,000) and p-AKT(Ser473) (1:2,000). Blots were then washed 3x for 10 min each in PBS-T and incubated in secondary antibody. Secondary antibodies used were sheep-anti-mouse (Amersham, Piscataway, NJ) and donkey-anti rabbit (Amersham) at a 1:10,000 dilution in milk block for 1 hour at room temperature. Blots were then washed again 3x for 10 min each in PBS-T. Chemiluminescence was assessed using WESTERN LIGHTNING-*Plus*-ECL horseradish peroxidase (PerkinElmer, Waltham, MA) and exposed to Amersham Hyperfilm ECL film (GE Healthcare, Piscataway, NJ). Densitometry was done utilizing Adobe Photoshop CS2 v9.0.2 histogram feature.

Immunocytochemistry

Jurkat cells were treated with test compounds or DMSO vehicle for 16 hours at 37° C. Samples were fixed in 4% paraformaldehyde for 20 minutes and then permeabilized with 0.1% Triton X-100 for 15 minutes. Samples

were then washed and resuspended in PBS/1%BSA and spun onto glass slides with a Shandon Cytospin3 cytocentrifuge (Thermo Scientific, Asheville, NC) at 600 rpm for 5 minutes. Slides were blocked in TBS buffer with 0.1% Triton X-100, 2% BSA, and 0.1% azide for 10 minutes, then incubated with active caspase-3 rabbit polyclonal antibody (BD Bioscience, San Jose, CA) diluted 1:200 in PBS/1%BSA for 60 minutes at room temperature. Slides were washed 3 times, then incubated with Alexa Fluor 568 goat anti-rabbit IgG secondary antibody (Invitrogen) diluted 1:1000 in PBS/1%BSA for 60 minutes at room temperature. Slides were washed 3 times then incubated with 50nM DAPI (Sigma) for 3 minutes. Slides were washed, allowed to dry briefly, and a coverslip was mounted to each slide with a drop of Prolong Gold (Invitrogen) and allowed to dry overnight. Slides were then imaged on a Nikon eclipse E600 fluorescence microscope (Nikon Instruments Inc., Melville, NY).

Statistical analyses

For mouse xenograft results, p-values were calculated utilizing Wilcoxon rank sum test (non-parametric test) due to non-normal distribution of tumor emittence data. Alpha level = 0.05, two-tailed test. For each p-value, comparison of interest was vehicle control vs. LDK-treated emittance for the pertinent experimental timepoint.

Phosflow experiments

Phosflow staining of Ramos B cell lymphoma and IL-3-dependent BaF3 pro-B cell lines was performed using BD Phosflow antibodies (BD BioSciences, San Diego, CA), BD Fix Buffer I and BD Perm Buffer III according to the manufacturer's protocol. Non-viable cells were excluded based on staining with Fixable Blue (Invitrogen, Carlsbad, CA) used according to the manufacturer's protocol. Dasatinib was purchased from Toronto Research Chemicals (Toronto, ON Canada) and JAK Inhibitor I was purchased from Calbiochem. Immunofluorescence was analyzed using a SORP LSRII (BD Biosciences) equipped with 4 lasers emitting at 488nm (100mW), 633nm (20mW), 405nm (25mW) and 355nM (25mW).

AKT double phosphomimetic mutagenesis.

The pTRE2-hyg vector (Clontech) containing myristoylated AKT was a kind gift of Steven Grant, MD (Virginia Commonwealth University) and has been described previously (Supplemental Reference 1). AKT double phosphomimetic mutations (T308D/S473D) were introduced into the myr-AKT construct using Agilent

Technologies QuikChange Lightning™ Multi-Site Diected Mutagenesis Kit (Cat# 210515-5) according to the manufacturer's instructions. For AKT(T308D) mutagenesis, the primer used was 5'-GGTGCCACTATGAAG**GA**CTTCTGCGGAAC GCCG-3'. For AKT(S473D) mutagenesis, the primer used was 5'-ACTTCCCCCAGTTC**GA**CTACTCA GCCAGTGG-3' (mutated bases shown in bold font). Sequence-verified myristoylated AKT(T308D/S473D) constructs (myr-AKT-DD) were introduced into Jurkat cells via nucleofection using the LONZA Amaxa™ Cell Line Nucleofector Kit V (Cat# VCA-1003) according to the manufacturer's instructions for optimized delivery to Jurkat Clone E6.1 cells. Nucleofected cells were then selected in 0.5mg/mL hygromycin for two weeks. The pLVX-Tet-On (Clontech) tetracycline-response control vector was utilized to generate lentivirus via standard methods in HEK293 cells. Jurkat cells previously selected in hygromycin for stable expression of the myr-AKT-DD construct were transduced with pLVX-Tet-On carrying lentivirus then selected in dual 0.5mg/mL neomycin/hygromycin for two weeks before testing for myr-AKT-DD transgene expression and LDK resistance.

***In vitro* kinase assay**

In vitro kinase assay was performed by SignalChem, Inc. (Richmond, BC). LDK was tested in triplicate against 33 purified kinase/phosphatases (See Supplemental Table 3) and their peptide targets, utilizing four increasing LDK concentrations of 0.2μM, 1μM, 5μM, and 25μM. Read-out for kinase assay was incorporation of ^{33}P. Read-out for phosphatase assay was absorbance at 410nm utilizing pNPP as substrate. The general kinase/phosphatase inhibitor staurosporine was used at 1μM as positive control. Further specific *in vitro* kinase assay methods may be found online at www.signalchem.com. An additional 451 kinases were tested by KINOME*Scan* (San Diego, CA) at 1μM LDK. Further information regarding KINOME*Scan* methods may be found online at www.kinomescan.com.

Cell cycle analysis

Cell cultures were suspended in media at a density of 500,000 cells/mL and exposed to the treatment conditions in 6-well cell culture plates for the indicated time at 37°C. Cells were harvested, washed with PBS, and fixed with 70% ethanol at 4°C for a minimum of 2 hours. Fixed cells were washed with PBS and stained with 10μg/mL propidium iodide (Invitrogen) with 1mg/mL RNase A (Invitrogen) for 30 minutes at 37°C, then placed on ice prior to analysis. DNA staining and cell cycle analysis was then done by flow cytometry.

LDK mouse blood serum level determination

Initial pharmacokinetic analysis was performed by Advinus, Inc. (Bangalore, India) (See Supplemental Fig. 7). Briefly, male Swiss Albino mice were divided into two groups and given a single dose bolus of LDK either intravenously at 3mg/kg via tail vein injection or orally at 15 mg/kg via gavage feeding. LDK solution was prepared by dissolving it in an aqueous diluent consisting of 5% N,N-dimethylacetamide, 5% Cremophor-EL, and 5% dextrose at pH 6.0 and filter-sterilizing it through a 0.22µm filter syringe. LDK for IV administration was resuspended in diluent to a concentration of 0.5 mg/mL with an injection volume of 6 mL/kg. LDK for oral administration was resuspended in the same diluent to a concentration of 1.5 mg/mL with an administration volume of 10 mL/kg. Following LDK administration, three treated mice were assessed per time point per treatment for blood serum LDK levels via retro-orbital blood draw and serum separation followed by LC-MS analysis. Pharmacokinetic parameters were calculated using non-compartmental analysis tool of WinNonlin Enterprise (Version 5.1.1) software (Pharsight Inc, Sunnyvale, CA). For LDK blood serum level determination following maximum tolerated dose study (See Supplemental Fig. 7), male NOD-SCID mice were divided into four groups of five mice each and injected IP b.i.d. for two weeks with either diluent only or 16, 80, or 200 mg/kg LDK, respectively. 24 hours following the last injection, mice were exsanguinated and serum was separated for LC/MS analysis of LDK serum levels by J.C.

Liquid chromatography-mass spectrometry (LC-MS)

For LC-MS analysis of LDK, an integrated system consisting of two Shimadzu LC-10AD VP pumps, a CBM-20A controller and an API 365 triple quadrupole mass spectrometer modified with an Ionics EP10+ source was employed. Parameter optimization was performed by direct infusion of LDK dissolved in acetonitrile. The parent mass of 287.2 m/z and the daughter mass of 144.2 was determined to be optimal for quantification in the positive mode. An HPLC method was developed using a HyperClone 100 x 4.6 mm 3 ODS column (Phenomenex, Torrance, CA). Solvents employed for this were MS grade acetonitrile and 5 mM ammonium formate buffer, pH 3.2. Flow rate was 0.5 mL/min. The column was held initially at 10% acetonitrile for 1 minute followed by a linear gradient to 90% acetonitrile over 4 minutes. This concentration was held for 2 additional minutes followed by a downward ramp back down to 10% acetonitrile. The column was re-equilibrated for 4 minutes at 10% acetonitrile. Using this method the retention time for LDK was determined to

be 6.3 minutes. A calibration curve was generated with the lower limit of detection (LOD) determined to be 6.25 ng/mL. A liquid-liquid extraction method was developed and optimized for the analysis of LDK in serum and tissue by spiking bovine serum with LDK and extracting twice with equal parts of toluene.

Isolation and analysis of mouse tissues

Groups of 3 animals per dose of drug were evaluated every 3 to 4 days by peripheral blood analysis and for cellularity and immunophenotype of cells in spleen and thymus. Peripheral blood was collected from the retro-orbital sinus and subjected to differential cell counting using a Serono System 9010+CP hematology counter (Serono Diagnostics, Allentown, PA). Spleen and thymus tissue was dissociated in Hank's Balanced Salt Solution (HBSS) containing 5% newborn calf serum, red blood cells were eliminated by ammonium chloride lysis. Cell counts were determined as above and 2×10^5 cells were incubated with labeled monoclonal antibodies to detect CD4, CD8, and CD19. Flow cytometry was performed using a FACScan flow cytometer (BD Biosciences, San Jose, CA; modified by Cytek Development, Fremont, CA). Four-micron thick sections were cut and stained with hematoxylin and eosin. Mouse tissues were examined for evidence of necrosis or toxicity by A.A.

B-ALL cell culture and treatment

Primary human B-ALL samples were cultured in StemSpan (Stem Cell Technologies, Vancouver, BC) serum-free expansion medium for hematopoietic cells supplemented with 1 mM L-glutamine, 10mM Hepes, 0.1mM non-essential amino acids, and 1mM sodium pyruvate. Cells were treated with test compounds or vehicle for 72 hours. During the last 16 hours of culture the cells were pulsed with [^{3}H]-thymidine. At the end of the incubation period the cells were harvested and run on a scintillation counter to measure dpm as a readout of cell proliferation.

CML clonogenic and viability analysis

Methylcellulose clonogenic assays were carried out by plating 10^3 CML-CP^{CD34+} or Ph+ALL MNCs 0.9% MethoCult (Stem Cell Technologies) in the presence of the cytokine cocktails described above, and either untreated or treated with LDK (0.1, 1.0, 3.0, 10.0μM) or imatinib (2.5μM). Colonies (>100μm) from primary cells were scored on day 12. Trypan blue exclusion was used to assess cell viability.

CD34+ hematopoetic stem/progenitor cell isolation and assay for LDK sensitivity

Umbilical cord blood samples were received within 48 hours of harvest. Samples were centrifuged and the pellet was suspended in red blood cell (RBC) lysis buffer and incubated on ice for 5 minutes. Cells were then pelleted, washed with PBS/2 mM EDTA, layered over cold Ficoll, and centrifuged at 1,800 RPM for 30 minutes. Mononuclear cells were then collected and washed in PBS/2 mM EDTA. CD34+ separation was then performed with an AutoMACS Pro separator and CD34 Multisort MicroBeads from Miltenyi Biotec (Auburn, CA). The CD34+ cells were then cultured in RPMI supplemented with 10% FBS, StemSpan® CC100 cytokine cocktail (STEMCELL Technologies, Vancouver, BC), and 50 ng/mL recombinant human thrombopoietin (Invitrogen, Carlsbad, CA). Cells were immediately plated in 96-well plates, treated with compound or vehicle, and incubated for 48 hours. After incubation the cell viability was determined by MTT analysis.

Supplemental Reference

1. Hahn M, Li W, Yu C, Rahmani M, Dent P, Grant S. Rapamycin and UCN-01 synergistically induce apoptosis in human leukemia cells through a process that is regulated by the Raf-1/MEK/ERK, Akt, and JNK signal transduction pathways. *Mol Cancer Ther*. 2005; 4(3):457-70.

CHAPTER 5

CONCLUSION

Summary and perspectives

Within the last 50 years, great progress has been made towards curing ALL, with cure rates rising from single digits to currently ~80% for children and ~50% for adults.[1] However, this progress has come with a dear price since it has come in the form of intensification of applied chemotherapy regimens.[2] Such treatment intensification carries with it a concomitant increase in detrimental side effects for both the short- and long-term. Among other side effects, adult survivors of childhood cancer treatment, in comparison to their untreated siblings, are 54 times more likely to have a major joint failure and replacement, 15 times more likely to have congestive heart failure, 14.8 times more likely to have a second primary cancer, and 10 times more likely to have severe cognitive dysfunction, to name only a few detrimental long-term side-effects (See Chapter 1, Table 1.7).[3]

There is, therefore, clearly a great need for improvement in treating childhood cancers, and ALL is the most common form of childhood cancer. For a clinical course of treatment to be considered to be "successful," clearly more must be taken into consideration than merely 5-year Kaplan-Meier statistical survival rates. Not only survival, but overall long-term quality of life must be the final clinical and research goal for this field. Furthermore, ~20% of childhood and ~50% of adult ALL cases still cannot

be cured currently even with these improvements.[1] Moreover, these statistics are slightly worse when considering T-ALL cases alone, which fare worse overall than B-ALL cases.[4]

The primary objective for this study was to identify such novel compounds as may have the desired combined traits of effectively eliminating T-ALL blasts while not causing significant harm to collateral healthy tissues. This objective appears to have been met with the identification of the novel compound Lenaldekar (LDK), which shows efficacy in treating human T-ALL both *in vitro* and *in vivo* without observable toxicity or endorgan damage to model organisms. Furthermore, LDK does not exhibit general cell-cycle effects as do traditional chemotherapy regimens. Moreover, LDK shows a one-log difference in the IC_{50} sensitivities of leukemic blasts in comparison to healthy circulating lymphocytes, thus exhibiting a useful therapeutic window for treatment. An additional unexpected benefit from this study was that LDK shows efficacy in treating most types of leukemia, including glucocorticoid-resistant T-ALL as well as treatment-refractory relapsed B-ALL and CML.

A followup goal after identifying such novel targeted therapeutic compounds was to characterize the molecular mechanism of action of the identified compound(s). Because LDK's efficacy was not dependent on the presence or absence of PTEN, it was deemed unlikely that it acted through down-regulation of the NOTCH1 pathway. Instead LDK shows down-regulation of the PI3K/AKT/mTOR (P/A/mT) pathway upon treatment, as exhibited by de-phosphorylation of AKT, mTOR, and p70S6 Kinase. Based on recent results, it seems possible that LDK may achieve this effect via binding and inactivating Insulin-Like Growth Factor 1 Receptor (IGF1-R), which is known to activate

the P/A/mT pathway. In addition to down-regulation of the P/A/mT pathway, LDK also exhibits a second, independent effect of G2/M block in most sensitive cell lines. The mechanism of action of the G2/M block is currently undergoing investigation.

An additional goal of the thesis was to determine whether or not the zebrafish could be a feasible model organism for conducting such a drug screening. Indeed, the zebrafish proved to be an excellent model organism for this study. As a vertebrate teleost, it shows significant molecular and anatomical homology to the human immune system.[5] Furthermore, at 5dpf, zebrafish already have fairly well-developed organ systems, including a thymus with visible developing T-cells.[6] Simultaneously, 5dpf larvae are still small enough to fit comfortably within the 96-well test plate format, thus saving both space and money. In addition, the starting hypothesis that compounds which selectively eliminate immature T-cells developing in the zebrafish thymus might also eliminate developmentally-arrested human leukemic blasts was also validated by this study.

Future directions

The ultimate goals of this study are to bring targeted T-ALL therapies to the clinic which improve on current treatment regimens in the form of improved T-ALL survival rates with a simultaneous reduction in detrimental side-effects. In order to reach these important goals, several additional steps need to be taken first. While a great deal of molecular characterization work has already been done, further work must still be done in order to optimize LDK's activity. Furthermore, additional animal studies in mammalian models must be conducted before a Phase I clinical trial can be authorized.

Up to this point, molecular characterization of LDK's mechanism(s) of action has shown down-regulation of the P/A/mT pathway as well as an independent G2/M cell

cycle arrest. Completion of LDK's molecular characterization will require identification and validation of LDK's direct biochemical target(s). Through pull-down experiments using biotinylated LDK, at least two putative molecular targets have been identified, IGF1-R and a second additional target that is currently deemed to be classified proprietary information and therefore will not be discussed in this document at this time.

Identification of LDK's direct molecular targets is essential to the process of optimizing LDK's therapeutic activity. Through three-dimensional modeling *in silico,* putative binding sites for LDK on its molecular targets can be identified. From this information, effective modifications can be proposed for LDK's chemical structure with the intent of increasing its specificity, potency, or preferably both. LDK currently shows an IC_{50} of ~1 μM in Jurkat cells, whereas a good drug's IC_{50} is typically considered to be in the nanomolar range (David Bearss, personal communication). Therefore, additional structure-activity relations (SAR) work needs to be done with the LDK molecule.

Additional work can also be done to further characterize LDK's potential for treating leukemia in combination therapy with other therapeutic drugs. In this study, LDK slowed progression of human T-ALL in a mouse xenograft model, and one zebrafish model of T-ALL, *rag2*:c-Myc-ER, showed an excellent long-term remission response to LDK treatment. However, results for LDK treatment of other zebrafish T-ALL models developed in our lab, including *Shrek, Oscar the Grouch,* and *Hulk,* did not show the same degree of efficacy (K. Frazer, pers. communication). It is possible that these three LDK-resistant lines may use different or additional biochemical pathways for T-ALL leukemogenesis than that utilized by the *rag2*:c-Myc-ER line. If such is the case, LDK

may be effective in treating these leukemias in combination with other drugs that target the relevant effector pathways.

Although not the primary focus of this study, LDK has also shown some efficacy in treating at least some epithelial cancer cell lines, including lung, breast, ovarian, and prostate cancer as well as Ewing sarcoma (Trede lab, unpublished data). Although LDK exhibits particular specificity for hematological malignancies, this does not rule out the possibility that it may be useful in treating other epithelial cancers as well. The P/A/mT pathway is found to be up-regulated in ~50% of all cancers, and is a common mechanism of chemo- and radiation resistance encountered in the clinic.[7] Thus, a novel therapeutic that down-regulates this pathway may have the potential to be very useful in treating both hematological and epithelial malignancies, either as monotherapy or in combination with other treatment modalities currently utilized in the clinic.

References

1. Pui CH, Robison LL, Look AT. Acute lymphoblastic leukaemia. *Lancet*. 2008; 371:1030-1043.

2. Fielding A. The treatment of adults with acute lymphoblastic leukemia. *Hematology Am Soc Hematol Educ Program*. 2008; 381-389.

3. Oeffinger KC, Mertens AC, Sklar CA, et al. Chronic health conditions in adult survivors of childhood cancer. *N Engl J Med.* 2006; 355(15):1572-82.

4. Litzow MR. Evolving paradigms in the therapy of Philadelphia-chromosome-negative acute lymphoblastic leukemia in adults. *Am Soc Hematol Educ Program*. 2009:362-70.

5. Postlethwait, JH, Woods IG, Ngo-Hazelett P, et al. Zebrafish comparative genomics and the origins of vertebrate chromosomes. *Genome Res*. 2000; 10:1890-1902.

6. Jin H, Xu J, Wen Z. Migratory path of definitive hematopoietic stem/ progenitor cells during zebrafish development. *Blood.* 2007; 109:5208-5214.

7. Steelman LS, Chappell WH, Abrams SL, et al. Roles of the Raf/MEK/ERK and PI3K/PTEN/Akt/mTOR pathways in controlling growth and sensitivity to therapy-implications for cancer and aging. *Aging.* 2011; 3(3):192-222.

APPENDIX

SUPPLEMENTARY DATA

Introduction

The primary purpose of this thesis project was to first utilize a zebrafish drug screen to identify novel small molecule compound(s) with the potential to treat human T-ALL effectively. Once identified in zebrafish, the second goal was to characterize the molecular mechanism of action responsible for the drugs' observed efficacy in treating human T-ALL and possibly other types of cancer as well. During the course of this project, many experiments were performed which could not be included in the published *Blood* article (see Chapter 4), but were still relevant to the fulfillment of the primary research aims.

The purpose of this Supplementary Data Appendix is to present these additional unpublished experiments with their results as they relate to the goals of the thesis project. These supplementary experiments fall into two general categories: (1) Characterization of LDK's molecular mechanism of action in treating T-ALL (Figures A.1 - A.6), and (2) Identification of other solid cancer types which also show sensitivity to LDK along with some characterization of the molecular mechanisms(s) of action responsible for the observed effects of LDK in these other solid cancer types (Figures A.7 - A.8).

Experimental results and conclusions

LDK impact on AKT downstream phosphorylation target GSK-3β

This experiment demonstrates that LDK treatment of Jurkat T-ALL results in decreased phosphorylation of GSK-3β, which is a direct downstream phosphorylation target of AKT kinase. The effect seems to be maximized at 3.2μM. Hence, LDK appears to down-regulate function of the AKT pathway and possibly downstream pathways controlled by GSK-3β, such as glucose metabolism and Wnt signaling (Figure A.1).

LDK impact on AKT downstream phosphorylation target p-BAD

The results of this experiment are partially unexpected. The constitutively active double-phosphomimetic AKT-DD construct is expected to be more active than wild-type AKT. Hence, expression of AKT-DD would be expected to elicit hyper-phosphorylation of AKT's downstream phosphorylation target BAD. However, expression of AKT-DD was inversely correlated with phosphorylation of BAD in this experiment. The reason for this observation is unknown. We speculate that the double phosphomimetic AKT possibly lacks the specific tertiary conformation required for efficient phosphorylation of BAD. However, within each cell line, the results are as expected with LDK treatment resulting in down-regulation of phospho-BAD in comparison to DMSO-treated controls (Figure A.2).

Constitutively active mTOR partially rescues LDK-treated Jurkat T-ALL

In this experiment, transduction of adenoviral mTOR into Jurkat cells rendered them partially resistant to LDK treatment. As expected, constitutively active mTOR (CA) had a more profound rescue effect than did wild type mTOR (WT). This experiment

demonstrates that down-regulation of mTOR activity in Jurkat T-ALL is responsible for at least some of LDK's lethality. However, since the rescue was only partial, other effects of LDK may also be involved in its mechanism of action. This explains why merely over-expressing mTOR in LDK-treated cells is insufficient for rescue (Figure A.3).

Characteristics of Jurkat LDK-resistant cell line derivatives Res 3 and Res 6

In this experiment, Jurkat cells were deliberately conditioned to be LDK-resistant via constant incubation in gradually increasing concentrations of LDK over several cell passages. Once resistant cell lines were generated, the P/A/mT pathway was assayed for LDK treatment effects in parental Jurkat versus LDK-resistant Jurkat lines. The results show highly similar effects on phosphorylation of the Thr308 residue of AKT (phosphorylated by PDK1) among the three cell lines assayed. However, there is a marked difference among the cell lines in phosphorylation status of the Ser473 residue of AKT, which is phosphorylated by mTOR(C2). The two LDK-resistant lines tested show a marked increase in baseline p-S473AKT status with continuing presence of p-S473AKT even with LDK treatment. In correlation with the results shown in the experiment depicted in Figure A.3, this experiment also indicates that down-regulation of mTOR activity may be essential for LDK-mediated toxicity in Jurkat cells (Figure A.4).

Spatiotemporal isolation of phospho-Aurora B kinase in HeLa cells

The purpose for this experiment was to further narrow down the specific mitotic timing of the observed G2/M delay in LDK-treated cells. Aurora B kinase is known to regulate abscission, which is the last checkpoint in the cell division process before separation of the two daughter cells. Immunostaining was employed in order to ascertain

both temporal and spatial distribution of p-Aur B in the treated versus control cells. HeLa cells were utilized because they are adherent and therefore more amenable to immunostaining than Jurkat cells. Furthermore, HeLa cells, though not LDK-sensitive, display a G2/M delay upon LDK treatment, similar to that observed in Jurkat cells.

These results were unexpected based on earlier observations in LDK-treated Jurkat cells. The number of HeLa cells displaying "midbody" p-Aur B, which is the form observed at the abscission checkpoint, was only ~50% of the number observed in untreated control cells. Furthermore, the number of p-Aur B-positive cells observed in metaphase was twice that counted in control cells. Moreover, the fact that half of the p-Aur B positive metaphase cells had no organized spindle structure suggests that LDK may be interfering with assembly of the mitotic spindle in HeLa cells.

Both Jurkat and HeLa cells show G2/M delay upon treatment with LDK. However, these data indicate that LDK may elicit a different impact on the G2/M transition in HeLa cells than what it does in Jurkat T-ALL. In Jurkat T-ALL, the timing of the G2/M delay has been isolated to occurring after metaphase but before cytokinesis (See Figure 4.4). By contrast, these observations in HeLa cells indicate an earlier LDK-mediated G2/M delay centered around (pro-)metaphase when the mitotic spindle is forming. The difference in the observed timing of the LDK-mediated G2/M delay may be at least partially responsible for the difference in sensitivity to LDK treatment between these two cell lines (Figure A.5).

LDK treatment results in increased autophagy in Jurkat cells

The purpose of this experiment was to determine whether autophagy might be playing a role in LDK-mediated toxicity in Jurkat cells. Indeed, the relative amount of

cleaved LC3-II (14KDa) in LDK-treated cells appears to increase at the 4, 6, and 8 hour timepoints. However, given that the relative increase does not rise above 1.5, it is unlikely that autophagy has a major role in LDK-mediated toxicity. It is also unknown whether or not the observed increase in cleaved LC3 is a bystander or a direct effect of LDK treatment (Figure A.6).

Ewing Sarcoma is LDK-sensitive and shows G2/M delay upon LDK treatment

Ewing sarcoma cell lines A673 and TC71 have consistently shown moderate sensitivity to LDK treatment with IC_{50}s of ~1µM and 3µM, respectively. The purpose of this set of experiments was to characterize the mechanism of LDK-mediated lethality in Ewing sarcoma. Both cell lines tested demonstrated G2/M delay upon LDK treatment, similar to that observed in Jurkat cells. However, unlike Jurkat cells, neither cell line showed down-regulation of p-AKT(S473) upon LDK treatment, as demonstrated by phos-flow analysis. These results indicated that down-regulation of the P/A/mT pathway, and specifically mTOR(C2), may not play a significant role in Ewing Sarcoma's sensitivity to LDK treatment. Rather, the G2/M delay may play a far more significant role in LDK's effect on this particular cancer cell type (Figure A.7).

MCF7 breast cancer derivatives Msp-Ron and sfRon are LDK-sensitive

MCF7 is a typical ER+ breast cancer cell line and, like Ewing Sarcoma, has exhibited consistent moderate sensitivity to LDK treatment with an IC_{50} of 2.3µM, as determined in the NCI60 assessment. This set of experiments was done using two derivatives of parental MCF7s. MCF7-Msp-Ron has been transduced with a cell surface receptor/intracellular signaling domain protein (Msp-Ron) which requires activation via

docking of the Msp ligand with the Msp receptor for activation of the Ron intracellular signaling domain. MCF7-sfRon, by contrast, has been transduced with a constitutively active form of the Ron signaling domain that is not dependent on Msp ligand docking for activation.

MCF7-Msp-Ron is slightly more sensitive to LDK treatment than is MCF7-sfRon and shows no phosphorylation of AKT at baseline control. By contrast, MCF7-sfRon does show AKT activation at baseline, indicative of the constitutively active nature of the sfRon construct. This difference in baseline AKT activation may explain at least in part the observed difference in LDK sensitivity between the two cell lines. Unlike Jurkat cells, MCF7-sfRon exhibits S-phase delay upon LDK treatment (panel C), suggesting that LDK may interfere with DNA synthesis in this cell line, which interference may be contributory to LDK-mediated toxicity in MCF7-sfRon cells and in all MCF7 cells in general (Figure A.8).

Appendix conclusion

The purposes of the experiments presented in this section were to further characterize LDK's mechanism of action in sensitive cells and to expand on identifying additional cancer cell types besides leukemia that may show sensitivity to LDK treatment, as well as the relevant mechanism(s) involved. The results indicate that LDK likely functions via multiple non-exclusive mechanisms of action, including down-regulation of the P/A/mT pathway, S-phase delay, G2/M delay, and possibly autophagy. The results vary among cell types and cell lines, suggesting that the mechanism of action most critical can vary depending on the cell type tested. The results also suggest that

epithelial cancers may also exhibit sensitivity to LDK via the same or different mechanisms as that found in leukemias.

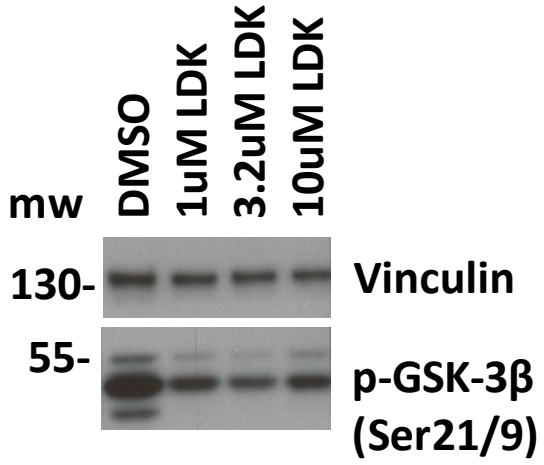

Figure A.1. LDK impact on AKT downstream phosphorylation target GSK-3β. Jurkat cells were treated with either DMSO vehicle or the indicated concentration of LDK for 12 hours then probed for phosphorylation of GSK-3β. De-phosphorylation is seen at an LDK treatment concentration as low as 1μM. Vinculin = loading control.

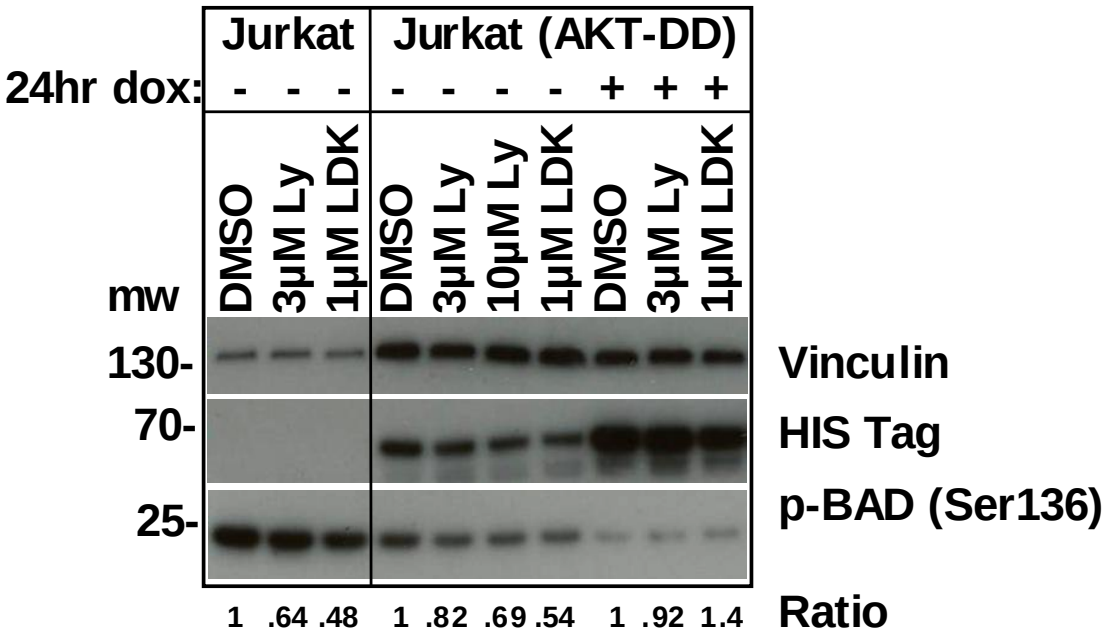

Figure A.2. LDK impact on AKT downstream phosphorylation target p-BAD. Parental Jurkat cells and Jurkat cells transduced with a doxycycline-inducible and constitutively active form of AKT (AKT-DD-6xHIS tag) were incubated for 12 hours with the indicated inhibitors at the indicated concentrations. Jurkat(AKT-DD) was tested both with and without 24 hour preincubation with doxycycline activation. Phosphorylation of BAD was then probed via Western blot. Within each cell line, LDK treatment is observed to result in down-regulation of p-BAD. Vinculin = loading control.

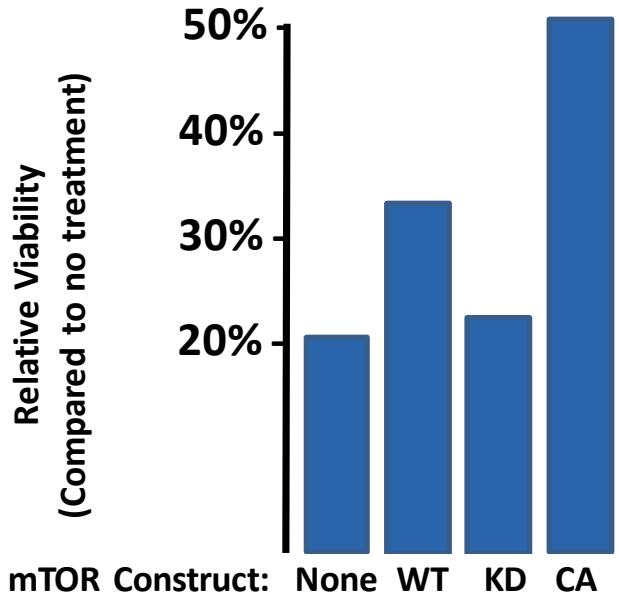

Figure A.3. Constitutively active mTOR partially rescues LDK-treated Jurkat T-ALL. Jurkat T-ALL was transduced with adenoviral mTOR constructs, including wild-type (WT), kinase-dead (KD) and constitutively active (CA). Transduced cells were then treated with 10μM LDK for 48 hours and relative viability was assessed via MTT assay. WT mTOR elicited weak rescue (~33% vs 20%) while CA mTOR elicited a moderate rescue (~50% vs 20%) compared to either untransduced cells ("none") or cells transduced with KD mTOR adenovirus ("KD").

A.

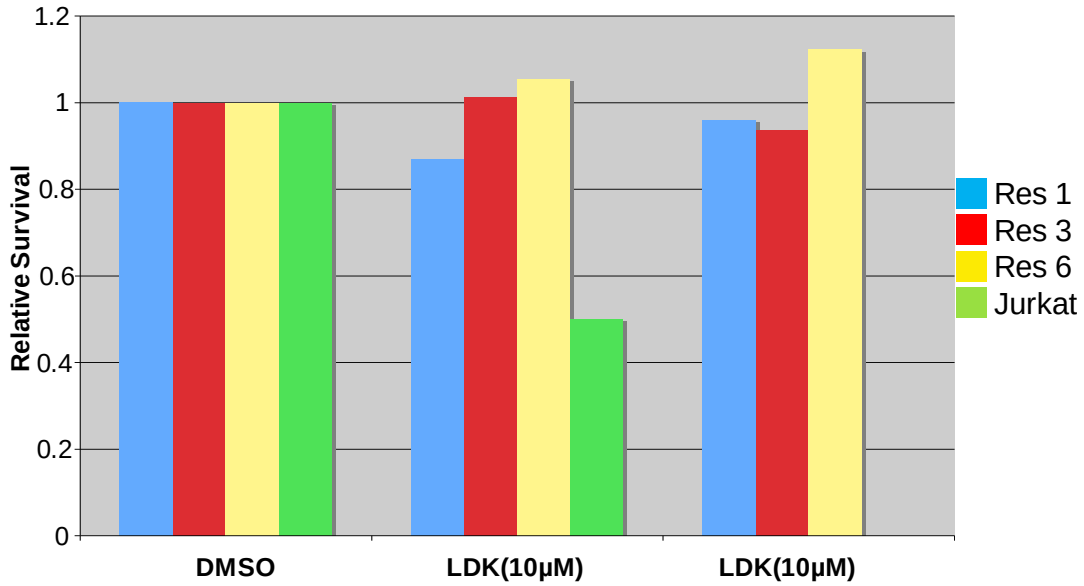

B.

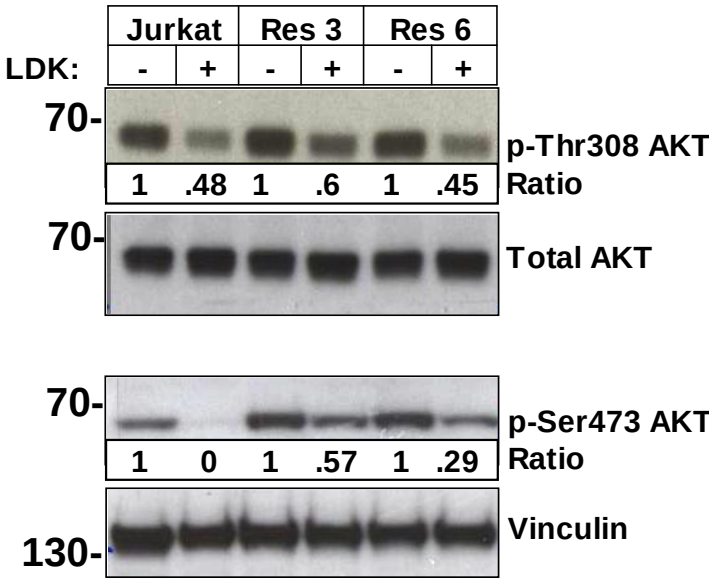

Figure A.4. Characteristics of Jurkat LDK-resistant cell line derivatives Res 3 and Res 6. LDK-resistant Jurkat cell lines were created via continuous incubation of parental Jurkat T-ALL cells in LDK over multiple cell passages. (A) Resistant lines 3 and 6 showed the highest viability and best resistance to 10μM LDK treatment as determined by MTT assay. (B) LDK-resistant lines Res 3 sand Res 6 show down-regulation of p-AKT(Thr308) upon LDK treatment comparable to that of parental Jurkat cells. P-AKT(Ser473) is strongly up-regulated in the LDK-resistant lines compared to parental Jurkat cells, indicative of increased mTOR complex 2 activity.

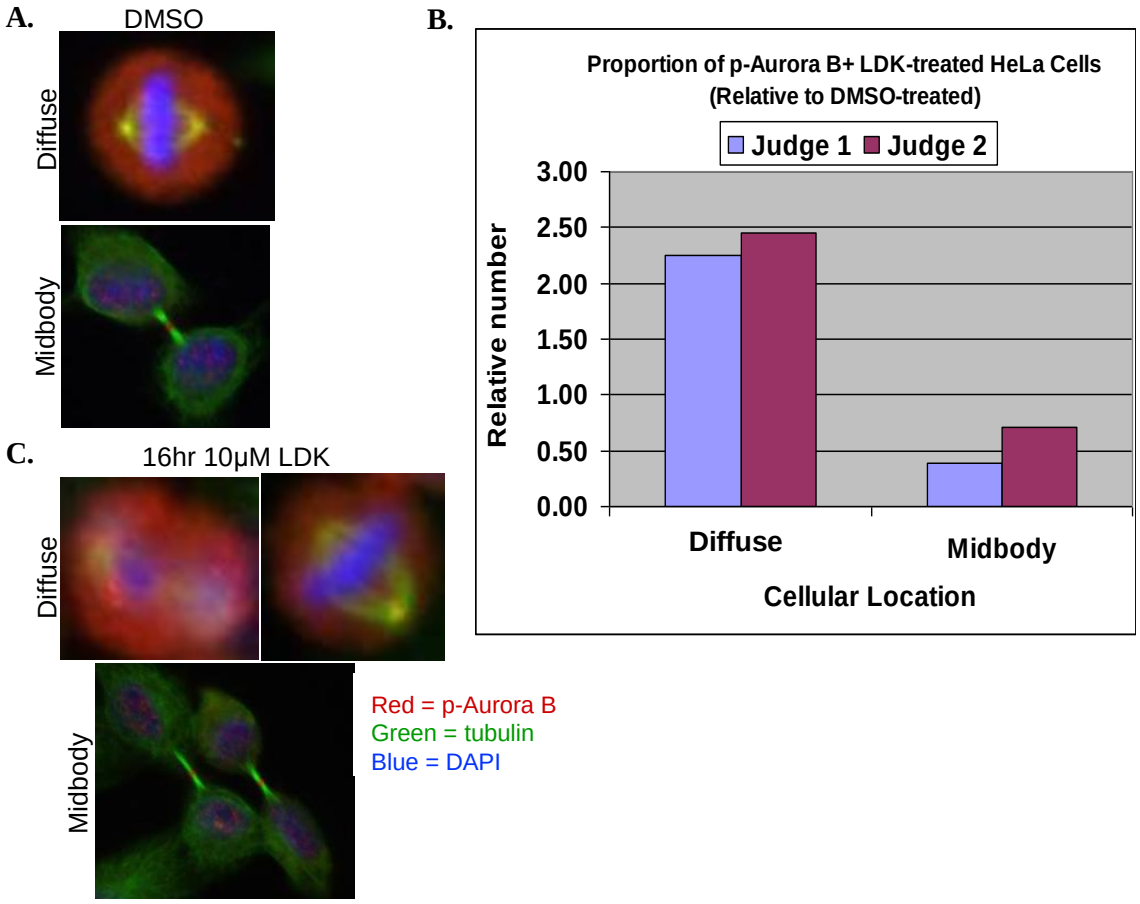

Figure A.5. Spatiotemporal isolation of phospho-Aurora B kinase in HeLa cells. Most LDK-sensitive cell lines tested to date, including both suspension and adherent cell lines, have exhibited G2/M block upon LDK treatment. Assessment of cyclin A, cyclin B1, and phospho-histone H3 (pH3) expression patterns in LDK-treated cells indicates that the G2/M block occurs after metaphase (see Figure 4.4 in Chapter 4). (A) Assessment of phospho-Aurora B kinase (p-Aur B) midbody expression patterns indicates that the G2/M block occurs after metaphase but before cytokinesis. (B) Immunostaining for p-Aur B kinase in HeLa cells shows that in LDK-treated cells, approximately twice as many are positive for diffuse p-Aur B compared to vehicle-treated cells. Of these LDK-treated p-Aur B positive cells, approximately half (C) lack any obvious organized spindle structure while (A) all observed vehicle-treated p-Aur B positive cells show an organized spindle structure.

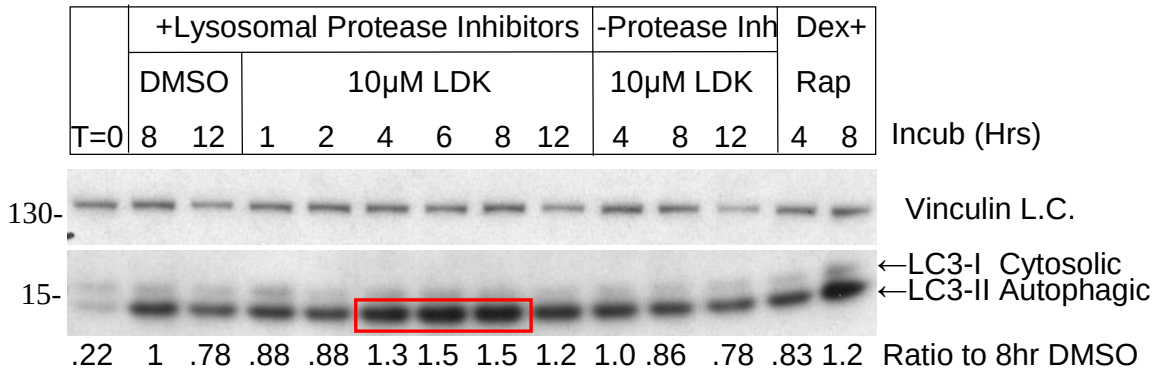

Figure A.6. LDK treatment results in increased autophagy in Jurkat cells. To determine whether LDK treatment increases autophagy in Jurkat cells, Jurkat cells were probed for cleaved LC3 on a western blot as a marker of autophagy. The cleaved form of LC3, LC3-II (14KDa), indicative of autophagy, increases (red box) in comparison to full-length cytosolic LC3-I (16KDa) with LDK treatment. (Dexamethasone + Rapamycin = positive control for autophagy induction).

A.

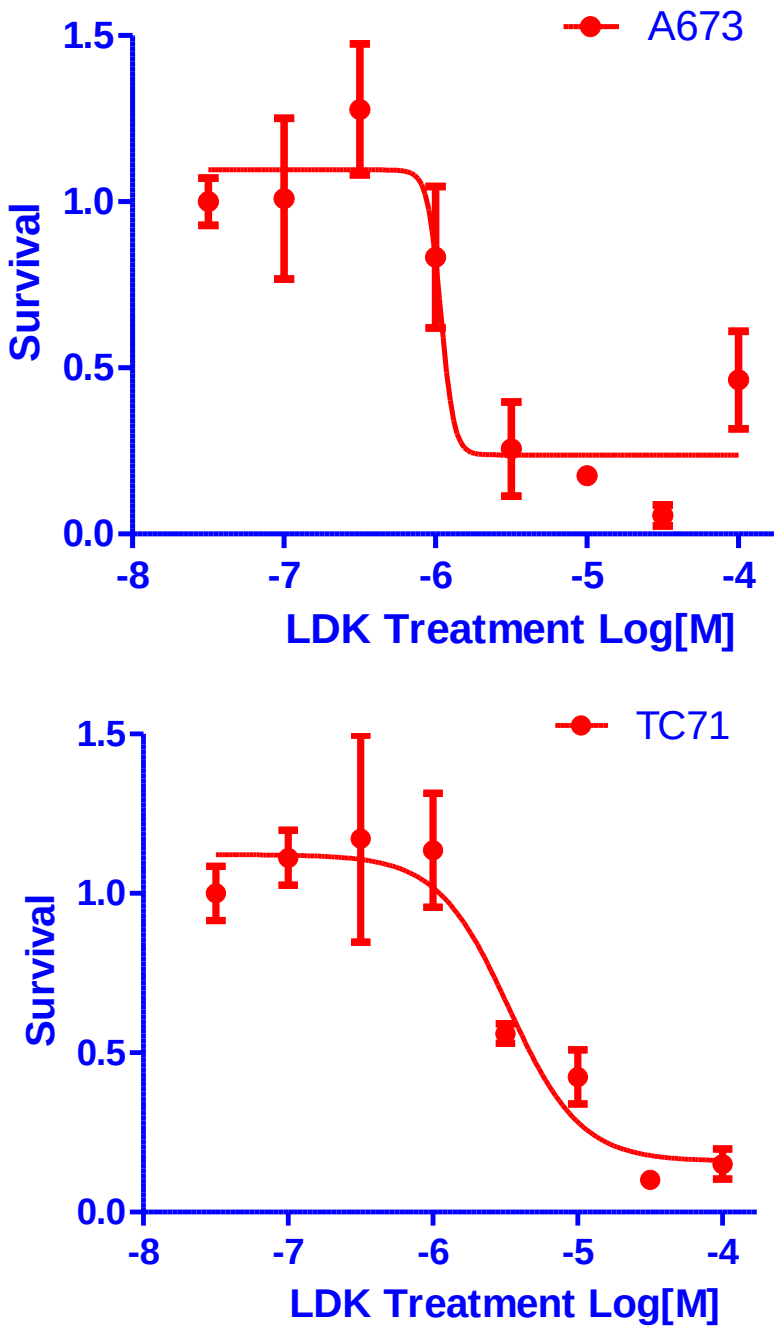

Figure A.7. Ewing Sarcoma is LDK-sensitive and shows G2/M delay upon LDK treatment. (A) IC_{50} dose response for LDK treatment of Ewing sarcoma cell lines A673 and TC71 which show IC_{50}s of ~1µM and ~3µM, respectively. (Error bars = St.Dev.). (B-C) LDK treatment cell cycle and AKT effects in Ewing sarcoma. Upper panels - Both A673 and TC71 show G2/M delay upon LDK treatment. Lower panels - Despite LDK sensitivity, neither cell line shows a change in quantified p-AKT(Ser473) with LDK treatment as determined via phos-flow assessment.

B.

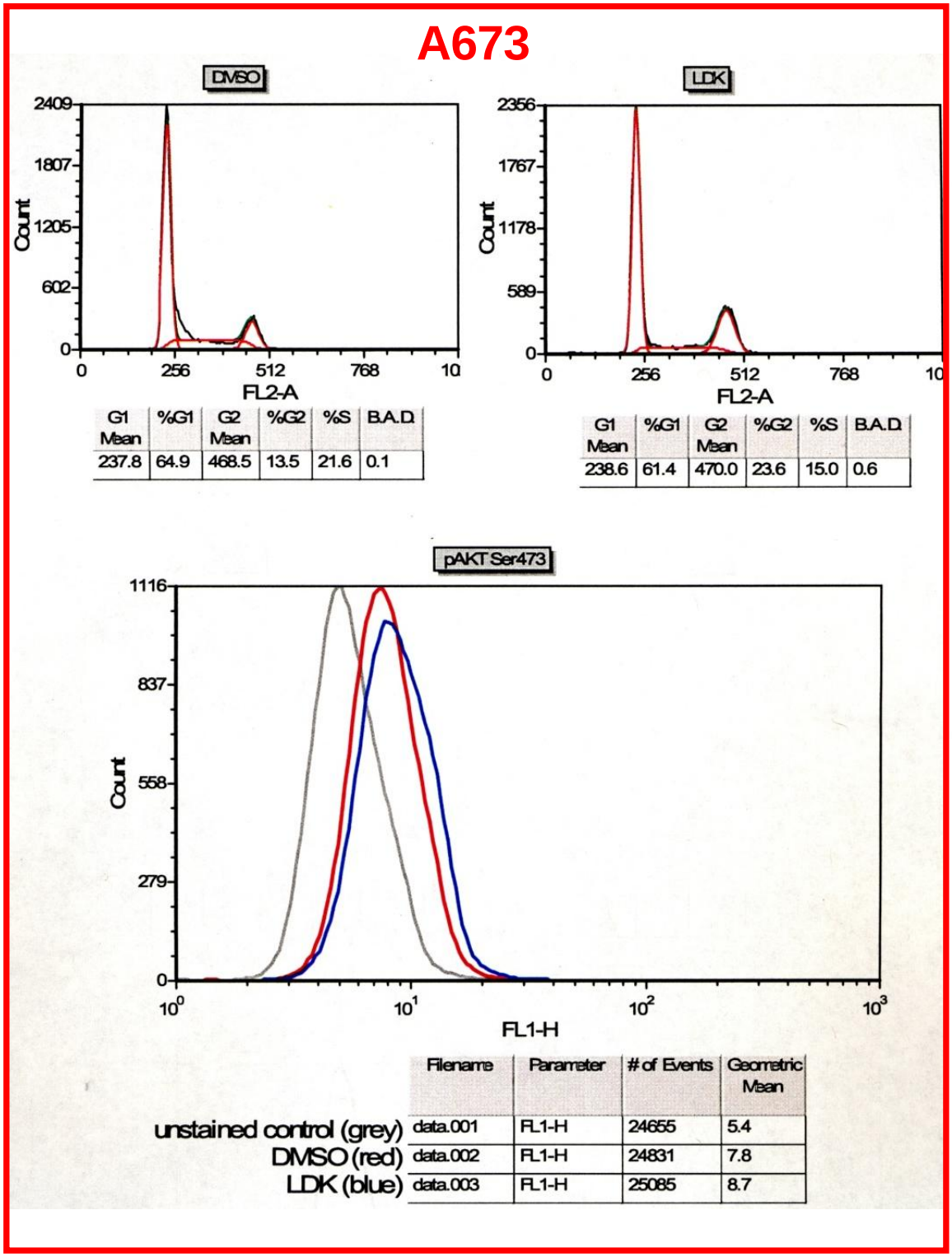
A673
DMSO
2409
1807
1205
602
0
Count
0
256
512
768
FL2-A
G1 Mean | %G1 | G2 Mean | %G2 | %S | B.A.D.
237.8 | 64.9 | 468.5 | 13.5 | 21.6 | 0.1
LDK
2356
1767
1178
589
0
Count
0
256
512
768
FL2-A
G1 Mean | %G1 | G2 Mean | %G2 | %S | B.A.D.
238.6 | 61.4 | 470.0 | 23.6 | 15.0 | 0.6
pAKT Ser473
1116
837
558
279
0
Count
10^0
10^1
10^2
10^3
FL1-H
Filename | Parameter | # of Events | Geometric Mean
unstained control (grey) | data.001 | FL1-H | 24655 | 5.4
DMSO (red) | data.002 | FL1-H | 24831 | 7.8
LDK (blue) | data.003 | FL1-H | 25085 | 8.7

C.

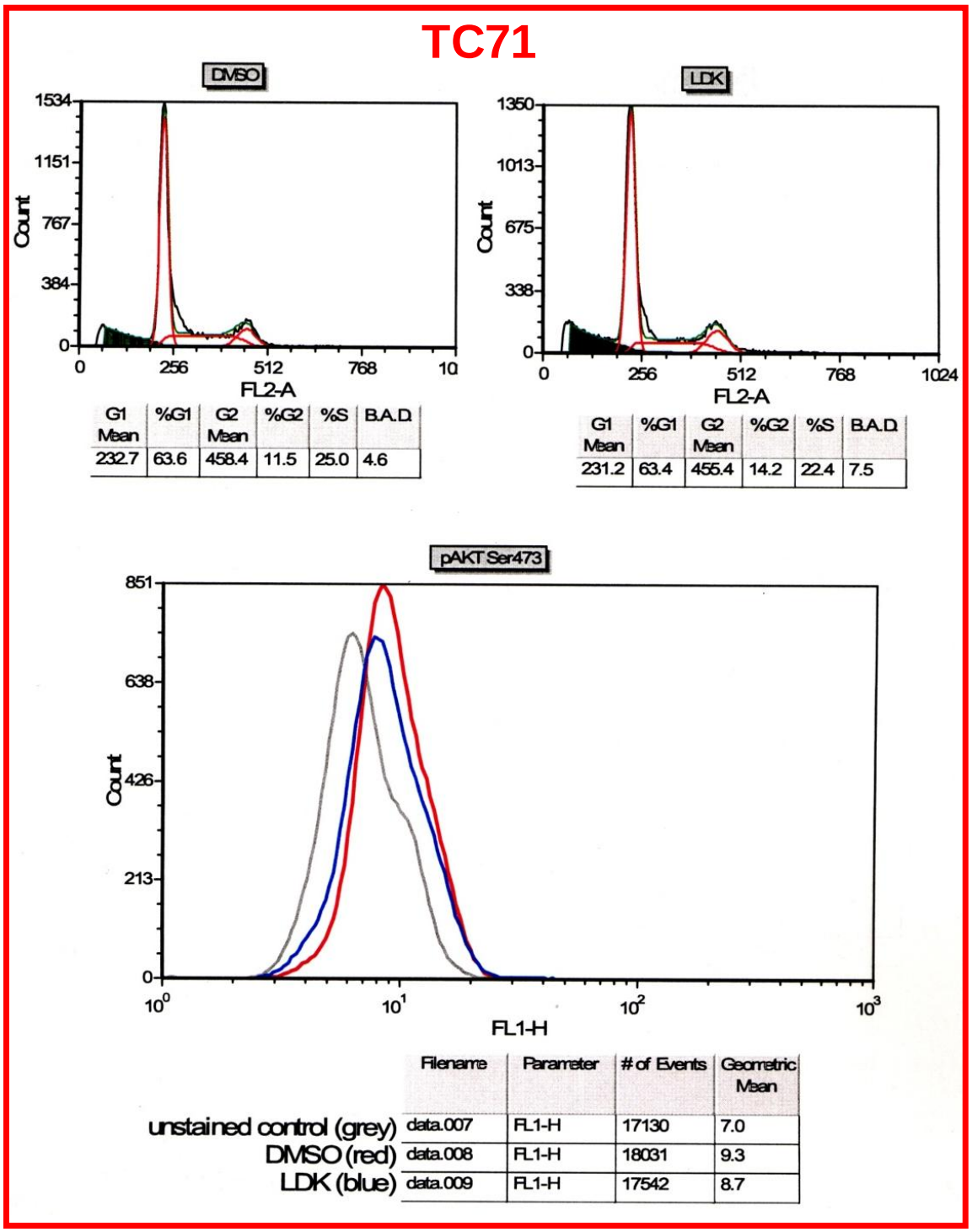
TC71
DMSO
1534
1151
767
384
0
Count
0
256
512
768
10
FL2-A
G1 Mean | %G1 | G2 Mean | %G2 | %S | B.A.D.
232.7 | 63.6 | 458.4 | 11.5 | 25.0 | 4.6
LDK
1350
1013
675
338
0
Count
0
256
512
768
1024
FL2-A
G1 Mean | %G1 | G2 Mean | %G2 | %S | B.A.D.
231.2 | 63.4 | 455.4 | 14.2 | 22.4 | 7.5
pAKT Ser473
851
638
426
213
0
Count
10^0
10^1
10^2
10^3
FL1-H
Filename | Parameter | # of Events | Geometric Mean
unstained control (grey) | data.007 | FL1-H | 17130 | 7.0
DMSO (red) | data.008 | FL1-H | 18031 | 9.3
LDK (blue) | data.009 | FL1-H | 17542 | 8.7

A.

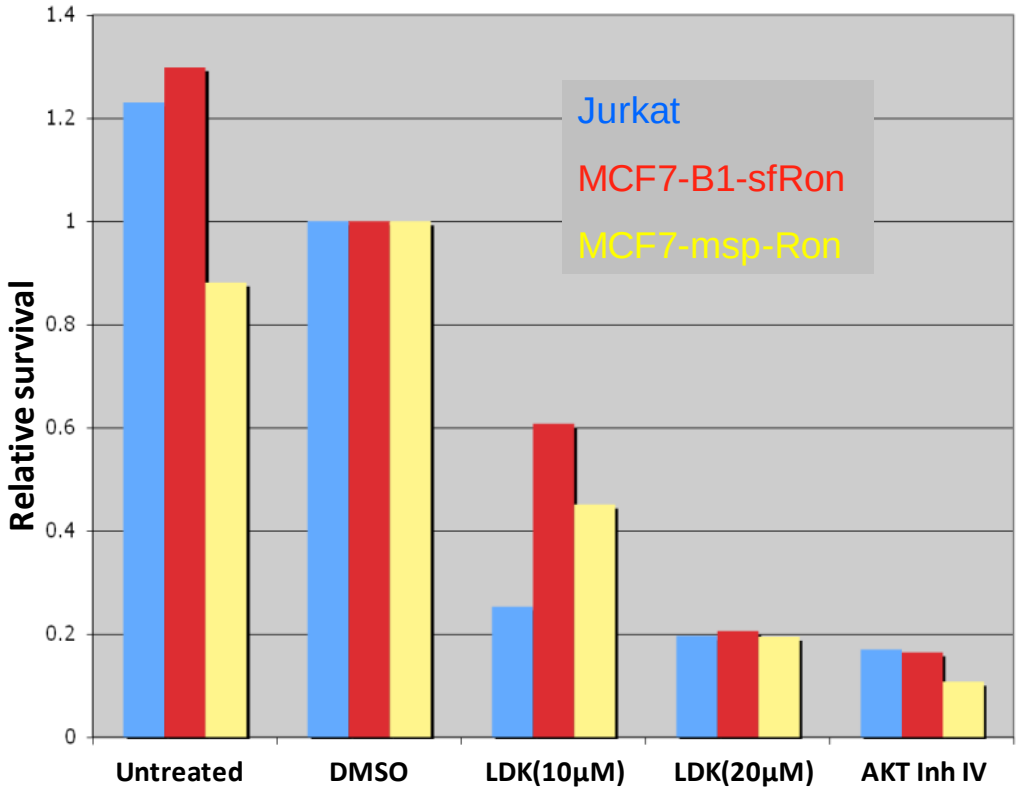

B.

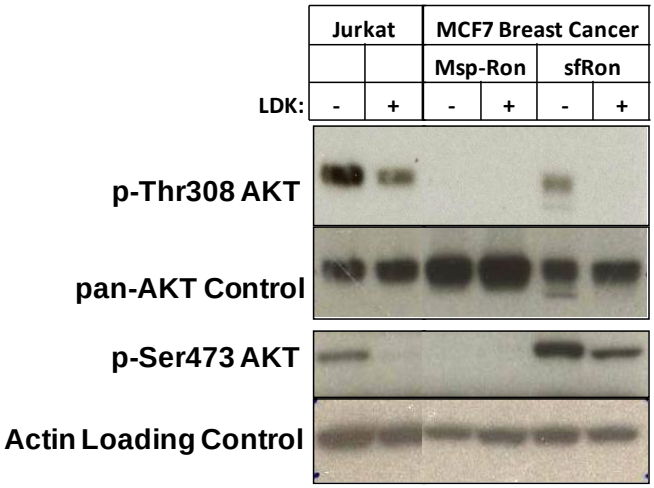

Figure A.8. MCF7 breast cancer derivatives Msp-Ron and sfRon are LDK-sensitive. (A) LDK dose-response determination for MCF7-Msp-Ron and MCF7-sfRon. Both cell lines show LDK IC_{50}s of ~10µM. (B) Western blot determination of p-AKT (Thr308 and Ser473) in LDK-treated MCF7-derived cell lines. MCF7-sfRON shows auto-activation of the AKT pathway which is down-regulated by 12 hours LDK treatment @ 10µM. Actin and pan-AKT = loading controls. (C) MCF7-sfRON shows S-phase cell cycle delay upon 10µM LDK treatment for 48 hours.

C.

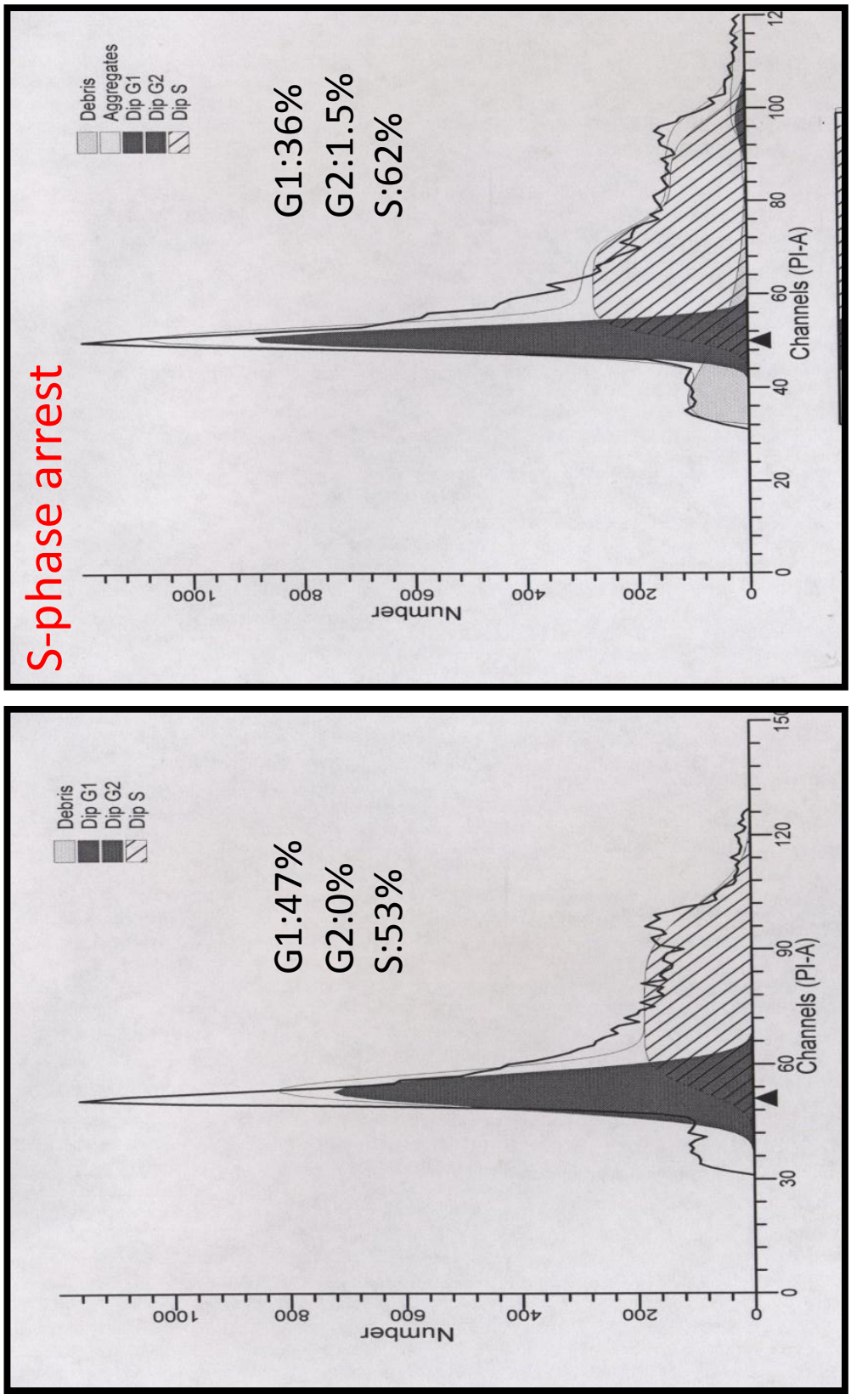
S-phase arrest
Debris
Aggregates
Dip G1
Dip G2
Dip S
G1:36%
G2:1.5%
S:62%
Number
Channels (PI-A)
48 Hrs incubation in LDK
Debris
Dip G1
Dip G2
Dip S
G1:47%
G2:0%
S:53%
Number
Channels (PI-A)
48 Hrs incubation in DMSO